Carbonate secreting organisms in clastic shelf systems and their potential as environmental archive

An interdisciplinary perspective on past and present marine ecosystems

Dissertation

Universität Bremen
Fakultät für Geowissenschaften

vorgelegt von
André Klicpera
Bremen, November 2014

Universität Bremen

Dissertation

zur Erlangung des Doktorgrades der Naturwissenschaften
(Dr. rer. nat.)

am Fachbereich Geowissenschaften
der
Universität Bremen

vorgelegt von

André Klicpera

im November 2014

Wissenschaftliche Betreuung und Begutachtung:

Prof. Dr. Hildegard Westphal

Leibniz Zentrum für Marine Tropenökologie
Abteilung Biogeochemie / Geologie
Fahrenheitstr. 6
D-28359 Bremen
Deutschland

Prof. Dr. André Freiwald

Senckenberg am Meer
Abteilung Meeresgeologie
Südstrand 40
D-26382 Wilhelmshaven
Deutschland

Weitere Mitglieder der Prüfungskommission:

Prof. Dr. Hans-Joachim Kuss, Dr. Jens Lehmann, Dr. Claudia Wienberg, Alex Janßen

Tag des öffentlichen Kolloquiums:
24. März 2015

Hiermit erkläre ich, daß ich die vorliegende Dissertation selbständig und ohne Zuhilfenahme unerlaubter Hilfsmittel erstellt habe. Weder diese noch eine ähnliche Arbeit wurde an einer anderen Abteilung oder Hochschule im Rahmen des Prüfungsverfahrens vorgelegt, veröffentlicht oder zur Veröffentlichung vorgelegt. Ferner versichere ich, daß die Arbeit unter Einhaltung der Regeln guter wissenschaftlicher Praxis der Deutschen Forschungsgemeinschaft (DFG) entstanden ist.

Bremen, den 01.11.2014

To my parents Günter and Marlies Klicpera

for their endless support and encouragement

No part of this dissertation or the publications included may be reproduced, stored in a retrieval system, or transmitted in any form or by any means, electronic, mechanical, photocopying, recording, or otherwise, without indicating the reference:

Klicpera, A. (2015) *Carbonate secreting organisms in clastic shelf systems and their potential as environmental archive. An interdisciplinary perspective on past and present marine ecosystems.* PhD thesis, Faculty for Geosciences, University of Bremen, Germany. 215 pp.

Klicpera, A., Michel, J., and H. Westphal (2015) *Facies patterns of a tropical heterozoan carbonate platform under eutrophic conditions: the Banc d'Arguin, Mauritania.* Facies 61:421. Doi:10.1007/s10347-014-0421-5

Klicpera, A., Taylor, P.D., and H. Westphal (2014) *Bryozoans on the move: Adaptations to hard substrate–limiting tropical heterozoan carbonates (Banc d'Arguin, Mauritania).* Marine Biodiversity (online first). Doi:10.1007/s12526-014-0279-3

Klicpera, A. and H. Westphal (2014) *Shallow water sediments of the Banc d'Arguin*. In: Westphal, H. et al. (Eds) Report of Cruise Maria S. Merian 16/3 – Phaeton – Paleoceanographic and paleo-climatic record on the Mauritanian shelf. Oct. 13 – Nov. 20, 2010, Bremerhaven (Allemagne) – Mindelo (Cap Verde). Maria S. Merian-Berichte, Leibniz-ZMT, Bremen, Germany. 136 pp. Doi:10.2312/cr_msm16_3

Klicpera, A., Taylor, P.D., and H. Westphal (2013) *Bryoliths constructed by bryozoans in symbiotic associations with hermit crabs in a tropical heterozoan carbonate system, Golfe d'Arguin, Mauritania.* Marine Biodiversity 43:429–444. Doi:10.1007/s12526-013-0173-4

Klicpera, A., Hanebuth, T.J.J., Carranza, A., and H. Westphal (2015) *The stable isotope record of a Late Pleistocene bivalve (Eurhomalea exalbida) from the Uruguayan Shelf: implications for palaeoenvironmental reconstructions.* (in preparation for submission)

Acknowledgements

First and foremost, I want to thank my supervisor Hildegard Westphal. She has taught me, both consciously and un-consciously, how good scientific work is done. I appreciate all her contributions of time, ideas, and funding to make my Ph.D. experience productive and stimulating. The joy and enthusiasm she has for her work as scientist and director of a prestigious international research institute was contagious and motivational for me, even during frustrating times in the Ph.D. pursuit.

Many of these chapters would not have been possible without the professional support of my highly valued colleagues at the Leibniz Center for Tropical Marine Ecology (ZMT) and the Center for Marine Environmental Sciences (MARUM) of the University of Bremen. Till J.J. Hanebuth, Hendrik Lantzsch, and Julien Michel, representative for all those who contributed to my research and provided support, are mentioned here.

André Freiwald (Marine Research Department at Senckenberg am Meer, Germany) is thanked for a second review of this dissertation as well as for his contribution of time and effort.

I am especially thankful to Paul D. Taylor (Museum of Natural History, United Kingdom) for giving me the opportunity to study our sedimentary samples from Mauritania at one of the oldest and most prestigious museums in the world. He contributed invaluable background knowledge and support in his function as one of the few bryozoan experts worldwide.

Other international co-operations with Alvar Carranza, Fabrizio Scarabino (both Museum National de Historia Natural, Uruguay) and Felipe García Rodruígez (Universidad de la República, Uruguay) were highly interesting and stimulating. I am particularly thankful for the opportunity to study the mollusk reference material hosted at the Natural History Museum in Montevideo and, of course, for the local support. The field trips and workshops organized by Felipe helped us to spread our ideas for future collaborations and scientific research.

Nereo Preto (University of Padua, Italy), Guillem Mateu-Vicens (University of the Balearic Islands, Spain) and Marco Taviani (University of Bologna, Italy) are acknowledged for their professional advice and support during various research visits and research cruises. Nereo, our Espresso sessions were hilarious and the time after the most productive part of the day!

Axel Munnecke and Matthias López Correa (both University Erlangen-Nürnberg, Germany) are thanked for their local support during my research visit and for the excellent organized course on carbonate microfacies (also known as "Flügel Course"). You did a great job and I appreciate having had the opportunity to attend!

Past and present members of the carbonate sedimentology workgroup are acknowledged for contributing immensely to my personal and academic education at the MARUM and later at the ZMT in Bremen. The group has been a source of friendship as well as good advice for problem solving discussions. I am particularly thankful to Claire Reymond and my Ph.D. student fellows Natalia Herrán Navarro, Thomas Mann, Peter Müller, and Andre Wizemann. Our countless, often highly emotional discussions and, of course, the interesting collaborations were a great panel to spread our ideas.

Tom, our expedition to Indonesia was more than exciting and the fieldwork on a number of uninhabited remote atoll islands was a great experience. Although the customs-disaster was frustrating in the beginning, we did a great job and, what is more, in the end we managed to get all important sediment samples back to Germany, even though I had to go without my luggage.

Matthias Birkicht is thanked for the endless discussions on how laser-particle-sizers do really work and how they contribute to the work of a sedimentologist, or maybe not.

Furthermore, I want to appreciate the enthusiasm, intensity and willingness of Sebastian Flotow in his function as ZMT all-rounder. His support and advice in the thin section lab and during our countless SEM and µCT sessions were invaluable. Sebastian, thank you for your professional thin sections and geological preparations, even when I provided most of the material at last minute.

Captain Friedhelm von Staa, his officers and crew of RV Maria S. Merian (cruise MSM16-3) are acknowledged for their excellent support of our measurement and sampling program and for creating a very friendly atmosphere on board.

The MARUM (DFG-Research Center / Excellence Cluster "The Ocean in the Earth System"), the DFG Senate Commission on Oceanography and the Leibniz Center for Tropical Marine Ecology (ZMT) are acknowledged for providing infrastructure and financial support for this research.

Last but not least I want to thank Diana for her endless support and patience throughout this project and who shares my passion for geology and traveling.

Abstract

The following dissertation investigates the potential of carbonate-secreting organisms as biogenic archive of past and present environmental conditions.

Recent efforts have given a high priority in marine research and, in particular, in climate reconstructions to produce biogeochemical proxies of characteristic oceanographic settings that can be integrated with other high-resolution climatic archives. Such records encompass terrestrial tree-ring data, speleothems, ice-cores, sediments and biogenic carbonates, each characterized by unique strengths and shortcomings. Biogenic carbonates of marine origin, for example, represent valuable high-resoluted, but comparably little used archives. Among the biogenic carbonates, mollusk shells offer a comparably short window (years to centuries) with a temporal high resolution covering sub-daily tidal cycles. As a consequence, robust climatological interpretations based on mollusk shells often demand for complex and time-consuming master-chronologies. Corals and other slow-growing marine carbonate secretors, in contrast, cover a longer time-span (centuries to millennia), but often with a significant lower temporal resolution.

Numerous marine organisms produce hard parts, which are usually precipitated in geochemical equilibrium with the ambient seawater and thus perfectly document the response of marine life to a changing environment. In their function as supporting structure, most of these hard parts are made out of accretionary precipitated calcium carbonate (e.g., bivalve shells, sea urchin spines or bryozoan and coral skeletons) and provide an abundant occurrence in most recent marine deposits, but also in the geological record. Such carbonate secreting organisms and their remains accumulate either *in-situ* or hydrodynamically transported to extensive sedimentary deposits covering today extensive areas of the marine realm from the shallow shelf seas to the deep ocean and from tropical latitudes to polar regions. The resulting carbonate-rich sediments and rocks provide an invaluable archive of both, short term environmental events usually in a sub-seasonal to millennial-scale resolution, but also long-term evolutionary trends of individual marine organisms covering geological time scales. These trends include, for example, structural modifications of the skeleton and other hard parts due to mutation and natural selection.

Besides a temporal resolution, those archives provide a spatial dimension covering large-scale community structures of ecosystem-wide extent down to individual-scale modifications of µm-sized skeletons of biological morphotypes (e.g., planktonic foraminifera, cheilostome bryozoans, and others).

With the first pioneering studies by Epstein et al. (1951; 1953), who focused on biologically precipitated skeletal carbonate of mollusks and its use for the reconstruction

of palaeo-water temperatures on the basis of stable oxygen isotopes, a first biogeochemical fingerprint of a large group of marine invertebrates was established that allowed to interpret past environmental conditions. A precise understanding of the controlling processes involved such as the incorporation of elements and biological factors like metabolically-driven fractionation processes allows for the interpretation of the characteristics of a habitat, its environmental condition and, not least, of associated steering parameters. Later in the 1970s, Lees & Buller (1972) developed the concept of carbonate grain association types, which was another breakthrough in carbonate sedimentology and allowed for the interpretation of sedimentological patterns based on facies studies. Both concepts provide a valuable framework for the investigation of biogenic carbonates such as sediments, rocks or individual sediment constituents. However, under complex oceanographical settings or under natural or anthropogenic induced disturbances (e.g., upwelling, industrial/agricultural induced eutrophication) both concepts can show weaknesses and thus clearly demand for detailed analyses of associated drivers and players.

This dissertation shows how a combined approach of interdisciplinary research (e.g., geology, marine biology and biogeochemistry) can enhance our understanding and the assessment of the functioning of modern and ancient marine archives in their function as ecosystem-specific records. By using the present as an invaluable key to the past, we can interpret and relate shifting marine communities, their adaptation capabilities as a result of environmental constraints and their geochemical fingerprint to changing environmental conditions and associated steering factors. Moreover, we can infer from these archives documented in ancient carbonate systems and preserved in the geological record valuable models for future developments such as anthropogenic induced coastal eutrophication as a growing concern in areas with high population rates.

Kurzfassung

Die vorliegende Dissertation untersucht das Potential karbonatischer Organismen als biogenes Archiv für vergangene und gegenwärtige Umweltbedingungen.

Aktuelle Bemühungen der Meeresforschung konzentrieren sich auf die Rekonstruktion des Erdklimas und der Etablierung biogeochemischer Proxys zur Charakterisierung vergangener Ozeanbedingungen, um diese in bestehende Klimaarchive einzuhängen zu können. Solche Datenreihen umfassen überwiegend terrestrische Archive wie Bauringdaten, Speläotheme, Sedimente und Eiskerne, aber auch marine Ablagerungen sowie biogene Karbonate. Jedes dieser Archive für sich bietet besondere Vorzüge, aber auch diverse Einschränkungen, die maßgeblich deren Anwendungsbereich charakterisieren. Molluskenschalen, als Beispiel biogener Karbonate, liefern über einen vergleichsweise kurzen Zeitraum (Jahre bis Jahrhunderte) sehr hochauflösende Archive (z.B. Tidenzyklen) sodaß deren klimatologische Aussagekraft maßgeblich von aufwendigen Master-Chronologien abhängt. Korallen und andere langsam wachsende Organismen decken einen weitaus längeren Zeitraum ab (Jahrhunderte bis Jahrtausende), zeigen aber meist eine deutlich geringere temporale Auflösung.

Zahlreiche marine Organismen produzieren Skelette und Hartteile welche weitgehend im geochemischen Gleichgewicht mit dem umgebenen Meerwasser abgeschieden werden und somit als biogene Rückmeldung einer sich verändernden Umwelt dienen können. In ihrer Funktion als Stützstruktur innerhalb eines Organismus oder einer Kolonie sind diese Hartteile überwiegend aus Kalziumkarbonat aufgebaut (z.B. Muschelschalen, Seeigelstachel, oder Skelette von Korallen und Bryozoen) und zahlreich in rezenten und geologischen Ablagerungen vertreten. Durch Akkumulation vor Ort oder durch Wasserenergie verfrachtet sammeln sich karbonatische Organismen und deren Überreste zu ausgedehnten Ablagerungen an. Heute bedecken diese biogenen Sedimente weite Bereiche des Ozeanbodens von den flachen Schelfmeeren bis in die Tiefsee und von tropischen Latitüden bis in die Polargebiete. Die daraus resultierenden Sedimente und Gesteine liefern zahlreiche biogenen Archive, die Rückschlüsse über kurzzeitige Umweltereignisse zulassen, aber auch evolutionäre Trends individueller Organismengruppen in Folge von Mutation und natürlicher Selektion aufzeigen.

Neben der für die Klimaforschung wichtigen temporalen Auflösung liefern solche biogenen Sedimente und die darin enthaltenen karbonatischen Archive auch eine räumliche Komponente. Diese ermöglicht wichtige Aussagen über lokal abgegrenzte Bereiche bis hin zu Ökosystem-weiten Gemeinschaftsstrukturen verschiedener Organismengruppen. Auf Organismen-Niveau lassen sich zudem kleinsträumliche

Anpassungen einzelner Individuen (z.B. Morphotypen planktonischer Foraminiferen oder cheilostomer Bryozoen) an ein bestimmtes Habitat identifizieren.

Mit den ersten wegweisenden Studien von Epstein et al. (1951, 1953), die sich mit dem geochemischen Fingerabdruck biogen gebildeter Skelettstrukturen und deren Potential zur Rekonstruktion von Paläo-Wassertemperaturen beschäftigten, etablierte sich die Geochemie als wichtiges Werkzeug zur Interpretation vergangener Umweltparameter. Ein genaues Verständnis über die Einbindung chemischer Elemente sowie die Analyse artspezifischer metabolischer Fraktionierungsprozesse bei der Karbonatbildung ermöglichen zudem die Interpretation von Lebensraum, Umweltbedingungen und, nicht zuletzt, die damit verbundenen Steuerungsparameter. Später in den frühen 1970er Jahren folge das Konzept der Karbonatkorn-Assoziationen von Lees und Buller (1972), welches einen weiteren Durchbruch bei der Interpretation sedimentologischer Abfolgen und deren räumliche Verteilung darstellte. Dieses Konzept ermöglichte die biogenen Bestandteile eines Sediments den vorherrschenden Umweltbedingungen zuzuordnen und ermöglichte erstmals einen direkten Vergleich von marinen Ablagerungen aus verschiedenen Klimazonen. Obwohl beide Konzepte ein wichtiges Rahmenwerk zur Untersuchung und Analyse karbonatischer Komponenten bieten, stoßen diese insbesondere unter komplexen ozeanographischen Bedingungen wie mariner Eutrophierung (z.B. Nährstoffeintrag durch marinen Auftrieb, oder industrieller / landwirtschaftlicher Abwässer) an ihre Grenzen. Detaillierte Betrachtungen assoziierter Steuerungsfaktoren und deren Einfluß auf Lebensgemeinschaften sind somit die Grundlage einer robusten Interpretation – für rezente Studien ebenso wie für Paläoumweltrekonstruktionen.

Die vorliegende Dissertation knüpft an dieser Stelle an und verwendet einen kombinierten interdisziplinären Ansatz aus Geologie, mariner Biologie und Biogeochemie um unser Verständnis zur Beurteilung und Funktion mariner Bioarchive zu erweitern. Hierbei dient die Gegenwart als Schlüssel zur Vergangenheit und ermöglicht die Interpretation und Verknüpfung historischer Daten und geologischer Archive mit Umweltfaktoren und deren Steuerungsgrößen. Darüber hinaus läßt die Vielzahl mariner Klimaarchive nicht selten wertvolle Aussagen über zukünftige Entwicklungen mariner Ökosysteme zu, die insbesondere im Hinblick auf anthropogen induzierte Eutrophierung sensibler Küstenräume in Folge von Überbesiedlung und zunehmender Urbanisation zunehmend ins Zentrum der gegenwärtigen Diskussion gerückt sind.

Table of Contents

Acknowledgements ..... *i*
Abstract ..... *iii*
Kurzfassung ..... *v*
Table of Contents ..... *vii*
List of Figures ..... *ix*
List of Tables ..... *x*
List of Supplements ..... *x*
I. General introduction *1*
II. Objectives *3*
III. Research areas offshore Uruguay and Mauritania *5*
III.1 The Northwest African Shelf *6*
III.2 The Southeast South American shelf *15*
IV. Materials sampled and investigated *21*
IV.1 R/V Poseidon Cruises 346 and 366 (Mauritania) *21*
IV.2 R/V Maria S. Merian Cruse MSM16-3 (Mauritania) *21*
IV.3 R/V Meteor Cruise M78-3a (Uruguay) *23*
V. Methods used in this study *25*
V.1 Sedimentological analysis *25*
V.2 Geochemical analysis *27*
V.3 Compositional analysis *29*
V.4 Classification and determination of sediments and biogens *29*
V.5 Software processing *30*
V.6 Statistical analysis *31*
VI. Outline of research *32*
VII. Sediment response to environmental steering factors *34*
VIII. First publication *35*
VIII.1 Introduction *38*
VIII.2 Study area *39*
VIII.3 Oceanographic Setting *41*
VIII.4 Material and methods *43*
VIII.5 Results *45*
VIII.6 Discussion *56*
VIII.7 Conclusions *66*
VIII.8 Acknowledgements *67*
VIII.9 References *68*

IX. Biological interactions and morphological adaptations as a tool in marine environmental research 73
X. Second publication 75
X.1 Introduction 78
X.2 Study area 79
X.3 Material and methods 82
X.4 Results 85
X.5 Discussion 91
X.6 Conclusions 100
X.7 Acknowledgements 101
X.8 References 102
XI. Third publication 105
XII. Bivalve shells as environmental archives 109
XIII. Fourth manuscript 111
XIII.1 Introduction 114
XIII.2 Study area 115
XIII.3 Material 119
XIII.4 Methods 121
XIII.5 Results and Discussion 126
XIII.6 Conclusions 136
XIII.7 Acknowledgements 138
XIII.8 References 139
XIV. Summary and conclusions 144
XIV.1 Main outcomes of the first publication 144
XIV.2 Main outcomes of the second and third publication 145
XIV.3 Main outcomes of the fourth manuscript 145
XV. Perspectives and implications for future research 146
XVI. Appendix 148
XVI.1 Institutional cooperation 148
XVI.2 List of co-authors 149
XVI.3 Compiled literature 150
XVI.4 Peer-reviewed conference contributions and cruise reports 164
XVII. Supplements to the first publication (Mauritania) 165
XVIII. Supplements to the second and third publication (Mauritania) 170
XIX. Supplements to the fourth manuscript (Uruguay) 191
XX. Epilogue 199

List of Figures

Fig. III.1: Study areas offshore Mauritania and Uruguay and Atlantic Ocean circulation pattern 6
Fig. III.2: Depth versus salinity diagrams for the Golfe d'Arguin for winter and summer season 8
Fig. III.3: Satellite Image and regional oceanography of the Golfe d'Arguin 11
Fig. III.4: Chl-a and SST for the years 2005 to 2012 in the Golfe d'Arguin area 12
Fig. III.5: SST and Chl-a values since 2005 for the Golfe d'Arguin 14
Fig. III.6: SST and SSS distribution over the Argentine and Uruguayan Shelf 17
Fig. III.7: Satellite Image and regional oceanography of the southeastern South American Shelf 18
Fig. III.8: T/S Diagrams for winter and summer season offshore northern Argentina and Uruguay 19
Fig. IV.1: Research cruise sampling sites along the Mauritanian Shelf 23
Fig. IV.2: Research cruise core sampling sites along the southeastern South American Shelf 24
Fig. VIII.1: Golfe d'Arguin bathymetry and sample stations offshore northern Mauritania 40
Fig. VIII.2: Sea Surface Temperature and Chlorophyll-*a* concentration in the Golfe d'Arguin 42
Fig. VIII.3: Carbonate content and grain size distribution in the Golfe d'Arguin 47
Fig. VIII.4: Skeletal and non-skeletal grain groups in the Golfe d'Arguin 49
Fig. VIII.5: Dendrogram of grain assemblages (F1 to F4B) from the Golfe d'Arguin. 54
Fig. VIII.6: Bulk sediments collected along the platform margin (Banc d'Arguin, Mauritania) 60
Fig. VIII.7: Local distribution of sedimentary facies patterns in the Golfe d'Arguin 61
Fig. VIII.8: Facies model of Golfe d'Arguin based on sedimentological analyses 64
Fig. X.1: Bryoliths sampling areas in the Banc d'Arguin offshore Mauritania 80
Fig. X.2: Bryoliths showing hermit crab symbiont and internal/external structures 86
Fig. X.3: Turritellid-nucleated bryoliths showing external and internal features of encrustation 87
Fig. XI.1: Heterozoan carbonates and bryozoan colonies form the Banc d'Arguin 108
Fig. XIII.1: Present-day oceanographical setting of the study area in southeastern South America 116
Fig. XIII.2: Modern oceanographical settings of the Argentinean and Uruguayan shelf 118
Fig. XIII.3: Sampling procedures of the deglacial bivalve species from southeastern South America 123
Fig. XIII.4: Regional map of southeastern South America with $\delta^{18}O_{water}$ and salinity (Sal) data 125
Fig. XIII.5: Shell height-at-age curves of fossil and modern specimens of bivalve species *E. exalbida* 128
Fig. XIII.6: The shell-intern growth record of the fossil specimen *E. exalbida* 130
Fig. XIII.7: Stable oxygen and carbon isotope profiles analyzed in the outer shell layer of *E. exalbida* 133

List of Tables

Tab. VIII.1: Sampling stations and gears of the R/V MS Merian cruise 16-3 44
Tab. VIII.2: Oceanographic data extracted from CTD measurements (cruise MSM16-3) 46
Tab. VIII.3: Measurements conducted during cruise MSM16-3 in the outer Banc d'Arguin, Mauritania 52
Tab. VIII.4: Identified mollusk taxa from the inner shelf of the Golfe d'Arguin, Mauritania 53
Tab. VIII.5: Facies characteristics of analyzed samples collected in the Golfe d'Arguin 55
Tab. VIII.6: Modern and ancient heterozoan carbonates in subtropical to tropical warm-water settings 65
Tab. X.1: Stations sampled in the Banc d'Arguin providing bryozoan – hermit crab associations 82
Tab. X.2: Bryolith specimens sampled from the Baie du Lévrier and the outer Banc d'Arguin 83
Tab. X.3: Astogenetic size variation of bryolith forming bryozoans 89
Tab. X.4: Environmental parameters of the Mauritanian and New Zealand carbonate systems 99
Tab. XIII.1: Sampling locations of bivalve shell material offshore Uruguay 119
Tab. XIII.2: AMS ^{14}C ages for shell-carbonate samples from the Uruguayan Shelf 126
Tab. XIII.3: Shell carbon ($\delta^{13}C_{shell}$) and oxygen ($\delta^{18}O_{shell}$) isotopes from bivalve sample material 132

List of Supplements

Suppl. XVII.1: Map of the Golfe d'Arguin anno 1747 165
Suppl. XVII.2: Summary of Cenozoic carbonate deposit types 166
Suppl. XVII.3: Component analysis and determination of bivalve grains from the Golfe d'Arguin 167
Suppl. XVII.4: Component analysis and determination of gastropod grains from the Golfe d'Arguin 169
Suppl. XVIII.1: Living Bryoliths 170
Suppl. XVIII.2: Bryozoan skeletons identified from Mauritanian sediments 171
Suppl. XIX.1: Fossil and recent bivalve shells sampled offshore Uruguay 191
Suppl. XIX.2: Thin section and SEM images showing internal growth structures of analyzed bivalves 192
Suppl. XIX.3: XRD analyses of bivalve shell carbonate - Pitar rostratus (extern shell). 193
Suppl. XIX.4: XRD analyses of bivalve shell carbonate - Pitar rostratus (intern shell) 194
Suppl. XIX.5: XRD analyses of bivalve shell carbonate - Eurhomalea exalbida (extern shell). 195
Suppl. XIX.6: XRD analyses of bivalve shell carbonate - Eurhomalea exalbida (intern shell) 196
Suppl. XIX.7: δ13C- and δ18O-measurements from bivalve specimen *Pitar rostratus* 197
Suppl. XIX.8: δ13C- and δ18O-measurements from bivalve specimen *Retrotapes exalbidus* 198

I. General introduction

The impact of climate change, rising sea level and the fingerprint of human induced ocean eutrophication and acidification make comprehensive studies on marine ecosystems more crucial than ever in order to apply sustainable ecosystem services (Wells and Daborn, 1997; Freiwald et al., 2004; Kleypas et al., 2006; André et al., 2009; Burke et al., 2011; IMROP, 2013; IPCC 2013, 2007). Today, more than half of all people worldwide are living in the vicinity to the sea. The ocean provides an important source of food, employment opportunities, traffic infrastructure, energy and a variety of touristic hotspots to sum up some of the most important economic factors (Bosch et al., 2010). However, seven out of the ten largest cities worldwide with more than 10 million inhabitants are threatened by continuously rising sea level and coastal erosion due to weather extremes and a long-term changing climate. Moreover, a vast number of countries located within the tropical climate belt and a steadily increasing number of remote island communities are dramatically affected by monsoon-related extreme weather events and are thus confronted with the phenomenon of climate migration (Sharkey, 2013).

This trend is especially remarkable considering that the world population is continuously growing with variable growth rates ranging between 2.2% (for 1963) and 1.1% (for 2012) see (WPP, 2012). Today, the UN projects predict a global population expected to reach between 8.3 and 10.9 billion by 2100 (WPP, 2012). As a direct result of overpopulation, most of the highly sensible coastal marine ecosystems are already dramatically threatened by human disturbances such as agricultural-induced eutrophication of marine environments, but also waste, industrial pollution and, not least, overfishing (Bosch et al., 2010; Burke et al., 2011; IMROP, 2013). Those interferences influence the majority of coastal-near marine ecosystems in the vicinity to larger human populations and are thus well known to be key-drivers causing the destruction of important key habitats such as coral reefs, seagrass plains and mangrove forests (IPCC, 2013). Such marine environments, however, are of fundamental value, because they provide, besides a major contribution to coastal stabilization and protection, a number of important nursery services to marine fish and shellfish stocks and host the highest beta-biodiversity worldwide (Burke et al., 2011). Fish and mollusks, in particular, are known to become an increasingly important food source of the future and represent an indispensable source of nourishment for a large number of wading and migrating birds (e.g., Wadden Sea, Germany and Banc d'Arguin, Mauritania) today (IMROP, 2013). With the fourth and fifth Assessment Report by the Intergovernmental Panel on Climate Change (IPCC) published in 2007 and 2013, respectively, the problems and impacts of climate change on ecosystem level were brought to the forefront and clearly highlighted

that our awareness and understanding of such marine systems is still correspondingly small.

While these reports clearly highlight the need for more fundamental research in increasingly affected marine environments, only a handful places worldwide provide natural laboratories in which the impact of environmental disturbances can be investigated under natural conditions. The Golfe d'Arguin offshore of northern Mauritania is due to year round upwelling and iron-rich dust input from the desertic hinterland one of the most productive marine areas in our modern ocean (IMROP, 2013). In its shallower parts, mixed carbonate-siliciclastic deposits accumulate to extensive successions that provide a valuable history of benthic marine organisms. These deposits prospered for thousands of years under natural eutrophic conditions and thus represent an invaluable marine archive of what we can expect from a future marine ecosystem in the absence of coral reefs (Westphal et al., 2010; Klicpera et al., 2015).

The application of marine organisms as biogenic archives is thus an essential part of ongoing marine research that allows to establish both, long-lasting climate records but also shorter and more highly resolved archives covering data down to sub-daily cycles. Marine carbonate secreting organisms play a key-role because they provide a number of modern representatives of organisms we know from the geological record. Using the present as a key to the past we can better understand the processes and mechanisms that drove global climate change in ancient times and it might help to understand environmental developments and changes on ecosystem level we expect in the future (André et al., 2009; Schöne and Gillikin, 2012; Gordillo et al., 2014).

Biogenic sediments and their constituents are an ideal source of environmental data because they are widespread from the shallow shelves to the deep sea and from the tropics to the polar realm. Shells and hard parts, in particular, provide invaluable morphological features developed in response to environmental conditions (see First publication). The modern life-style of organisms and their relationship to other biota can furthermore provide valuable insights into biological associations, biocoenoses and symbiotic partnerships where a poor fossilization potential hampers the documentation in the fossil record (see Second publication and Third publication). The biogeochemical fingerprint of biologically precipitated carbonate represents an ultimate tool to reconstruct environmental conditions through time as long as the sample material is not diagenetically altered. Used by scientists for decades, the reconstruction of aquatic settings and the environmental context under which the sediment producer had lived has today become a key-tool in geosciences and opens up a "window into the past". Although the calibration of such data is often coupled to kinetic effects or species-specific metabolic interferences that demand for modern representatives as calibration standards, the palaeo-temperature reconstruction based on stable oxygen and carbon isotopes or supported by rare-element ratios (Sr/Ca, Mg/Ca) has developed to a well-established technique today (see Fourth manuscript).

II. Objectives

Regional and global environmental changes (e.g., climate change, ocean acidification, natural and anthropogenic-induced eutrophication, marine pollution) are altering the chemistry and thus decline the health status of the ocean, sometimes at rates exceeding those in recent sedimentary and geological records (e.g., IPCC Reports 2013, 2007; Burke et al., 2011; Gattuso and Hansson, 2011). Such environmental disturbances have a significant impact on the marine biota and, in particular, on carbonate secretors. These changes in ecosystem conditions may lead to shifts in biological and ecological communities and manifest in an altered sedimentation pattern, which gives valuable insights into past and present processes.

Calcareous red and green algae, foraminifers, corals, sponges, bryozoans, brachiopods, echinoderms, mollusks and crustaceans play a dominant role as a primary carbonate source in most tropical and extra-tropical marine ecosystems along the continental shelves and further offshore. Some of these organisms build in extensive frameworks and are able to shape their environment by building reefs and hardbottom communities (Tucker, 1996; Flügel, 2004). The role of hard-bottom communities and reefs in coastal protection and for resource management is essential, as they provide shelter, food and habitat to numerous species of fish and invertebrates. Similarly, such marine communities are extremely vulnerable to physical damage from recreational and commercial activities, from the impacts of human development and, potentially, eutrophication of coastal waters (Burke et al., 2011; Riegl et al., 2013).

Such impacts, often acting on ecosystem-level, are well documented in numerous bioarchives precipitated by marine invertebrates (Gordillo et al., 2014). Supported by fundamental studies using the light dependence-related classification concept of carbonate grain associations (*sensu* Lees and Buller, 1972; James, 1997) and the more detailed carbonate grain assemblages (*sensu* Nelson, 1988; Hayton, 1995 and others), a useful basic framework is established that allows to interpret pure carbonate and mixed carbonate-siliciclastic deposits in modern and ancient sedimentary records. These descriptive approaches, however, are not always reliable, in particular, in those environmental settings with enhanced nutrient input. Where light is absent, carbonates develop that are reminiscent of cool-water communities even under tropical conditions, thus causing environmental misinterpretations where additional information on environmental conditions is not available (Westphal et al., 2010).

The objective of the presented dissertation is to contribute to filling this gap in our knowledge by providing an interdisciplinary ecosystem-based approach to classify modern and ancient marine environments and their drivers and players in the context of sedimentology, marine biology and geochemistry:

The investigated study areas off northwest Africa (Golfe d'Arguin) and off southeast South America (Río de la Plata Shelf) play a key-role in the Atlantic-wide ocean circulation system. The two shelfal environments host important large marine ecosystems and provide fishing grounds of highest socio-economical importance. Characterized by a number of distinct ocean-atmosphere couplings, coastal upwelling phenomena and seasonal-controlled shifts in the local ocean circulation pattern, these marine ecosystems represent important global players and are thus extremely vulnerable to the impact of anthropogenic induced climate change. A complex oceanography and seasonal shifting frontal zones manifest in the distribution of benthic organisms. Most processes and relationships, however, are still not completely understood and clearly deserve more attention in the context of environmental change (Pastor, 2008; Michel, 2009).

The detailed objectives of this study based on a multi-disciplinary approach are:

(1) — **Sedimentology/Geology** (Golfe d'Arguin, Mauritania, NW Africa)

A large-scale analysis of the modern and sub-recent sedimentary biofacies and taxonomic distribution patterns of carbonate-secreting organisms (e.g., facies-indicators, ecological key species) are undertaken in the shallow Banc d'Arguin. The objective of this study is to identify potential production areas and the effect of environmental steering parameters (e.g., eutrophication, upwelling, water energy, water temperature) on the tropical heterozoan carbonates and to deduce information for future scenarios.

(2) — **Marine Biology/Ecology** (Golfe d'Arguin, Mauritania, NW Africa)

This study focuses on the identification and evaluation of modern inter-specific relationships (e.g., biocoenoses and symbiotic interactions) between bryozoans and pagurid crabs. These partnerships are seen as a response to natural environmental constraints such as limited hardbottom availability and restricted habitat conditions. These biocenoeses are characteristic for the shallow marine and extreme low-diverse tropical ecosystem in the Golfe d'Arguin and provide new information that increases the knowledge of similar associations from the geological record.

(3) — **Sclerochronology/Geochemistry** (Río de la Plata Shelf, Uruguay)

This study deals with the application of sub-recent and fossil macro-benthos as potential bioarchive of oceanographic and environmental changes in a temporal highest resolution. Sclerochronological/geochemical approaches were applied on cold to temperate water large bivalve shells in order to track seasonal-controlled and long term (decadal to millennial) shifts in the thermohaline shelf front offshore Uruguay since the late Pleistocene.

III. Research areas offshore Uruguay and Mauritania

This dissertation investigates shallow-marine continental shelf deposits and the role of carbonate secreting organisms therein in their function as environmental bioarchive. Today a multitude of oceanographic studies investigate recent and past environmental parameters of marine ecosystems by relying on the ability of carbonate precipitating biota to record physico-chemical parameters of the water column (see Gillikin, 2005; André et al., 2009; Azzoug et al., 2012; Schöne and Gillikin, 2012; Butler et al., 2013; Klicpera et al., 2014; 2015; Gordillo et al., 2014 and references therein). However, under complex oceanographic conditions, these studies have also shown that environmental steering parameters, the ability of inter-specific interaction to cope with constraints, and even species-dependent metabolic effects on isotope fractionation play a key-role and represent the backbone of a robust environmental reconstruction (see details in e.g. Grossman and Ku, 1986; Elliot et al., 2003; Gillikin et al., 2005; Kanazawa and Sato, 2007; Lopez-Correa et al., 2010 and references therein). Neglecting one or a combination of these controls might result in misinterpretations as shown by Edinger et al., (2002), especially for historical or fossil material when the environmental context is largely unknown.

This dissertation provides new insights into the epicontinental shelf platform (<30 mbsl) offshore northern Mauritania (Golfe d'Arguin, see First publication, Second publication and Third publication) and the shallow-marine (<200 mbsl) shelf deposits offshore northern Argentina and Uruguay (Río de la Plata Shelf, see Fourth manuscript) and. Sea bottom substrata are characterized by a siliciclastic-dominated (Uruguay) and mixed carbonate-siliciclastic (Mauritania) sedimentation in which the carbonatic macro-benthos is of special interest for environmental interpretations.

Additionally influenced by an intense input of terrigenous material from the hinterland and a complex and nutrient-rich oceanographic setting (upwelling, riverine runoff and input of iron-rich desertic dust), both areas are far from being classical carbonate depositional environments (Campos et al., 2008; Michel et al., 2009). However, understanding carbonate sedimentation even under such complex and limiting environmental parameters is of highest importance for marine research and beyond as these marine environments might serve as natural laboratories that help to investigate a multitude of ecosystem services in the context of climate change and resource management (IMROP, 2013).

The ecosystems offshore Northwest Africa and Southeastern South America are linked into the large-scale oceanographic circulation pattern (see Fig. III.1), forming the North and South Atlantic gyre, respectively (see e.g., monitoring reports Wells and Daborn, 1997 and IMROP, 2013). These ocean gyres are particularly important for the central role they play in the thermohaline circulation and the worldwide climate.

Moreover, coastal near boundary currents are known to induce upwelling (e.g., Eastern Boundary Current *cf.* Canary Current) which pushed the primary production and makes coastal and offshore waters to economical important fishing grounds. Additional fertilization by iron-rich desertic materials from the Saharan hinterland make the waters offshore Mauritania to indispensable natural resource of highest socio-economic values (Goudswaard et al., 2007; IMROP, 2013).

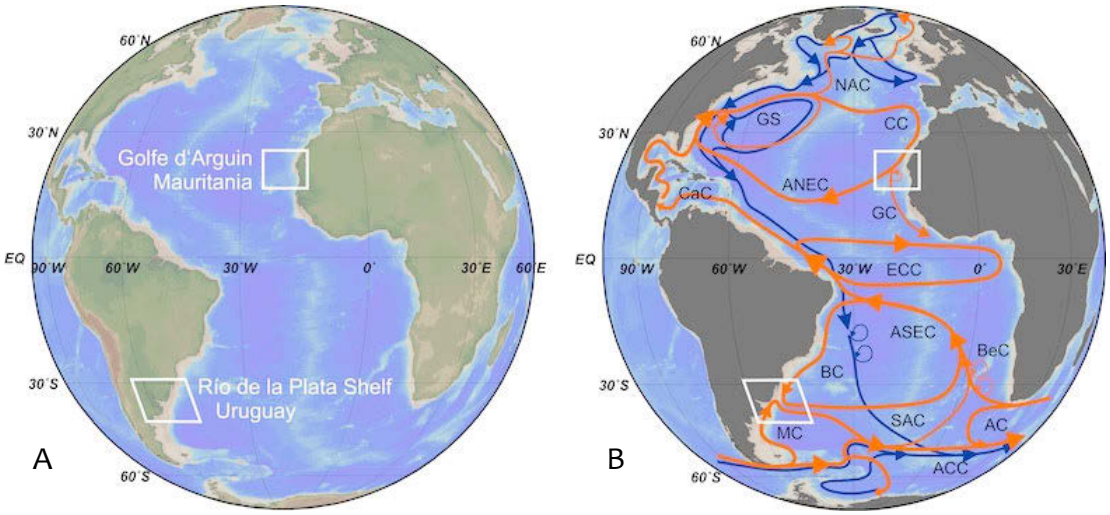

Figure III.1: Location of the research areas offshore Mauritania (Golfe d'Arguin hosting the shallow-marine Banc d'Arguin platform) and Uruguay (Rio de la Plata Shelf) illustrated in (A). Schematic Atlantic-wide ocean circulation pattern (B) are shown as near-surface currents (orange) and deep currents (blue). North Atlantic Current (NAC), Gulf Stream (GS), Canary Current (CC), Atlantic North Equatorial Current (ANEC), Caribbean Current (CaC), Guinean Current also known as Mauritanian Current (GC), Equatorial Counter Current (ECC), Atlantic South Equatorial Current (ASEC), Benguela Current (BeC), Brazil Current (BC), Malvinas Current (MC), South Atlantic Current (SAC), Aguilhas Current (AC), Antarctic Circumpolar Current (ACC).

III.1 The Northwest African Shelf

The sedimentary depositional system on the shelf and continental slope off northern Mauritania hosts one of the rare modern occurrences of eutrophic large-scale tropical ecosystems (known as tropical heterozoan carbonates). Here, the nutrient-enriched upwelling waters warm up in the shallows and are further fertilized by the influx of Saharan dust from the desertic hinterland. The resulting facies in the Golfe d'Arguin shows dominating bivalve fragments, barnacles and foraminifers, which refer to the heterozoan association (Piessens, 1979; Michel et al., 2011a; 2011b). By definition, the attributes of the Mauritanian shelf sedimentation do not simply fit into commonly used carbonate classifications and demonstrate the multi-dimensional ecological control of carbonate sedimentation (Westphal et al., 2007; 2010; 2014). Understanding the relationships between controlling natural steering parameters and the 'atypical'

sedimentation is important, because as it represents a analogue for ancient and future conditions. From a climatological and oceanographical perspective, the shelf of Mauritania is exceptionally sensitive and offers the unique opportunity to put a variety of environmental parameters into a chronologic and causal context.

III.1.1 Geological Setting

The Northwest African continental margin is of highest scientific interest to a wide range of geological and oceanographical studies, as it belongs together with the Northeast American continental margin to the oldest passive margins of our modern oceans (Seibold, 1982). The first rifting activity of the central Mid-Atlantic Ridge began during late Triassic to mid Jurassic times with average seafloor spreading rates of 2.5 cm per year (Davison, 2005). Since then thick sediment accumulations have developed on most parts of both mature passive continental margins, which cover the early evolution documented in deeply buried rocks (Seibold, 1982). Despite their common origin, the American and Northwest African continental margin developed fundamental differences during their history, such as the structure of the margin including orogenic and volcanic activities; the palaeo-climate of the margins and hinterland; and the palaeo-oceanography of adjacent regions of the North Atlantic Ocean (Seibold, 1982).

Characterized by prograding sedimentation on a subsiding basement, the Northwest African continental margin was formed during the Mesozoic and most parts of the Cenozoic (Nutter et al., 1971). Sediment accumulations covering the Paleozoic basement are estimated to be between 2 and 3 km in thickness along the northern Mauritanian coastline, extending to more than 10 km in distal directions (Wissmann, 1982). Pleistocene regression events ended to shape the shelf surface as a marine erosion plane, while recent depositional processes did not have a significant affect the shelf morphology (Nutter et al., 1971). Modern sedimentation along the Northwest African continental margin shows a mixed carbonate-siliciclastic character, with components provided by marine biological production, fluvial input of mud from the Atlas region and Senegal river, and aeolian inputs from the desertic hinterland (Summerhayes et al., 1976; Piessens, 1979; Holz et al., 2004; Michel et. al., 2009; Hanebuth et al., 2013). Extensive Northwest African shelf areas north of 20 °N provide average carbonate contents of >70 % with intermediate contents of 50 to >70 % between 20 °N and 19 °N (Golfe d'Arguin area) and decreasing contents of <30 % south of 19 °N, which can be related to environmental steering parameters (Fütterer, 1980).

III.1.2 Oceanographical Setting

The oceanography offshore Northwest Africa is closely coupled to the anticyclonic North Atlantic gyre, which is an essential element of the North Atlantic Meridional Overturning Circulation (MOC). Four distinct ocean currents form this large-scale ocean gyre: (1) the western boundary Gulf Stream (GS); (2) the North Atlantic Current (NAC); (3) the eastern boundary Canary Current (CC); and (4) the Atlantic North Equatorial Current (ANEC) (see e.g., Sverdrup et al. (2006) and Fig. III.1B). Driven by primary forces (e.g., solar heating causing thermal expansion of ocean water, salinity differences and trade winds) and secondary forces (e.g., Coriolis effect, gravitation, sea bottom and shelf morphology) the currents form a clockwise rotating circulation system in the northern Atlantic Ocean (Fig. III.1B). Intensified by global wind systems such as the trade winds and the prevailing Westerlies (anti-trades), this gyre keeps in permanent rotation. As a result, coastal-near boundary currents transport either warm temperated (western boundary currents; WBC) or cold temperated (eastern boundary currents, EBC) water masses along the continental margins, thus playing an important role in the heat transfer from the tropics to the polar realm and vice versa.

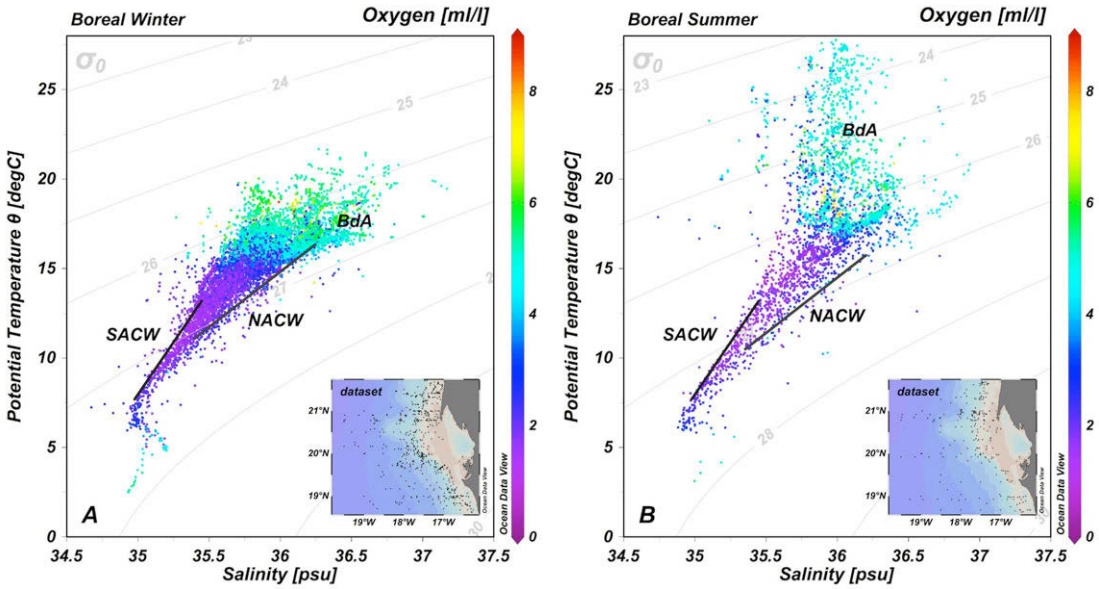

Figure III.2: Temperature versus salinity in relation to dissolved oxygen in the Golfe d'Arguin area (19 °W – 16 °W; 21.5 °N – 19 °N). Boreal winter season (Jan-Mar) is shown in (A), boreal summer season (Jul-Sep) is shown in (B). Data compiled from NASA, *Modis aqua* (http://disc.sci.gsfc.nasa.gov/giovanni).

Along the Northwest African Shelf, the Canary Current is an important supplier of cool and nutrient-rich surface waters. Intensified by trade winds during winter season, this

EBC pushes cold and less saline North Atlantic Central waters (NACW), but also marginal layers of South Atlantic Central Water (SACW) onto the Mauritanian Shelf (Fig. III.2A), where it warms up under tropical temperatures (Mittelstaedt, 1991; Sevrin-Reyssac, 1993; Matsuzaki et al., 2011). A frontal zone separates salty NACW (>36 PSU) and the less saline SACW (<35 PSU) in water depths >200 m and characterizes the NW African oceanography as one of the most complex upwelling systems in the world, see also (Abrantes, 1991). During summer season (Fig. III.2B), however, an intensified anti-current from southern direction (Guinean Current, GC and Equatorial Countercurrent, ECC) determine the water circulation in the coastal near settings (e.g., Golfe d'Arguin), resulting in a stagnation of upwelling activity south of 20° N (Mittelstaedt, 1991).

III.1.2.1 The eastern boundary Canary Current

Along the northern Mauritanian coast, the Canary Current provides cool surface waters from the North and induces upwelled waters to swell onto the shelf and into the photic zone (Barton et al., 1998). This eastern boundary is well known for centuries (Peters et al., 1996) and thus one of the best-studied ocean current system in the Atlantic Ocean. It flows year-round along the African coast from north to south between 30 °N and 10 °N and extends offshore to approximately 20 °W (Fedoseev, 1970; Wooster et al., 1976; Batten et al., 2000). The Canary Current is wide (approx. 1000 km), a typical feature of eastern boundary currents, on average 500 m deep and slow-flowing in the order of 10-30 cm*s^{-1} (= 8.6-25.9 km*d^{-1}). For comparison, its western counterpart the Gulf Stream proceeds at the order of several hundreds of kilometers per day. Surface-near waters provided by the Canary Current to the NW African Shelf are cool and enriched in nutrients, because it entrails upwelling waters from the coastal regions on its way south (Mittelstaedt, 1991).

When the current reaches the area between 20 °N and 15 °N, it begins to flow in a western direction, primarily controlled by the influence of the Equatorial Countercurrent that forms together with the Guinean Current (see Fig. III.3B) a northward directed component along the southern Mauritanian Shelf. Both Currents collide offshore northern Mauritania (Golfe d'Arguin) and are deflected in a western direction, where they form the Atlantic North Equatorial Current. Although both currents flow in the same direction, they show different velocities. As a consequence, two anti-cyclonic gyres form at the border between them.

In spring the Canary Current weakens along with a weakening of the trade winds, while the Equatorial Countercurrent strengthens. An anti-cyclonic gyre forms to the west of the current. The summer brings about further weakening of the trade winds, coinciding with a reduced water inflow from the north. The cyclonic gyres on the shelf weaken or disappear completely. The Equatorial Countercurrent, on the other hand, is at its peak and shifts in northern direction, separating the Canary Current from the coast.

During autumn the Canary Current is at its weakest, however, some of its characteristics are very similar to those during winter (Gyory et al., 2013). The current passes through the Canary archipelago, the influence of the Equatorial Countercurrent is the same as in winter, and the strong cyclonic gyres form once again. Stramma and Siedler (1988) reported the highly variable nature of the Canary Current, providing indications of even a northward-directed flow during Nov-Dec 1984, Apr-May 1985, and Sep-Oct 1985.

III.1.2.2 The Northwest African upwelling scenario

Governed by an eastern boundary current, trade winds and temperature cycles of sea surface waters, the Northwest African Shelf is characterized by an high primary production that is pushed by upwelling activities. Upwelling is generally strongest in the periods February to June and October to December (Kuipers et al., 1993). Furthermore, the upwelling cell offshore Northwest Africa is known to vary both, seasonally and inter-annually (Fütterer, 1983; Hagen, 2001). It moves from a northward position during summer (33 °N to 20 °N) in southern direction (25 °N and 10 °N) during winter, following roughly the meridional extension of the trade winds, that is defined by the position of the Inter Tropical Convergence Zone (ITCZ).

The upwelling duration ranges from one month at the latitudinal periphery (10 °N and 33 °N) to permanent upwelling activity (25 °N to 20 °N) in between (Van Camp et al., 1991; Hagen, 2001). As a consequence, large planktonic blooms characterize the oceanography offshore Mauritania (see e.g., Fig. III.4A), making this region to an important nesting ground of fish stock and thus to a bioreactor with one of the highest production rates in our modern oceans (Binet et al., 1998). Pushed by high nutrient settings and additional subtropical to tropical water temperatures, the primary productivity in the Golfe d'Arguin and offshore Cap Blanc (21 °N) provides maximum values of 325 g C $m^{-2}yr^{-1}$ (annual mean of 200 g C $m^{-2}yr^{-1}$). The Chlorophyll-*a* values largely exceed 20 mg per m^3 (Chl-*a*) with maximum intensities during boreal spring and summer (Marañón and Holligan, 1999), see also Fig. III.4 and Fig. III.5. The high primary production in the Golfe d'Arguin pushes the trophic state of ocean waters off Mauritania towards eutrophic conditions. Reduced trophic conditions such as meso- or oligotrophic waters are restricted to coastal near environments in the inner shelf areas of the Golfe d'Arguin (Schemainda et al., 1975; Quack et al., 2007).

III.1.3 The Golfe d'Arguin

The Golfe d'Arguin is formed by an epicontinental rimmed platform along the northern Mauritania Shelf. It stretches between the northernmost tip of the Baie du Lévrier (21.1 °N) and Cap Timiris (19.2 °N) over a latitudinal distance of about 200 km (Fig. III.4).

Influenced by the post-glacial transgression, this wide gulf extends today for over 150 km from coastline to shelf break (in 80-110 mbsl) with a gentle gradient of approx. 0.3 m*km^{1} (Hanebuth and Lantzsch, 2008). As a result, a shallow marine ecosystem of more than 15.000 km^{2} has developed in the past few millennia, characterized by shallows of 5-10 m water depth and a number of moving shoals not deeper than 5 mbsl.

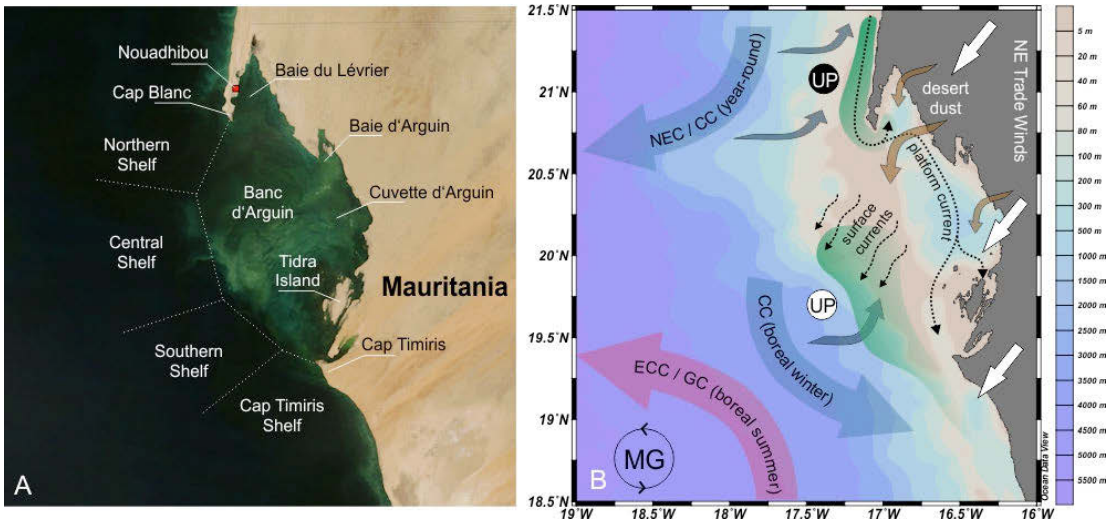

Figure III.3: Satellite image showing phytopigmentation of Mauritanian shelf waters and shelf zonation (A); Regional oceanography of the northwest Mauritanian Shelf (B). Areas of year-round upwelling activity marked as black circle, seasonal upwelling activity as white circles, eutrophic waters shaded in green. The cool Canary Current (CC) detaches from the shelf and forms the North Equatorial Current (NEC). The warm Mauritanian Current reaches the Golfe d'Arguin during boreal summer formed by deflected braches of the Equatorial Counter Current (ECC) and Guinea Current (GC). In a more seaward position the detaching currents form the Mauritanian Gyre (MG). This satellite image scene was captured by the Moderate Resolution Imaging Spectroradiometer (MODIS) on NASA's Terra satellite on December, 2006.

Towards the southern Golfe d'Arguin the shallow shelf shows extensive sub- to intertidal areas with seagrass plains in the vicinity of Tidra Island (Wolff et al., 1993a; Hanebuth and Lantzsch, 2008; Michel et al., 2009; Westphal et al., 2010), see Fig. III.3. Furthermore, these Intertidal plains serve as an important breeding site and settle ground for a large number of migrating birds, feeding on the rich mollusk and decapod fauna (Hoffmann, 1988; Campredon, 2000; Van der Geest, 2013). Since 1989 the inner Golfe d'Arguin (approx. 12.000 km^{2}) have been a marine protected area (National Parque Banc d'Arguin, NPBA) and belong to the Unesco World Heritage List (http://whc.unesco.org/en/list/506).

The hydrology of the Golfe d'Arguin and the shallow-marine Banc d'Arguin is closely coupled to the Canary Current that pushes cool, low-saline and nutrient enriched upwelling waters onto the shelf and into the gulf (Fig. III.2). Driven by maritime winds (trades winds) and continental winds (Harmattan) the waters circulate over the platform, where they warm up (> 25 °C) and increase in salinity (>39 PSU), see Fig. III.5.

On their way over the platform most of the eutrophic, phytopigmented waters decrease in their trophic level and grade towards mesotrophic and finally oligotrophic conditions when they reach the seagrass plains and intertidal areas in the vicinity around Tidra Island (Berghuis et al., 1993), see also (Fig. III.3A).

The residence time of platform waters is known to be variable and ranges between 18 and 34 days (Sevrin-Reyssac, 1993). Moreover, the whole Golfe d'Arguin is characterized by a high water energy (Piessens, 1976) that is strongest in the northern parts where the shelf faces swell coming from northwestern direction. Tidal (1-1.5 m amplitude *cf.* Hanebuth and Lantzsch, 2008) and wind-driven currents (Mittelstaedt, 1976; Peters, 1976) intensify the water energy regime with surface current velocities of 1 to >2 m per second (personal observation during sampling).

The Banc d'Arguin sea surface temperatures (SST) oscillate throughout the year between 17.5 and 29 °C (Fig. III.4A), see Ould Mahfoudh et al. (1991) for details and between 15.4 and 25.8 °C more offshore (Quack et al., 2007). Coldest SST are related to upwelling activities during boreal spring (February to June), whereas the warmest temperatures are observed in boreal summer (Kuipers et al., 1993), see also Fig. III.4 for 2012 SST and related Chl-*a* values (Fig. III.5).

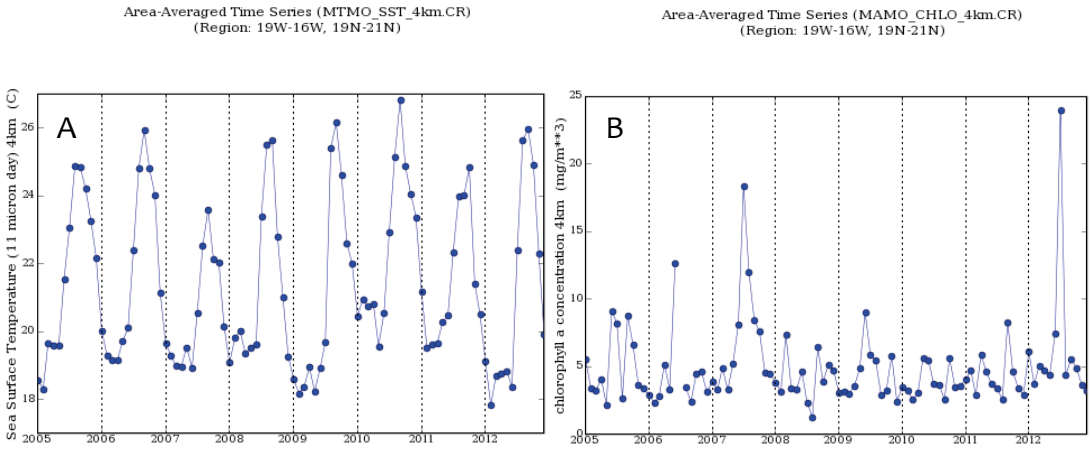

Figure III.4: Remote sensing sea surface temperature (A) in degrees Celsius and chlorophyll-a (B) in mg per cubic meter for the Golfe d'Arguin area. Quarterly concentration of Chl-*a* and related SST for 2012 are shown in Fig. III.5. Data compiled from NASA, Modis *aqua* (http:// http://disc.sci.gsfc.nasa.gov/giovanni).

Additionally fertilized by iron-rich desert dust (Fig. III.3B), the Golfe d'Arguin waters host a very unique mixed carbonate-siliciclastic sedimentation system, whose response to the environmental context is atypical in the modern world (Westphal et al., 2010; Michel et al., 2011a; 2011b). Sedimentary deposits of the Banc d'Arguin and Baie du Lévrier (<5 to

30 mbsl) are characterized by an extreme low-diverse tropical heterozoan fauna, dominated by the calcareous remains of filter-feeders.

Pushed by year-round tropical water temperatures of >15 to <30 °C (Fig. III.1A) and high Chl-a concentrations of up to > 20 mg per m^3 (Fig. III.4B and Fig. III.5), largely aphotic locally dysoxic conditions, the carbonate grain association refers to Foramol (*cf.* Lees and Buller, 1972) grading to Barnamol (*cf.* Hayton et al., 1995) in the shallows and Bimol (*cf.* Hayton et al., 1995) towards the upwelling fronts.

Locally smaller patches of Bryomol (*cf.* Nelson et al., 1988b) are known (Klicpera et al., 2013, see Second publication and Third publication). Such a sediment composition, however, is far from being typical for a tropical carbonate depositional environment and thus often related to slightly cooler water temperatures of higher latitudes (Westphal et al., 2010; Michel et al., 2011a; 2011b; Reymond et al., 2014).

Tropical, light dependent calcifying biota such as green algae, zooxanthellate corals or photo-symbiotic foraminifers are completely absent, thus providing no stability capabilities for the sea bottom substratum, nor coastal protection against waves and storms. However, the platform margin of the Banc d'Arguin shows a large-scale hardbottom community (mostly barnacles and mollusks) that forms a reef-like structure. Large sites providing hardbottom substrata, the ideal settle ground for fixo-sessil filter feeders, were mapped south of Cap Blanc (Domain, 1985). This platform rim separates the deeper high-energetic areas along the outer shelf from middle and inner shelf areas that provide typical lagoonal features. A semi-enclosed basin (Cuvette d'Arguin) characterizes the innermost platform of the Banc d'Arguin, which is refilled by sediments of largely terrestrial origin (Westphal et al., 2010; Michel et al., 2011a; 2011b; Aleman et al., 2013).

Coastal near environments and the southern Banc d'Arguin, in contrast, show large and shallow seagrass plains (Vermaat et al., 1993). Towards the outer shelf the water depth increases and typical platform features are continuously overprinted by muddy to silty accumulations of siliciclastic material. These deposits form large wedge-like bodies (*cf.* Arguin mud wedge; Timiris mud wedge *sensu* Hanebuth and Lantzsch, 2008) along the central and southern outer shelf (see also Hanebuth et al., 2013). Submarine canyon structures of assumed fluviatile origin cut into the outermost shelf and slope along the southwestern margin of the Golfe d'Arguin. These canyons channelize sediments as well as water from the shelf into the deep sea and are preserved as turbiditic succession (Hanebuth and Henrich, 2009).

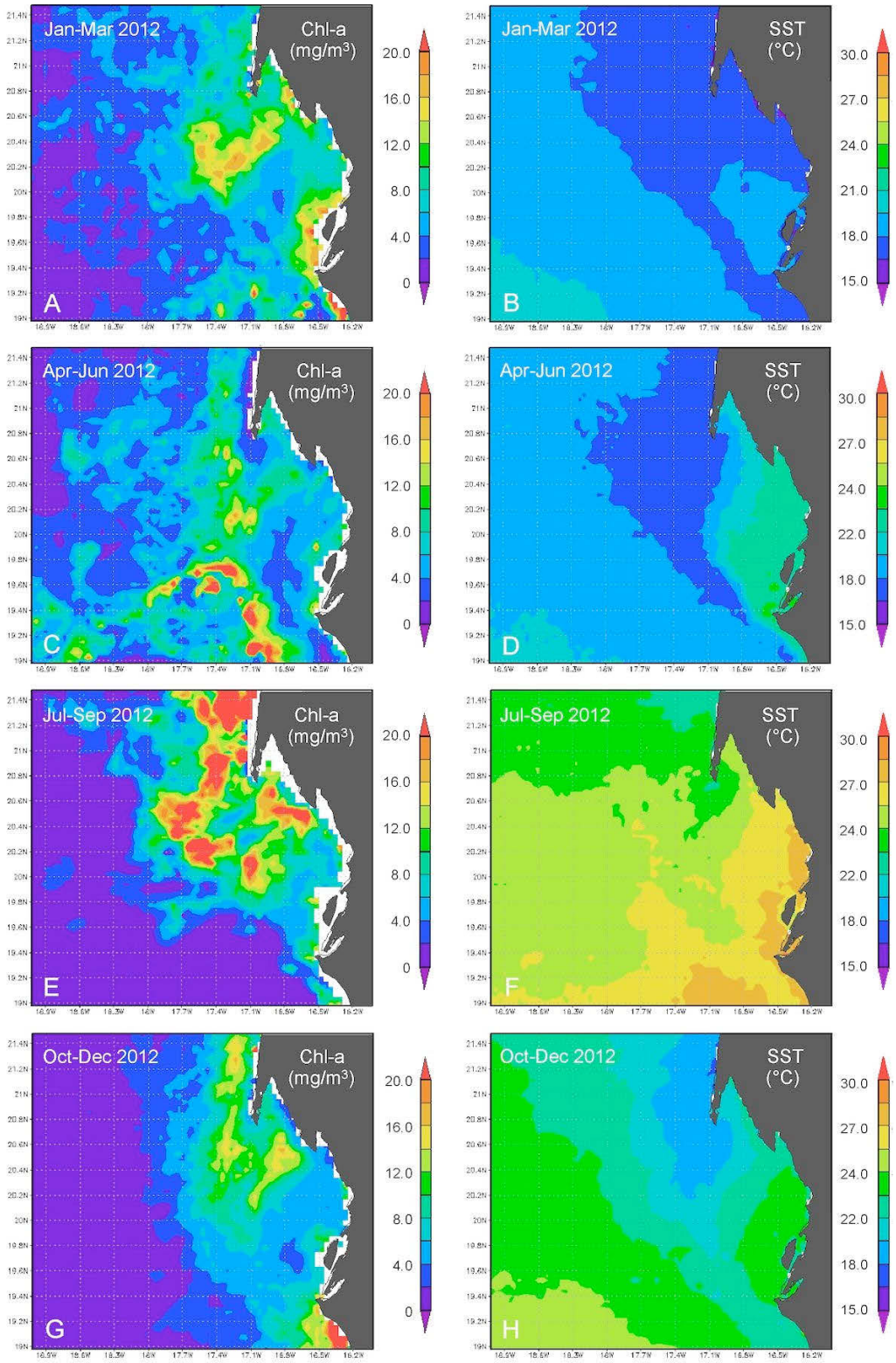

Figure III.5: Quarterly Chl-a concentrations (A, C, E, G) and related SST (B, D, F, H) for the year 2012 in the Golfe d'Arguin area and offshore northern Mauritania, compiled from NASA *Giovanni* (Modis *aqua*).

III.2 The Southeast South American shelf

The southeastern South American (SESA) Shelf and adjacent marine areas are today dominated by (1) the worldwide highest energetic ocean confluence zone (2) enormous sediment load and freshwater runoff from the second largest drainage basin of the South American continent and (3) a monsoonal climate. Each of these environmental parameters undergoes a highly dynamic variability (e.g., in precipitation, current intensity) over short (seasonal to centennial) and long (millennial to glacial-interglacial) time scales (Campos et al., 2008; Matano et al., 2010). Although this region plays a key role in the South American climatic system and in the Atlantic-wide ocean circulation, regional changes in precipitation, ocean-atmosphere couplings, the routes and budgets of material transported from land to ocean as well as the effects of human activity on shallow-water sedimentation and ecology are up to today poorly understood and clearly deserve more attention, see Fourth manuscript.

III.2.1 Geological setting

The earliest tectonic processes that were identified to be responsible for the separation of the South American platform from the African platform are ancient, probably dating back to the Triassic and represent the initial phase of the break-up of the Gondwana continent (Ribeiro, 2006). As a result, the first rifting activity began along the Brazilian continental margin from French Guyana to the Amazon delta and dates back between Late Triassic to Middle Jurassic times (230-170 million years ago). The following period from Middle Jurassic to Early Cretaceous (170-120 million years ago) was characterized by extended rifting activities, which took also place along the Argentinian, Uruguayan and Brazilian coasts (Ribeiro, 2006). Both, the South American and African continents became completely separated at the beginning of the Late Cretaceous between 98 and 93 million years ago (Cesero and Ponte, 1997).

The SESA continental margin was significantly influenced during the last glaciation (LGM, 21 thousands years ago). Sea level dropped some 120 meters below the present-day sea level resulting in an exposure of the shelfal plains (Wells and Daborn, 1997; Violante and Parker, 2004). The following post-LGM transgression was significantly involved of the formation and shaping of the modern SESA continental shelf that stretches roughly from Cape Frio, Brazil (23 °S) to the south of Burdwood's Bank, Argentina (55 °S) and represents today the largest shelf system in the southern hemisphere. The shelf shows a very distinctive bathymetry, hydrography, productivity and biological community structure and forms with a total area of 2.7 million km^2 (Bisbal, 1995) one of the most important ecosystems in our modern world. The SESA shelf encompasses the Patagonian Shelf Large Marine Ecosystem and the South Brazil Shelf Large Marine Ecosystem extending seawards from the coast of southeastern Brazil,

Uruguay and Argentina to the steep continental slope down to a depth of approximately 1000 mbsl. Relatively narrow at its northern end (approximately 70 km at Cape Frio, the shelf plain widens progressively to the south, where it reaches a maximum width of some 850 kilometers at southernmost Argentina (49 °S) (Bisbal, 1995).

The study area offshore northern Argentina and Uruguay (36 °S) is located at the confluence of two well-defined physiographic units: (1) the Uruguayan-Brazilian Shield, a mostly Precambrian basement and (2) the Argentine "Pampa" sedimentary basin. Consequently, the coastal environment has very contrasting characteristics. The northern Uruguayan coast is dominated by sandy beaches with bars, sand ridges, dunes and some minor cliffed areas which have developed over a variety of geological formations (Violante and Parker, 2004). Towards the south, the northern shore of Argentina, in contrast, is characterized by marshes, lagoons, great mudflats, shores and ancient beach ridges that form the north Buenos Aires coastal plain (Bisbal, 1995). Towards Cabo San Antonio, active dune fields and dune ridges alternate with marshes.

The Río de la Plata between northern Argentina and Uruguay separates these two morphological entities. It deals as the collector of the second largest drainage basin of the continent, covering 3.170.000 km^2 (Tossini, 1959; Depetris and Griffin, 1968; Depetris, 1973) and is formed by the junction of Uruguay and Paraná rivers. The catchment area includes parts of the territories of Argentina, Brazil, Bolivia, Paraguay and Uruguay that are transported from the source in the hinterland to the sinks located on the shelf and in the deep sea basin offshore southern Brazil (Krastel et al., 2012).

III.2.2 Oceanographical Setting

The oceanography of the southeastern South American continental shelf is dominated by two distinct shelf water masses. Subantarctic Shelf water and subtropical shelf water is provided by the Subantarctic Shelf Current (SASC) and Subtropical Shelf Current (STSC), respectively. These waters of different physicochemical properties form a sharp and distinct oceanographic front offshore Uruguay (Emilsson, 1961; Piola et al., 2000; Ortega and Martínez, 2007). It runs approximately southward from the near coastal region at 32°S to the shelf break and is quite stable seasonally and inter-annually (Piola et al., 2000; 2008; Palma et al., 2008). Two major western boundary currents flow along the southeastern South American continental margin: (1) the southward flowing warm and saline Brazil Current (BC; >20 °C, >36 PSU) proceeding with a maximum in velocity of 0.8 m/s (De Mello e Sousa et al., 2006); and (2) the northward flowing, cold and less saline Malvinas Current (MC; <15 °C, <34.2 PSU), see also Fig. III.6.

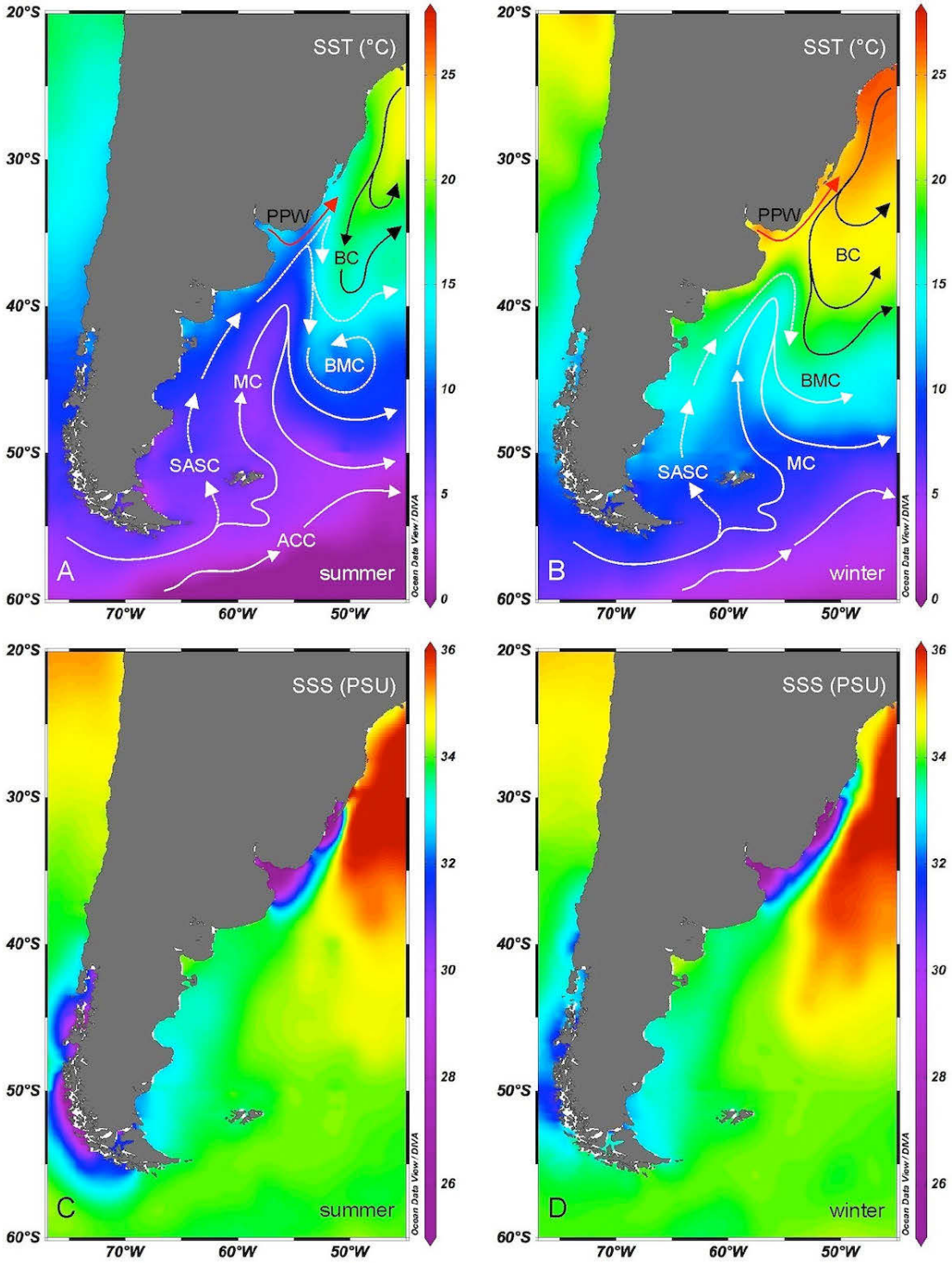

Figure III.6: Sea surface temperature (SST) for austral summer (A) and austral winter (B) and sea surface salinity (SSS) for austral summer (C) and austral winter (D) over the South Eastern South American shelf. Antarctic Circumpolar Current (ACC); Malvinas Current (MC); Subantarctic Shelf Current (SASC); Plata Plume water (PPW); Brazil Current (BC); and Brazil Malvinas Confluence Zone (BMC). Data provided by Ocean Data Atlas 2009, coverage ¼ degree, climatological mean.

The currents have their core below 1 km water depth but influence the surface waters significantly (Piola and Matano, 2001). Both currents collide near 38 °S (Fig. III.6) and produce a highly energetic confluence zone, which extends hundreds of kilometers offshore into the Argentine Basin (Fig. III.7B). It is assumed that the intensity of these individual currents and the depths of the boundaries between water masses have significantly changed since glacial times (Arz et al., 1999; Curry and Oppo, 2005; Negre et al., 2010) but precise data are largely absent.

III.2.3 The Río de la Plata and adjacent shelf areas

In addition to the offshore shelf currents (SASC and STSC) and the large-scale western boundary currents (MC and BC), the Río de la Plata plays an important role in the local oceanographic settings. It provides a huge amount of freshwater (670 km^2/yr) and suspended sediment load (130*10^6 km^2/yr) from the hinterland to the shelf and beyond. Collected and transported from the second largest (3.2*10^6 km^2) drainage basin in South America (Depetris and Pasquini, 2007) the suspended material that is provided to the shelf significantly controls regional and local sedimentation pattern and provide a valuable substratum for a number of benthic marine organism (Carranza et al.; 2008; 2010).

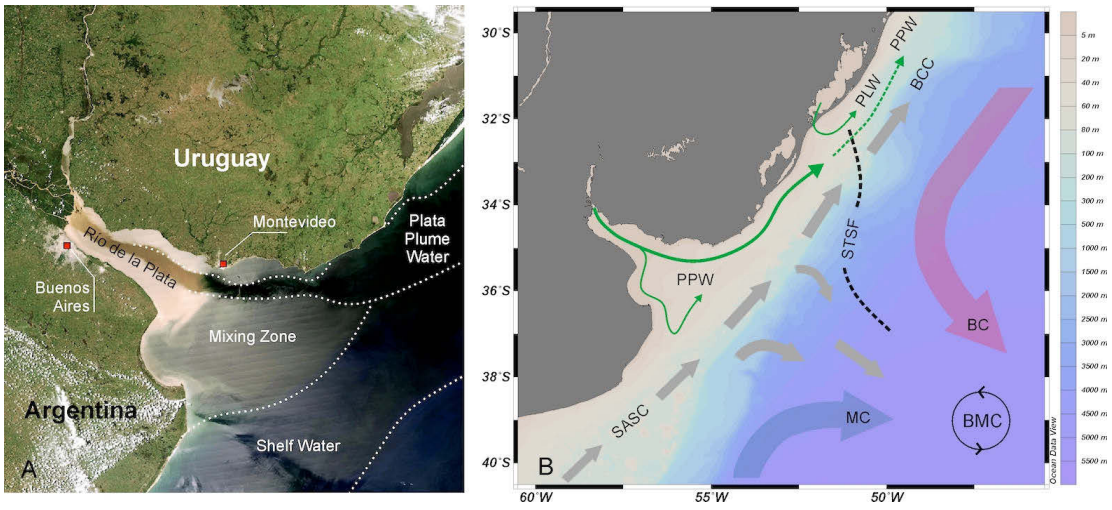

Figure III.7: Satellite Image showing Río de la Plata Plume Water (PPW) extending in northeastern direction (A); Regional oceanography of the Southeastern South American Shelf between Argentina and Uruguay (B). Subantarctic Shelf Current (SASC), Malvinas Current (MC); Subtropical Shelf Front (STSF); Brazil-Malvinas Confluence (BMC); Patos Lagoon Water (PLW); Brazil Countercurrent (BCC).

The Plata-derived reduced saline waters extend in northeastward direction along the coastline (PPW, Fig. III.7). Here it mixes with seasonally drained lagoonal waters (Patos Lagoon water; PLW). This buoyant freshwater plume can extend beyond Latitude 26°S in winter and retreats to 32°S in summer (Piola et al., 2000). Sharp changes in distribution are closely tied to a seasonally reversing wind direction (northeastward in winter, southwestward in summer; Piola et al., 2005).

The hydrological setting in the Uruguayan Shelf (<150 mbsl) is dominated by Subantarctic Shelf Waters (SASW), the Subtropical Shelf Waters (STSW) and low salinity Plata plume waters provided by the Río de la Plata (Fig. III.8). The SASW and STSW shelf currents flow in opposite direction and thus form a sharp and characteristic hydrographic boundary. This oceanographic front shows large horizontal temperature and salinity gradients (Fig. III.6) and is known as the Subtropical Shelf Front (STSF; Piola et al., 2000). The shelf surface waters undergo a large seasonal temperature change, shown in Fig. III.6. South of 33 °S, the amplitude of the Sea Surface Temperature (SST) exceeds 9 °C and reduces to <3 °C north of 23 °S (Piola et al., 2000). Seasonal SST provided by World Ocean Atlas 2009 (WOA09) (Antonov et al., 2010; Locarnini et al., 2010) show this high temperature variability offshore Uruguay which peaks in the range of 20 to 24 °C at the end of January and are at their lowest at the beginning of August within the range of 7 to 13 °C (Fig. III.8A, B).

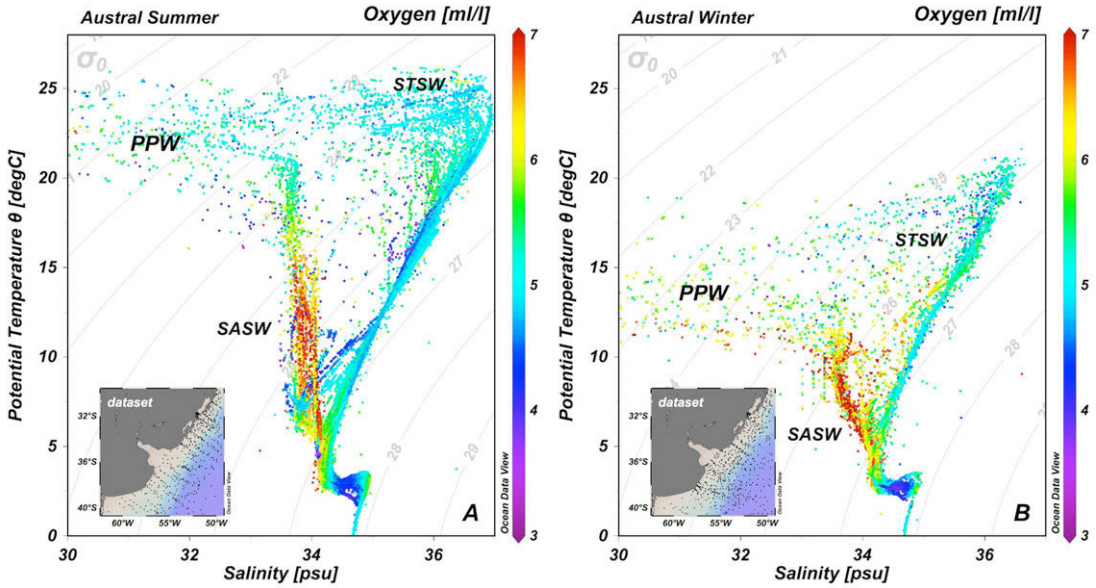

Figure III.8: T-S diagrams in relation to dissolved oxygen along the southeastern South American shelf (60 °W – 45 °W; 30 °S – 40 °S). Austral summer season (Jan-Mar) is shown in (A), austral winter season (Jul-Sep) is shown in (B). Low salinity Plata plume water (PPW), Subtropical shelf water (STSW) and Subantarctic shelf Water (SASW). Data compiled from NASA; http://disc.sci.gsfc.nasa.gov/giovanni

Sea Surface Salinity (SSS) pattern south of 37 °S show little variations (~33.6 to 33.7 PSU). Between 37 °S and 35 °S low salinity waters (<25 to 30.0 PSU) originating from the Rió de la Plata estuary reach the open shelf and form a buoyant plume (Plata Plume Water, PPW) that extends from the river mouth along the Uruguayan coastline in northern direction to southern Brazil (Emilsson, 1961; Piola et al., 2000). A second important freshwater runoff is provided by the Patos Lagoon near 32 °S (Fig. III.6 and Fig. III.8) (Burrage et al., 2008; Campos et al., 2008).

The autochthonous fauna off the Uruguayan coasts shows temperate-cold and temperate-warm components, which are characteristic for a marine environment influenced by seasonal varying water masses. The Argentine Biogeographic Province spans from 36° to 43° S along the coasts, but it extends onto the inner shelf areas off Uruguay. The Magellanic Biogeographic Province occurs along the coasts from 43°to 56 °S, but it expands also northwards into the deep waters on the outer Uruguayan shelf (Carranza et al., 2008; 2010). On the continental shelf, the transition between both faunal assemblages follows a southwest–northeast direction in 70 to 100 m water depth off Uruguay and, in addition, the Plata River region seems to act as a biogeographic barrier for many warm-temperate and subtropical species. Nevertheless, the available information about marine biodiversity and environmental perturbation as well as about its history is still restricted to few areas.

IV. Materials sampled and investigated

Sedimentological and biological samples used in the present thesis were collected during three research cruises offshore Mauritania (Poseidon cruises POS346, Westphal et al., 2007; POS366, Zonneveld et al., 2010; and Maria S. Merian Cruise MSM16-3, Westphal et al., 2014) and Uruguay (Meteor Cruise M78-3a, Krastel et al., 2012). All cruises followed a common research objective, which focused on the investigation of sediment dynamics and sediment transport from „source to sink". Within this objective, an extensive set of sedimentological cores (e.g., gravity cores, vibro-cores and box cores), as well as surface samples (e.g., Van-Veen grabs) and physico-chemical measurements of the water column (e.g., miniCTD, CTD-rosette) were taken in order to collect and compile a robust dataset for environmental investigations for interpretations.

IV.1 R/V Poseidon Cruises 346 and 366 (Mauritania)

Material collected during Poseidon cruises 346 (2006/2007) and 366 (2008) was additionally investigated and existing sedimentological data provided in Michel et al. (2009; 2011a; 2011b) were used and implemented in the present study in order to get a full sedimentation picture of the Golfe d'Arguin off Mauritania (see First publication). Material and Methods of this material follows roughly the instructions as documented within the Doctoral thesis of J. Michel, 2009 – University of Bremen and in the cruise reports (Westphal et al., 2007; Zonneveld et al., 2010).

IV.2 R/V Maria S. Merian Cruse MSM16-3 (Mauritania)

In addition to the previous research cruise to the Golfe d'Arguin, the shallow marginal areas of the Banc d'Arguin were one of the research foci of the latest cruise to Mauritania, which was conducted in late 2010 (see Westphal et al., 2014). Of special interest for the presented study was the extreme shallow-marine carbonate production, which developed in a eutrophic heterozoan carbonate system. The seafloor substratum is characterized by a mixed carbonate-siliciclastic composition in which cool-water related faunal elements dominate as a consequence of nutrient-rich and cool upwelling waters. These deposits are thus a central part of this thesis and were sampled for the first time since the pioneering studies by Piessens (1979) and Koopman et al. (1979). However, research in this marine environment is extremely limited due to water depth of largely less than 5-10 meters below sea level.

During MSM16-3 we used an auxiliary zodiac vessel in order to access even shallowest areas during low tide. Equipped with an sediment echo-sounder, a winch for Van-Veen grab sampling, a miniCTD for physico-chemical properties of the water column and a Secchi-disk, we were able to collect a comprehensive dataset including 125 surface grab samples distributed over 4 sampling areas described in the following:

The Baie du Lévrier (Fig. IV.1; A) provides two zodiac stations (GeoB14783, GeoB14786). Most of the sample materials studied were collected from 45 sampling sites arranged in two N-E orientated transects in the vicinity of Cansado Harbor (Nouadhibou, Mauritania). Coastal near areas are heavily influenced by ship traffic and thus characterized by muddy, sometimes anoxic sediments, while the sampling sites in the central Baie du Lévrier were more ventilated showing typical barnacle-rich deposits with variable amounts of siliciclastic material. Water depths of sediment samples range between 6 and 16 mbsl. The central part of the Banc d'Arguin (Fig. IV.1; B) provides one zodiac station (GeoB14833), of which 22 sampling sites were studied. This station is furthest from the coastline and provides a sea bottom substratum that is rich in shells. The deepest samples show muddy silts and fine sands throughout. As a consequence of its proximity to the Arguin mud wedge depocenter most samples show a low-diverse mollusk association (mostly *Donax burnupi* and *Venus crassatina* bivalves) with variable amounts of barnacle fragments and siliciclastics. One curiosity of this sampling station is the presence of in-situ egg-sized Bryoliths (Suppl. XVIII.1), symbiotic associations between hermit crabs and bryozoans that cover the sea floor (see Second publication). Water depths of sediment samples taken range between 30 and 20 mbsl.

The southern Banc d'Arguin (Fig. IV.1; C) is characterized by its proximity to the inter-tidal areas of Tidra Islands and its location close to the Timiris mud wedge depocenter. This area provides two sampling stations (GeoB14748 and GeoB14812), which are situated relatively close to each other. The sea bottom substratum of 43 sediment sampling sites grades from muddy silt to coarse sandy material with a high amount of barnacle remains, benthic foraminifers, sea urchins (*Heliophora sp.*) and mollusks. The siliciclastic content is always high due to desertic hinterland close by. Water depths of sediment samples range between 5 and 38 mbsl.

The vicinity of the Cap Timiris Shelf (Fig. IV.1; D) shows a faunal composition that reminds of samples from the northern Banc d'Arguin. One sampling station (GeoB14725) provides 15 sampling sites, characterized by high amounts of barnacle fragments and *Donax burnupi* shells. Additionally the samples are enriched in bryozoans of which cupuladriid colonies are abundant in most samples. Towards deeper water settings, the variety in bryozoans increases with, erect, fenestrate and encrusting growth forms that are shown in detail in Suppl. XVIII.2. The siliciclastic content is still high. Water depths of sediment samples range between 7 and 26 mbsl.

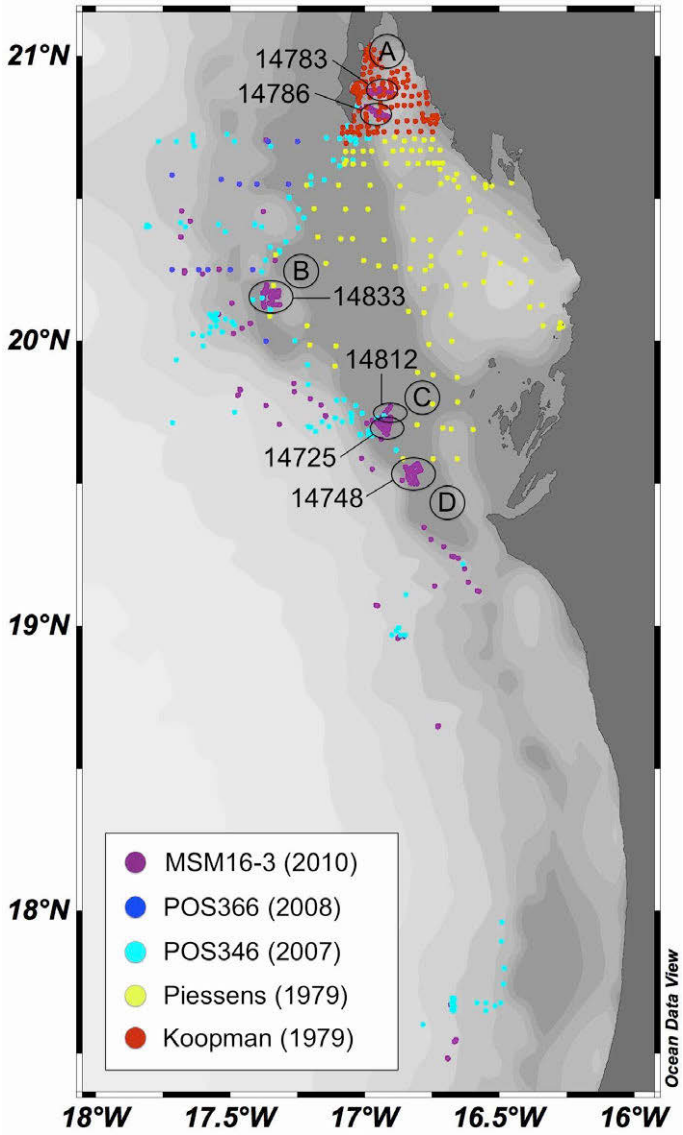

Figure IV.1: Sampling sites and location of historical data along the Mauritanian Shelf (n = 764). Poseidon research cruises (POS366, POS 346) focused on the outer shelf and slope settings, while the latest Merian cruise (MSM16-3) also investigated the platform margin of the middle shelf. Additional historical datasets (Piessens, 1979; Banc du Arguin and Koopman et al., 1979; Baie du Lévrier) conducted during a 1979 undertaken research campaign were implemented in this study. Shallow-marine zodiac sampling sites analyzed within this study are marked; Baie du Lévrier (A); Central Banc d'Arguin (B); Southern Banc d'Arguin (C) and Cap Timiris Shelf (D). Increasing brightness in gray scale (offshore areas) refer to an increasing water depth.

IV.3 R/V Meteor Cruise M78-3a (Uruguay)

Four sedimentary cores were sampled offshore Uruguay within the scope of this study for carbonate secreting organisms suited best as archive of palaeo-oceanographic proxies (Suppl. XIX.1). The cores are situated along the Uruguayan shelf from distal to proximal and from north to south. Additionally, the seafloor morphology and sequence stratigraphy were mapped by means of hydro-acoustic and seismic techniques.

Gravity core 13813-4 was taken in the inner shelf setting (57 mbsl) and provided a recovery of 1028 cm. The surface of core 13813-4 is characterized by autochthonous faunal elements (mostly bivalves and other mollusks) of which one representative

bivalve specimen (*Pitar rostratus*) was collected for geochemical analyses (stable isotopes and radiocarbon dating).

Box core 13839-2 (18 cm recovery) and **vibro core 13836-2** (507 cm recovery) were taken along the outer shelf environment in 67 mbsl and 134 mbsl respectively. Core surfaces (upper 10 cm) showed accumulations of dead, but still articulated bivalve shells (mostly mass accumulations of *Zygochlamys patagonica* and some large shelled *Venus antiqua*), of which one specimen from each core was collected for radiocarbon dating.

Vibro core 13802-2 (341 cm recovery) was taken at the shelf break in 141 mbsl of which a large, thick-walled articulated bivalve shell (*Retrotapes exalbidus*) was collected from the base (335-341 cm) for geochemical analyses and radiocarbon dating.

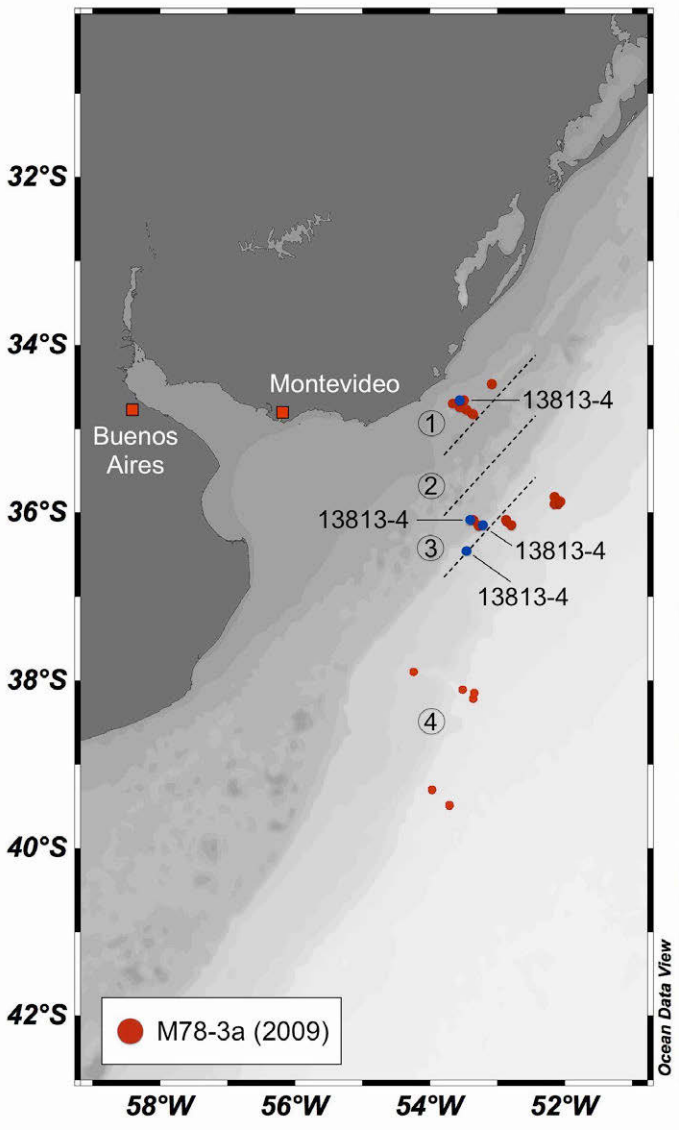

Figure IV.2: Core sampling sites along the SESA Shelf offshore Uruguay and Northern Argentina (n = 47). During Merian cruise M78-3 leg a the inner and outer shelf, as well as the slope were investigated and sampled for core and surface material in order to reconstruct the sedimentation history and the transport of terrestrial sediments from 'source to sink'. (1) Inner shelf settings; (2) middle shelf settings; (3) outer shelf settings and shelf break; (4) slope settings and incised valley structures. Stars indicate core material investigated and sampled for biogenic archives. Increasing brightness in gray scale (offshore areas) refer to an increasing water depth.

V. Methods used in this study

V.1 Sedimentological analysis

Sediments recovered during research cruise (MSM16-3, see Westphal et al., 2014), were pretreated directly on board the research vessel. Sediment samples were macroscopically classified into two textural groups that define their pre-treatment: (1) Coarse-grained and unconsolidated materials were washed under deionized water and dried at +60 °C in an oven for at least 48 h; (2) Fine-grained materials that show mostly muddy silts and fine sands. These were immediately wet-stored as bulk samples in a cooling facility at +4 °C to avoid aggregate formation and to reduce biodegradation of organic material. Sedimentary material sampled during research cruises POS346 and M78-3a, also part of this research project, were pretreated as specified in corresponding cruise reports, see e.g., Westphal et al. (2007) and Krastel et al. (2012).

V.1.1 Grain-size analysis of material >500 µm (Sieving method)

Sediments were washed and dried before they were spitted down to samples of 150-200 g each. Sample material characterized by aggregated particles, most likely a result of enrichments in clay content or salt recrystallization, were treated with "Calgon" (Sodium hexametaphosphate, $Na_6P_6O_{18}$) for disaggregation as suggested by Tucker (1996). Depending on the intensity of aggregated grains, all samples were additionally treated in an ultrasonic bath for approx. 2 min. Sediments showing sensitive material (e.g., small mollusk shells, planktonic foraminifers, bryozoans) were omitted from ultrasonic treatments, in order to avoid destruction of shell material.

Sediment samples were divided in two main fractions (coarse material, >0.5 mm and fine material <500 µm) depending on grain diameter, to improve accuracy of the following grain-size measurements and to reduce the duration of the analytic procedure. The coarse fraction >500 µm was again wet sieved using a Retsch sieve shaker (AS-200) for at least 15 min. per sample and fractionated in the grain size classes 500 µm, 1000 µm and 2000 µm. All sieved coarse fractions were then dried and weighted to document individual fraction weights. Grain size classifications and size classes of sediment samples follow the scheme of Wentworth (1922).

V.1.2 Grain Size analysis (Laser particle analysis)

The fine fraction <500 µm was analyzed by means of a laser particle sizer (Horiba LA-950). This analytic device determines the absolute abundances of solid particles in an individual sample and recalculates the percentages of particle size classes by internal algorithms. Although this device is certified for particles up to 3000 µm in diameter, we experimentally determined an unexpected high standard deviation, especially for particles >1000 µm in diameter. To avoid this systematic error, which is caused due to different particle shapes of the calcareous material (platy, elongated, spherical), the fine fraction (<500 µm) was used for laser particle analyses only. To improve the precision of measurements an average of three replicates (of approx. 1-5 g) was used of which each single replicate was measured three times. Each sub-sample was treated with "Calgon" (Sodium hexametaphosphate, $Na_6P_6O_{18}$) where necessary and additionally placed in an ultrasonic bath for 2 min in order to remove aggregates. The fine-grained samples were analyzed at particle size classes of <63 µm, 63-125 µm, 125-250 µm and 250-500 µm following the classification scheme of Wentworth (1922).

V.1.3 Core description

During research cruises to Uruguay (M78-3a) and Mauritania (POS346 and MSM16-3) a number of different coring devices were used. Each coring device is specialized for different types of seafloor substratum and, of course, the temporal resolution of the sedimentary record, given by the research question. In total, a multitude of gravity cores, vibro cores and giant box cores were recovered during each cruise, additionally complemented by a range of grabs (e.g., Van Veen grab) that were used to recover surface material. Material recovery by giant box corers was directly documented and processed aboard the research vessel and washed immediately down to the fractions 1.0 mm, 2.0 mm and 5.0 mm (see also cruise reports, Westphal et al., 2007; Krastel et al., 2012 and Westphal et al., 2014). Vibrio cores and gravity cores were cut in core segments of 1 m each and directly stored in an cooling facility at 4 °C. These segments were later opened in the core laboratory at University of Bremen and MARUM and visually described for sediment color, lithostratigraphic units and sorting structures of material. Afterwards sub-samples were taken from the core for preliminary radiocarbon dating and thin section analyses. Moreover, the sedimentary material taken from the cores were analyzed for high-resolution climate archives (see Fourth manuscript), grain size distributions, component composition and facies architecture (see e.g., Hanebuth et al., 2013). Lithostratigraphic logs of cores were digitized based on photographic material and core log data using Corel Draw (ver. 15) and Psicat (ver. 1.0.4).

V.2 Geochemical analysis

V.2.1 Micromill and dental-drill sampling of accretionary carbonate

For high-resolution microsampling a Merchantek (New Wave) MicroMill system equipped at the Geozentrum-Nordbayern (University Erangen-Nürnberg) was used. This micro-drilling device is designed for high-resolution sampling in order to recover sample powder for chemical and isotopic analysis, see e.g., Dettman and Lohmann (1994). This technique is excellent for microsampling of serially grown successions of accretionary biogenic carbonate, such as growth bands of bivalve shells that are preserved in the chondrophore or outer layer of the shell. To avoid contamination of calcareous material only fresh and not altered parts were used for sampling. Horizontal drilling speed was adjusted to 100 µm/sec, with a maximum drilling depth of ~280 µm milled in eight, consecutive passes of 35 µm depth. The sampling track distance was 100 µm. Additionally, a dental drill with optional micro saw-blade was used to cut samples from the shell (e.g., radiocarbon samples, SEM samples or powder material for XRD analysis).

V.2.2 Radiocarbon dating of biogenic carbonate

Biological samples (e.g., shell material) were sampled for AMS ^{14}C dating. To avoid contamination or mismeasurements of eroded material, we collected fresh, articulated and, where possible, in-situ calcareous material from cores. Larger biogenic components (e.g., macro bivalve shells) were sampled in both, a juvenile shell position in the umbo (dorsal) and in an adult position near the ventral margin (ventral). Powder (~30-50 mg) was drilled from marginal transects of ~10 mm length, set parallel to the growth rings comprising less than 2 (annual) growth increments. Poznan Radiocarbon Laboratory in Poland carried out all further pre-cleaning procedures. ^{14}C ages are reported in uncalibrated ages (^{14}C yrs BP), 1σ calibrated range (cal. yrs BP) and intercept calibrated kilo-years before present (cal. kyrs BP). The AMS ^{14}C dating of life-collected bivalves (e.g., *P. rostratus* specimen) is reported in percent Modern Carbon (pMC). Shells were calibrated applying the MARINE09 dataset (Reimer et al., 2009) using CALIB v. 6.0 (http://calib.qub.ac.uk/calib/), marine reservoir effect corrections were not applied.

V.2.3 Carbonate mineralogy (XRD)

X-ray diffraction pattern analyses of carbonate powder (<20 µm particle size) were analyzed by the Central Laboratory for Crystallography and Applied Material Sciences, ZEKAM, University of Bremen). The X-ray diffraction were measured on a Philips X'Pert Pro multipurpose diffractometer equipped with a Cu-tube (k" 1.541, 45 kV, 40 mA), a

fixed divergence slit of ¼°, a 16 samples changer, a secondary Ni-Filter and the X'Celerator detector system. Continuous scans from 3 – 85° 2θ were analyzed with a calculated step size of 0.016° 2θ. Mineral identification was achieved by means of the Philips software X'Pert HighScore™. The determination of crystal sheet distances in Angstroem (10 nanometer) as well as the identification of calcite and aragonite was realized by using the X-ray diffraction interpretation software MacDiff 4.25 (Petschick et al., 1996), see also data provided as supplementary protocols (Suppl. XIX.3-12).

V.2.4 Measurements of stable isotopes from biogenic carbonate

Micro-drilled powder samples (5 mg) were analyzed using a Kiel III carbonate preparation line connected online to a ThermoFinnigan MAT 252 mass-spectrometer (Rosenbaum and Sheppard, 1986; Kim et al., 2007). All isotope values are reported in the conventional δ-notation in per mill relative to V-PDB (Vienna Pee Dee Belemnite) by assigning a $\delta^{13}C$ value of +1.95 ‰ and a $\delta^{18}O$ value of -2.20 ‰ to NBS19. Reproducibility was checked by replicate analyses of laboratory standards and is greater than ± 0.5 ‰ 1σ (1 std. dev.), see also data provided as supplementary protocols (Suppl. XIX.7 and Suppl. XIX.8).

V.2.5 Carbonate content

The carbonate content of four replicates per sample was measured as a percentage of the bulk sediment. Each replicate was prepared by using either a sample splitter (for dry and unconsolidated material), or directly taken from a randomly chosen sampling point within the wet bulk sample. For the measurement, the carbometer analysis based on Müller and Gastner (1971) was applied, an easy and effective way to determine the carbonate content of a sediment sample from CO_2 pressure. For this, all replicates were dissolved in technical hydrochloric acid (30 % HCl). In order to avoid effects of the intra-daily changing barometric pressure, the carbometer device was calibrated twice a day (pre- and post-calibration), for long measuring campaigns we applied a third calibration in between. The internal error of the carbometer is usually below 1.0 %, however, for samples with an unexpected low carbonate content (siliciclastic-rich samples) of less than 50 % the double sample weight was dissolved to improve accuracy (see also recommendations in Müller and Gastner, 1971).

V.3 Compositional analysis

V.3.1 Scanning electron microscopy

Description and determination of the components present in the sediment samples is based mainly on optical investigations under the macroscope, but scanning electron microscope (SEM) results of microscopic biogenic particles are also included. SEM images were taken with a Tescan Vega 3 SEM (SE detector at 20kV) at the Leibniz ZMT-Bremen, Germany. Additional backscatter electron images (BSE) were prepared at 15kV, sometimes in low-vacuum mode to avoid sensible specimens and important material from being gold-sputtered (see e.g., Second publication). SEM images of bivalve shell microstructures were taken using a Zeiss Supra40 SEM at 5.0 kV at the University of Bremen, Germany (see Fourth manuscript). Both SEM units were equipped with Oxford EDX detector providing valuable information about the composition of the investigated samples (see also Suppl. XIX.2). Additional high-resolution tomographic scans of small biogenic structures were realized using a Skyscan µCT unit attached to the Tescan Vega 3 SEM. This tomographic device provides a nominal resolution of 350 nm to 8 µm per pixel and is able to reconstruct a 3D model of microsamples not larger than 4mm in diameter. During the tomography the specimens were scanned at angular increments of 0.45° rotation steps over a period of 11 hours to provide a high-resolution virtual 3D model of the sample.

V.3.2 Optical microscopy

For the investigation of thin sections and loose biogenic sediment particles (see component analysis in First publication and Suppl. XIX.2) a manual Leica stereo macroscope (Leica S6D) and a Leica polarizing microscope (Leica DM EP) was used, each equipped with a Leica digital camera (DMC2900) providing a 3-megapixel CMOS sensor.

V.4 Classification and determination of sediments and biogens

Sedimentary material was classified into grain-size fractions according to Wentworth (1922). Quantification and determination of dominating bioclasts and biogens was performed on the fraction 500 µm, 500 – 1000 µm and >1000 µm using a minimum of 300 identifiable grains where possible. Component analysis of grains < 500 µm in diameter are not part of this study. Carbonate grain assemblages refer to the bimodal classification of Lees and Buller (1972) and James (1997), that accentuates the light dependence of carbonate-producing benthic organisms (see also Suppl. XVII.2).

Taxonomy of mollusks follows the systematic database of Malacolog 4.1.1 (http://www.malacolog.org), based on Rosenberg (2009) as well as Ardovini and Cossignani (2004) and Huber (2010). Determination of single bivalve specimens used for isotopic analyses (see Fourth manuscript) were performed at the Museo Nacional de Historia Natural (MNHN), Montevideo, Uruguay, see also Suppl. XIX.1.

All samples were compared with reference material, holotype specimens and identified down to species level. Internal features and shell layer configurations of bivalve mollusks follows the revised terminology as suggested by Schöne et al. (2011). Sedimentary material and single bryozoan species (e.g., bryoliths; Second publication) were compared with reference material and holotype specimen at the Natural History Museum (NHM) London, UK. All specimens were identified down to genus level, where possible down to species level. Bryozoan terminology and zoarial growth forms follows the classification by Nelson (1988b).

V.5 Software processing

V.5.1 CTD DATA Processing

CTD raw data were processed using Seasoft CTD data acquisition software for Windows XP. Data were directly converted with Ocean-Sneaker's Tool (www.awi.de) in order to make them readable for visual processing software such as Ocean Data View (http://odv.awi.de).

V.5.1 Satellite remote sensing and historical oceanographic data

Time series of oceanographic parameters (e.g., SST, SSS, Chl-*a*) in monthly, seasonal, annual and decadal resolution were acquired by using the online platform "NASA Giovanni" (http://disc.sci.gsfc.nasa.gov/giovanni) hosted by the Goddard Earth Sciences Data and Information Services Center (GES DISC). The National Oceanographic Data Center (NOAA) provided additional oceanographical data that were extracted from the online database "World Ocean Atlas 2009" (WOA09).

V.5.2 Ocean Data View (ODV)

Time series of oceanographic data acquired from NASA Giovanni database and the NOAA World Ocean Atlas (WOA09), as well as *in-situ* measurements (e.g., CTD, Secchi-disk, biofacies) taken during research cruises (POS346 and MSM16-3) were processed and

visualized in the software package Ocean Data View version. 4.5.7. (www.odv.awi.de), provided by the AWI (Schlitzer, 2012). In order to enhance the color contrast of gridded surface maps and profiles the revised color scheme "JetPlus" according to Haddock (2010) was applied. This ODV plugin provides an optimized color scheme that is advantageous when figures are converted from RGB to CMYK for printing.

V.6 Statistical analysis

V.6.1 Gradistat Grain size data analysis for Excel

Grain size raw data from laser particle measurements were converted in an plain-text format and analyzed in *GRADISTAT* according to Blott and Pye (2001). This Excel-based program is suitable for calculating particle size measurements for sieve and laser granulometer data and provides a quick analysis of single and multiple data entries. The latest version of *GRADISTAT* is available under www.kpal.co.uk/gradistat.html. Statistic formulas used in this study to calculate grain-size related parameters follow the instructions documented in Blott and Pye (2001).

V.6.2 Cluster analysis in JMP

Statistical analyses of the quantified grains were performed using JMP for Mac (version 9.0.1). A hierarchical cluster analysis (Ward's minimum variance method) was used to group the samples with similar compositions (Ward, 1963). This method calculates the distance between two clusters, which is the ANOVA sum of squares between the two clusters added up over all the variables. At each generation, the within-cluster sum of squares is minimized over all partitions obtainable by merging two clusters from the previous generation. The sums of squares are easier to interpret when they are divided by the total sum of squares to give the proportions of variance (squared semi-partial correlations). Ward's method joins clusters to maximize the likelihood at each level of the hierarchy under the assumptions of multivariate normal mixtures, spherical covariance matrices, and equal sampling probabilities. The sedimentary biofacies groups were determined on the basis of dominating biogenic and abiogenic components excluding unidentified grains, see component analysis in First publication.

VI. Outline of research

The outcomes of this dissertation are presented in four peer-reviewed studies that are introduced in the following chapters. Towards the end of this dissertation a summary and conclusion chapter will highlight the key findings before the chapter on future perspectives will introduce the reader into further implications of the research project.

1) Facies patterns of a tropical heterozoan carbonate platform under eutrophic conditions: the Banc d'Arguin, Mauritania

The First publication provides the sedimentological background of the carbonate depositional system that forms the Banc d'Arguin offshore Mauritania. For the first time we combine new, existing and historical data, in order to reconstruct the full sedimentation picture in the entire Golfe d'Arguin.

The northern Mauritanian Shelf is an excellent example of a trophic-controlled tropical shelf. The marine environment is characterized by eastern boundary currents that induce nutrient-rich upwelling waters to swell onto a wide epicontinental platform (Banc d'Arguin) where they warm up to >25 °C. The resulting facies is mixed carbonate-siliciclastic, in which cool water related foramol associations dominate besides a suppressed tropical molluskan fauna, while chlorozoan associations are completely absent. Reduced water depths of less than 10 m and a maximum platform extension of more than 100 km has limited the understanding of the sediment deposition in the Banc d'Arguin and beyond so far.

Here, we reconstruct for the first time potential carbonate production areas and provide a comprehensive depositional model that exhibits a characteristic facies zonation. This study sheds light on the role of the facies zonation in the Banc d'Arguin and underlines the importance of environmental steering factors that control the distribution of carbonate precipitating organisms.

2) Bryoliths constructed by bryozoans in symbiotic associations with hermit crabs in a tropical heterozoan carbonate system, Golfe d'Arguin, Mauritania

The Second publication highlights the importance of understanding biological and ecological interactions of marine carbonate secreting biota that provides valuable insights into their marine environment. Symbiotic associations between two different organisms are known to represent adaptations to local environmental constraints. Bryolith fossil, are reported from deposits dating back to Jurassic times, however, this is

the first time *in-situ* bryoliths were investigated with both symbiotic partners alive. These associations between a hermit crab and multilamellar encrusting bryozoans document a very close „mutualistic“ relationship with benefits for both partners.

The second study highlights the extreme nature of the Mauritanian carbonate depositional system, which is characterized by a number of natural environmental constraints. As a consequence the faunal community is extremely low in diversity. The remaining filter-feeding specialists are well adapted to this environment and form a number of atypical associations in order to survive.

3) Bryozoans on the move: Adaptations to hard substrate–limiting tropical heterozoan carbonates (Banc d'Arguin, Mauritania)

The high adaptation potential of marine carbonate secretors is also the topic in a Third publication that highlights the presence of mobile and semi-mobile bryozoans (Cupuladriids and multilamellar encrusting forms) as a result of the high sedimentation rate and limited hardbottom availability in the shallow Banc d'Arguin, Mauritania.

4) Recent versus deglacial seasonal variability of the south-eastern South American shelf front recorded from venerid bivalves

The Fourth manuscript deals with the role of carbonate secreting organisms and their function as bioarchive of palaeo-oceanographic proxies. It furthermore highlights the importance of sclerochronological and geochemical approaches in order to reveal the skeletal record of bivalve mollusks dating back to the Late Pleistocene. In the frame of this study the importance of recent analogue specimens is exposed, a prerequisite in order to "calibrate" species-dependent metabolic effects on isotope fractionation, which is far from being well-understood.

The first study is dedicated to the Southeast South American shelf, an oceanographic region that is of highest importance for the South Atlantic circulation and beyond. It is characterized by one of the highest-energetic confluence zones worldwide formed by the collision of cold Malvinas Current and warm Brazil Current. Moreover, the Rió de la Plata estuary and connected river systems in the hinterland transport freshwater and suspended sediments from the second largest drainage system in South America to the ocean. Finally, the atmospheric system is characterized by the South American monsoon system and seasonally varying winds. Such ocean-atmosphere couplings are known to play a key-role in the displacements of shelf water bodies and play a key-role in the distribution of physico-chemical seawater properties along the shelf. Bivalve shells collected from gravity and vibro-cores represent valuable bioarchives dating back to late Pleistocene times.

VII. Sediment response to environmental steering factors

Marine carbonates of biogenic origin play a major role in oceanographical sciences, not least, because they provide a number of excellent high-resolution archives of environmental conditions. Globally, approximately 10 % of all carbonate production occurs within shallow marine settings, comprising the light saturated zone within the first 10 to 20 meters below sea level. Between the deep marine basins and the shallow marine shelfal environments around 60 % of the total biogenic carbonate production is performed by reef constructing organisms that form complex communities (Milliman, 1974; Tucker an Wright, 2009). Coral reefs, hardbottom communities, *Halimeda* populated reef flats and associated marine environments, for example, host a large number of the marine biodiversity.

Production rates of such carbonate factories are high but can vary depending on specific individuals and changing environmental parameters (e.g., temperature, salinity, water depth, nutrient and substrate availability). The mean carbonate production rate ranges between 1.5 and 4.5 kg $CaCO_3$ m^{-2} yr^{-1}, equivalent to a carbonate deposition rate of 0.5–1.5 mm yr^{-1} or 0.5–1.5 m ky^{-1} (Kendall and Schlager 1981; Tucker and Wright 2009). Where optimum conditions and healthy ecosystems exist for the growth of marine carbonate precipitating organisms, then it appears that the carbonate production rate is fairly constant, regardless of the types of organisms involved (Hallock, 1981).

However, such well-balanced ecosystems are extremely vulnerable to natural and anthropogenic-induced disturbances such as pollution or nutrient-input. The Golf d'Arguin offshore Mauritania provides a natural laboratory to study the effect of natural nutrient input (e.g., upwelling, iron-rich sand) on a shallow marine carbonate factory (Klicpera et al., 2015).

The key-findings, based on a large-scale environmental survey presented in the following publication (see Chapter VIII) indicate a distinct facies pattern characterized by light independent carbonate secretors as a result of reduced light transparencies of the water column. Coral reefs and light-associated biota, typical elements for a tropical setting in low latitudes, are completely absent, while the whole ecosystem shifted towards robust filter-feeders (heterozoan association) with a high reproduction cycle. Accumulations of shells and hard-part remains form extensive ridges and shallows that are threatened in navigation since centuries (see Suppl. XVII.1) and which limit nowadays research due to the inaccessibility of the shallow marine carbonate bank.

VIII. First publication

Facies patterns of a tropical heterozoan carbonate platform under eutrophic conditions: the Banc d'Arguin, Mauritania

André Klicpera, Julien Michel, Hildegard Westphal

Facies 61:421 (2015)
DOI: 10.1007/s10347-014-0421-5

this page is intentionally left blank

Facies patterns of a tropical heterozoan carbonate platform under eutrophic conditions: the Banc d'Arguin, Mauritania

André Klicpera[1], Julien Michel[2], Hildegard Westphal[1,3]

1 Leibniz Center for Tropical Marine Ecology (ZMT), Bremen, Germany
2 Center for Marine Environmental Sciences (MARUM), University Bremen, Germany
3 Department of Geosciences, University of Bremen, Germany

Abstract

High nutrient, tropical carbonate systems are known to produce sediments that, in terms of skeletal composition are reminiscent of their extra-tropical counterparts. Such carbonate systems and associated carbonate grain assemblages in the tropics are rare in the present-day world and clearly deserve more attention. Nonetheless, it is crucial to gain a better understanding of those ecosystems, including their drivers and players because such settings potentially represent models for ancient depositional systems as well as for predicted future environmental conditions.

One of the modern occurrences of eutrophic tropical carbonate systems is the northern Mauritanian Shelf. The marine environment is characterized by an eastern boundary upwelling system that pushes cool and nutrient-rich intermediate waters onto a wide epicontinental platform (Golfe d'Arguin) where the waters warm up to tropical temperatures. The resulting facies is mixed carbonate-siliciclastic with a dominant foramol association grading into bimol and barnamol grain assemblages in the shallowest areas forming the Banc d'Arguin. Besides this cool water-related heterozoan association, the carbonate sediment is characterized by tropical molluskan species, while chlorozoan biota (e.g., corals and algal symbiont-bearing foraminifers) are entirely absent.

We here present a first comprehensive facies analysis of this model example of eutrophic tropical carbonates. Furthermore, we reconstruct the loci of carbonate production and provide a conclusive depositional model of the Banc d'Arguin that received little attention to date due to its poorly accessible nature.

Corresponding author: André Klicpera, Leibniz Center for Tropical Marine Ecology (ZMT), Fahrenheitstraße 6, D-28359 Bremen, Germany and Center for Marine Environmental Sciences (MARUM), University of Bremen, Germany

First publication

VIII.1 Introduction

The impact of climate change, rising sea level, and the fingerprint of human-induced eutrophication make comprehensive studies on tropical marine ecosystems more important than ever for predicting future developments (Hallock 2005; Solomon et al. 2007; Taylor et al. 2012). Marine ecosystems in low latitudes such as mangroves, seagrass meadows, and coral reefs provide a wide range of socio-economic services, besides their important role as biodiversity hotspots that need efficient protection against the disturbances by human activity (Myers et al. 2000; Hoegh-Guldberg et al. 2007; Gilman et al. 2008; Gattuso and Hansson 2011; Fourqurean et al. 2012). Therefore, research integrating environmental steering factors, processes and threats on carbonate sedimentation is essential to acquire reliable insights into future developments of coastal marine ecosystems.

Biogenic sediments provide a range of proxies that can be used to reconstruct environmental conditions and settings through time (Scholle et al. 1983; Mutti and Hallock 2003; Halfar et al. 2004; Pomar et al. 2004; Wright and Burgess 2005). Particularly, the analysis of carbonate grain assemblages has become a key tool for palaeo-environmental reconstructions from the tropics up to the polar realm (Chave 1967; Lees and Buller 1972; Hayton et al. 1995; James et al. 1997). Such biofacies pattern shed light on the spatial and temporal distribution of marine ecosystems in relation to past and present climatic conditions.

In the last decades, two major classification concepts of carbonate sediments have been developed. The first one is based on a combination of composite terms, such as foramol (foraminifers and mollusks) and chlorozoan (chlorophyta, hermatypic corals and mollusks) (Lees and Buller 1972), while the more recent concept uses a bimodal approach (photozoan vs. heterozoan carbonate association), accentuating the presence or absence of photosymbiotic carbonate-producing benthic organisms (James et al. 1997). Both schemes provide a framework for the interpretation of modern and ancient carbonate deposits in various environmental contexts (see case studies in Flügel 2010). However, the terms heterozoan and photozoan have become, in some cases, simplified synonyms for the descriptive approach to classify non-tropical, cold-water versus tropical, warm-water regimes (cf. Nelson 1988; Nelson et al. 1988). The ongoing discussion demonstrates that both concepts have strengths and shortcomings, but that the influence of a wider range of environmental controls needs to be considered (Hallock 1988; Betzler et al. 1997a, 1997b; Brandano and Corda 2002; Samankassou 2002; Pomar et al. 2004; Brandano et al. 2009; Kindler and Wilson 2010; Westphal et al. 2010; Betzler et al. 2011; Schäfer et al. 2011; Reijmer et al. 2012). Knowledge of the ecological context and environmental steering parameters is thus crucial for an interpretation of sub-recent and fossil facies (Martín et al. 1996, 2001; Samankassou 2002; Perry and Taylor 2009; Barange et al. 2010; Doney et al. 2012). Among those factors are biological evolution, temperature, salinity, trophic conditions, water depth, oxygen and CO_2 concentrations, Mg/Ca ratio in

the seawater, alkalinity, bathymetry, type of substrate, sea water light penetration, internal waves and water stratification (see Westphal et al. 2010 and references therein). Neglecting one or a combination of these controls might result in palaeo-environmental misinterpretations (cf. Edinger et al. 2002; Samankassou 2002; Pomar 2004). The restricted occurrences of modern heterozoan carbonate depositional systems in tropical latitudes provide a key to better constrain the multi-dimensional ecological control on carbonate sedimentation (Halfar et al. 2004; Kindler and Wilson 2010; Westphal et al. 2010; Schäfer et al. 2011; Reijmer et al. 2012).

Here we discuss the Golfe d'Arguin offshore northern Mauritania as one of the present-day tropical heterozoan carbonate factories. Previous sedimentological studies took place in different parts of the shelf such as the Baie de Lévrier (Koopmann et al. 1979), the outer shelf (Hanebuth and Lantzsch 2008; Michel et al. 2011a, b; Hanebuth et al. 2013; Klicpera et al. 2013, 2014), the innermost shelf (Barusseau et al. 2010; Aleman et al. 2014) and in the vicinity of Tidra Island (Proske et al. 2008). However, none of these studies provides a comprehensive picture of the sedimentary facies distribution. One reason for the rather low research intensity is the restricted access to the shallow waters of the Banc d'Arguin. It cannot be accessed by larger research vessels and is by far too extensive for coverage by small boats (Wolff et al. 1993c).

In this study, we combine samples from the outer Banc d'Arguin (Westphal et al. 2007; 2014) with earlier investigations from the inner Banc d'Arguin (Piessens 1979) to a comprehensive facies pattern model. The aim is to identify areas of tropical heterozoan carbonate production and facies distribution by reconstructing the sedimentation dynamics in the Golfe d'Arguin and to infer from this example general patterns of eutrophic tropical carbonate deposition.

VIII.2 Study area

Off northern Mauritania, the narrow West African shelf (~50 km in width) opens up into a wide gulf of more than 150 km in east-west extension (Einsele 1972; Piessens 1979). The so-called Golfe d'Arguin (GdA; Fig. VIII.1) stretches between the Baie du Lévrier (BdL; 21°10'N) and the Cap Timiris Shelf (CTS; 19°20'N) over a distance of about 200 km (Piessens and Chabot 1977).

The depositional profile of the northern GdA describes a flat-topped platform (gradient 0.3 m km^{-1}; Fig. VIII.1, transect A), on which extensive carbonate deposits (Banc d'Arguin; BdA) developed in largely <10 meters below sea level (mbsl). Vast areas of the BdA are covered by mixed carbonate-siliciclastic sediments dominated by barnamol assemblages (balanids and mollusks) *sensu* Hayton et al. (1995) plus admixed aeolian siliciclastics (Sarnthein and Walger 1974; Westphal et al. 2007; 2014). Those sediments accumulate into extensive shoals, occasionally reaching causing water depth below

5 mbsl (Prévost 1746; Piessens 1979; Sevrin-Reyssac 1993). The bank-edge forms a sharp morphological step, suddenly deepening from 10–20 mbsl down to 30–50 mbsl, and separates the inner shelf environments (<5–10 mbsl; carbonate bank) from those of the outer shelf (>30 mbsl; open platform, see Hanebuth et al. (2013).

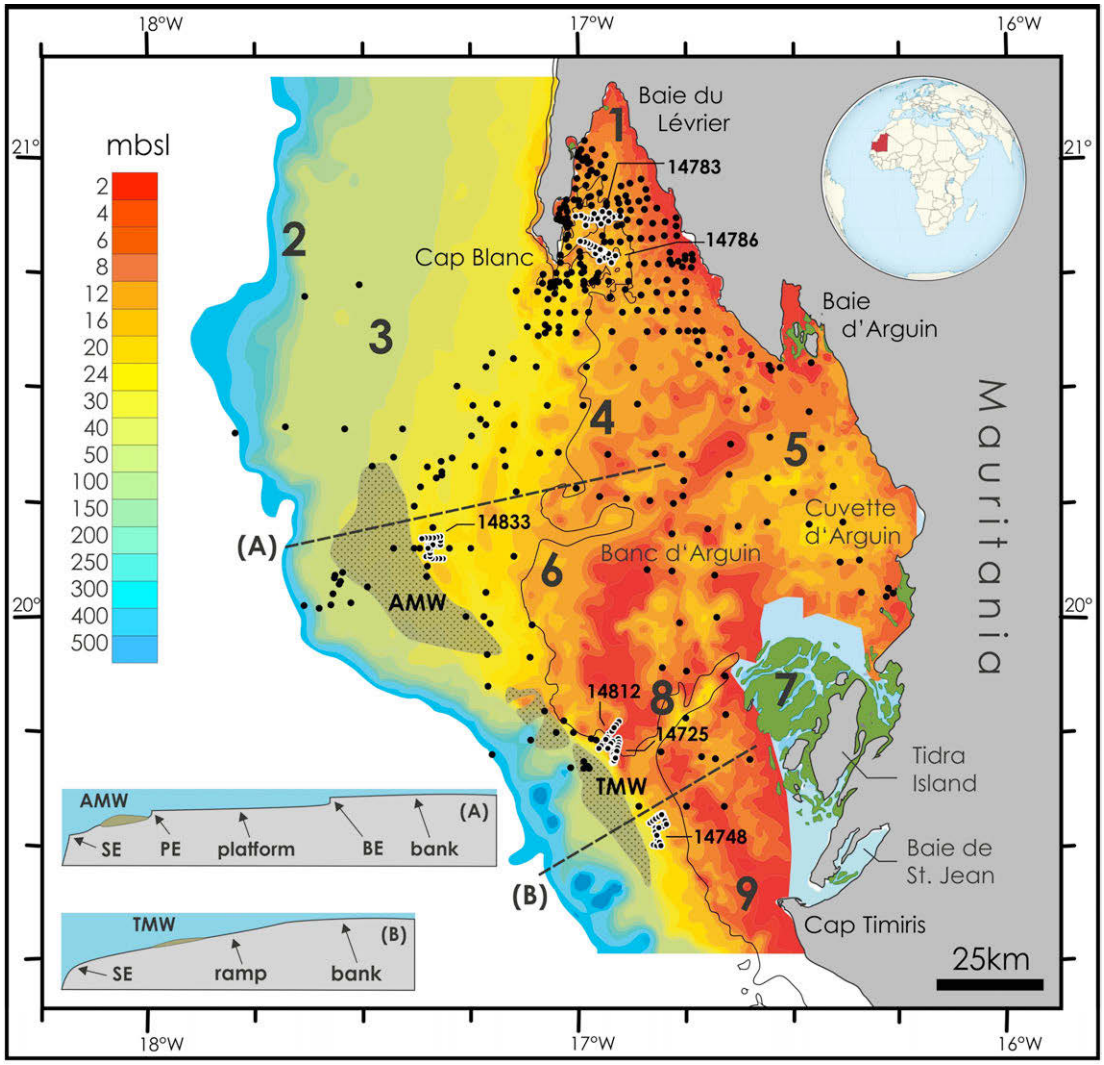

Figure VIII.1: The Golfe d'Arguin off northern Mauritania and the shallow Banc d'Arguin with vast areas <10 meters below sea level (mbsl). White circles indicate MSM16-3 sampling sites; black dots sampling sites compiled from other studies (Piessens, 1979; Michel et al., 2011a). The shallow bank-edge follows roughly the 10-20 m isobaths, while the shelf-edge of the outer platform is located in 80 to 100 mbsl. Fine-grained sedimentary bodies characterize the Arguin (AMW) and Timiris (TMW) mud wedges deposited in a platform-like depositional setting in the northern gulf (transect A) and a ramp-like setting in the south (transect B). Bathymetry according to Aleman et al. (2010, 2014); regional map modified after Hanebuth and Lantzsch (2008). Fine-grained deposits are the Arguin (AMW) and Timiris (TMW) mud wedges situated in a platform-like depositional setting (transect A) and a ramp-like setting in the south (transect B), respectively. Profile nomenclature: *SE* shelf-edge, *PE* platform-edge, *BE* bank-edge (*sensu* Hanebuth et al. (2013)); topographic features in the entire Golfe d'Arguin: *1* Baie du Lévrier, *2* shelf break (in 80-110 mbsl) *3* outer shelf, *4* Bank d'Arguin margin, *5* inner Banc d'Arguin (Cuvette d'Arguin), *6* central outer Banc d'Arguin, *7* Tidra Island intertidal zone, *8* southern Banc d'Arguin, *9* Cap Timiris shelf.

Foramol assemblages (foraminifers and mollusks) *sensu* Lees and Buller (1972) and bimol assemblages (bivalve mollusks) *sensu* Hayton et al. (1995) with admixed aeolian silt characterize the platform cover in the outer shelf (Sarnthein and Walger 1974; Piessens 1979; Michel et al. 2009). In the central and southern outermost shelf, silt-sized quartzose materials (mode at 35 µm) form confined bodies referred to as the Arguin mud wedge (AMW) and Timiris mud wedge (TMW) cf. Hanebuth and Lantzsch (2008). These deposits started to form with transgressional inundation early in the Holocene and have grown continuously and rapidly over the past 9 kyrs (Sarnthein and Diester-Haass, 1977; Hanebuth and Lantzsch 2008). Locally, the AMW and TMW deposits are incised by gullies and canyons towards the shelf break lying at around 80–110 mbsl (Hanebuth et al. 2013). The southernmost GdA describes a homoclinal ramp profile (gradient 3–4 m km^{-1}) with vast intertidal plains around Tidra Island (Wolff et al. 1993a, b; Proske et al. 2008; Fig. VIII.1, transect B).

VIII.3 Oceanographic Setting

The oceanography of NW Africa is characterized by tropical waters (>24°C; <35‰) of the northward-directed Guinea Current and cool waters of the southward flowing Canary Current (<24°C; >35‰). Additionally, nutrient-enriched upwelling waters (<18°C; <36‰) are pumped onto the shelf and into the photic zone by Ekman transport, induced by equatorward Trade Winds that control the eastern boundary Canary Current (Maigret 1972).

During winter, a branch of the Canary Current is displaced as far south as 20°N, while during summer, the Guinea Current and thus tropical waters dominate the hydrology of the GdA (Mittelstaedt 1991; Van Camp et al. 1991).

As a result, a perennial upwelling cell occurs year-round north of 21°N (Cap Blanc), whereas the upwelling activity is seasonal-controlled south of this latitude and in the study area (maximum upwelling intensities February–June and October–December cf. Sevrin-Reyssac 1993; Fig. VIII.2). These oscillating upwelling conditions allow for water stratification to develop during non-upwelling periods and nutrients to concentrate in calm photic water layers where they push the primary production (Huntsman and Barber 1977). As a consequence, the primary productivity off Cap Blanc is one of the highest worldwide with values exceeding 325 g C m^{-2} yr^{-1} (annual mean of 200 g C m^{-2} yr^{-1}) and Chlorophyll *a* (Chl-*a*) values of 3 to >10 mg m^{-3} (Marañón and Holligan 1999; Fig. VIII.2).

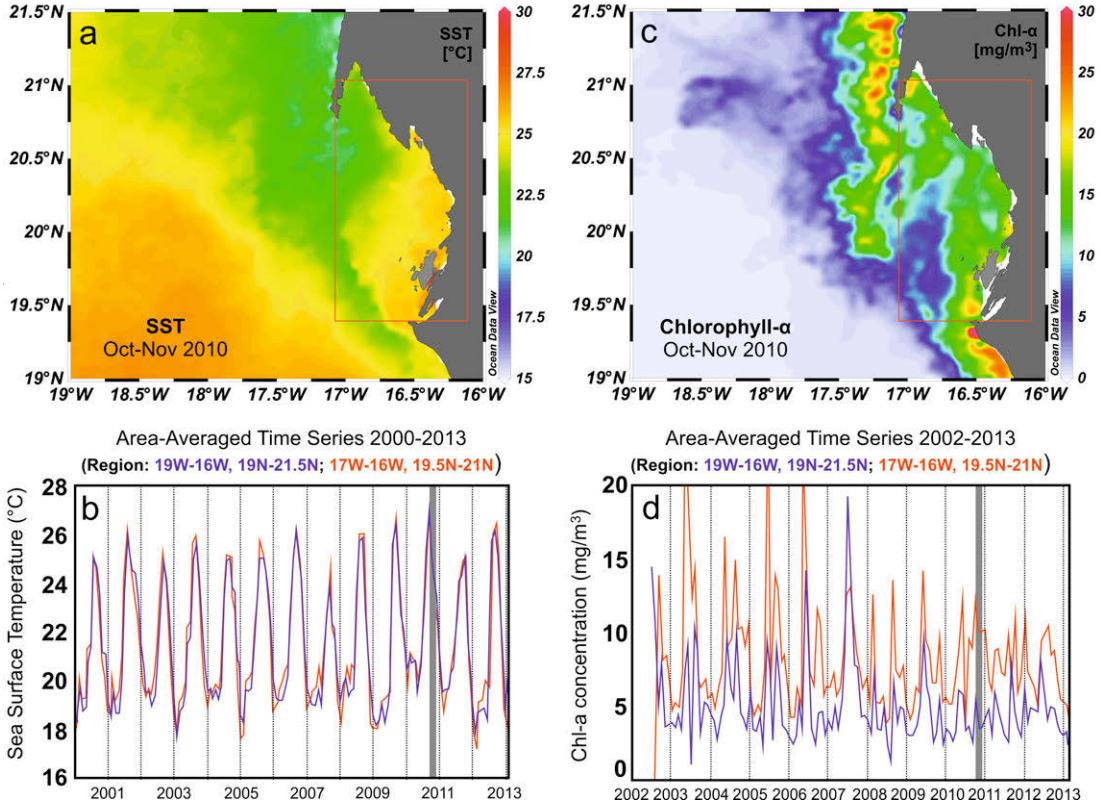

Figure VIII.2: Sea surface temperature (a) and Chlorophyll-*a* concentration (c) based on remote-sensing data (Acker and Leptoukh 2007) for the time of sampling (Oct-Nov 2010). Area-averaged SST time series from 2000 to 2013 (*MODIS terra*) are given in (b), area-averaged Chl-*a* time series from 2002 to 2013 (*MODIS aqua*) in (d). Grey bars in b and d indicate the time of sampling, blue curve present regional data, the red curve data limited to the Banc d'Arguin.

Mean annual water temperatures (>23°C) in the GdA show a pronounced seasonality with lowest sea surface temperatures (SST) of 16–17°C recorded near Cap Blanc (April–May) corresponding to spring upwelling. Maximum water temperatures of >26°C occur during September–October (Fig. VIII.2) in the nearshore and intertidal areas around Tidra Island (Sevrin-Reyssac 1993). Strong insolation in spring and summer leads to a pronounced temperature gradient across the area and a high seasonal variability (Peters 1976; Koopmann et al. 1978; 1979; Ould Dedah 1993; Hagen 2001).

Strong surface currents (2–3 m s^{-1}) characterize the GdA, particularly the shallow BdA, and are related to tidal currents, the wind regime and upwelling swell. In restricted areas, such as the Baie de Saint Jean (BdSJ) the conditions become extreme with highest water temperatures and salinities reaching hypersaline concentrations (Sevrin-Reyssac 1993).

VIII.4 Material and methods

Surface sediments were collected during the research cruise "PHAETON" aboard the R/V Maria S. Merian (MSM16/3, October–November 2010; Westphal et al. 2014). To access the shallow, westernmost parts of the BdA from the seaside, an auxiliary zodiac was deployed from the research vessel. Six remote sites within the BdL (station IDs 14783, 14786), along the central BdA (station ID 14833), the southern BdA (station IDs 14812, 14725), and in the CTS area (station ID 14748) were sampled (Tab. VIII.1). For each of these stations, 15–24 sub-samples (Sed_{Bulk}) were taken using a Van Veen grab (surface sediments; N=125). Additionally, oceanographic profiles of the water column were measured with a miniCTD probe (temperature and salinity; N=49) and a Secchi disk (light penetration depth; N=44).

VIII.4.1 Carbonate content

Carbonate contents were determined as the mean weight percentage (wt% $CaCO_3$) of four replicates per bulk sample (N=468) following the carbometer method of Müller and Gastner (1971). The internal error of this procedure is less than ±1% $CaCO_3$. To improve precision, the carbometer device was calibrated at least twice daily with a calcium carbonate standard (99.5% $CaCO_3$).

VIII.4.2 Grain size determination

Sediment samples were classified on board the vessel into two textural groups that defined their further treatment: (1) coarse-grained bulk sediments (N=75) that were washed and dried at +60°C; (2) fine-grained materials (N=45), directly wet-stored as bulk material in a cooling facility at +4°C to reduce biodegradation of organic material. Back to the laboratory, the coarse-grained samples were dry-sieved by means of a sieve shaker, while the fine-grained sediments were first split at 500 µm and then either wet-sieved (>500 µm) or analyzed by means of a laser granulometer (<500 µm; cf. Blott et al. 2004). Laser granulometer raw data were re-calculated in Gradistat (Blott and Pye, 2001) to make the applied techniques and datasets comparable.

Additional grain-size data were extracted from Piessens (1979), Koopmann et al. (1979) and Michel et al. (2011a) and re-calculated to make the applied techniques and datasets comparable. All data were subsequently split in eight grain-size classes (<62 µm, 62–125 µm, 125–250 µm, 250–500 µm, 500–1000 µm, 1000–2000 µm, and >2000 µm) following Wentworth (1922). Measurements are given as the weight percentage (wt%) of the bulk sediment.

Table VIII.1: Sampling stations and gears of the R/V MS Merian cruise 16-3 in the Golfe d'Arguin, Mauritania, Locations: BdL, Baie du Lévrier; BdA, Banc d'Arguin; CTS, Cap Timiris Shelf; mbsl, meters below sea level; CTD, conductivity, temperature, depth probe; SD, Secchi disk; COMP-DARA, station sub-samples (=site ID) analyzed for component data; COMP-MOL, station sub-samples (=site ID) analyzed for mollusk assemblages.

Station (ID)	**14783**	**14786**	**14833**	**14812**	**14725**	**14748**
Latitude	20°87'N	20°81'N	20°16'N	19°73'N	19°71'N	19°53'N
Longitude	-16°94'W	-16°94'W	-17°35'W	-16°92'W	-16°91'W	-16°82'W
Location	BdL	BdL	Central BdA	Southern BdA	Southern BdA	CTS
WD (range in mbsl)	6 – 13	4.5 – 16	20 – 30	4.5 – 38	6 – 26	8 – 31
Sediment grabs (N=)	23	22	22	20	15	23
CTD casts (N=)	9	9	5	7	9	10
SD casts (N=)	7	9	5	7	6	10
COMP-DATA (sites=)	-1, -7, -12	-2, -9, -14	-6, -17, -20	-6, -10	-3, -6, -2	-6, -9, -13
COMP-MOL (sites=)	-7	-9	-7, -21	-10	-2	-10, -11

VIII.4.3 Component analysis

The component analysis was undertaken on surface sediments by determining a minimum of 300 skeletal grains per fraction (N=18823 counts). Analyzed component groups are given as mean percentages of the three coarsest fractions (>500–1000 µm, 1000–2000 µm and >2000 µm) of sediments sampled at three sites per station (N=18; Tab. VIII.1). The high identification potential (>94%) of the fraction >500 µm allowed to differentiate bivalves, gastropods, foraminifers, bryozoans, echinoderms, serpulids, coralline red algae, balanids, and undeterminable bioclasts. Bivalve and gastropod grains were determined, where possible, down to species level (N=3287; Suppl. XVII.3 and Suppl. XVII.4). Non-skeletal grains are classified as siliciclastics, aggregates, pellets, and undeterminable material.

Additional samples were provided by an environmental monitoring program carried out by the Mauritanian government (BdSJ sediments; IMROP, 2013). Other component data were taken from Piessens (1979), Koopmann et al. (1979) and Michel et al. (2011a). All data were re-calculated on a percentage basis excluding unidentified components and standardized with respect to component groups used to allow direct comparability. The abundance scale used follows the recommended classification scheme cf. Flügel (2010) p. 262.

VIII.4.4 Statistical analysis and mapping program

Sedimentary facies types were determined on the basis of grain size and composition of the sediment. A hierarchical cluster analysis (dendrogram using Ward's method; Ward 1963) was performed using JMP data analysis software for MacOS version 9.0.2 (Fig. VIII.5) to statistically distinguish groups and clusters of samples. Non-determinable grains were not included in the statistical analysis.

Mapping of facies data was achieved using Ocean Data View (ODV) version 4.6.2. Areas of poor sample resolution were interpolated by the Diva gridding method provided in ODV (Schlitzer 2012). The resulting facies map was later processed in a vector graphics software and manually translated in a hexagonal grid (Fig. VIII.7) to allow a better overview of facies zones identified.

VIII.5 Results

VIII.5.1 Oceanographic data

CTD casts from the outer BdA give a total temperature range (water column) between 18.2 and 24.3°C (mean=20.6°C; October–November 2010). SSTs range between 18.7 and 24.3°C (mean=21.1°C); sea bottom temperatures (SBT) show values between 18.2 and 24.3°C (mean=19.8°C). The highest temperature contrast (entire water column) is observed in the southern BdA, where SBTs and SSTs range between 18.2°C and 24.3°C respectively (mean=20.3°C). The lowest temperature contrast occurs in the central BdA where SBTs and SSTs range between 19.4°C and 21.2°C respectively (mean=19.9°C; Tab. VIII.2).

CTD-based salinity measurements show a total range between 35.1 and 38.0‰ (mean=36.0‰) that correspond to the range of sea surface salinities (SSS; mean=36.1‰). Sea bottom salinities (SBS) range from 35.9–36.5‰ (mean=36.0‰). Greatest contrasts occur in the southern BdA, where the mixed surface water layer ranges between 35.8‰ and 38.0‰ (mean=36.0‰). The lowest SSS range was measured in the central BdA with values between 35.7‰ and 36.4‰ (mean=36.0‰; Tab. VIII.2).

Table VIII.2: Oceanographic data extracted from CTD measurements (cruise MSM16-3) undertaken in the Golfe d'Arguin, Mauritania. Bold and italic values indicate maximum and minimum values, respectively. SSS, sea-surface salinity; SBS, sea-bottom salinity; SST, sea-surface temperature; SBT, sea-bottom temperature.

October-November 2010 (MSM16-3)	**Baie du Lévrier** (14786; 14783) (N = 584)			**Central Banc d'Arguin** (14833) (N = 366)			**Southern Banc d'Arguin** (14725; 14748; 14812) (N = 943)		
	Mean	Max	Min	Mean	Max	Min	Mean	Max	Min
Salinity (‰)	36.04	36.79	35.33	35.95	36.44	35.66	36.04	**38.03**	*35.12*
SSS	36.06	36.57	35.54	35.99	36.40	35.73	36.14	**38.03**	*35.12*
SBS	36.12	**36.46**	36.02	35.93	35.94	35.93	36.03	36.34	*35.88*
Temperature (°C)	21.54	24.08	19.58	19.97	21.23	19.36	20.30	**24.34**	*18.17*
SST	22.41	24.08	21.10	20.85	21.23	20.30	21.11	**24.33**	*18.66*
SBT	20.84	21.78	19.58	19.67	19.99	19.36	19.76	**24.32**	*18.17*

Secchi disk measurements (Tab. VIII.3) show a light penetration averaging at 3 mbsl (N=43). Lowest water transparencies of <2 mbsl (N=10) are observed in the BdL and in the southern BdA (station 14748). Intermediate water transparencies of 2–4 mbsl (N=22) are ubiquitous with the exception of the central BdA where transparencies of >4 mbsl (N=11) are observed. Greater light penetration depths occur in the southern BdA (stations 14725, 14812) and near the CTS (Tabs. 2, 3).

Multi-annual remote sensing data show well-defined seasonal cycles. Area-averaged SSTs range from 18–26°C for the entire area (19.0°N–21.5°N; 19.0°W–16.0°W) and are slightly higher for the GdA (19.0–27.0°C; 19.5°N–21.0°N; 17.0°W–16.0°W) (Fig. VIII.2a, b). The Chl-*a* concentrations show a seasonal pattern oscillating around 5 mg m^{-3} for the entire area with prominent peaks in the order of 10 to >20 mg m^{-3} for the GdA (Fig. VIII.2c, d).

VIII.5.2 Sedimentary facies

VIII.5.2.1 Surface sediment texture

The outer BdA is covered by two sediment types: (1) Coarse-grained bioclastic sands with minor portions of rounded quartz (N=75) and (2) quartzose sands with a low amount of

coarse skeletal grains (N=45). Rocky hardgrounds occur along the bank margin resulting in empty grabs (station 14748; N=5) or in the recovery of cemented aggregates.

Towards the outer shelf (>30 mbsl; Fig. VIII.1, transect A), the bioclastic sands grade into quartzose sands and silts with increasing water depth (Fig. VIII.3b, c, d). Silt-sized muddy bodies (AMW, TMW) separate the outermost shelf with locally exposed erosion surfaces from the shelf break (Fig. VIII.1, see Hanebuth et al. 2013 for nomenclature used).

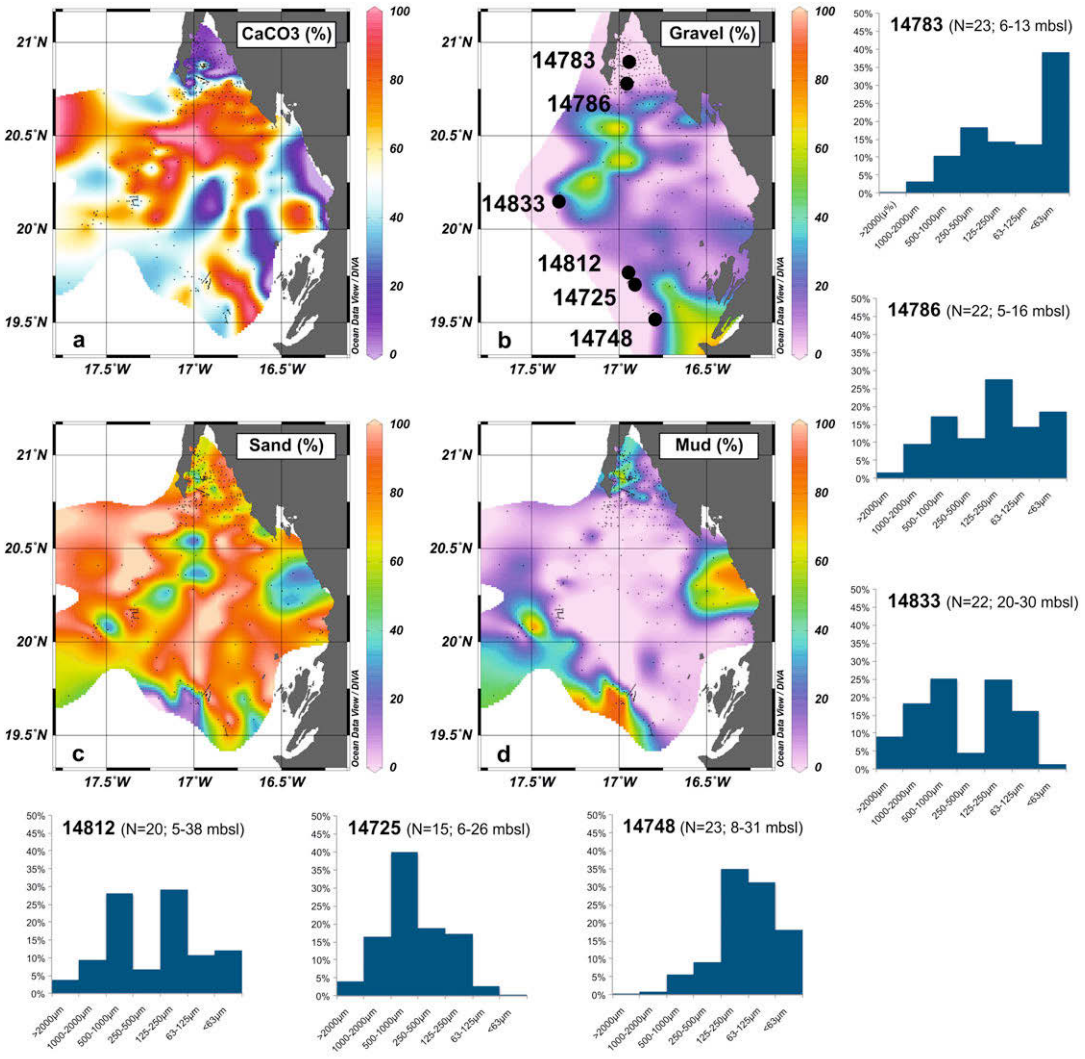

Figure VIII.3: Carbonate content (a) and large-scale grain-size distribution of gravel (b), sand (c) and mud (d) of surficial sediments sampled in the Golfe d'Arguin (Mauritania). Data are compiled from the present study and additional data taken from Koopman et al. (1979), Piessens (1979) and Michel et al. (2011a) using Ocean Data View (ODV) version 4.6.1 (http://odv.awi.de; Schlitzer 2012). The bar diagrams in the right and lower panel show the grain-size distribution in localized sampling sites cf. b sampled during MSM16-3.

VIII.5.2.1 Carbonate content

Dry bulk sediments from the outer BdA and BdL range from 16–85% in calcium carbonate content (N=468; Tab. VIII.3) Highest values are recorded in the BdL (34–85%; mean=56%) and in the southern BdA (21–85%; mean=55%). Sediments from the central BdA range from 39–45% (mean=42%), while the southernmost CTS shows lowest measured contents ranging from 16–52% (mean=37%).

Over the entire GdA, carbonate contents exceed >80% in the northern GdA and in the vicinity of Cap Blanc with slightly decreasing contents from north to south and from shallow to deeper water. Lowest carbonates contents occur in nearshore settings and around Tidra Island (Fig. VIII.3a).

VIII.5.2.2 Grain-size distribution

Sand-sized fractions dominate (82%) the bulk sediments from the BdA and BdL throughout (N=113; Fig. VIII.3) with fine-grained (125–250 µm) and coarse-grained (500–1000 µm) sands averaging at 25% and 21%, respectively. Silt and clay-sized materials (<63 µm) average at 14%; gravel-sized sediments (>2000 µm) at 3%.

Restricted areas such as the BdL show a shift towards finer grain-size classes, dominated by sand-sized fractions (70%) with fine-grained sand accounting for 21% and medium-grained sand (250–500 µm) for 15% of the bulk sediment. Silt and clay-sized materials average at 29%; gravel-sized at material not more than 1%. Particle size curves (Fig. VIII.3) show monomodal distributions in the southern BdA (mode 500–1000 µm at station 14725) and the CTS (mode 125–250 µm at station 14748) or polymodal distributions of particles in the BdL (stations 14783, 14786), the central BdA (station 14833) and the southern BdA (station 14812).

GdA-wide, grain-size distributions show a dominance of sand-sized classes with larger areas covered by 80–100% sand (Fig. VIII.3c) south of Cap Blanc and towards the outer shelf, in the central to southern BdA and around Tidra Island. Gravel-rich deposits occur in the area between the central BdA and Cap Blanc as well as in the CTS (Fig. VIII.3b). Periplatform muds (<63 µm) are restricted to the BdL (<40%), the Cuvette d'Arguin (<60%) and to off-bank settings below the storm wave-base (>20 mbsl). On the outer shelf (>50–100 mbsl), the AMW and TMW show accumulations in the silt to fine-sand range (35–125 µm) of <40% and <80%, respectively (Fig. VIII.3d).

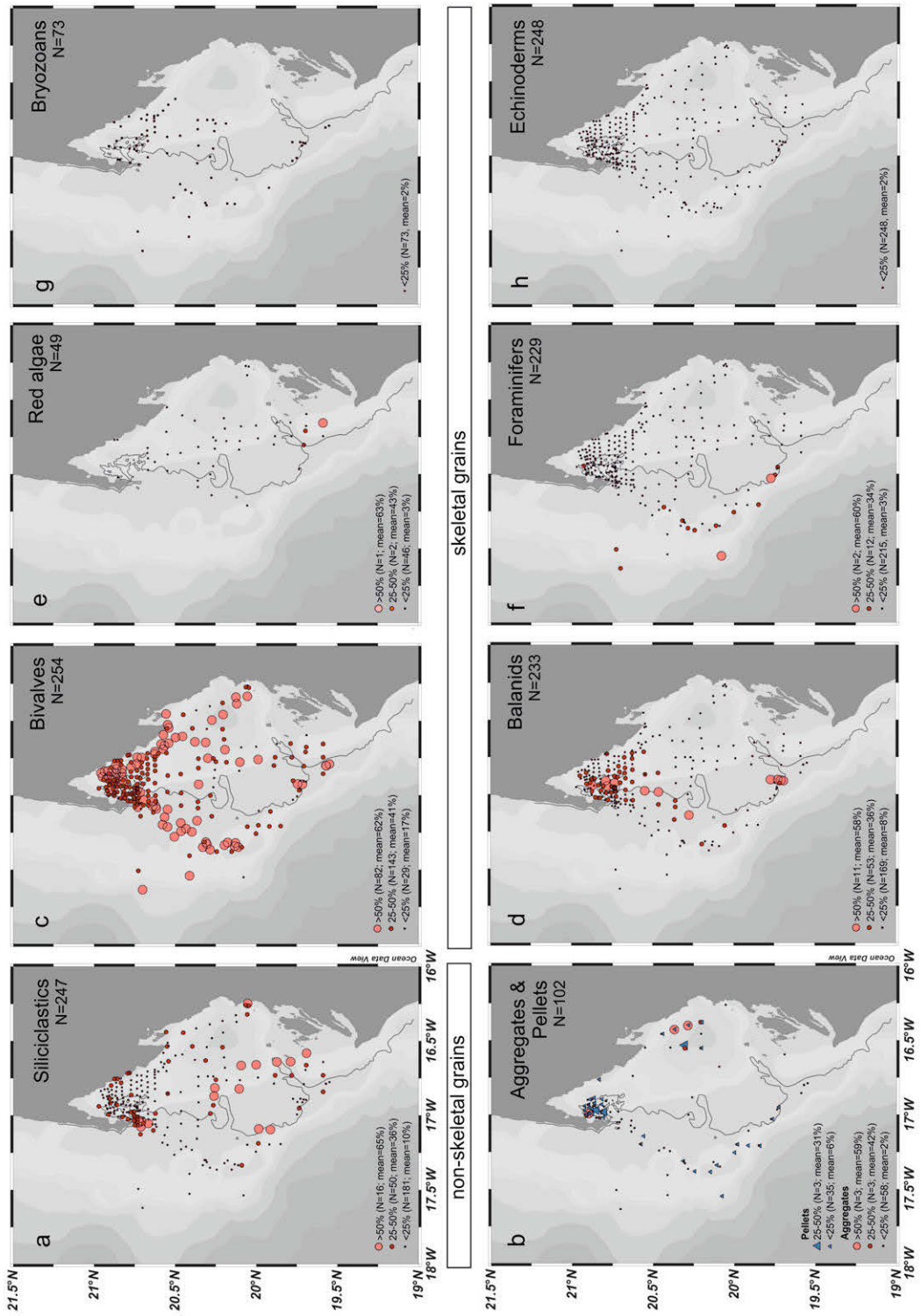

Figure VIII.4: Relative abundance of non-skeletal grains (a, b) and skeletal grains (c to h) in the Golfe d'Arguin offshore Mauritania are shown in. Thin black line indicates the bank-edge in 10-20 mbsl. Data are compiled from the present study and additional data extracted from Koopman et al. (1979), Piessens (1979) and Michel et al. (2011a).

VIII.5.2.1 Non-skeletal components

Abiogenic grains are rare to sparse constituents throughout the outer BdA sediments averaging at 3% of the component-analyzed samples (fractions >500 µm). Siliciclastics average at 2% with a maximum of 9% in the southern BdA (station 14725). Aggregated grains average at 1% but can show elevated contents of up to 5% (BdL, station 14783).

Over the entire GdA, abiogenic grains occur in quantities exceeding >25% of the component-analyzed samples (fractions >500 µm) along nearshore areas (e.g., Cap Blanc, Cuvette d'Arguin, Timiris Island) but also offshore in the AMW area. Siliciclastics (quartz grains; Fig. VIII.4a) average at 19% with local enrichments (<89%) south of Cap Blanc and in the southern BdA. Fecal pellets average at 8% with maximum contents of up to 35% restricted to low energy settings such as the BdL and the Cuvette d'Arguin (Fig. VIII.4b). Aggregates average at 6% but can reach contents of 63% along nearshore environments (e.g., south of Cap Blanc; BdL) and close to submarine outcrops. Accumulations in aggregates (>50%) can also occur as allochthonous deposits within low-energy regimes (e.g., Cuvette d'Arguin; Fig. VIII.4b).

VIII.5.2.2 Skeletal components

Mollusks – The variety of mollusk grains present in the BdA and BdL sediments is characteristic for an environment influenced by mixed coastal and open marine conditions (Michel et al. 2011a, b) Whole and reworked shells occur as common to abundant constituents in most sediment types and water depths averaging at 50% of the component-analyzed materials (fractions >500 µm). Highest contents (82%) were found in the central BdA.

The GdA-wide distribution of mollusk shells shows abundant contents averaging at 56% (fractions >500 µm) and a maximum of up to 93% in the central BdA and around Cap Blanc. Lower contents of 83% occur the northern Cuvette d'Arguin and in nearshore setting close to the Baie d'Arguin.

Balanids – Hard substrate-related balanid grains (*Balanus* cf. *trigonus;* Darwin, 1854) are ubiquitous in the outer BdA (Gruvel 1912). Such balanid accumulations average at 35% (fractions >0.5mm) with highest concentrations of 67% in the northern BdL (station 14783). Percentages around 55% occur in the southern BdL (station 14786) and in the southern BdA (stations 14725 and 14812).

Over the entire GdA, balanid grains average at 17% (fractions >500 µm; Fig. VIII.4d) with dominant occurrences (>50%) restricted to shallow subtidal waters (<10 mbsl) in the BdL (60%), the northern BdA (56%), and in the southern BdA (58%). Balanid sands can accumulate to extensive shoals forming shallows of <5 mbsl more than 100 km offshore. The majority of balanid grains recovered from the BdA are disarticulated plates,

however, some entire shells are found as clusters attached to rocks (southern BdA) or to larger mollusk shells such as *Venus crebrisulca* in the central BdA.

Coralline red algae – Sediment samples from the outer BdA and BdL provide no significant records of coralline red algae, however, their abundance over the entire GdA averages at 6% (fractions >500 µm; Fig. VIII.4e) with enrichments of up to 63% restricted to the southern BdA.

Foraminifers – Foraminifers are very rare (<2%) in the outer BdA. The GdA-wide distribution of foraminifers averages at 5% (Fig. VIII.4f) with higher concentrations in fine-grained sediments alongside the outer shelf and in the CTS area. Highest occurrences (>30%; Fig. VIII.6g, h) of the bulk sediment were identified as *Tetragonostomina rhombiformis* (Mikhalevich, 1975). Other sparse to common distributed taxa are the benthic taxa *Siphonaperta* sp., *Quinqueloculina* sp., *Eponides* sp., *Homotrema* sp. and the planktonic *Globigerinoides ruber* (Cushman, 1927).

Bryozoans – Samples from the BdA margin and BdL show rare to sparse bryozoan records averaging at 2% (fractions >500 µm). Highest contents are restricted to the southern BdA (station 14812) where bryozoans may reach up to 10% of the sediment constituents.

The same quantity in distribution and local appearance applies for the entire GdA. In the central BdA, abundant *in situ* bryoliths were identified formed by symbiotic associations between the bryozoan *Acanthodesia commensale* (Kirkpatrick & Metzelaar, 1922) and hermit crabs (Klicpera et al. 2013). Other common (<10%) bryozoans in the CTS area are free-living cupuladriid colonies (e.g., *Discoporella* spp., *Reussirella* spp., and *Cupuladria* spp.; Klicpera et al. 2014)

Echinoderms – Remains of echinoderms average at 1% (fractions >500 µm) in the samples from the BdA. However, their abundance in the fraction >2 mm can be as high as 7%, especially in the southern BdA where the infaunal species *Heliophora orbicularis* (Linnaeus, 1758) is a common constituent in surficial sediments (Fig. VIII.6e).

The GdA-wide distribution of echinoderm grains averages at 2% (Fig. VIII.4h) with local accumulations of up to 18% of the sediment constituents in the southern BdA and up to 17% in the outer shelf area south of Cap Blanc (northern BdA).

Table VIII.3: Measurements conducted during cruise MSM16-3 in the outer Banc d'Arguin, Mauritania. BdL, Baie du Lévrier; BdA, Banc d'Arguin; CTS, Cap Timiris Shelf

Station (ID)	**14783**	**14786**	**14833**	**14812**	**14725**	**14748**
Location	BdL	BdL	central BdA	southern BdA	southern BdA	CTS
Depth range (mbsl)	6 - 13	4.5 - 16	20 - 30	4.5 - 38	6 - 26	8 - 31
Secchi Disk (mbsl)	1.5	1.9	6.4	3.3	3.8	3.3
Chl-*a* (mg m^{-3})	8.3	8.3	4.5	3.9	3.9	8.3
% $CaCO_3$ / mean	34-85 / 56	40-83 / 57	39-45 / 42	21-85 / 42	15-84 / 56	31-52 / 37
Dominant biota	balanids, mollusks	balanids, mollusks	bivalves	balanids	balanids	bivalves

VIII.5.3 Mollusk taphonomy

Mollusk assemblages from the BdA were further investigated taxonomically for their ecological significance in the study area. In total 109 taxa are identified from 3657 mollusk shells that were picked from eight sampling sites in BdL and BdA and one additional sample from the BdSJ (fractions >500 µm). Among these, 3287 identified bivalve grains account for 90% of the mollusk grains (Fig. VIII.4c) and clearly highlight the dominance of bivalve mollusks in the GdA. Sediment samples from the outer BdA and BdL show high abundances of the bivalves *Donax burnupi* (Sowerby III, 1894) with >50% (occasionally >90%) in BdL and CTS; *Timoclea ovata* (Pennant, 1777) with >50% in CTS area, and *Papillicardium papillosum* (Poli, 1791) with 30–50% in BdL area of the component analyzed fractions (see Tab. VIII.1). The complete list of bivalve and gastropod taxa identified is given as supplements to this study (see for detail analyses Suppl. XVII.3 and Suppl. XVII.4).

Over the entire GdA, extensive deposits of *Venus crebrisulca* (Lamarck, 1818) shells indicate economically significant stocks that were investigated in Goudswaard et al. (2007). In nearshore areas, the species *Senilia senilis* (=*Anadara senilis*; Linnaeus, 1758) yield abundant archeological material and represents the main mollusk exploited by ancient human populations living in the GdA hinterland (Barrusseau et al. 2007). The deeper outer shelf (>30 mbsl) shows remains and *in situ* records of *Pinna rudis* (Linnaeus, 1758) and scattered shells identified as the chemosymbiotic bivalve *Solemya togata* (Poli, 1791) prospering in muddy to fine-grained sediments (Westphal et al. 2014).

Table VIII.4: Identified mollusk taxa in more than rare abundance (>5% of mollusk grains) from the inner shelf of the Golfe d'Arguin, Mauritania. Abundance scale cf. Flügel (2010) p. 262. A, abundant (>50%); VC, very common (30-50%); C, common (10-30%); S, sparse (5-10%); R, rare (2-5%); VR, very rare (<2%). Locations: Locations: BdL, Baie du Lévrier; BdA, Banc d'Arguin; CTS, Cap Timiris Shelf; BdSJ, Baie de Saint Jean. Mollusk substrate: M, mud; sM, sandy mud; fS, fine Sand; Sa, sand. Mollusk environment: Tr, tropical; ST, subtropical; TE, temperate; COS, cosmopolitan; UP, upwelling-related.

	Depth range (mbsl)	Substrate	Ecology	Environment	14783-7	14786-9	14833-7	14833-21	14812-10	14725-2	14748-10	14748-11	Baie de Saint Jean
					BdL		***Central BdA***		***southern BdA***		***CTS***		***BdSJ***
Bivalvia													
Carditamera contigua	*1-5*	*rock*	*SF*	*TR, UP*	VR				S	S			
Cerastoderma cf. edule	*1-100*	*Sa*	*SF*	*COS*									C
Chama crenulata	*0-60*	*Rock*	*SF*	*TR*	VR		VR	VR	C	S	R	VR	
Corbula gibba	*3-100*	*sM, fS*	*OM, B*	*TE*	C	C		VR					
Cuna gambiensis	*1-20*	*sM, fS*	*PP*	*TR-ST, UP*	S	S			VR		VR	VR	
Donax burnupi	*1-40*	*Sa*	*PP*	*TR-ST, UP*	VR	R	**A**	**A**	S	R	**VC**	**VC**	
Dosinia sp.	*3-20*	*Sa*	*PP*	*COS*	R	S	VR	VR	VR		VR	VR	C
Fraginae sp.1	-	-	-	-									C
Gregariella petagnae	*>3*	*fS, Sa*	*OM*	*COS*					R	C	VR		
Nuculana bicuspidata	*1-60*	*sM, fS*	*OM*	*TR, UP*	C	C							
Papillicardium papillosum	*20-60*	*Sa*	*SF*	*COS*	**VC**	C	VR		VR			VR	
Tellina densestriata	*15-35*	*fS*	*OM*	*TR*		S							
Tellina rubicincta	*10-100*	*sM, fS*	*OM*	*TR-ST*		S							
Timoclea ovata	*30-200*	*fS, Sa*	*PP*	*COS*	VR	VR	R	C	**VC**	C	**A**	**VC**	
Venus crebrisulca	*4-25*	*Sa*	*PP*	*TR-ST, UP*			VR	VR		C			
Carditamera contigua	*1-5*	*rock*	*SF*	*TR, UP*	VR				S	S			
Gastropoda													
Bittium reticulatum.	*0-5*	*S*	*HV*	*COS*									S
Pusillina sp.	*18-50*	*m / fS*	-	-									C
Rissooidea	*>2*	-	-	-									C
Tricolia pullus	*0-10*	*rock*	*HV*	*COS*							S		

VIII.5.4 Integrated facies analysis

The facies-type definition of surficial sediments is based on a cluster analysis (N=251; Fig. VIII.5) gathering data from the present study and from the literature (re-analyzed datasets; cf. section Material and methods). In total, six grain-assemblages (F1 to F4 including subgroups F3A, F3B, F4A and F4B) are distinguished (Fig. VIII.7), whose characteristics and interpretations are listed in Tab. VIII.5.

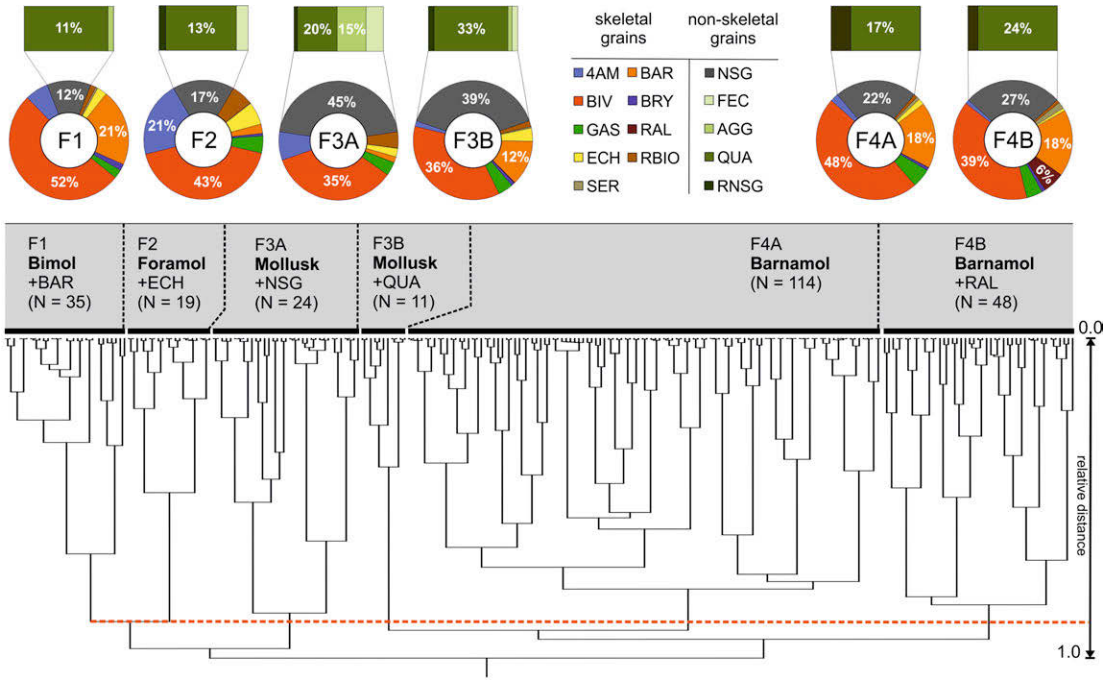

Figure VIII.5: Dendrogram and sediment composition of grain assemblages (F1 to F4B) from the Golfe d'Arguin. The hierarchical clustering follows the Ward's method and is based on 251 sediment samples compiled from Koopmann et al. (1979); Piessens (1979); Michel et al. (2011a, b) and the present study. Abbreviations used: *4AM* foraminifers, *BIV* bivalves, *GAS* gastropods, *BAR* barnacles, *BRY* bryozoans, *RAL* red algae, *ECH* echinoderms, *SER* serpulids, *RBIO* remaining bioclasts, *NSG* non-skeletal grains, *FEC* fecal pellets, *AGG* aggregates, *QUA* siliciclastics, *RNSG* remaining non-skeletal grains.

Table VIII.5: Facies characteristics of analyzed samples collected in the Golfe d'Arguin. Sample dataset is based on surficial sediment samples collected in the late 1970 (Koopman et al. 1979; Piessens 1979) and from two former cruises in 2007 (POS346; Westphal et al. 2007; Michel et al. 2001a, b) and MSM16-3 in 2010 (Westphal et al. 2014; this study). GdA, Golfe d'Arguin; BdA, Banc d'Arguin; BdL, Baie du Lévrier; mbsl, meters below sea level.

Facies	F1	F2	F3A	F3B	F4A	F4B
Number of samples referring to facies	N = 25	N = 19	N = 24	N = 11	N = 114	N = 48
Skeletal grain assemblage	bivalve dominated; bimol grain assemblage	mollusks and benthic foraminifers; foramol grain assemblage	mollusks and non-skeletal grains; mixed mollusk-non-skeletal grain assemblage type A	mollusks and non-skeletal grains; mixed mollusk-non-skeletal grain assemblage type B	mollusks and balanids; barnamol grain assemblage type A	mollusks and balanids; barnamol grain assemblage type B
Depth range (meters below sea level)	subtidal to slope 6 and 161 mbsl	subtidal 15 and 42 mbsl	subtidal to outer shelf 5 and 89 mbsl	subtidal 8 and 38 mbsl	subtidal to outer shelf 13 and 72 mbsl	subtidal 4 and 10 mbsl
Carbonate content (wt% $CaCO_3$)	carbonate content between 16 and 91% (mean=57%)	carbonate content between 11 and 85% (mean=51%)	carbonate content between 1 and 87% (mean=25%)	carbonate content between 11 and 93% (mean=42%)	carbonate content between 1 and 89% (mean=18%)	carbonate content between 1 and 88% (mean=45%)
Skeletal grains (with abundant and minor components)	skeletal grains (88%); incl. bivalves (52%), balanids (21%)	skeletal grains (83%); incl. bivalves (43%), benthic foraminifers (21%), echinoderms (6%)	skeletal grains (55%); incl. bivalves (35%), benthic foraminifers (8%), gastropods (4%)	skeletal grains (61%); incl. bivalves (36%), balanids (12%), gastropods (4%), echinoderms (4%)	skeletal grains (78%); incl. bivalves (48%), balanids (18%)	skeletal grains (73%); incl. bivalves (39%), balanids (18%); calcareous red algae (6%)
Non-skeletal grains (with abundant and minor components)	non-skeletal grains (12%); incl. siliciclastics (11%)	non-skeletal grains (17%); incl. siliciclastics (13%)	non-skeletal grains (45%); incl. siliciclastics (20%), aggregates (16%), pellets (9%)	non-skeletal grains (39%); incl. siliciclastics (33%)	non-skeletal grains (22%); incl. siliciclastics (17%)	non-skeletal grains (27%); incl. siliciclastics (24%)
Grain size range	medium-grained sand to gravel	silt to medium-grained sand	silt to coarse-grained sand	medium-grained sand to gravel	medium-grained sand to gravel	coarse-grained sand to gravel
Grain sorting	moderate to good	moderate to good	poor to moderate	moderate to good	good	moderate to good
Substratum for carbonate producers	sand to gravel	muddy silts to sand	silts to sands	sands	rocky bank-edge	sand with hardgrounds
Occurrences in the Golfe d'Arguin	F1 concentrates in the northern GdA along both, the coast and the outer margin of the BdA. Restricted occurrences are observed in the intertidal areas of the southern BdA (Figs. 4C; 6C, D; 7)	F2 is common in restricted areas in the outer shelf where it covers a corridor off the bank margin that extends from the BdL to the southern BdA following roughly the 30 m isobaths (Figs. 4F; 6G, H; 7)	F3A shows a patchy distribution that is limited to restricted areas within the BdL and the inner BdA (Cuvette d'Arguin) (Figs. 4B; 6, 7)	The distribution of F3B shows no clear pattern with accumulations in the inner southern BdA and intertidal areas (Figs. 4A; 7)	F4A shows a clear pattern extending from Cap Blanc in southward direction along the outer BdA margin to the southern BdA (Figs. 4D; 7)	F4B occurs in the central BdA and a North-South extending corridor in the southern BdA (Figs. 4D; 6E, F, 7)
Facies interpretation	High energetic subtidal environment under the influence of upwelling swell (*Donax*-rich deposits along the bank edge). The limited occurrence of living species is interpreted as sporadic productions related to upwelling-controlled food availability.	Low energetic subtidal environment below the wave base (outer shelf), often preserved in a patchy distribution related to the complex hydraulic regime. Chemosynthetic bivalve taxa indicate constraining conditions (limited light, oxygen, food settings).	Low energetic subtidal environment in the inner shelf setting and BdL where calmer water conditions occur. The high amount of non-skeletal grains (e.g., aggregates and peloids) is interpreted as a shallow basinal setting in proximity of a rocky shore.	Medium energetic subtidal environment widespread over the entire GdA. Often characterized as transition- facies between productive zones and siliciclastic sources (e.g., hinterland, intertidal areas around Tidra Island).	High energetic shallow subtidal environment along the bank-edges that provide extensive rocky outcrops. The accumulation of balanid remains under such strong hydrological conditions indicates a production *in-situ* or close by	Medium energetic shallow subtidal environment with parautochthonous deposits of balanids, mollusks and *in-situ* records of red-algae that argue for eu- to mesophotic conditions. Possibly, offshore extensions of the intertidal flats around Tidra Island.

VIII.6 Discussion

Cool water-related grain assemblages in the GdA highlight a strong environmental control under which marine carbonate-secreting biota have developed. A complex oceanographic regime and the co-occurrence of tropical key-species together with a dominant cool water-related community suggest that temperature-depth relationships alone may not account for the presence of heterozoan carbonates in low latitudes. The following environmental parameters were identified to have an significant effect on the formation of tropical heterozoan carbonates at the GdA: (1) upwelling-induced high nutrient water conditions, (2) low water transparencies due to high Chl-*a* levels and resuspended sediments, (3) a strong hydrological regime, and (4) annual high water temperatures. Additionally, the availability of hard bottoms and other topographical shelf features in the shallow BdA act as steering factors affecting carbonate production. The impact of those controls on benthos ecology, sediment formation, reworking, and distribution results in a characteristic facies zonation (Fig. VIII.7) that is discussed in the following sections.

VIII.6.1 Oceanographic parameters

VIII.6.1.1 Temperature

The remote sensing SST dataset (Fig. VIII.2) and the studies of Cuq (1993), Ould Dedah (1993), and Ould Mahfoudh et al. (1991) showed that water temperatures in the GdA undergo significant seasonal variations. This pattern is attributed to the changing influence of (1) the tropical Guinea Current (<35‰, >24°C); (2) the temperate Canary Current (>35‰, <24°C) coupled with upwelling-induced cool intermediate waters, and (3) shallow subtidal to intertidal coastal waters (BdA and BdL; >39‰, >28°C) heated by solar-driven evaporation. Seasonal displacements of either cold (Canary Current) or warm (Guinean Current) water masses in the GdA thus cause a pronounced hydrographic heterogeneity in both, a spatial and temporal dimension (Sevrin-Reyssac 1993).

The CTD dataset taken in October–November 2010 (MSM16-3) indicates a temperature contrast of up to 5.6°C (18.7–24.3°C; Tab. VIII.2) in the southern BdA. This significant variation in temperature is related to cold upwelled waters (<20°C) and warm coastal waters (>22°C) from the intertidal settings close by. The temperature variation, however, is in agreement with Ould Dedah (1993) reporting a maximum temperature variability of up to 9°C in the southern BdA. Such upwelling-induced cool water intrusions in epicontinental seas cause distinct thermal fronts, to which the benthos adapts by forming 'atypical' eurythermal communities in the shallow bank (cf. Westphal et al. 2010; Michel et al. 2011a; Schäfer et al. 2011; Reijmer et al. 2012; Tab 6). Nonetheless, such

conditions puts intensive stress on most carbonate secreting biota and explains the absence of temperature-sensitive groups (e.g., chlorozoan biota; Halfar et al. 2006).

VIII.6.1.2 Salinity

Similar to water temperature, salinity pattern display distinct variations over the year with values between 35.5 and 37.0‰ for the seaward part of the BdA and values exceeding 38‰ for inshore environments (Ould Dedah 1993). CTD measurements taken in October–November 2010 (MSM16-3) agree with those of previously reported ranges showing a range between 35.1 and 38.0‰ (mean=36.1‰) for the outer BdA and BdL. Again, highest contrasts are identified in the southern BdA, where salinity-depleted waters of the Guinean Current collide with salinity-enriched coastal waters. Highest salinity records are reported from isolated and restricted bays in the innermost BdA such as the semi-enclosed BdSJ, where salinities can exceed 52.0‰ and peak up to 80.0‰ (Sevrin-Reyssac 1993). Apart from these extremes, the salinity contrast in the southern BdA and other nearshore areas under upwelling control (BdL; Tab. VIII.2) is restrictive to stenohaline biota, while euryhaline species (e.g., osmoregulating balanids cf. Anderson (1994), mollusks cf. Michel et al. (2011a), and *Zostera noltii* seagrass meadows cf. Vermaat et al. (1993) prosper under such conditions.

VIII.6.1.3 Nutrients and photic zone

Trophic-controlled settings with eutrophic conditions are known to influence the formation of chlorozoan versus heterozoan communities in tropical marine environments (Hallock and Schlager 1986; Birkeland 1987; Halfar and Ingle 2003; Halfar et al. 2004, 2006; Pomar et al. 2004; Reijmer et al. 2012). The nutrient availability in the GdA is thus the most important steering factor coupled with the following environmental controls: (1) seasonal trade winds that push the Canary Current south of 21°N, inducing upwelling of nutrients (Mittelstaedt 1991; Sevrin-Reyssac 1993; Barton 1998; Martinez et al. 1999; Pastor et al. 2008); (2) calm water conditions during non-upwelling periods that allow waters to stratify and phytoplankton to grow in the photic layer (Huntsman and Barber 1977) and (3) seasonal offshore-directed winds from the Saharan hinterland providing iron-rich dust as additional fertilizer (Sarnthein and Walger 1974; Sarnthein and Diester-Haass 1974; Brust et al. 2011).

Hence, eutrophic waters play a key role in the ecology of the GdA (see also Fig. VIII.2c, d), particularly in those areas where the plankton-enriched water layers can interact with macrobenthic communities in the shallow BdA (cf. Wolff et al. 1993c). These contact zones were identified in the bank-edge along a corridor stretching from north to south between Cap Blanc and Cap Timiris (Fig. VIII.7). Here, the highest Chl-*a* values occur

with peaks of >20 mg/m^3 (Chl-*a*; Fig. VIII.2d). Secchi-disk measurements support the eutrophic to mesotrophic nature of the outer BdA with oligotrophic waters restricted to the innermost shelf where extensive seagrass meadows prosper. This eutrophic environment makes the NW African waters to one of the most productive areas of our oceans (Marañón and Holligan 1999). A high biological productivity (cf. Berghuis et al. 1993) is furthermore indicated by the sedimentological record indicating largely dysoxic and aphotic conditions in the outer shelf of the GdA. Such limiting settings hamper the development of photoautotrophic carbonate biota (e.g., zooxanthellate corals, calcareous green algae, photosymbiont-bearing foraminifera), while filter-feeding, light independent marine organisms prosper. Profiteers are fast growing high nutrient-related mollusks (e.g., chemoautotrophs; cf. Michel et al. 2011a), filter-feeding balanids and bryozoans; cf. Klicpera et al. 2013; 2014).

VIII.6.1.4 Thermocline and hydrodynamic regime

CTD casts taken in the proximal outer shelf and bank environment (topographic nomenclature cf. Hanebuth et al. 2013) show a poor water stratification throughout due to water depths of largely <30 mbsl (Tab. VIII.1). In addition, offshore-directed winds and a M2-type tidal regime (principal lunar semi-diurnal with amplitudes averaging at 1.61 m; Wolff and Smit 1990) result in strong bank-top currents (velocities of >3 m s^{-1}), often appearing as a series of stationary waves of up to 1 m in height along the BdA margin (Westphal et al. 2014). These observations agree with local topographic features such as hardgrounds along bank- and platform margin, occasionally incised by valleys and large-scale gullies at the BdA margin and in the outer shelf (Fig. VIII.1). Moreover, these features are indicative of a complex oceanography with density currents following topographic contours (Peters 1976). The high-energy setting has also been reported by Sevrin-Reyssac (1993) who related the high diversity of marine environments in the BdA to the complex and strong hydrology. Such hydrological conditions, in particular, make it challenging for marine biota prospering under low energy regimes, while infaunal or sessile epifaunal filter-feeding taxa benefit from it.

VIII.6.1.5 Shelf morphology and substrate

Shelf morphology and substrate relationships were shown in Betzler et al. (1997a, b), Pomar (2001), Pomar and Ward (1995), (1999), and Pomar et al. (2004) to be important drivers of carbonate production. While vast areas of the platform-like northern BdA (Fig. VIII.1, transect A) are covered by mixed carbonate-siliciclastic sands, exposed Mid-Pleistocene erosion surfaces along the bank margin provide extensive escarpment structures and hard grounds (details in Hanebuth et al. 2013). Such hard substrates meet the ecological requirements of most hard ground-related biota (e.g., certain bivalves,

balanids, bryozoans) in the GdA and might explain the high amount of balanid grains several tens to up to 100 kilometers away from rocky shoreline (see also Domain 1985; Duineveld et al. 1993; Michel et al. 2011b; Klicpera et al. 2013, 2014).

Towards the southern GdA, the shelf profile turns into a ramp profile (Fig. VIII.1, transect B) with a significant siliciclastic input derived from intertidal settings close-by. The development of a platform in the northern GdA and a ramp in the southern half might be related to different relationships between shelf morphology and biotic settings (see Betzler et al. 1997a, b) or unknown regional differential tectonics (cf. Hanebuth et al. 2013).

VIII.6.1.6 Terrigenous influence

Input of terrigenous material into the GdA occurs throughout the year but increases during winter storms attributed to Harmattan trade winds (Holz et al. 2004; Michel et al. 2009; Mulitza et al. 2010). Lying adjacent to and downwind of the Saharan desert and Sahel zone, the GdA is connected to a large source of silt-sized aeolian dust (Sarnthein and Walger 1974; Sarnthein and Diester-Haass 1974; Glaccum and Prospero 1980), and lies beneath the prevailing dust-loaded wind trajectories. D'Almeida (1989) estimated the amount of Saharan dust at 0.6–0.7 Pg (1 Pg = 10^9 metric tons) $year^{-1}$, of which about one-third is blown into the North Atlantic Ocean (Duce et al. 1991).

The absence of fluvial runoff turns aeolian dust into the only terrigenous source of bioavailable nutrients (e.g., iron and phosphorous-rich dust; Brust et al. 2011). Winnowing and partitioning lead to redistribution across the shelf and to selective downslope transport along topographically and hydrodynamically defined pathways (Michel et al. 2009; Hanebuth and Henrich 2009). More sand-sized terrestrial input comes from migrating siliciclastic dunes that occupy the coastline bordering the innermost BdA (cf. Mount 1984). Minor amounts of siliciclastics are hydrodynamically reworked submarine palaeo-dunes of which some onshore records are exposed in the Cap Blanc area (Westphal et al. 2014).

As a result, resuspended aeolian sediments affect most marine habitats in the BdA thus causing reduced water transparencies and aphotic conditions below 2 mbsl. Such settings are restrictive to light-dependent, sessile and slow-growing organisms, not capable to adapt to high sedimentation rates and low light conditions. In contrast, fast-growing soft-bottom dwellers (e.g., certain infaunal mollusks) non-sensitive to high terrestrial loads and aphotic conditions prosper under such setting.

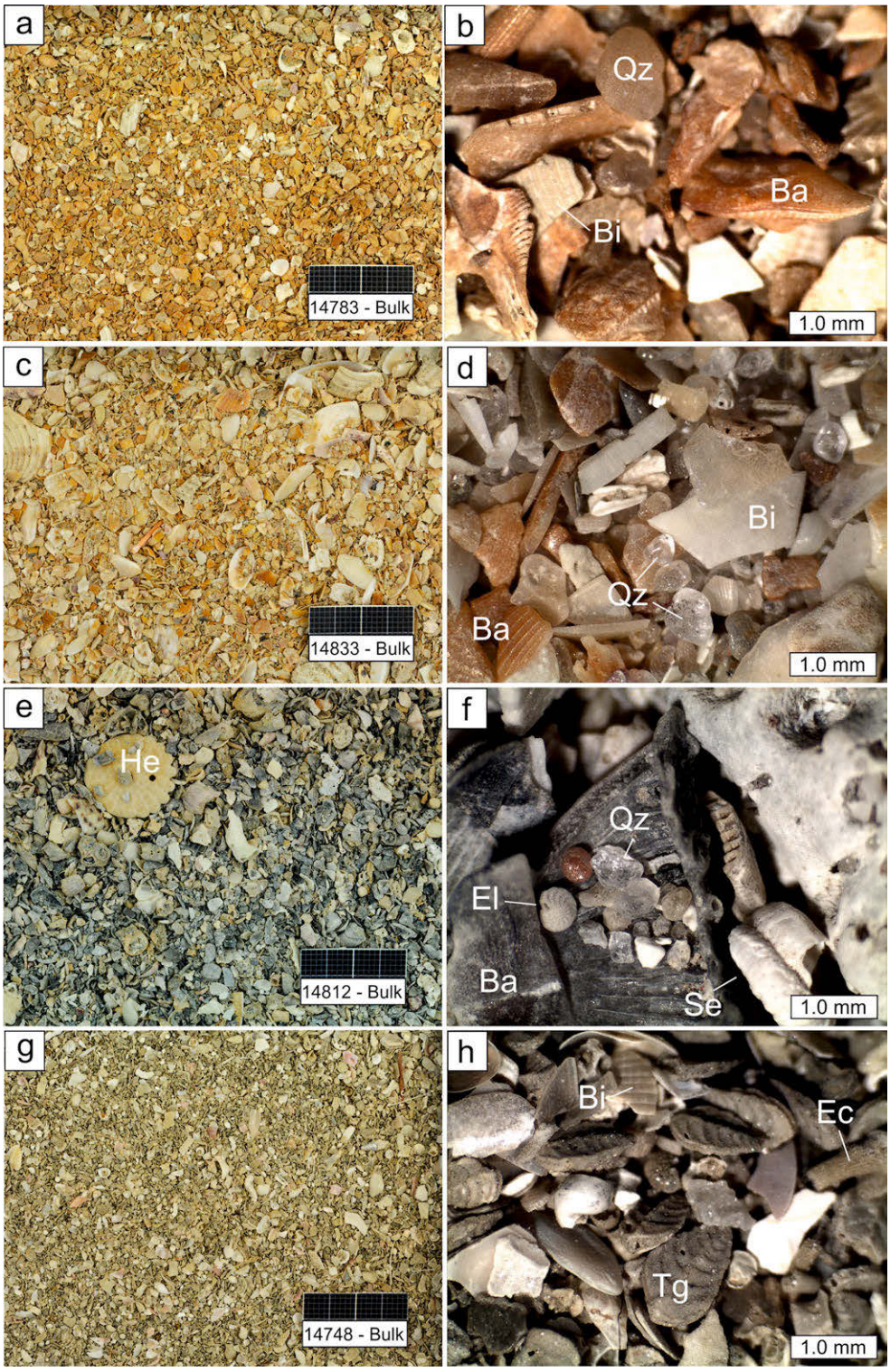

Figure VIII.6: Bulk sediments collected during MSM16-3 cruise along the platform margin (Banc d'Arguin, Mauritania). Baie du Lévrier sample (barnamol assemblage, 14783) in (a, b); central Banc d'Arguin sample (bimol assemblage, 147833) in (c, d); southern Banc d'Arguin sample (barnamol assemblage with siliciclastics, 14812) in (e, f); and Cap Timiris Shelf sample (foramol assemblage with *Tetragonostomina rhombiformis* (Tr), 14748) in (g, h). Abbreviations used: *Qz* quartz, *Ba* balanids, *Bi* bivalve mollusks, *Se* serpulids, *Ec* echinoderm fragments, *He Heliophora* sp., *El Elphidium* sp..

VIII.6.2 Facies distribution across the entire Golfe d'Arguin

Present biogenic sediments, represent a mixture of fresh (Fig. VIII.6c, h; herein called modern) and relict material (Fig. VIII.6a, e; herein called sub-recent) that have been generated in the last several thousand years (detailed radiocarbon ages in Michel et al. 2011a).

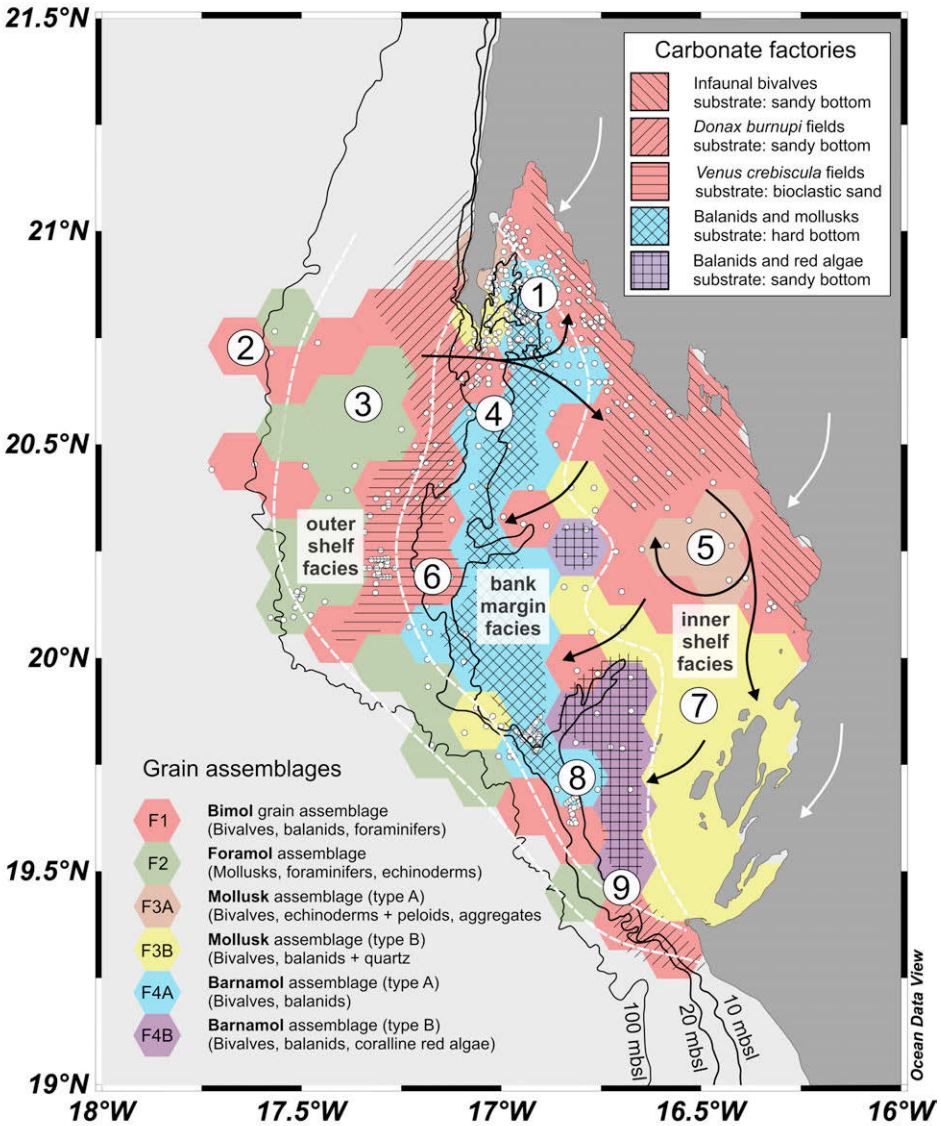

Figure VIII.7: Local distribution of sedimentary facies, grain assemblages and carbonate factories in the Golfe d'Arguin (Mauritania). Black arrows indicate swell and wind-controlled surface currents, white arrows the prevailing wind trajectories; numbers are topographic shelf features: *1* Baie du Lévrier, *2* shelf break (in 80-110 mbsl), *3* outer shelf, *4* Bank d'Arguin margin, *5* inner Banc d'Arguin (Cuvette d'Arguin), *6* central outer Banc d'Arguin, *7* Tidra Island intertidal zone, *8* southern Banc d'Arguin, *9* Cap Timiris shelf; the bank-edge follows roughly the 10-20 m isobaths and the shelf-edge along the 100 m isobaths.

Three larger facies belts are distinguished in the GdA: (1) a mollusk-dominated inner shelf facies, locally enriched in (a) bivalves (F1; northern GdA), (b) mud with peloids and aggregates (F3A, intrabank depression) or (c) siliciclastics (F3B, southern GdA and intertidal plains); (2) a bank margin facies characterized by (a) high amounts of balanids and mollusks (F4A) and (b) enrichments in coralline red algae (F4B, southern BdA); and (3) an outer shelf facies showing scattered parautochthonous and allochthonous skeletal material (benthic foraminifers, mollusks, echinoderms) in silty to fine-sandy siliciclastic material (Figs. 7, 8).

VIII.6.2.1 Inner shelf facies

The inner shelf shows contrasting marine environments. Bimol grain assemblages (F1) dominate and cover more than 50% of the inner shelf facies (Fig. VIII.7, Tab. VIII.5). North of 20°N, the GdA (including bank-margin and outer shelf areas) is covered by up to 75% of sediments referring to the assemblage F1. This pattern coincides with the maximum southward displacement of the Canary Current during winter (Mittelstaedt 1991; Hagen 2001; Pastor et al. 2008), which is known to induce upwelling offshore and thus pushes the primary production. Trajectories of oceanic swell and surface currents suggest that the inner shelf bivalve community is linked to food-enriched waters provided by upwelling (Fig. VIII.7). Such bimol assemblages are also known from other modern upwelling regions such as the Western Sahara shelf (Summerhayes et al. 1976), the southern Australian shelf (James et al. 1992; 2001), the Gulf of California (Halfar et al. 2004, 2006) or the Gulf of Panama (Reijmer et al. 2012) and clearly demonstrate that a high-productive but low-diverse bimol assemblage can exist in low latitudes.

Parts of the innermost shelf (Cuvette d'Arguin; Fig. VIII.1) show increasing water depths (>20 mbsl) with a low-energy mollusk grain assemblage (F3A) dominated by benthic foraminifers, aggregates and peloid grains in a very fine-grained matrix (Fig. VIII.7, Tab. VIII.5). These elements indicate calm hydrological conditions below storm wave-base, a setting limited to restricted marine environments in the Cuvette d'Arguin and in the BdL that are protected from oceanic swell (Aleman et al. 2014).

The southern inner shelf facies around Tidra Island is characterized by intertidal conditions with extensive seagrass plains and a dominant siliciclastic input. The sedimentary cover shows an undifferentiated infaunal mollusk grain assemblage (F3B) with high contents of terrestrial quartz grains due to the proximity to the desertic hinterland (Fig. VIII.7, Tab. VIII.5). Seagrass plains (*Zostera noltii*) represent the largest primary producer of organic carbon (Wolff and Smit 1990) and provide similarly a rich food resource and habitat for intertidal mollusk and decapod species. The abundant bivalve *Anadara senilis,* for example, provides a biomass contribution of (8.1 g m^{-2} ash free dry weight = 48% of total tidal flat total biomass; Wolff et al. 1993b) thus representing the

most important macrobenthic mollusk taxon in the intertidal inner shelf and a main contributor nearshore bimol assemblages.

VIII.6.2.2 Bank-margin facies

The facies distribution in the outer BdA shows a dominant barnamol assemblage (F4A; Fig. VIII.7; Tab. VIII.5) that covers the entire bank-margin (10-20 mbsl) along a narrow corridor from the BdL over the central BdA down to the CTS (19.5°N). Exposed Mid-Pleistocene erosion surfaces provide submarine hardgrounds along the bank margin that favor the development of a light-independent and suspension-feeding balanid community, able to cope with strong hydrodynamics and eutrophic conditions. Modern and sub-recent balanid remains (mostly preserved as disarticulated plates) are ubiquitous in all samples from the bank-margin and BdL and indicate an important, yet relatively poorly investigated contributor of carbonate. Although barnamol assemblages are usually associated with cool-temperate water regimes (cf. Hayton et al. 1995), balanids are today cosmopolitan players due to human-mediated translocations (Carlton et al. 2011).

Larger bimol grain assemblages (F1, Fig. VIII.7) appear close to upwelling hotspots (south of Cap Blanc and in the CTS area) and indicate high-nutrient settings by an often-dominant appearance of *Donax burnupi* (1-40 mbsl) and *Venus crebrisulca* (4-25 mbsl). The ecological requirements of these two species agree with upwelling conditions; they are known for their high productivity in nutrient-rich waters (cf. Ansell 1983).

Towards the southern BdA, barnamol assemblages are enriched in remains of calcareous red algae (F4B; Fig. VIII.7; Tab. VIII.5). Although the presence of red algae could not be confirmed by the MSM16-3 cruise, a number of studies provide data on restricted red-algae occurrences (Piessens 1979; Koopmann et al. 1979; John et al. 2004). Some even confirm the presence of Maërl-forming taxa (e.g, *Lithothamniom* sp.; *Lithophyllum* sp.) in the outer BdA (Birkett et al. 1998; Jackson 2003; Goudswaard 2007). Based on the component analysis of GdA-wide data, red-algal contents remain low (<3% in the inner BdA) with restricted enrichments of up to >50% (fractions >500 µm; Fig. VIII.4e) in the southern BdA (Piessens 1979).

VIII.6.2.3 Outer shelf facies

The outer shelf (>30 mbsl) shows sediments with a fine-grained quartzose texture and scattered reworked bioclasts of the foramol assemblage (F2; Figs. 4g, h; 7; Tab. VIII.5). Skeletal grains are largely reworked by biological (e.g., boring sponge *Cliona* sp.) and physical abrasive processes, implying that the material originates from remote production areas (e.g., bank-, nearshore environments). Such processes were shown in

Hallock (1988) to significantly influence carbonate production and accumulation, especially under eutrophic tropical conditions. The outer shelf thus acts as a large-scale depositional plane for parautochthonous and allochthonous skeletal and fine-clastic material (e.g., AMW, TMW; Fig. VIII.8) deposited under comparatively little hydrodynamic activity und below the storm-wave base (Michel et al. 2009). The presence of endobenthic chemosymbiotic bivalves (e.g., *Anodontia* sp., *Solemya togata*) in the outer shelf underlines the constraining nature of this environment characterized by an upwelling-induced high productivity with resulting dysoxic and aphotic sea bottom conditions (Fig. VIII.7, and Fig. VIII.8).

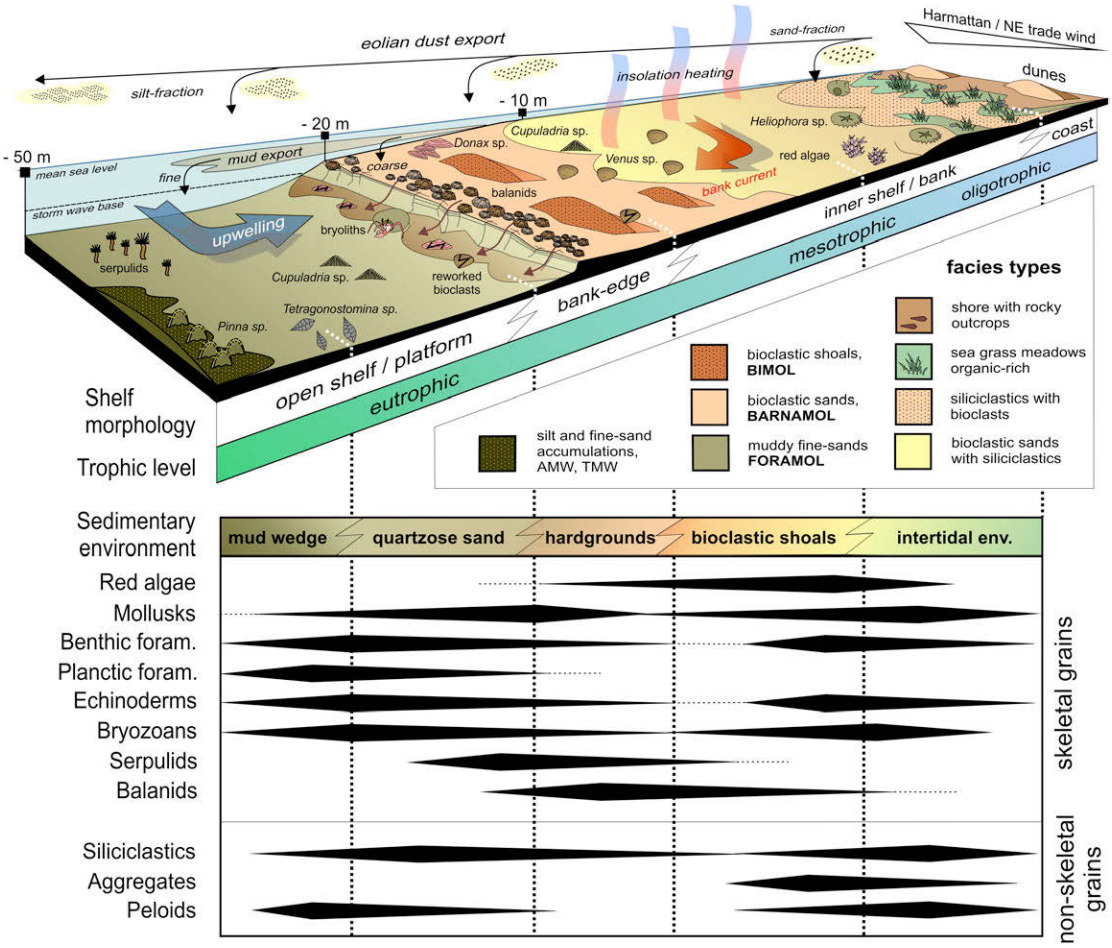

Figure VIII.8: Facies model of an idealized transect from the outer shelf (platform environment; 20-50 mbsl) over the bank-edge in 10-20 mbsl to the inner shelf (Banc d'Arguin; <10 mbsl) and intertidal plains of the coastal-near environments (<5 mbsl). Skeletal and non-skeletal grains characterize the depositional environments and define grain assemblages that organize in related facies zones cf. Fig. VIII.7.

VIII.6.3 Past and present tropical heterozoan carbonate systems

The sedimentary composition in the GdA largely corresponds to the temperate-water foramol association *sensu* Lees and Buller (1972). Within this association, distinct heterozoan grain assemblages exist, whose constituents show both, elements typical of extra-tropical carbonates (e.g., mollusks, balanids, bryozoans, foraminifers, red algae), and tropical indicators (e.g., tropical bivalves and gastropods), see Kindler and Wilson (2010) for details. This dichotomy suggests that modern heterozoan carbonate formation is not straightforward, and that classical depositional models *sensu* Lees and Buller (1972) or James (1997) should be used carefully and with critical reflection. As shown in this study, the oceanographic setting largely overprints carbonate formation by seasonally shifting thermal fronts, intermittent mixing processes and an upwelling-induced high-nutrient regime causing low light conditions. Coastal environments, in contrast, are less influenced by upwelling phenomena, but show more terrestrial influences.

This 'atypical' modern carbonate production is reflected best in the diversity pattern of bivalves representing ubiquitous components in all samples from the GdA. Their biodiversity is remarkably low (approx. 200 species; cf. Michel et al. 2011a, b) compared to other tropical and sub-tropical locations (650-1200 species cf. Crame 2000), while their composition shows cosmopolitan-, and endemic NW African and tropical taxa (Tab. VIII.4, Suppl. XVII.3).

Table VIII.6: Selected modern and ancient heterozoan carbonates in subtropical to tropical warm-water settings. Data extracted from Westphal et al. (2010) and Reijmer et al. (2012).

Location	Latitude/ Longitude	Temp (°C)	Chl-a (mg/m3)	Trophic regime	Carbonate grain	Environmental steering factors	Period (Age)	Reference
Golfe d'Arguin (NW-African Shelf)	20 °7'N 16° 59'W	<18 – >26	3 – >10	mesotrophic to eutrophic	foramol, bimol, barnamol	upwelling, dust-input	modern	this study; Michel et al. 2011a
Gulf of Panama	8° 7'N 79° 34'W	20 – 28	0.2 – >10	mesotrophic to eutrophic	foramol, barnamol	upwelling	modern	Reijmer et al. 2012
Gulf of California	27° 50 'N 111° 58'W	10 – <19	<1 – 1.5	oligotrophic to eutrophic	chlorozoan	upwelling	modern	Halfar et al. 2006
Gulf of Mexico (Yucatan Shelf)	22° 22'N 88° 31'W	17 – 30	1	mesotrophic to eutrophic	foramol	upwelling	modern	Logan et al. 1969
Gulf of Mexico (West Florida Shelf)	27° 44'N 84° 3'W	18 – 30	0.5	mesotrophic	chloralgal	nutrients fluvial input	modern	Goud and Steward 1956
Gulf of Mexico (Nicaragua Rise)	14° 8'N 82° 16'W	25 – 30	0.2 – 0.3	oligotrophic to mesotrophic	chloralgal	upwelling	modern	Hallock et al. 1988
Balearic Islands (W-Mediterranean)	39° 21'N 2° 4'E	tropical	changing trophic conditions		foramol, rhodalgal, chlorozoan	changing climate, terrigenous input	Miocene	Pomar et al. 2004
Latium-Abruzzi Platform (Apennines)	41° 51'N 13° 53'E	subtropical to tropical	change from oligotrophic to eutrophic settings		foramol, rhodalgal, chlorozoan	orogenic activity	Miocene	Brandano and Corda 2002

Such a pattern is characteristic of eutrophic marine environments favoring the development of high productive filter-feeding communities (e.g., bivalves, balanids, bryozoans) that are adapted to only sporadic food availability and changing hard substrate availability. Similar heterozoan carbonate environments are known from other modern and ancient settings worldwide (see also Tab. VIII.6). The carful analysis of carbonate sediments including associated drivers and players, ideally on species level, is the key to identify the environmental context and to achieve a robust reconstruction or palaeoenvironmental settings. The GdA provides such a valuable example for a world without coral reefs and thus serves as a modern analogue for conditions preserved in the fossil record.

VIII.7 Conclusions

(1) Modern heterozoan carbonates in the tropical Golfe d'Arguin off northern Mauritania are characterized by a strong multi-dimensional control that is attributed to upwelling-induced eutrophic settings, illuminations and tropical water temperatures governing a shallow marine carbonate factory (Banc d'Arguin).

(2) A characteristic foramol association with distinct bimol and barnamol grain assemblages in the shallowest areas exists. Dominant components are bivalves, balanids, benthic foraminifers and other filter feeders – subordinate components are serpulids, echinoderms and red algae. Photosymbiotic organisms such as zooxanthellate corals are entirely absent, although the setting is tropical.

(3) By combining new and existent surface sediment data, we could reconstruct the full sediment pattern in the Golfe d'Arguin. Sedimentary components are mixed carbonate-siliciclastic showing a well-adapted, light independent marine biota whose skeletal remains are organized in six mollusk-dominated assemblages and along three larger facies belts.

(4) This modern analogue of a tropical heterozoan carbonate system demonstrates the response of a shallow marine ecosystem to eutrophication and desertification. Moreover, it clearly demonstrates that a "cool water-related" heterozoan carbonate fauna can exist in low-latitude high-nutrient settings. It thus provides invaluable insights for the classification and interpretation of tropical eutrophic settings in the fossil record and provides an important model for future perspectives in the context of climate change.

VIII.8 Acknowledgements

Participants and crew of the Maria S. Merian Cruise MSM-16 leg 3 are acknowledged for providing support. We are grateful to the Mauritanian authorities for their permission to carry out research in their territorial waters. Many thanks are due to Abdoul Dia from the Mauritanian Institute for Oceanographic Research (IMROP) for his collaboration during the cruise. Thanks to Michael Sarnthein (University of Kiel) for providing additional sample material. Nicolas Aleman and Raphaël Certain (both CEFREM, Perpignan) are acknowledged for additional bathymetric data. The manuscript benefitted immensely from reviews by Franz T. Fürsich (GeoZentrum Nordbayern) and one anonymous reviewer. The DFG Senate Commission on Oceanography is thanked for providing funding for the research cruise to HW. This project was partial funded through the DFG Research Center/Cluster of Excellence MARUM (Sediment Dynamics, SD2) and is part of the PhD thesis of AK.

VIII.9 References

Acker JG, Leptoukh G (2007) Online analysis enhances use of NASA Earth science data. Eos Trans Am Geophys Union 88:14–17. doi:10.1029/2007EO020003

Aleman N, Certain R, Courp T, et al. (2010) Le Golfe d'Arguin: Carte morpho-bathymétrique 1/250

Aleman N, Certain R, Dia A, Barusseau JP, Courp T (2014) Post-glacial filling of a semi-enclosed basin: The arguin basin (Mauritania). Mar Geol 349:126–135

Anderson DT (1994) Barnacles: Structure, function, development and evolution. Chapman and Hall, London, 357 p

Ansell, AD (1983) The biology of the genus Donax. In: McLachlan A, Erasmus T, (eds) Sandy beaches as ecosystems. Dr .W. Junk Publishers, The Hague pp 607–636

Barange M, Field J, Harris R, Hofmann E (2010) Marine ecosystems and global change. Oxford University Press, Oxford

Barton ED (1998) Eastern boundary of the North Atlantic: Northwest Africa and Iberia. In: Robinson AR, Brink KH (eds) The Sea. JohnWiley & Sons Inc., New York, pp 633–657

Barusseau J-P, Vernet R, Saliège J-F, Descamps C (2007) Late Holocene sedimentary forcing and human settlements in the Jerf el Oustani Ras el Sass region (Banc d'Arguin, Mauritania). Géomorph Reli Process Environ 7:7–18

Berghuis EM, Duineveld GCA, Hegeman J (1993) Primary production and distribution of phytopigments in the water column and sediments on the upwelling shelf off the Mauritanian coast (Northwest Africa). Hydrobiologia 258:81–93

Betzler C, Brachert TC, Braga JC, Martin JM (1997a) Nearshore, temperate, carbonate depositional systems (lower Tortonian, Agua Amarga Basin, southern Spain): implications for carbonate sequence stratigraphy. Sediment Geol 113(1-2):27-53

Betzler C, Brachert TC, Nebelsick J (1997b) The warm temperate carbonate province: A review of the facies, zonations, and delimitations. Cour Forsch-Inst Senckenberg 201:83-99

Betzler C, Braga JC, Jaramillo-Vogel D, Romer M, Hubscher C, Schmiedl G, Lindhorst S (2011) Late Pleistocene and Holocene cool-water carbonates of the Western Mediterranean Sea. Sedimentology 58(3):643-669

Blott SJ, Pye K (2001) GRADISTAT: a grain size distribution and statistics package for the analysis of unconsolidated sediments. Earth Surf Proc Land 26(11):1237-1248

Blott SJ, Croft DJ, Pye K, et al. (2004) Particle size analysis by laser diffraction. Geol Soc Lond Spec Publ 232:63–73. doi: 10.1144/GSL.SP.2004.232.01.08

Birkeland C (1987) Nutrient availability as a major determinant of differences among coastal hard-substratum communities in different regions of the tropics. In: Birkland C (ed) Differences between Atlantic and Pacific tropical marine coastal ecosystems: Community Structure, Ecological Processes and Productivity. UNESCO Reports in Marine Science, Paris, pp 45–90

Birkett DA, Maggs CA, Dring MJ (1998) Maerl (volume V). An overview of dynamic and sensitivity characteristics for conservation management of marine SACs. Scot Ass for Mar Sci (UK Marine SACs Project), pp 1–116, (www.english-nature.org/uk-marine/reports/pdfs/maerl.pdf)

Brandano M, Corda L (2002) Nutrients, sea level and tectonics: constrains for the facies architecture of a Miocene carbonate ramp in central Italy. Terra Nova 14:257–262

Brandano M, Frezza V, Tomassetti L, Cuffaro M (2009) Heterozoan carbonates in oligotrophic tropical waters: The Attard member of the lower coralline limestone formation (Upper Oligocene, Malta). Palaeogeogr Palaeoclimatol Palaeoecol 274:54–63. doi:10.1016/j.palaeo.2008.12.018

Brust J, Schulz-Bull DE, Leipe T, Chavagnac V, Waniek JJ (2011) Descending particles: From the atmosphere to the deep ocean - a time series study in the subtropical NE Atlantic. Geophys Res Lett, 38:L06603. doi:10.1029/2010gl045399

Carlton JT, Newman WA, Pitombo FB (2011). In the wrong place - alien marine crustaceans: Distribution, biology and impacts. Springer Netherlands, Dordrecht. doi:10.1007/978-94-007-0591-3

Chave K (1967) Recent carbonate sediments: an unconventional view. Geol Educ 5:200–204

Crame JA (2000) Evolution of taxonomic diversity gradients in the marine realm: Evidence from the composition of Recent bivalve faunas. Paleobiology 26:188–214

Cuq F (1993) Remote sensing of sea surface and coastal features in the area of the Golfe d'Arguin, Mauritania. Hydrobiologia 258:33–40

D'Almeida GA (1989) Desert aerosol: characteristics and effects on climate. In: Leinen M, Sarnthein M (eds) Palaeoclimatology and palaeometeorology: Modern and past patterns of global atmospheric transport. Kluwer Academic Publishers, Dordrecht, pp 311–338

Duineveld GCA, De Wilde PAWJ, Berghuis EM, Kok, A (1993) The benthic infauna and benthic respiration off the Banc d'Arguin (Mauritania, Northwest Africa). Hydrobiologia 258:107–117
Domain F (1985) Carte sédimentologigue du plateu continental Mauretanien 1:200.000. Nouadhibou
Doney SC, Ruckelshaus MJ, Duffy E, et al. (2012) Climate change impacts on marine ecosystems. Ann Rev Mar Sci 4:11–37. doi:10.1146/annurev-marine-041911-111611
Duce RA, Liss PS, Merrill JT, Atlas EL, Buat-Menard P (1991) The atmospheric input of trace species to the world ocean. Global Biochem Cycles 5:193–259
Einsele G, Herm D, Sarnthein M, Schwarz HU (1972) Bericht über die Landesexpedition nach Senegal und Mauretanien in Ergänzung zur Meteorfahrt 25/71.- Techn Bericht Deutsche Forschungsgemeinschaft 1-28
Edinger EN Copper P, Risk MJ, Atmojo W (2002) Oceanography and reefs of recent and Paleozoic tropical epeiric seas. Facies 47:127–149
Flügel E (2010) Microfacies of carbonate rocks: analysis, interpretation and application. Springer, Berlin, Heidelberg
Fourqurean JW, Duarte CM, Kennedy H, et al. (2012) Seagrass ecosystems as a globally significant carbon stock. Nature Geosci 5:505–509. doi: 10.1038/ngeo1477
Gattuso JP, Hansson L (2011) Ocean acidification. Oxford University Press, Oxford.
Gilman EL, Ellison J, Duke NC, Field C (2008) Threats to mangroves from climate change and adaptation options: A review. Aquat Bota 89:237–250. doi: 10.1016/j.aquabot.2007.12.009
Glaccum RA, Prospero JM (1980) Saharan aerosols over the tropical north Atlantic. Mineral Mar Geol 37:295–321
Gould HR, Steward RH (1956) Continental terrace sediments in the northeastern Gulf of Mexico. In: Hough JL, Menard HW (eds) Finding ancient shore lines, vol 3. SEPM Special Publication, pp 2–19
Goudswaard PC, Smaal AC, Wagué A (2007) The ecological implications of exploitation of the bivalve *Venus rosalina* in Mauritanian waters, Report No. C124A-07.Wageningen Imares, Amsterdam, 132 p
Gruvel A (1912) Mission Gruvel sur la cote occidentale d'Afrique (1909–1910) et collection du Museum d'histoire naturelle Les Cirrhipedes. Bull Mus Hist Nat Paris 18:344–350
Hagen E (2001) Northwest African upwelling scenario. Oceanol Acta 24:113–128
Halfar J, Godinez-Orta L, Mutti M, et al. (2004) Nutrient and temperature controls on modern carbonate production: An example from the Gulf of California, Mexico. Geology 32:213-216. doi:10.1130/G20298.1
Halfar J, Godinez-Orta L, Mutti M, Valdez-Holguin JE, Borges JM (2006) Carbonates calibrated against oceanographic parameters along a latitudinal transect in the Gulf of California, Mexico. Sedimentology 53:297–320
Halfar J, Ingle Jr. JC (2003) Modern warm-temperate and subtropical shallow-water benthic foraminifera of the Southern Gulf of California, Mexico. J Foram Res 33(4):309-329
Hall-Spencer JM (1998) Conservation issues relating to maerl beds as habitats for molluscs. Journal of Conchology, Spec Publ 2: 271–286
Hallock P (2005) Global change and modern coral reefs: New opportunities to understand shallow-water carbonate depositional processes. Sediment Geol 175:19–33. doi:10.1016/j.sedgeo.2004.12.027
Hallock P (1988) The role of nutrient availability in bioerosion: consequences to carbonate buildups. Palaeogeogr Palaeoclimatol Palaeoecol 63:275–291
Hallock P, Hine AC, Vargo GA, Elrod JA, Jaap WC (1988) Platforms of the Nicaraguan rise: examples of the sensitivity of carbonate sedimentation to excess trophic resources. Geology 16:1104–1107
Hallock P, Schlager W (1986) Nutrient excess and the demise of coral reefs and carbonate platforms. Palaios 1:389–398
Hanebuth TJJ, Mersmeyer H, Kudrass HR, Westphal H (2013) Aeolian to shallow-marine shelf architecture off a major desert since the Late Pleistocene (northern Mauritania). Geomorphology 203:132–147
Hanebuth TJJ, Henrich R (2009) Recurrent decadal-scale dust events over Holocene western Africa and their control on canyon turbidite activity (Mauritania). Quat Sci Rev 28:261–270. doi:10.1016/j.quascirev.2008.09.024
Hanebuth TJJ, Lantzsch H (2008) A Late Quaternary sedimentary shelf system under hyperarid conditions: Unravelling climatic, oceanographic and sea-level controls (Golfe d'Arguin, Mauritania, NW Africa). Mar Geol 256:77–89. doi:10.1016/j.margeo.2008.10.001
Hayton S, Nelson C, Hood S (1995) A skeletal assemblage classification system for non-tropical carbonate deposits based on New Zealand Cenozoic limestones. Sed Geol 100:123–141
Hoegh-Guldberg O, Mumby PJ, Hooten J, et al. (2007) Coral reefs under rapid climate change and ocean acidification. Science 318:1737–42. doi: 10.1126/science.1152509
Holz C, Stuut JW, Henrich R (2004) Terrigenous sedimentation processes along the continental margin off NW Africa: implications from grain-size analysis of seabed sediments. Sedimentology 51:1145–1154

Huntsman SA, Barber RT (1977) Primary production off northwest Africa: the relationship to wind and nutrient conditions. Deep-Sea Res 24:25–33
IMROP (2013) Atlas maritime des zones vulnérables en Mauritanie—Un appui à la gestion écosystémique et équitable. IMROP, Nouhadibou, Mauritania, 156 p
Jackson A (2003) BIOTIC Species Information for Lithothamnion corallioides. (http://www.marlin.ac.uk/biotic/)
James NP, Clarke JAD (1997) Cool-water carbonates. SEPM Spec Publ No. 56
James NP, Bone Y, Von der Borch CC, Gostin VA (1992) Modern carbonate and terrigenous clastic sediments on a cool water, high energy, mid- latitude shelf: Lacepede, southern Australia: Sedimentology 39:877–903
James NP, Bone Y, Collins LB, Kyser TK (2001) Surficial sediments of the Great Australian Bight: Facies dynamics and oceanography on a vast cool-water carbonate shelf: J Sediment Res 71:549–567
John DM, Prud'homme van Reine WF, Lawson GW, Kostermans TB, Price JH (2004) A taxonomic and geographical catalogue of the seaweeds of the western coast of Africa and adjacent islands. Beih Nova Hedwigia 127:1–139
Kindler P, Wilson MEJ (2010) Carbonate grain associations: their use and environmental significance, a brief review. In: Mutti M, Pliller WE, Betzler C (eds), Carbonate Systems During the Oligocene-Miocene Climate Transition. Int Assoc Sedimentol Spec Publ. Wiley-Blackwell, Chichester (West Sussex), pp 35–48
Klicpera A, Taylor PD, Westphal H (2013) Bryoliths constructed by bryozoans in symbiotic associations with hermit crabs in a tropical heterozoan carbonate system, Golfe d'Arguin, Mauritania. Mar Biodiv 43:429–444. doi:10.1007/s12526-013-0173-4
Klicpera A, Taylor PD, Westphal H (2014) Bryozoans on the move: Adaptations to hard substrate-limiting tropical heterozoan carbonates (Banc d'Arguin, Mauritania) Mar Biodiv. doi:10.1007/s12526-014-0279-3
Koopmann BJ, Sarnthein M, Schrader H (1978) Sedimentation influenced by upwelling in the subtropical Baie du Levrier (West Africa) In: Boje R, Tomczak M (eds) Upwelling Ecosystems, Proc III Int Symp. Springer Verlag, pp 282-288
Koopmann BJ, Lees A, Piessens P, Sarnthein M (1979) Skeletal carbonate sands and wind-derived silty marls off the Saharan coast: Baie du Léevrier, Arguin Platform, Mauritania. Meteor Forsch-Ergebn C:15–57
Lees A, Buller AT (1972) Modern temperate-water and warm-water shelf carbonate sediments contrasted. Mar Geol 13:M67–M73
Logan BW, Harding JL, Ahr WM, Williams JD, Snead RG (1969) Late Quaternary sediments of Yucatan Shelf, Mexico. In: Bass MN, Cebulski DE, McBirney AR (eds) Carbonate sediments and reefs, vol 11. Yucatan Shelf, Mexico. AAPG Memoir, pp 5–128
Maigret J (1972) Campagnes expérimentale de pêche des sardinelles et autres espèces pélagiques (juillet, 1970-octobre 1971). Tome I. Observations concernant l'océanographie et la biologie des espèces. Sec Stat Aff Etrang France; Mis Pêche et Mar March; Mauritanie. SCET- International, BCE P 083, Paris pp 140
Marañón E, Holligan PM (1999) Photosynthetic parameters of phytoplankton from 50N to 50S in the Atlantic Ocean. Mar Ecol Progr Ser 176:191–203
Martín JM, Braga JC, Betzler C (2001) The Messinian Guadalhorce corridor: the last northern, Atlantic-Mediterranean gateway. Terra Nova 13(6):418-424
Martín JM, Braga JC, Betzler C, Brachert T (1996) Sedimentary model and high-frequency cyclicity in a Mediterranean, shallow-shelf, temperate-carbonate environment (uppermost Miocene, Agua Amarga Basin, southern Spain). Sedimentology 43(2):263-277
Martinez P, Bertrand P, Shimmield GB, et al. (1999) Upwelling intensity and ocean productivity changes off Cape Blanc (northwest Africa) during the last 70,000 years: geochemical and micropalaeontological evidence. Mar Geol 158:57–74
Michel J, Vicens GM, Westphal H (2011a) Modern heterozoan carbonates from a eutrophic tropical shelf (Mauritania). J Sediment Res 81:641-655. doi:10.2110/jsr.2011.53
Michel J, Westphal H, Von Cosel R (2011b) The mollusk fauna of soft sediments from the tropical, upwelling-influenced shelf of Mauritania (northwestern Africa). Palaios 26:447–460. doi:10.2110/palo.2010.p10-148r
Mittelstaedt E (1991) The ocean boundary along the northwest African coast: Circulation and oceanographic properties at the sea surface. Progr Oceanogr 26:307–355. doi:10.1016/0079-6611(91)90011-A.
Mount JF (1984) Mixing of siliciclastic and carbonate sediments in shallow shelf environments. Geology 12:432–435
Mulitza S, Heslop D, Pittauerova D, et al. (2010) Increase in African dust flux at the onset of commercial agriculture in the Sahel region. Nature 466:226–8. doi:10.1038/nature09213

Müller G, Gastner M (1971) The "Karbonate-Bombe", a simple device for the determination of the carbonate content in sediments, soils and other materials. N Jb Miner Mh 10:446–469
Mutti M, Hallock P (2003) Carbonate systems along nutrient and temperature gradients: some sedimentological and geochemical constraints. Int J Earth Sci 92:465–475. doi:10.1007/s00531-003-0350-y
Myers N, Mittermeier RA, Mittermeier CG, et al. (2000) Biodiversity hotspots for conservation priorities. Nature 403:853–8. doi:10.1038/35002501
Nelson CS (1988). An introductory perspective on non-tropical shelf carbonates. Sediment Geol 60:3–12.
Nelson CS, Keane SA, Philip SH (1988) Non-tropical carbonate deposits on the modern New Zealand shelf. Sediment Geol 60:71–94
Ould Dedah S (1993) Wind, surface water temperature, surface salinity and pollution in the area of the Banc d'Arguin, Mauritania. Hydrobiologia 258:9–19
Ould Dedah S, Dobrovine B (1992) Atlas hydrologique des eaux superficielles de la Baie du Lévrier. Département Ressources et Environment et Laboratoire d'Hydrologie et Environment, Centre National de Recherches Oceanographiques et des Peches (IMROP); http://hdl. handle.net/1834/516
Ould Mahfoudh MOTS, Dobrovine B, Ould Dedah S (1991) Atlas hydrologique des eaux superficielles du Banc d'Arguin. Département Ressources et Environment et Laboratoire d'Hydrologie et Environment, Centre National de Recherches Oceanographiques et des Peches (IMROP); http://hdl. handle.net/1834/518
Pastor M, Pelegri J, Hernandezguerra A, et al. (2008) Water and nutrient fluxes off Northwest Africa. Continenta Shelf Res 28:915–936. doi:10.1016/j.csr.2008.01.011
Perry C, Taylor K (2009) Environmental sedimentology. Wiley, New York
Peters H (1976) The spreading of the water masses of the Banc d'Arguin in the upwelling area off the northern Mauritanian coast. Meteor Forsch Ergebn 18:78–100
Piessens P, Chabot AG (1977) Bathymetry and sediments of the Arguin Platform, Mauritania, West Africa. Mém Inst Géol Univ Louvain 29:369–379
Piessens P (1979) Influence relative des sources de production et du transport dans la formation de faciès calcaires biogéniques: les sédiments quaternaires de la plate-forme d'Arguin (Mauritanie) et comparaison avec des régions côtières européennes (Irlande et Hébrides). Ph.D. thesis, Université Catholique de Louvain, Louvain-la-Neuve, 133 p
Prévost (1746) Carte de la Coste occidentale d'Afrique Depuis le Cap Blanc jusqu'a Tanit
Pomar L (2001) Types of carbonate platforms: a genetic approach. Basin Res 13:313–334. doi:10.1046/j.0950091x.2001.00152.x
Pomar L, Brandano M, Westphal H (2004) Environmental factors influencing skeletal grain sediment associations: a critical review of Miocene examples from the western Mediterranean. Sedimentology 51:627–651. doi:10.1111/j.13653091.2004.00640.x
Pomar L, Ward W (1995) Sea-level changes, carbonate production and platform architecture: the Llucmajor platform, Mallorca, Spain. Sequence stratigraphy and depositional response to eustatic, tectonic and climatic forcing. Academic Press, Dordrecht, 87 p
Pomar L, Ward W (1999) Reservoir-scale heterogeneity in depositional packages and diagenetic patterns on a reef-rimmed platform, upper Spain Miocene, Mallorca. Bull AAPG 83:1759–1773
Proske U, Hanebuth TJJ, Meggers H, Leroy SAG (2008) Tidal flat sedimentation during the last millennium in the northern area of Tidra Island, Banc d'Arguin, Mauritania. J. Afri Earth Sci. 50:37–48. doi:10.1016/j.jafrearsci.2007.09.002
Reijmer JJG, Bauch T, Schäfer P (2012) Carbonate facies patterns in surface sediments of upwelling and non-upwelling shelf environments (Panama, East Pacific). Sedimentology 59:32–56. doi:10.1111/j.1365-3091.2010.01214.x
Samankassou E (2002) Cool-water carbonates in a paleoequatorial shallow-water environment: The paradox of the Auernig cyclic sediments (Upper Pennsylvanian, Carnic Alps, Austria-Italy) and its implications. Geology 30(7):655–658
Sarnthein M, Walger, E (1974) Der äolische Sandstrom aus der W-Sahara zur Atlantikküste. Geol Rdsch 63:1065-1087
Sarnthein M, Diester-Haass, L (1977) Eolian-sand turbidites. J Sed Petrology 47:868-890
Schlitzer R (2012) Ocean Data View (ODV). http://odv.awi.de
Scholle PA, Bebout DG, Moore CH (eds) (1983) Carbonate Depositional Environments, AAPG Memoir 33, Tulsa, Oklahoma
Schäfer P, Fortunato H, Bader B, Liebetrau V, Bauch T, Reijmer JJG (2011) Growth rates and carbonate production by coralline red algae in upwelling and non-upwelling settings along the Pacific coast of Panama. Palaios 26(7):420-432

Sevrin-Reyssac J (1993) Hydrology and underwater climate of the Banc d'Arguin, Mauritania: a review. Hydrobiologia 258:1–8
Solomon S (2007) Climate Change 2007: The Physical Science Basis: Contributions of Working Group I to the Fourth Assessment Report of the Intergovernmental Panel on Climate Change (IPCC). Cambridge University Press, Cambridge
Summerhayes CP, Milliman JD, Briggs SR, Bee AG, Hogan C (1976) Northwest African shelf sediments: Influence of climate and sedimentary processes: J Geol 84:277–300
Taylor GT, Muller-Karger FE, Thunell RC, et al. (2012) Ecosystem responses in the southern Caribbean Sea to global climate change. Proc Nat Acad Sci USA 109:19315–20. doi:10.1073/pnas.1207514109
Van Camp L, Nykjaer L, Mittelstaedt E, Schlittenhardt P (1991) Upwelling and boundary circulation off Northwest Africa as depicted by infrared and visible satellite observations. Prog Oceanogr 26:357–402
Vermaat JE, Beijer JAJ, Gijistra R, et al. (1993) Leaf dynamics and standing stocks of intertidal *Zostera noltii* Hornem. and *Cymodocea nodosa* (Ucria) Ascherson on the Banc d'Arguin (Mauritania). Hydrobiologia 258:59–72
Ward Jr JH (1963) Hierarchical grouping to optimize an objective function. J Amer Statist Assoc 58(301):236-244
Wentworth CK (1922) A scale of grade and class terms for clastic sediments. J Geol 30:377–392
Westphal H, Freiwald A, Hanebuth T, and cruise participants (2007) Report and preliminary results of Poseidon cruise 346, MACUMA. Las Palmas (Spain) – Las Palmas (Spain), 28.12.2006 – 15.1.2007. Berichte Univ Bremen No. 260. 49 p
Westphal H, Beuck L, Braun S, Freiwald A, Hanebuth TJJ, Hetzinger S, Klicpera A, Kudrass H, Lantzsch H, Lundälv T, Vicens GM, Preto N, Reumont J, Schilling S, Taviani M, Wienberg V (2014) PHAETON - Paleoceanographic and paleoclimatic record on the Mauritanian Shelf – Cruise No. MSM16/3 - October 13 to November 20, 2010, Bremerhaven (Germany) – Mindelo (Cap Verde). MARIA S. MERIAN-Berichte, MSM16/3, DFG-Senatskomm Ozeanogr, 57 p. doi:10.2312/cr_msm16_3
Westphal H, Halfar J, Freiwald A (2010) Heterozoan carbonates in subtropical to tropical settings in the present and past. Int J Earth Sci 99:153–169. doi:10.1007/s00531-010-0563-9
Wolff WJ, Van der Land J, Nienhuis PH, De Wilde PAWJ (1993a) Ecological studies in the coastal waters of Mauritania. Hydrobiologia 258:vii–ix
Wolff WJ, Duiven AG, Duiven P, et al. (1993b) Biomass of macrobenthic tidal flat fauna of the Banc d'Arguin, Mauritania. Hydrobiologia 258:151–163
Wolff WJ, Land J, Nienhuis PH, De Wilde PAWJ (1993c) The functioning of the ecosystem of the Banc d'Arguin, Mauritania: a review. Hydrobiologia 258:211–222
Wolff WJ, Smit CJ (1990) The Banc d'Arguin, Mauritania as an environment for coastal birds. Ardea 78:17–38
Wright V, Burgess P (2005) The carbonate factory continuum, facies mosaics and microfacies: an appraisal of some of the key concepts underpinning carbonate sedimentology. Facies 51:19–25

IX. Biological interactions and morphological adaptations as a tool in marine environmental research

It is well known that functional morphological features of marine species (e.g., shell size, growth form and sculpture in mollusks) are evolutionary responses to environmental constraints (see e.g., Stanley, 1975; Wainwright, 1994 and reference therein). This relationship is also documented from the fossil record and characterizes the majority of the modern marine community, which have shown a number of intelligent strategies to cope with environmental constraints governing our oceans (Vogel, 1984). Wherever such challenging conditions (e.g., hydrodynamic regime, trophic levels, substrate availability and others) characterize the marine environment, some specialists developed the extraordinary ability to interact with organisms of different species (e.g., use of chemosymbionts or photosymbionts for nutrition or poisonous hydrozoa for protection), indicating a significant evolutionary step. Both symbiotic partners benefit from such a partnership by forming loose protocooperations (alliance between individuals to cope with environmental conditions), mutualistic relationships (closer non-obligatory symbiosis, see Second publication) or tight eusymbiotic relationships (obligatory symbiosis) (Douglas, 1994; 2010; Bradford and Schwab, 2012).

Besides the number of 'classical' symbiotic interactions between species, described in detail in e.g., Greene (1974), Smith (1992) and Moran (2006), some of the most impressive partnerships are described from decapod crustaceans with marine carbonate secreting organisms such as corals, mollusks, serpulids and bryozoans (see e.g., Williams and McDermott, 2004). These biocoenoses, both parasitic and symbiotic in nature, are known from various ancient and modern marine environments. They clearly express the adaptation capabilities of marine organisms to their environment and were described in a number of publications, see e.g., Boschma (1955); Taylor (1994); Taylor and Schindler (2004); Williams and McDermott (2004); Cadée (2007).

Among the marine carbonate secretors, bryozoans are a particularly useful group to study the response (e.g., modification of skeletal morphologies, intra- and inter-specific interactions) of marine organisms as a response to poor or 'atypical' environmental conditions (McKinney and Jackson, 1991). Fossil remains of bryozoans date back to Ordovician times but also modern specimens show a highly specialized skeleton with an intra-specific plasticity (variability) that characterizes growth and form of the skeletons (McKinney and Jackson, 1991; Smith, 1995; Taylor, 2005). This variability makes identifications of bryozoan taxa and environmental studies often to a complex and complicate, but in the end promising approach (see Suppl. XVIII.2).

Bryozoa are modular aquatic invertebrates, which are entirely colonial, except for one genus (*Monobryozoon ambulans*) that lives solitary. Each colony comprises a series of inter-connected, genetically identical individuals (zooids). Generally living as suspension feeders in marine waters, bryozoans prefer salinities between 32 and 37 ‰. Some species, however, can tolerate low salinities in brackish waters, while the class *Phylactolaemata* lives in freshwater habitats.

Bryozoans prefer waters with temperatures ranging from 10 to 30 °C but some Antarctic genera may tolerate water temperatures as low as -15 °C (Smith, 2005). A single zooid usually measure less than 0.5 mm in length but can reach a size exceeding more than 1.8 mm in length, most likely an adaption to limited substrate availability (Grischenko et al., 2002). Other authors see a correlation between zooid size and colony growth rate and seawater temperature, see e.g., Menon (1972), Smith (2005), Taylor (2005) and references therein. Most of the 6000 recent bryozoans species are found in shelfal environments under subtidal to intertidal conditions, but some were identified down do 6000 mbsl (Taylor, 2005). Although usually of minor significance in tropical reefs, bryozoans are major components of temperate shelf carbonate sediments and can reach dominant components and carbonate producers on the Australian (e.g., Wass et al. 1970) and New Zealand (e.g., Nelson et al. 1988b) shelves, see also Second publication. Bryozoan skeletons, colony organization and reproductive strategies are known to vary in size, structure and mode respectively with physicochemical properties of the water column (O'Dea and Jackson, 2009; O'Dea, 2009). Smallest colonies are less than 1 mm in diameter while the largest can exceed 1 m (Grischenko et al., 2002), thus making bryozoans to important sediment components and environmental indicators. Besides colony growth rate, the growth form of bryozoan colonies is also controlled by environmental conditions favoring the colony to form tree-like erect, mesh-like, free-living cup-like or singe and multiple encrusting growth habits (see Suppl. XVIII.2). Classifications of bryozoan growth forms can serve as valuable environmental indicators and are described in detail in e.g., Nelson (1988b).

Biocoenoses between bryozoans and other marine organism are rare known from mostly commensalistic relationships, few partnerships, however, are known to from tight mutualistic partnerships (e.g., Klicpera et al., 2013). A range of authors have shown this rare relationship to be closely coupled with environmental conditions such as substrate availability, water temperatures, salinities, nutrient settings and sedimentological properties of the environment, see e.g., Taylor (1994), Kidwell and Gyllenhaal (1998) and Klicpera et al. (2013).

The following studies highlights the non-obligate mutualistic symbiosis between bryozoans and hermit crabs and illustrates the adaptive capabilities and benefits from a close partnership in a highly dynamic environment. Our results show that this symbiotic relationship is closely linked to environmental constraints and parameters that govern this very complex ecosystem.

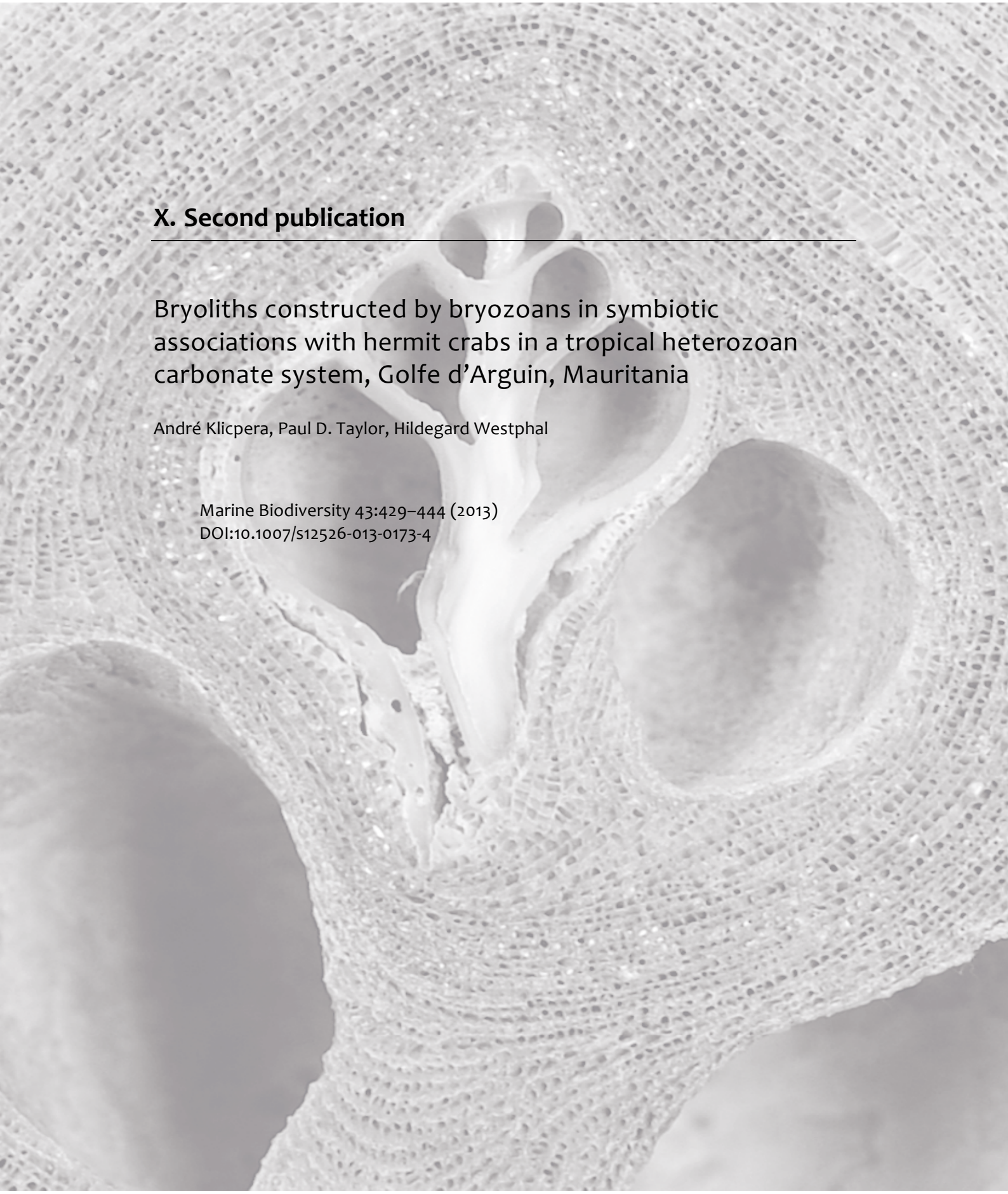

X. Second publication

Bryoliths constructed by bryozoans in symbiotic associations with hermit crabs in a tropical heterozoan carbonate system, Golfe d'Arguin, Mauritania

André Klicpera, Paul D. Taylor, Hildegard Westphal

Marine Biodiversity 43:429–444 (2013)
DOI:10.1007/s12526-013-0173-4

this page is intentionally left blank

Bryoliths constructed by bryozoans in symbiotic associations with hermit crabs in a tropical heterozoan carbonate system, Banc d'Arguin, Mauritania

André Klicpera[1], Paul D. Taylor[2], Hildegard Westphal[1,3]

1 Leibniz Center for Tropical Marine Ecology (ZMT), Bremen, Germany
2 Department of Earth Sciences, Natural History Museum London, UK
3 Department of Geosciences, University Bremen, Germany

Abstract

The Golfe d'Arguin offshore of northern Mauritania hosts a rare modern analogue for heterozoan carbonate production in a tropical marine setting. Dominated by ocean upwelling and with additional fertilization by iron-rich aeolian dust, this naturally eutrophic marine environment lacks typical photozoan communities. A highly productive, tropical cosmopolitan biota dominated by mollusks and suspension-feeders such as bryozoans and balanids characterizes the carbonate-rich surface sediments. Overall biodiversity is relatively low and the species present are tolerant against the eutrophic and low-light conditions, strong hydrodynamic regime governed by ocean upwelling, and unstable, soft-bottom seafloor with few hard substrata.

Here we describe an ectosymbiosis between the hermit crab *Pseudopagurus granulimanus* (Miers, 1881) and monospecific assemblages of the encrusting cheilostome bryozoan *Acanthodesia commensale* (Kirkpatrick and Metzelaar, 1922) that cohabits vacant gastropod shells. Nucleating on an empty gastropod shell, the bryozoan colonies form multilamellar skeletal crusts that produce spherical encrustations and extend the living chamber of the hermit crab through helicospiral tubular growth. This non-obligate mutualistic symbiosis illustrates the adaptive capabilities and benefits from a close partnership in a complex marine environment, driven by trophic conditions, high water energies and instable substratum. Sectioned bryoliths show that between 49 and 97 % of the solid volume of the specimens consists of bryozoan skeleton.

Corresponding author: André Klicpera, Leibniz Center for Tropical Marine Ecology (ZMT), Fahrenheitstraße 6, D-28359 Bremen, Germany and Center for Marine Environmental Sciences (MARUM), University of Bremen, Germany

Second publication

X.1 Introduction

Symbiotic associations between two or more different biological species are ubiquitous in terrestrial, freshwater and marine communities. Symbiosis played a key role in the emergence of major life forms on Earth and in the generation of biological diversity (Douglas, 1994; Moran, 2006). Many symbiotic relationships involve trophic associations and some – mutualisms – are beneficial to both partners (Boucher, 1988).

Symbiotic biocoenoses between decapod crustaceans and other organisms are known from various ancient and modern marine environments and have been topics for numerous studies; for example, see Stachowitsch (1980); Taylor (1994); Kidwell and Gyllenhaal (1998); Taylor and Schindler (2004); Williams and McDermott (2004); Cadée (2007) and references therein. Some of the best-known and most impressive symbioses involve associations between hermit crabs (Arthropoda) and sea anemones (Cnidaria). Hermit crabs of the species *Dardanus pedunculatus* (Herbst, 1804) establish close mutualistic symbioses with sea anemones (*Calliactis* sp.) that live attached to the external surfaces of the shell housings and provide protection and camouflage. Other crab species such as the Boxing Crab *Lybia tesselata* (Latreille, 1812) use the poisonous anemone *Triactis producta* (Klunzinger, 1877) attached to their claws to fight against predators and for protection (Williams and McDermott, 2004). The importance of some of these interspecific relationships to the crabs is evident from the crabs actively transferring their protective symbionts to a new shell when ecdysis forces a change in domicile (Karleskint et al., 2009, p. 431; Moen and Svensen, 2004, p. 261).

Here we describe a striking biocoenosis between the hermit crabs *Pseudopagurus granulimanus* (Miers, 1881) (see McLaughlin, 2012) and the anascan cheilostome bryozoan *Acanthodesia commensale* (Kirkpatrick and Metzelaar, 1922). A nodule-shaped domicile is formed by multilamellar growth of the bryozoan around an empty gastropod nucleus that was the initial housing for the hermit crab and which remains preserved in the center of the construction. Kidwell and Gyllenhaal (1998) adopted the term 'bryolith' *sensu* Reguant et al. (1991) to describe such bionodules with roughly spherical circumrotatory growth. The nuclei of these bryoliths collected from tidal channel deposits in the Pliocene of southeastern California were either skeletal or non-skeletal origin (for other examples see James et al., 2006). This growth pattern has also been recognized among other marine organisms, such as coralline algae (Adey and MacIntyre, 1973; Peryt, 1983), corals (Glynn, 1974; Kissling, 1973; Roff, 2007) and other bryozoan species (Rider and Enrico, 1979; Balson and Taylor, 1982; McKinney and Jackson, 1991; Reguant, 1991; Taylor, 1994).

We collected living and dead bryoliths from the tropical, shallow-marine Banc d'Arguin of NW Mauritania, where they constitute part of a heterozoan faunal community (Westphal et al., 2010; Michel et al., 2011a; 2011b). The aim of this study is to take a first step away from a merely descriptive view of bryolith growth and towards a

better understanding of environmental controls and habitat characteristics. Moreover, the collected specimens extend the sparse knowledge of *in situ* bryoliths inhabited by hermit crabs that reside in living-chambers enlarged by bryozoan growth and place this unusual symbiotic association in an environmental context.

X.2 Study area

The Golfe d'Arguin off Mauritania stretches from Cap Blanc to Cap Timiris over a latitudinal distance of about 200 km (Fig. X.1). It hosts an extensive modern heterozoan carbonate system that is rare in the present-day tropics (Westphal et al., 2010; Michel et al., 2011a; 2011b). The wide and shallow shelf was significantly influenced by post-glacial transgression, which resulted in an extensive shallow marine ecosystem of largely <10 m water depth with wide intertidal plains (Fig. X.1; IT) concentrated around Tidra Island and along the Mauritanian shoreline (Wolff et al., 1993; Hanebuth and Lantzsch, 2008). Since 1989 the inner part of the shelf has been a marine protected area (National Parque Banc d'Arguin; http://whc.unesco.org/en/list/506) and belongs to the Unesco World Heritage List . Moreover, it serves as an important settlement ground for a large number of migrating birds, which feed on the rich mollusk and decapod faunas (Hoffmann, 1988; Campredon, 2000).

X.2.1 Banc d'Arguin platform characteristics

From the modern coastline to the shelf break at a water depth of around 100 meters below sea level (mbsl) the central Banc d'Arguin stretches over a longitudinal distance of more than 150 km. It forms a rimmed depositional system *sensu* Ginsburg and James (1974) with a shallow epicontinental flat-topped platform (Fig. X.1). The rimmed shelf margin is located about 100 km off the coastline and shows a characteristic escarpment structure dividing the middle and outer shelf (>20 mbsl) from the shallow platform (<20 mbsl, large areas 5–10 mbsl) (Westphal et al., 2010). Large parts of the shelf are covered by bioclastic sediments dominated by heterozoan grain associations as a consequence of elevated nutrient levels due to upwelling and aeolian dust input (Westphal et al., 2010; Michel et al., 2011a; Westphal et al., 2014 and references therein).

The high insolation and the shallow waters on the platform result in tropical warm water temperatures (annual mean >23 °C, Ould Mahfoudh, 1991). These are characterized by an intense hydrodynamic regime mostly controlled by the Eastern Boundary Current (EBC), but are also influenced by the tidal regime and shelf morphology. Fertilized by upwelling and iron-rich dust from the Saharan desert and the Sahel zone, the waters off Mauritania are characterized by high primary productivity (> 3 mg*m^{-3} [Chl-*a*]), reduced

oxygen levels and a low light penetration of less than 2 m (Marañón and Holligan, 1999; Westphal et al., 2014).

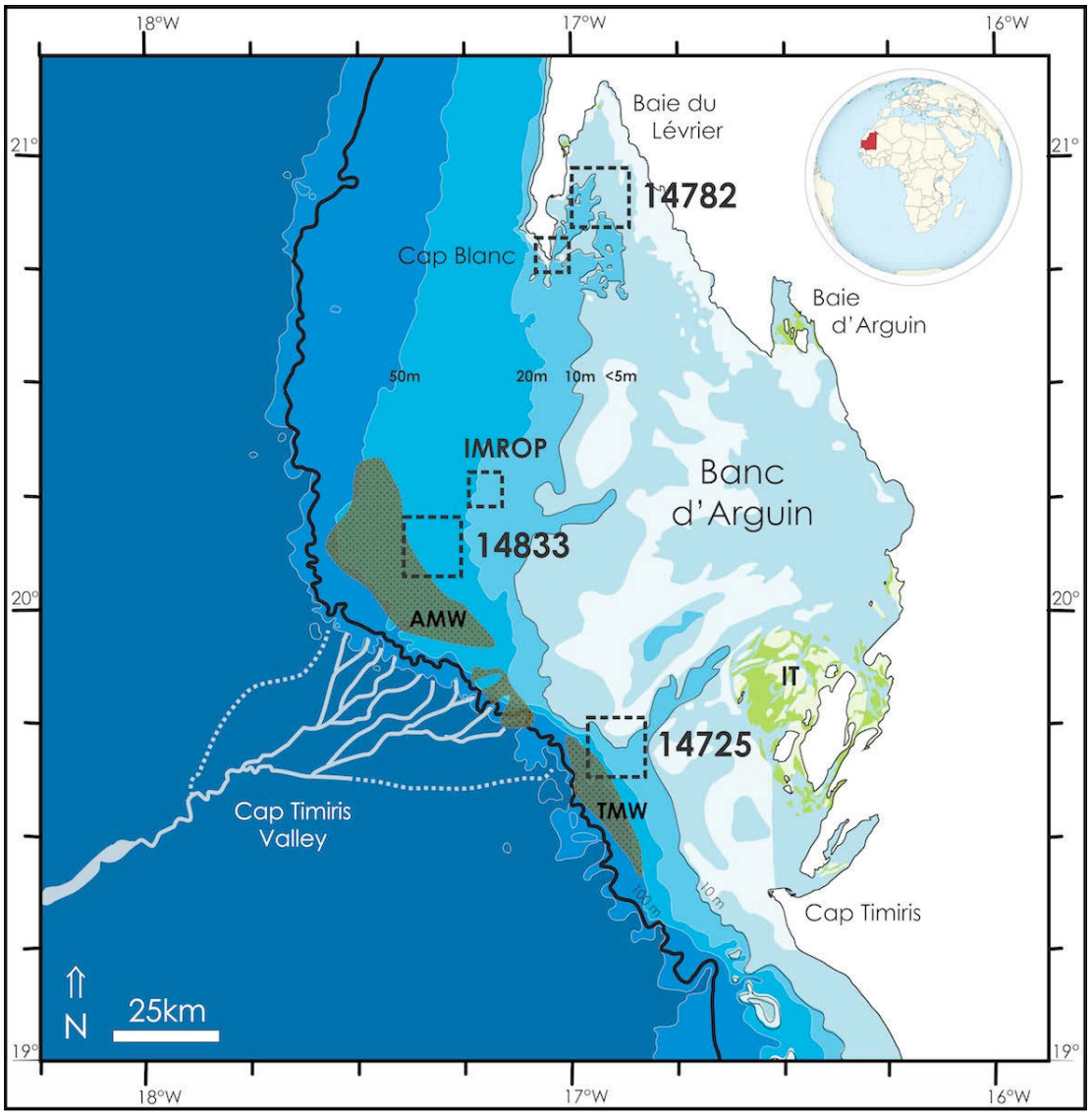

Figure X.1: The Banc d'Arguin sampling area (modified from Michel et al., 2011b after Hanebuth and Lantzsch, 2008) characterized by a shallow marine ecosystem. White patches on the inner shelf indicate shallows of <5 m water depth, while the southern region is typically intertidal and seagrass meadows (IT). The zodiac sampling was performed in the Baie du Lévrier (14782, 5-10 mbsl), along the outer platform rim of the central Banc d'Arguin (14783, 5-25 mbsl) and in the southern Banc d'Arguin 14725, 5-10 mbsl). Dark patches along the shelf break (solid dark contour line) represent high-accumulation bodies (AMW = Arguin mud wedge, TMW = Timiris mud wedge). "IMROP" indicates in-situ bryolith accumulations explored during a 2012 cruise of the R/V Al Awam.

As a consequence, the shelf lacks light-controlled photozoan elements expected in a tropical marine setting (Michel et al., 2011a; Reymond et al., 2013 submitted). Photoautotrophic organisms, such as photosymbiont-bearing benthic foraminifers, zooxanthellate corals and calcareous green algae, are entirely absent, and the system lacks any sediment trapping and stabilization capability apart from seagrass meadows in the coastal areas and deep-water coral mounds along the lower slope (Vermaat et al., 1993; Westphal et al., 2007; Michel et al., 2009; Eisele et al., 2013 submitted). In the absence of photoautotrophs, a low-diversity heterozoan fauna is developed characterized by suspension-feeders (Koopmann et al., 1979; Piessens, 1979; Michel et al., 2011a; 2011b) and light-independent biota (Westphal et al., 2014). Among these, the remains of mollusks, balanids and other crustaceans, bryozoans, echinoids and non-phototrophic benthic foraminifers provide a major share of the hard substrates available on the seabed for potential colonization by benthic organisms.

X.2.2 Sedimentological context

Sediments of the Banc d'Arguin show a mixed carbonate-siliciclastic composition (Westphal et al., 2010; 2014). The shallows (Fig. X.1; <20 mbsl) are dominated by a mixture of balanids and mollusks (Barnamol *sensu* Hayton et al., 1995) that grade towards the margins of the platform in coarse, bivalve-rich deposits (Bimol *sensu* Hayton et al., 1995). Abundant bivalve taxa in the vicinity of bryolith occurrences (central Banc d'Arguin, 14833) are upwelling associated *Donax burnupi* (Sowerby III, 1894) and large *Venus crebrisulca* (= *Venus rosalina*) (Sowerby II, 1853) that extend northwards to Cap Blanc; *Pinna rudis* (Linnaeus, 1758) in deeper muddy to fine-clastic sediments (~20-25 mbsl); and some rare chemosynthetic *Solemya togata*? (Poli, 1791) that indicate reduced conditions and thus the high productive nature and this ecosystem.

Gastropod shells are rare components in sediments from the central Banc d'Arguin (14833, Fig. X.1) that average in general <5 % of the bioclastic sediment fraction. However, the availability of empty gastropod shells has been reported as an important limiting factor of hermit crab population size (e.g., Kellog, 1976; Morris et al., 1989). The following gastropod taxa (in order of decreasing occurrence) are reported from study sites close to bryolith occurrences: *Stramonita* sp., *Nassarius* sp., *N. elatus*, *Mesalia mesal*, *Turridae* sp., *Tectonatica filosa*, *Turritella* cf. *biplicata, Crepidula porcellana, Eulimidae* sp., *Cerithiopsis* sp., *Gibberula* sp., *Volvarina* sp., *Granulina* sp., *Genota* sp., *'Mangelia' nuperrima, Basisulcata* sp., *Mathilda quadricarinata, Pyramidellidae* spp., *Acteon* sp., *Ringicula* sp., *Gibbula joubini, Bela* sp., *Natica fanel, Epitonium* sp., *Bivetiella cancellata, Marginella cleryi,* and *Turbonilla* sp. (Westphal et al., 2014).

Deeper environments along the outer central and southern shelf (>30 mbsl) are characterized by olive-green muddy substrata of mostly silt to fine-sand hat indicate high-

accumulation bodies (Hanebuth et al., 2013). These mud wedges (Fig. X.1) are composed of mostly aeolian and reworked silty material (Hanebuth and Henrich, 2009). Carbonate-richer sediments close by are characterized by a mixture of foraminifers and mollusks (Foramol after Lees and Buller, 1972).

A fourth, less frequent, carbonate grain association is a bryozoan-rich facies (Bryomol *sensu* Nelson et al., 1988b) that covers large parts of the outer shelf towards the southern shelf around Cap Timiris (Fig. X.1). Bryozoan growth forms and the morphological plasticity within species represent modifications of taxa to special environmental conditions (Amini et al., 2004; Taylor, 2005). The sea floor sediment in the southern Banc d'Arguin shows a composition dominated by siliciclastics and provides locally large abundances of cupuladriid bryozoans (e.g., *Discoporella* spp., *Reussirella* spp.), highly adapted to life on unstable, particulate substrates (Lagaaij, 1952; McKinney and Jackson, 1991). Besides the carbonate produces, which provide a major share (up to 90%) to the sediment, admixed fine-grained siliciclastics (quartz grains) of terrestrial origin are sourced from the Saharan hinterland (Westphal et al., 2007; 2014; Michel et al., 2009; 2011a; 2011b).

Table X.1: Study areas and sites sampled in the Baie du Lévrier (14782) and towards the south along the outer Banc d'Arguin (14833, 14725) providing bryozoan – hermit crab associations. Mean water depth (MWD); R/V Maria S. Merian (MSM); Van Veen grab (hBG); CTD probe (hCTD); Secchi disk (SD); Giant box corer (GKG).

Study Area	Site	No. of specimens	Latitude (N)	Longitude (W)	MWD (m)	Temp (°C)	Vessel	Sampling Gears
14782	-3	1	20°52.807'	16°59.533'	14 m	n/a	MSM	GKG
14833	-8	13	20°09.460'	17°19.267'	24 m	19.9	Zodiac	hBG, hCTD, SD
14833	-18	4	20°07.626'	17°20.459'	27 m	n/a	Zodiac	hBG
14833	-21	4	20°07.612'	17°18.878'	22.5 m	20.0	Zodiac	hBG, hCTD, SD
14725	-8	1	19°41.903'	16°55.033'	8 m	18.5	MSM	hBG, hCTD, SD

X.3 Material and methods

During the research cruise "PHAETON" on board the R/V Maria S. Merian (MSM16 leg 3, Oct.-Nov. 2010) off NW Mauritania the outer rim of the Banc d'Arguin was investigated and sampled (Westphal et al., 2014). A fast rescue zodiac was used in order to access shallow-marine sampling areas (<20 mbsl) in the Baie du Lévrier (14782), the central Banc d'Arguin (14833) and the southern Banc d'Arguin (14725). These three study areas (Fig. X.1, Tab. X.1) were subsampled at up to 22 sites (Tab. X.2), each of which was sampled by

a Van Veen grab of 1.5 liters volume and every third site by a hand-CTD probe and a Secchi disk.

Table X.2: Bryolith specimens sampled from the Baie du Lévrier and the outer Banc d'Arguin.

Specimens (GeoB-)	Bryolith		Weight (g)	Gastropod nucleus (family)	Area in %		
	length (mm)	width (mm)			*Shell*	*Bioer.*	*Bryoz.*
14833-8-1	43.30	38.60	34.93	*Naticidae*	14.2	1.2	84.6
14833-8-2	68.29	44.67	46.81	*Turritellidae*	4.3	2.7	93.0
14833-8-3	73.24	30.55	29.91	*Turritellidae*	49.5	1.4	49.1
14833-8-4	55.28	44.60	58.99	*Cassidae*	2.7	1.0	96.3
14833-8-5	57.40	39.96	53.14	*Cassidae*	1.2	3.7	95.1
14833-8-6	58.93	44.79	70.22	*Cassidae*	4.0	0.5	95.5
14833-8-7	54.93	40.22	55.20	*Naticidae*	9.0	0.8	90.2
14833-8-8	47.99	32.57	27.37	*Turritellidae*	3.3	0.7	96.0
14833-8-9	43.03	35.48	30.93	*Naticidae*	4.5	0.6	94.9
14833-8-10	51.67	39.84	52.81	*Naticidae*	6.3	0.5	93.2
14833-8-11	50.35	42.25	59.44	*Naticidae?*	7.1	1.4	91.5
14833-8-12	52.95	36.94	48.41	*Marginellidae*	3.3	0.9	95.8
14833-8-13	52.70	42.71	50.31	*Turritellidae*	2.5	0.5	97.0
14833-18-1	63.74	42.93	67.15	*Turritellidae*	0.9	2.4	96.7
14833-18-2	57.29	45.95	59.88	*Nassaridae?*	0.0	1.1	98.9
14833-18-3	42.83	38.66	29.70	*Naticidae*	8.5	3.1	88.4
14833-18-4	57.00	46.00	60.47	*not sectioned*			
14833-21-1	54.79	41.10	57.07	*Naticidae*	5.1	0.5	94.4
14833-21-2	41.71	33.02	21.48	*Naticidae*	10.6	1.1	88.3
14833-21-3	44.77	37.97	41.04	*Naticidae*	6.0	5.9	88.1
14833-21-4	43.73	33.57	29.67	*Naticidae*	9.8	2.8	87.4
14833-21-5	34.21	32.56	20.75	*not sectioned*			
14782-3-1	*reworked and abandoned bryolith, not sectioned*						
14725-8-1	*reworked and abandoned bryolith, not sectioned*						

Tab. X.2: Bryolith specimens sampled from the Baie du Lévrier and the outer Banc d'Arguin

The central Banc d'Arguin (14833) provided a great number of pagurid-occupied bryoliths, which were recovered from a water depth between 8 and 24 mbsl. Bryoliths were *in situ* with both symbiotic partners still alive, while abandoned and bioeroded

bryolith remains were collected from the Baie du Lévrier (14782) and the southern Banc d'Arguin (14725). A total of 24 bryolith specimens were sampled, 22 occupied by living hermit crabs and two abandoned (Tab. X.1 and Tab. X.2).

The 22 *in situ* collected specimens (Tab. X.2) were immediately prepared for conservation by removing biological material (the hermit symbiont was preserved in ethanol). The empty colonies were then externally cleaned under fresh water and dried in an oven (60 °C). Additional archive specimens were stored in ethanol and are accessible via the German Center for Marine Biodiversity Research (DZMB).

In order to prepare the bryoliths for analysis of the internal and external structure, we removed organic remains and tissue by treating them in 18 % H_2O_2 for at least 3 days. Specimens were sectioned and analyzed along the axial plane to reveal information about the internal anatomy and the gastropod shell nucleus (Fig. X.3D, E, F). Of the 24 bryoliths collected (Tab. X.2), 20 specimens were sectioned analyzed and subsampled for thin sections, scanning electron microscopy (SEM) and micro-tomography (µCT), while the two abandoned and bioeroded specimens were sectioned only (14782-3-1, 14725-8-1) and two other specimens were held back for later analyses (14833-18-4, 14833-21-5).

Bryozoan determination was aided by SEM analysis and comparisons with reference collections that include the types of *Acanthodesia commensale* (Kirkpatrick and Metzelaar, 1922) at the Natural History Museum, London (NHMUK). Additional SEM imaging and µCT scans were undertaken at the Leibniz Center for Tropical Marine Ecology (ZMT) in Bremen, Germany. The gastropod shell nucleus could be determined only down to family level because important outer shell features such as sculpture and color were inaccessible beneath the thick coating of bryozoan skeleton. The identification of the hermit crab as the species *Pseudopagurus granulimanus* (Miers, 1881) is based on literature reporting the identity of crabs from similar bryolith occurrences offshore Mauritania (see Cook, 1968; Taylor, 1994; McLaughlin, 2012).

X.3.1 SEM and µCT scans

SEM and µCT preparations were cut from external bryozoan skeletons using a dental drill equipped with a diamond-cutting disc. SEM images were taken by a Tescan Vega 3 SEM at 20kV (SE detector) linked to a Skyscan µCT, which provides a nominal resolution of 350 nm to 8 µm per pixel. µCT specimens were scanned at angular increments of 0.45° rotation steps over a period of 11 hours to provide a high-resolution scan (Fig. X.2F). Backscattered electron (BSE) images were prepared at 15kV in low-vacuum mode (Fig. X.2G, H). To assist taxonomic determination of the bryozoan and to provide data about its skeletal morphology and modular construction, 123 zooids from three bryolith specimens (14833-8-1, 14833-18-1 and 14833-21-1) were measured (Tab. X.3).

X.3.2 False-color analysis and tomographic processing

The internal anatomy of 20 bryolith images (Tab. X.2) were analyzed by coloring features of the frontal plane (Fig. X.3B, E, H) using a RGB false-color code. In order to determine the proportions (%) represented by the gastropod shell nucleus, the bryozoan cover and bioerosional traces, we analyzed red, green and blue pixels from the histogram data of each digital image in ImageJ v.1.45s (http://rsb.info.nih.gov). In all sections the gastropod shells were colored in red, the bryozoan colonies blue and losses due to bioerosion or abrasion in green (see Tab. X.2and Fig. X.2B, D). The hermit crab living chamber formed jointly by the gastropod shell and the bryozoan were excluded from the structural false-color analysis. Tomographic data (µCT) were later processed in OsiriX v.4.1.2 to calculate the proportion of bryozoan net area, which is skeleton ($CaCO_3$).

X.4 Results

X.4.1 Taxonomic identification of encrusting bryozoans

All collected bryolith specimens (Tab. X.2) are composed of a single anascan cheilostome bryozoan species determined as *Acanthodesia commensale* (Kirkpatrick and Metzelaar, 1922). This species was originally described as *Conopeum commensale,* while Cook (1968b) identified material from Ghana as *Membranipora commensale.* Along with other genera of *Membraniporidae* (see Taylor and Monks, 1997), *Acanthodesia* has a twinned ancestrula, a feature which is absent in *Conopeum* and, unfortunately, totally hidden by multilamellar overgrowths in the pagurid symbionts described here. While it seems likely that Kirkpatrick and Metzelaar's species is a membraniporid, it can no longer be placed in *Membranipora,* which is a specialized epiphyte with a thinly mineralized skeleton of aragonite. The best option available is to assign it to *Acanthodesia* (Canu and Bassler, 1919) pending a full morphological study. A commonly used synonym for the taxon *Acanthodesia commensale* is *Biflustra commensale* (Taylor, 1994; Grischenko et al., 2002)

X.4.2 Zooid dimensions

Dimensions of zooidal skeletons (zooecia) (n = 123) of three bryolith specimens (14833-8-1, 14833-18-1 and 14833-21-1) were measured using SEM and µCT scans (Fig. X.3). Terminology follows Winston et al. (1986). Lengths and widths of the zooids and their opesiae are shown in Tab. X.2.

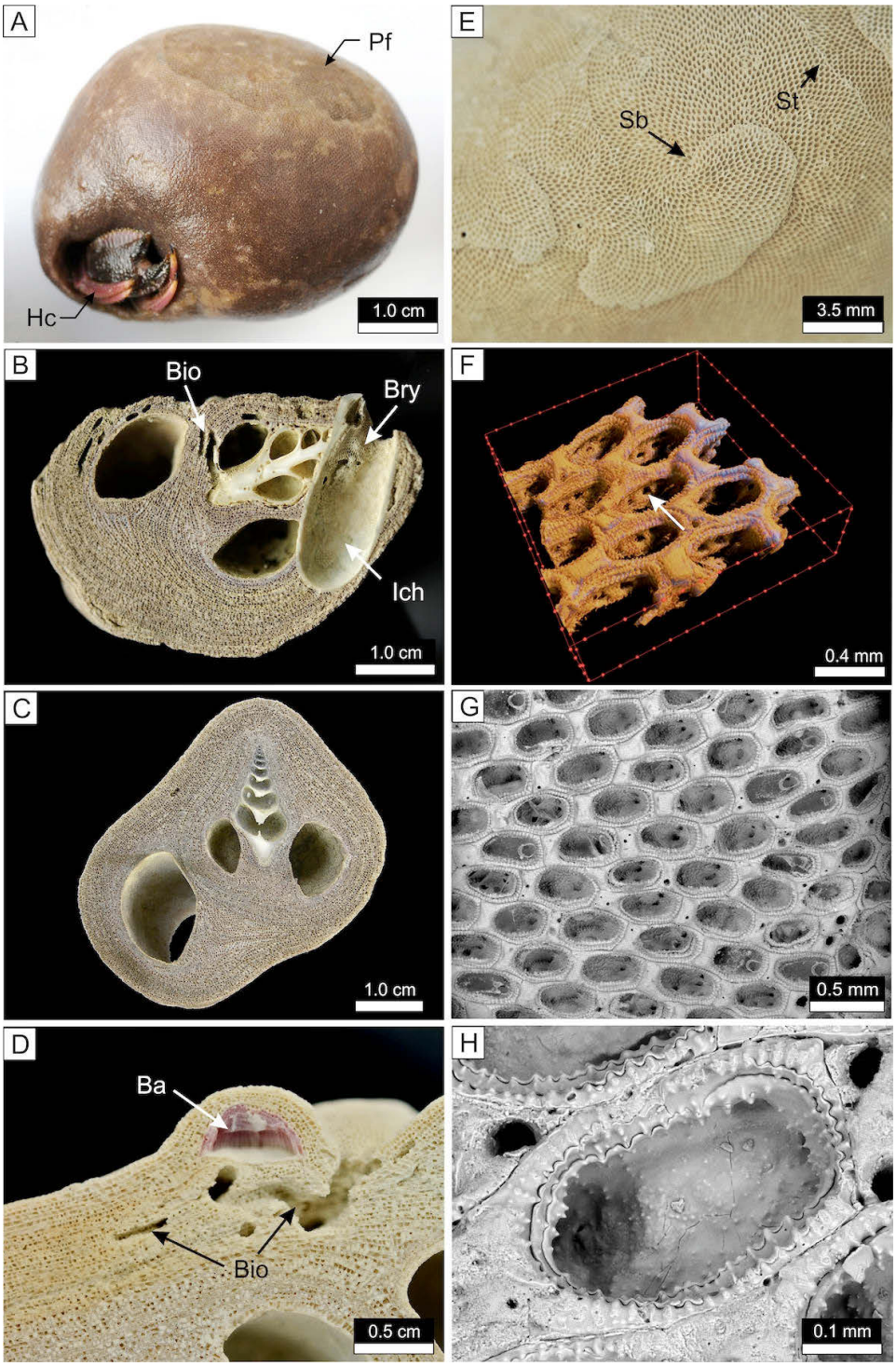

Figure X.2: (A) Bryoliths as in situ specimens showing hermit crab symbiont (Hc) and worn base of colony (Pf); (B) Sectioned view of an abandoned bryolith with bioerosional features (Bio), tube of ichnogenus Gastrochaenolites (Ich) and new bryozoan skeletons extending within the tube (Bry). (C) Section view of turritellid nucleated bryolith; (D) Internal features of colony thickening with ingrown balanid (Ba) and bioerosion (Bio); (E) External features of the outermost zooidal layers with spiral overgrowth (spiral budding) of older zooids (Sb) and standoff structures (St) where growing edges collided; (F) µCT 3D reconstruction of the external bryozoan skeleton with communication pores (arrow); (G, H) Backscattered SEM images of the bryozoan colony at different magnifications.

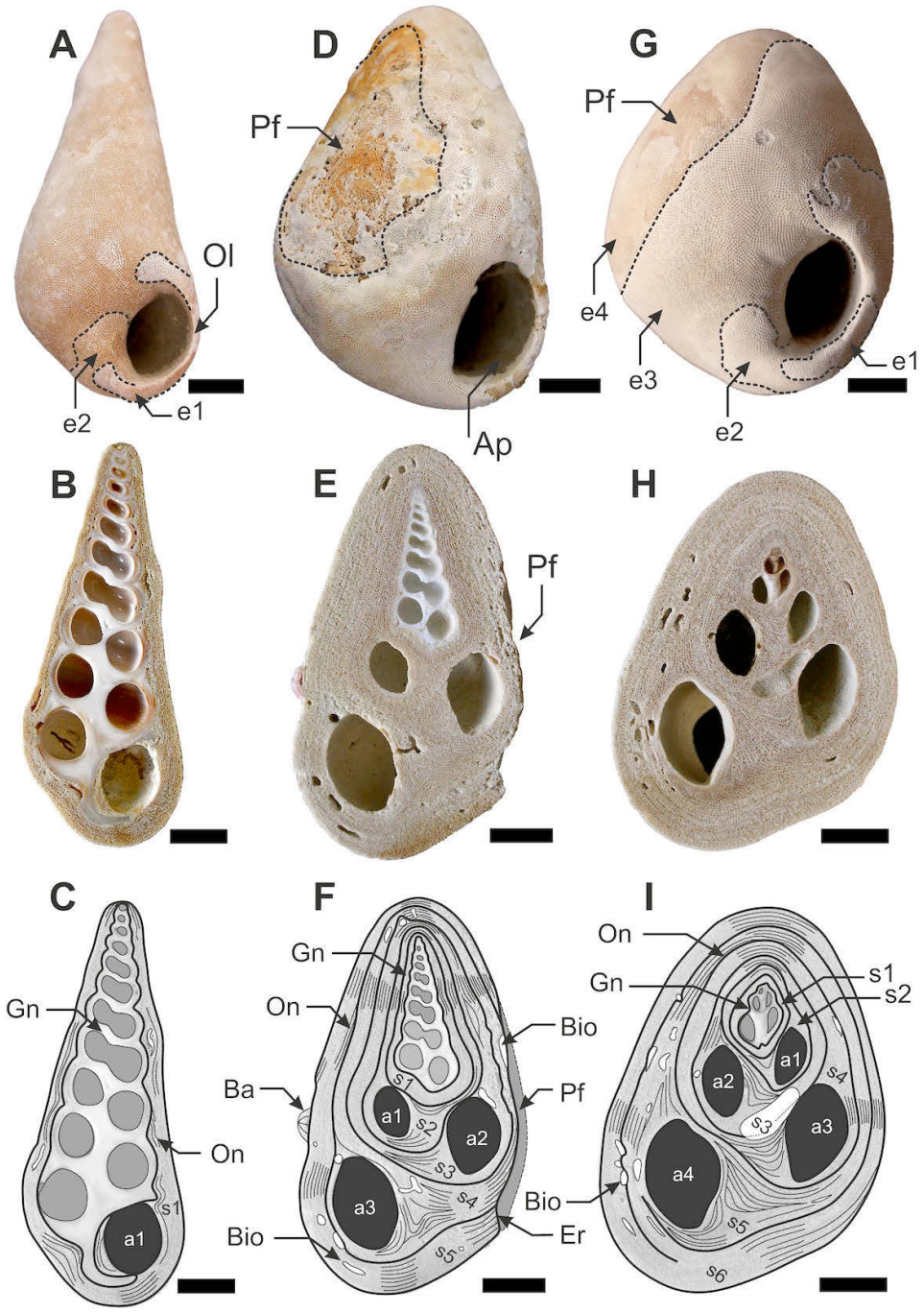

Figure X.3: (A) Turritellid-nucleated bryolith (specimen 14833-8-3) showing encrustation stages e1–e2, section view showing large gastropod nucleus (b) and illustration of internal anatomy (c); d turritellid encrusted bryolith (specimen 14833-8-2) showing pagurid facet (Pf), corresponding section view (e) and internal anatomy (f);g Cassid-nucleated bryolith (specimen 14833-8-5) showing encrustation stages e1- e4, section view (h) and corresponding illustration of internal anatomy (i); gastropod nucleus (Gn), aperture (Ap) apertural edge=outer lip (Ol), onlapping stratigraphy (On), bioerosion (Bio), barnacle (Ba), abrasion/erosion (Er), reconstructed living chambers (a1–a4) and corresponding growth sequences of the bryozoan skeleton (s1–s6). Scale bar 1 cm.

X.4.3 Bryozoan skeletal morphology

Zooidal skeletons of Acanthodesia commensale have calcified basal and vertical walls, the latter containing communication pores linking adjacent zooids (Fig. X.2F). Calcification of the frontal surface is limited in this species to a narrow, thickened rim, widest proximally, surrounding an oval opening (opesia) occupied by a filigree non-calcified membrane and operculum, which are usually destroyed during cleaning of the bryoliths by bleaching (Fig. X.2G, H). Additional, smaller openings at the corners of some zooids represent the reduced opesia of kenozooidal polymorphs. Prominent pustules are developed around the edges of the opesiae. Zooids are outlined by brown lines representing the surface expressions of the thin organic cuticles between the calcified components of the vertical walls of neighboring zooids. Ovicells and avicularia are absent in this species. The ancestrula is twinned in *Acanthodesia*, which separates this genus from the otherwise similar *Conopeum*.

X.4.4 Bryozoan skeleton weight

The calcitic bryozoan skeletons net weight of 20 analyzed bryoliths ranges between 4.4 and 20.1 g (mean 12.8 g). This calculation is based on the average net area of three representative bryozoan chambers scanned and analyzed using the µCT method. Individual chamber dimensions are in accordance with averages as shown in Tab. X.3. Skeletal net volume of 0.0131 mm^3 per zooecia volume (~0.0425 mm^3) was calculated from serially taken tomographic images (n = 429) using OsiriX software and then extrapolated for bryozoan gross areas of the bryolith.

X.4.5 Bryozoan colony thickening

Bryolith sections show multilamellar colonies of *Acanthodesia commensale* that envelop the gastropod shell nucleus in circumrotatory growth (Fig. X.2C and Fig. X.3B, E, H). Once the initial encrusting bryozoan layers reach the aperture of the gastropod shell, they develop a special pattern of growth that extends the living chamber (inhabited by a hermit crab) by prolonging the helicospiral structure of the shell (Fig. X.3C, F, I; a1-a4). The addition of usually 10 or more layers of zooids causes rounding of the bryolith nodule (Fig. X.3C, F, I), which tends to develop a massive, subspherical shape (Fig. X.2A and Fig. X.3A, D, G and Suppl. XVIII.1). The innermost layers of the bryolith indicate that the hermit crab occupant/s originally used the gastropod shell nucleus, with the bryozoan latter extending this chamber as a domicile (Taylor, 1994).

Table x.3: Astogenetic size variation of bryolith forming bryozoans identified as *Acanthodesia commensale.*

Specimen	**14833-8-1**	**14833-18-1**	**14833-21-1**
Zooid length (Lz)			
Mean ± SD (µm)	586 ± 47	560 ± 45	538 ± 63
Range (µm)	519-740	442-675	312-649
Zooid width (Wz)			
Mean ± SD (µm)	273 ± 29	271 ± 32	267 ± 32
Range (µm)	182-325	195-325	208-390
Opesia length (Lo)			
Mean ± SD (µm)	385 ± 35	385 ± 37	357 ± 60
Range (µm)	286-442	260-455	130-429
Opesia width (Wo)			
Mean ± SD (µm)	213 ± 28	227 ± 33	220 ±37
Range (µm)	156-273	156-312	78-273
Measurements	n = 39	n = 41	n = 43

Illustrations in Fig. X.3C, F, I clearly show that the colony progresses from an initial, shell coating phase (Fig. X.3C, F, I; s1), to a helicospiral phase of growth (Fig. X.3C, F, I; s2-s6). Depending on age, nucleus size and stage of encrustation (early and late), the gastropod shell is overgrown by bryozoan skeletons of variable thickness. Specimens listed in Tab. X.2 show lateral encrustations of bryozoan skeletons that range between 4 and 19 mm and comprise 10 and 53 layers respectively (Fig. X.3). As a result the bryolith specimens are variable in weight and range between 21 and 70 g (mean 46 g) with a total length of 34–73 mm.

Sectioned views (Fig. X.3) highlight the regularity of bryozoan skeleton successions originating from the nucleus with no evidence of periodic die-off (Fig. X.2C). The external view shows bryozoan skeletons overgrowing and fouling older skeletons (Fig. X.3A, G) through either eruptive or spiral budding (Fig. X.2E) starting from the growing edge. The presence of a twinned ancestrula or the zones of astogenetic change (diagnostic for fouling of two genetically different colonies) in the external bryozoan layers are not observed.

X.4.6 Gastropod shell nucleus

Sectioned specimens (Tab. X.2) revealed the identification of the nucleus in the center of each bryolith. Almost all specimens show an aragonitic gastropod shell nucleus (n = 19) with a net weight ranging from 0.59 to 14.75 g (mean 3.06 g), while one specimen (14833-8-13) showed a completely dissolved shell. The size of the gastropod shell ranges between 5 and 69 mm, while the shape varies depending on the gastropod taxon. Globose (e.g., *Naticidae*) and high-spired forms were identified (e.g., *Turritellidae*, Fig. X.3) that can control the external shape of the bryolith (Fig. X.3A, B, C). However, determination of the gastropod shell down to genus or species level is largely hampered by the thick bryozoan skeletons, which limit the identification of the shells to family level only. In addition to *Naticidae* (50 % of all bryoliths examined) and *Turritellidae* (25 %), gastropod shells of the families *Cassidae* (15 %), *Marginellidae* (5 %) and *Nassaridae* (5 %) also served as nuclei (Tab. X.2).

X.4.7 Erosional structures

Erosional structures are present in all specimens (Fig. X.2 and Fig. X.3), but never in sufficient abundance to cause major structural weakening. Exceptions are the abandoned specimens (14782-3-1, 14725-8-1), which show an intense bioeroded framework with flask-shaped cemented borings. These were determined as an incipient structure of the ichnogenus *Gastrochaenolites* (Leymerie, 1842) (Fig. X.2B, Ich). The majority of bioerosional features are, however, caused by the activities of smaller boring organisms (e.g., polychaete worms) (Fig. X.2B; Bio). Borehole openings on the outer surface of the bryoliths are rare and usually <1mm in diameter, while the exposed axial planes show a layer-parallel orientation of bioerosional structures (Fig. X.2D and Fig. X.3E, H). Naticid bryolith nuclei provide increased bioerosional features in the shell carbonate, while turritellid gastropod shells are less affected or show no indications of bioerosion. Balanid encrusters sometimes foul the outer surfaces of the bryozoan colonies (Fig. X.3, F; Ba) and some balanids were found embedded within the bryozoan skeleton (Fig. X.2D; Ba), indicating that fouled bryozoans were later able to overgrow the balanids. The undersides of the bryolith specimens are often abraded that cause truncations structures (Fig. X.3F; Er), and show irregular bryozoan encrustation or largely destroyed colonies (Fig. X.3D; Pf). This external bryolith structure is known as “pagurid facet” (*sensu* Ehrenberg, 1931; see also Taylor, 1994).

X.4.8 False-color analysis

Investigated bryoliths (n = 20) show thick and massive bryozoan encrustations. Apart from one specimen (14833-8-3) with 49.1 % bryozoan cover and <10 skeleton layers in which bryozoan cover is evidently reduced due to the relatively large size of the nucleus (Fig. X.3A, B, C), all specimens show 84.6 to 98.9% (mean 90.7%) bryozoan cover. Skeletons usually comprise more than 10 and up to 50 laminae, and can reach a total thickness of several centimeters. The contribution of the gastropod shell nucleus (Fig. X.3B, E, H) depends on shell taxon, shape and size. Percentages contributions of gastropod shells range from 1.2% (14833-8-5) to 49.5% (14833-8-3) (mean 7.6%), apart from one specimen (14833-18-2) in which the nucleus is completely dissolved.

Note that the reliability of these values as indicators of the proportional volume of bryozoan skeleton in the bryoliths is compromised by the fact that the orientation of the gastropod shell was unknown before cutting the bryoliths and obtaining the optimal axial sections was difficult. Bioerosional structures do not exceed 6% (mean 1.6%) in the axial planes and play a minor role in the composition of the bryoliths (see Tab. X.2 and Fig. X.2 and Fig. X.3).

X.5 Discussion

Bryoliths are formed by bryozoan colonies that grow circumferentially around biogenic or abiogenic nuclei. These structures have been recorded in modern and ancient marine ecosystems, as well as in various environmental contexts (see Flor, 1970; Piessens, 1979; Morris et al., 1989; Taylor et al., 1989; Taylor, 1994; Winker and Kidwell, 1996; Cuffey and Johnson, 1997; Kidwell and Gyllenhaal, 1998). While some bryoliths are nucleated on non-skeletal grains (e.g., Kidwell and Gyllenhaal, 1998; Cuffey and Johnson, 1997), those encrusting gastropod shells inhabited by hermit crabs document distinct symbiotic associations between these crustaceans and bryozoans (Morris et al., 1989; Taylor et al., 1998; Taylor, 1994; Kidwell and Gyllenhaal, 1998).

Modern bryolith occurrences are reported from the British Isles (Hayward and Ryland, 1979), Northwest Africa (Cook, 1964; 1968a; 1968b), North America to the Gulf of Mexico (Lagaaij, 1963; Winston, 1982; Morris et al., 1989) and New Zealand (Gordon, 1972; Taylor et al., 1989), see also Taylor (1994) and references therein. Among these, bryoliths from the tropical Golfe d'Arguin (Mauritania, NW Africa) provide interesting examples of an ectosymbiosis between two different marine species, while environmental parameters are unique but well known. Mass occurrences of *in situ* bryoliths were, besides the locations reported in this study, identified at 20°17'949 N - 17°11'811 W during a cruise of the Mauritanian Institute for Oceanographic Research and Fisheries (IMROP, 2013) conducted in late 2012 (Suppl. XVIII.1; J. Michel, pers. comm.); see also IMROP in

Fig. X.1. However, as with other such symbioses, both fossil and recent, the net benefit or cost to the two symbionts is largely unknown (Taylor et al., 1989; Taylor, 1994).

From a preservational point of view, this distinctive biocoenosis has a good potential for fossilization because the bryozoan secretes a massive skeleton with a colonial morphology diagnostic of the presence of a hermit crab symbiont. Protected by the multilamellar calcitic bryozoan skeleton, the aragonitic gastropod shell nucleus (see Tab. X.2) is shielded from active bioerosion and may be less prone to long-term diagenetic alteration (see also Taylor, 2005; Smith, et al. 2006). Fossil examples show either a solid-state transformation of gastropod shell aragonite to calcite or a refilling of dissolution voids by diagenetic calcite (e.g., Kidwell and Gyllenhaal, 1998). As a result, bryoliths can document symbiotic interactions as adaptations to environmental limitations even over geological time scales of millions of years. The earliest pagurid-inhabited bryoliths date back to the Middle Jurassic (Palmer and Hancock, 1973; Taylor, 1976; 1994).

X.5.1 Mauritanian bryoliths

The first Mauritanian pagurid-occupied bryoliths were collected from beach drift deposits near Cap Blanc (northern Golfe d'Arguin) and described as a new species (*Conopeum commensale*) by Kirkpatrick and Metzelaar (1922) (see also Cook, 1964; 1968a; 1968b; 1985; Taylor, 1994). Since then, several studies have shown that particular bryozoan species apparently prefer to settle on gastropod shells inhabited by hermit crabs. Cook (1968; 1985) demonstrated this selectivity for the species *Hippoporidra senegambiensis* and it is assumed to be the same for the species *Acanthodesia commensale*. Bryoliths are reported from Cap Blanc, Mauritania (Fig. X.1) that live in a close association with hermit crabs (*Paguridae*) and which occupy predominantly *Turritella* shells (Cook, 1968). Our analyses revealed that nuclei of 20 *in situ* collected bryoliths comprised a variety of gastropod taxa. This suggests that the hermit crabs and their subsequent bryozoan symbionts occupied gastropod shells more or less randomly, probably depending on local distributions and availability in the sediment.

X.5.2 Availability of gastropod shells

Bryolith nuclei (Tab. X.2) include a wide range of gastropod shells that are common along the Mauritanian shelf. Determined shells belong to *Naticidae* (n=10), *Turritellidae* (n=5), *Cassidae* (n=3), *Marginellidae* (n=1) and *Nassaridae* (n=1). Of these, the family *Naticidae* accounted for 50% of all bryolith nuclei examined. Selectivity of, or preference for, particular gastropod taxa or shapes is thus not evident. Ongoing analyses of the component distribution have shown that, although sediments are rich in mollusks (BIMOL and BARNAMOL associations, that grade locally to FORAMOL and BRYOMOL associations)

with bivalves and balanids as the dominant components, gastropod shells account for only 5% or less of the carbonate fraction (see e.g., Koopmann et al., 1979; Piessens, 1979; Ardovini and Cossignani, 2004; Westphal et al., 2007; Michel et al., 2009; 2011a; 2011b; Westphal et al., 2014). However, the rare presence of the turritellid *Mesalia* sp. accumulations in some restricted parts of the northern Banc d'Arguin and in the vicinity of Baie du Lévrier (pers. obs. and Westphal et al., 2014) might lead to locally increased frequencies of certain taxa, which are later used as hermit crab domiciles.

X.5.3 Structural analyses of bryoliths

The internal anatomy of the bryoliths exhibit unique growth patterns (illustrated in Fig. X.3C, F, I), which indicates that the bryozoan colony dynamically reconstructs the living chamber the hermit crab uses as its shelter (Fig. X.3C, F, I; a1-a4). The bryozoan skeletons develop a helicospiral tube that extends the original living chamber of the gastropod shell and provides the hermit crab with an enlarged cavity to occupy. Shape, size and spiral orientation of the reconstructed living chamber are triggered physically by the presence of the hermit crab that controls the growth of the bryozoan colonies along the apertural edge (Fig. X.3C, F, I; s1-s6) to a helicospiral trajectory (Taylor et al., 1989; Taylor, 1994).

Structural analyses of sectioned bryoliths revealed a multilamellar growth pattern, classified as celleporiform (ml-B) *sensu* Nelson (1988b) that encrust a gastropod shell nucleus (Fig. X.3). Apart from one specimen, covered by only a few (<10 laminae) bryozoan layers (14833-8-3, see Fig. X.3A, B, C), all bryoliths show a massive, continuous and exclusively monospecific accretionary growth, that argues for the presence of a single bryozoan colony. Overgrowing of older skeletons results in the formation of bionodules with subspherical to almost spherical shapes. This regular growth and the condition of external bryozoan colony, which was active and healthy in all *in situ* collected samples (Fig. X.2A, C), suggest that the symbioses are in good condition. Moreover, the bryozoan skeletons seem to compensate structural loss due to abrasion (e.g., movement of the colony by the hermit crab) or the bioerosional activities of carbonate-dissolving or encrusting biota (Fig. X.2D). The absence of any discontinuous internal layers (as described in Kidwell and Gyllenhaal, 1998) during the helicospiral phase of growth, argues for a permanent use of the bryolith by the hermit carb without periodic die-off (Fig. X.3C, F, I; s2-s6). Immediate reuse of the housing after ecdysis is indicated and reflects the fact that gastropod shell domiciles are relatively rare.

The base of each bryolith shows abrasion, known as a "pagurid facet", caused by dragging of the colony by the pagurid occupant. Corresponding sections show features similar to erosional truncation in a larger scale (Fig. X.3F; Er). Apart from specimen (14833-8-2; Fig. X.3D, E, F), most facets are poorly developed (see Fig. X.2A) and do not

seem greatly to affect the bryozoans. This argues for the presence of soft-substrates (e.g., coarser biogenic sands), rather than hardgrounds or sharp siliciclastics, which would produce better developed pagurid facets. The abandoned specimens (14782-3-1 and 14725-8-1) show distinct indications of macroborings determined as *Gastrochaenolites* (Fig. X.2B, Ich) and a range of microborings caused by the activity of polychaete worms (Fig. X.2B, Bio).

X.5.4 Bryozoan skeletons

The calcitic skeleton represents around 25-30% of the volume of a single bryozoan zooid. Fine organic-rich membranes separate individual bryozoan chambers (see also Fig. X.2G, H). These can be examined best by high-resolution tomographic scans to reconstruct the 3D shape and thus the volume of the zooecium. Extrapolated to the amount of bryozoan skeletons covering nucleus, the relative extra-weight for the hermit crab would range between 4 and 20g for the specimens examined and listed in Tab. X.2.

However, these analyses are based on µCT scans of three zooecia (Fig. X.2F) and provide only a rough estimate of the contribution of bryozoan skeletal material. Compacted skeletal layers typical in the older parts of colonies around the nucleus or enlarged zooecia in the center of the spiral tube (Fig. X.3H) might have an important influence on the calculation of net skeletal weight. Advanced high-resolution tomographic scans enabling to analyze the bryolith as a whole can provide much more precise 3D data and are planned for the two unprepared specimens held back for later analyses (see Tab. X.2).

X.5.5 Symbiotic interaction

This symbiosis provides important advantages for both participants, as well as some possible disadvantages. Unequivocal identification of a mutualistic (+/+), commensalistic (+/0) or parasitic (+/–) symbiosis is difficult, because comparative values of Darwinian fitness of each associate in and out of association have not been determined, a common problem in the study of symbioses (see Smith, 1992). Another measure of the advantages and disadvantages incurred by symbiosis is its effect on the rate of population growth but this too is difficult to determine (Smith, 1992; Taylor, 1994).

With regard to the Mauritanian symbiosis between bryozoans and pagurid crabs, we interpret the presence of an exclusively monospecific bryozoan cover (mean 91% along the axial plane) as making it likely that the bryozoan achieves a high reproductive fitness and population growth through its association with a hermit crab. Encrusting bryozoans of such large size are unusual. However, this association is a proto-cooperation in the

sense that neither the hermit crab nor the bryozoans are obligatory symbionts of one another (Taylor, 1994).

X.5.6 Advantages and disadvantages of the relationship

One of the most important advantages for the bryozoan colony is the provision of a long-lasting substrate that is protected against the high sedimentation rate and movement of unstable substratum and therefore not buried. The shelf morphology of the central Banc d'Arguin provides neither hardgrounds (minor rocky substrata are limited to the area south of Cap Blanc), nor protection against the strong hydrodynamic regime that causes permanent redeposition of unconsolidated reworked material. A mobile colony is thus a clear advantage that protects the bryozoans not only against physical damage but also from environmental changes in temperature, dissolved oxygen, and salinity, or from siltation (Morris et al., 1989). An analysis of the Mauritanian bryoliths showed that new bryozoan skeletons start to encrust preferentially older skeletons along the apertural edge (Fig. X.3A, G), pending a detailed morphological study of colony skeletons that would indicate genetically different colonies due to the presence of a twinned ancestrula or a zone of astogenetic change. According to Morris et al. (1989) this can be explained by the presence of a microbial surface flora near the outer lip (Fig. X.3; Ol) of the housing, which develops due to nutrition activities of the pagurid symbiont and the presence of fecal material. Feces are known to offer additional nutrition to various microbial groups and bryozoans (Ryland, 1976).

The hermit crab can benefit from the additional protection against predators afforded by the thick bryozoan coating and also from the provision of a continuously growing domicile which can potentially alleviate the need for the crab to switch shells as it grows (see Taylor, 1994; Kidwell and Gyllenhaal, 1998). The dynamically growing bryozoan cover offers the hermit crab a permanent domicile, presumably leading to less intraspecific competition for shells and fewer shell fights (Taylor, 1989; 1994). Also, the multilamellar carbonate skeletons precipitated by the bryozoan colonies may negate or lessen the shell-weakening impact of bioeroders which normally present significant problems for hermit crabs unable to repair or protect the gastropod shells they occupy (e.g., Williams and McDermott, 2004).

Disadvantages for the hermit crab are limited. The extra weight and bulk of the bryolith could theoretically lead to a reduced mobility for the crab and shift in the center of gravity could cause problems in locomotion when bryozoan colonies dominate the weight of the domicile. However, bryoliths that document this condition were not sampled from the Mauritanian Shelf and are to our knowledge not reported in the literature. While the bryozoan colony experiences no significant disadvantage from being associated with a hermit crab, abrasion and loss can occur of some zooids as the crab

drags its domicile over the seafloor (see Fig. X.3B; Pf) and around the aperture through movement of the crab in and out.

As a result of the points explained above we thus interpret this symbiotic association as a mutualistic relationship that provides benefits to both partners, helping them to cope with environmental conditions offshore of Mauritania.

X.5.7 Environmental steering factors

The identification of broad-scale environmental factors from the occurrence of pagurid bryoliths is difficult, not least because knowledge of both partners in the symbiosis is incomplete (see Taylor, 1994 and references therein). However, this *in situ* occurrence from offshore Mauritania provides some useful insights, which highlight the dominance of environmental steering factors interacting with the depositional system and autochthonous faunal communities.

The oceanographic setting offshore of Mauritania is complex and characterized by: (1) high-nutrient settings due to upwelling and iron-rich Saharan dust; (2) an intense hydrodynamic regime driven by upwelling swell, tidal currents and shelf morphology; and (3) largely aphotic conditions that limit the marine biodiversity to light-independent filter-feeding specialists (e.g., balanids, mollusk, bryozoans, echinoids and arthropods). Remains of these organisms cover large areas of the shallow Banc d'Arguin and Baie du Lévrier (Koopmann et al., 1979; Piessens, 1979; Wolff et al., 1993, Michel et al., 2009; 2011a; 2011b). Characterized by admixed siliciclastics (e.g., quartz-grains) provided by the Saharan hinterland or by migrating dunes, this marine depositional system has a mixed-carbonate-siliciclastic character (Westphal et al., 2010; 2014).

The shelf morphology is characteristic in providing few hardground substrates, while extensive areas of the shallow Banc d'Arguin are dominated by moving shoals of coarse sandy material and an intense hydrodynamic regime, in water depths largely <20 mbsl (Fig. X.1). The cool and nutrient-rich upwelling waters (> 3 mg*m^{-3} [Chl *a*]) see Westphal (2010) swell onto the shallow shelf where they warm up to >23 °C and favor the formation of a heterozoan facies that develops in tropical latitudes (Westphal et al., 2010; Michel et al., 2011a). Towards the shelf break in 80-110 mbsl the sediments of the outer shelf (Fig. X.1) are enriched in fine-clastic 'muddy' material of mostly terrestrial origin, less biogenic material, and locally large accumulations of drift bodies (Fig. X.1; AMW, TMW) composed of siliciclastic sands and remains of carbonate precipitating organism (Hanebuth and Henrich, 2009; Michel et al., 2009).

The bryoliths were collected from the central Banc d'Arguin (Fig. X.1; 14833) in water depths of around 25 mbsl where the sea bottom substratum is characterized by coarse bioclastic material classified as BARNAMOL and BIMOL *sensu* Hayton et al. (1995).

Sediments vary from well-sorted shelly sand in <20 mbsl to silty sand in water depths >30mbsl. Major components are, apart from remains of *Balanus sp*. and large clams of *Venus crebrisulca* (=*Venus rosalina*), the shallow infaunal species *Donax burnupi,* which accumulates in the north (south of Cap Blanc) up to monospecific deposits (Westphal, 2010; Michel, 2011b). *Donax burnupi* is known to be a dominant bivalve in high energy regimes, sandy beaches and shallow subtidal sandy flats under highly productive, tropical to subtropical conditions and represents an important environmental indicator (Michel et al., 2011b). Gastropod shells are rare components along the central Banc d'Arguin. Some locations in the vicinity of Cap Blanc show restricted enrichments in gastropod shells that probably account for the dominance of turritellid nucleated bryoliths reported by Cook (1968a; 1968b). The general levels along the Banc d'Arguin, however, do not exceed 5 % of the bioclastic fraction, which highlights the value of empty gastropod shells as suitable shelters for hermit crabs (Kellog, 1976).

This obvious lack in gastropod housings correlates with a dominance of other trophic-related biota (e.g., filter feeders, bivalves) that provide higher carbonate precipitation rates and whose remains cover large parts of the Banc d'Arguin, forming high-dynamic deposits. As a consequence, the hermit crab provides for its house-building symbiont a hard surface for settlement and probably nutritional resources (e.g., organic debris, fecal pellets, food particles, microbiota; Morris et al., 1989). Furthermore, it moves the colony away from environmental threads (e.g., changes in temperature, salinity, dissolved oxygen or siltation), protects the colony against physical abrasion (e.g., high water energy) and avoids burial of the bryolith (e.g., high sedimentation rates, moving clastic shoals) Taylor, 1994. Therefore we conclude that the hermit crab is re-using its valuable housing immediately after ecdysis, which in turn reduces intra-specific shell fights, provides camouflage (e.g., individual pigmentation) and protection against predators (e.g., thick colonies, egg-shaped bryolith).

This protective behavior provided by the hermit crab is shown best by the development of thick, monospecific and healthy bryozoan colonies that show high reproduction rates and the absence of any periodic die-off as reported by Kidwell and Gyllenhaal (1998) for Pliocene tidal channel deposits of the Imperial Formation of southeastern California.

X.5.8 Analogues from the New Zealand Shelf and southeastern California

Locations that show comparable hermit crab bryoliths are sparse, although important occurrences have been reported from the southern part of New Zealand (Taylor et al., 1989) and North America (Morris et al., 1989; Kidwell and Gyllenhaal, 1998). Of these, the depositional environments and ecological parameters of the Otago assemblages (New Zealand) are of special interest. Both the NW Mauritanian Shelf and the Otago Shelf

show a carbonate-siliciclastic depositional system, characterized by unstable substrata and the lack of rough sea bottom topography, needed to develop a rich and diverse epibenthic community. Carbonate production on the central New Zealand Shelf is largely suppressed due to the input of terrigenous material produced by physical weathering and active volcanism and transported to the shelf. The northern- and southernmost tips of New Zealand, however, provide high carbonate production with a calcium carbonate content of more than 75 %; (50–75 % for the Otago Shelf) (Nelson et al., 1988a). Bryozoan taxa are widespread along the shelf and are often the dominant skeletal contributors in all sediments, forming a BRYOMOL carbonate grain association *sensu* Nelson (1988b), see also Tab. X.4.

Hermit crab-occupied bryoliths are reported from the middle to outer Otago Shelf setting (69 – 87 mbsl) where they encrust gastropod shells, but also calcareous worm tubes (Nelson, 1988b). According to Taylor et al. (1989) 60 bryozoan taxa can be identified of which 13 species are capable of forming helicospiral extensions beyond the shell aperture. Although this relatively high diversity of hermit crab symbionts along the New Zealand Shelf is in contrast to the monospecific assemblages from Mauritania, their distributional pattern and species richness can be attributed to the presence of suitable substrates and replenished nutrient supplies (Taylor, 1989; Nelson, 1988b). The availability of a suitable substrate in Mauritania is limited; however, the permanent nutrient supply and tropical to subtropical water temperatures guarantee a high primary production. Trophically controlled regimes that provide a constant source of food, while the availability of substrata for bryozoans and hermit crabs are limited, are interpreted to be important factors that favor symbioses between hermit crabs and bryozoans.

Fossil bryolith occurrences are reported from the ~4 Ma Camel Head Member of the Imperial Fm. of southeastern California (Johnson et al., 1983; Winker and Kidwell, 1986), where they constitute part of tidal channel deposits. This depositional setting is characterized by tropical and dominantly siliciclastic conditions (Kidwell and Gyllenhaal, 1998).

Bryoliths from the Imperial Fm. show a colony growth that is different from both the Mauritanian and New Zealand bryoliths; however, its internal structure tells a lot about the environmental conditions and ecological parameters that govern this depositional system. Moreover, the Imperial Fm. bryolith forming species is determined as *Biflustra commensale*, which is often used as a synonym of the West African species *Acanthodesia commensale* (see Taylor, 1994; Grischenko et al., 2002). Pending a full morphological and systematical study, we here assume both bryozoans to be the same species, or at least very close relatives. A number of bryoliths from the Imperial Fm. are associated with the tidal channels, either in muddy oyster banks along channel margins or in the thalweg itself. Each environment hosts a different assemblage of bryolith morphotypes that is characterized by its internal anatomy.

Table x.4: Environmental and sedimentological parameters that characterize the Mauritanian (A) and New Zealand (B) carbonate depositional system.

Environmental or facies parameter	A - Mauritania modern shelf carbonates	B – New Zealand modern shelf carbonates (from Nelson, 1988a)
Latitude	Between 19 °N and 21 °N	Between 33 °S and 49 °S
Climate zone	Subtropical to tropical	Cool to warm temperate
Mean annual water temp.	>23 °C	13-19 °C
Minimum annual water temp.	18 °C	9-12 °C
Salinity	S = 35.8-36.1 PSU	S = 34.3-35.7 PSU
Water circulation	Strong tidal driven, wind driven	Open, strong storm swell, tidal influence
Shelf gradient	0.75m/km	0.25-2m/km
Reef structures	Absent	Absent (local oyster banks)
Sedimentation rate	Moderate to high	Low but variable
CaCO3 content	35-93 %	50-100 %
Terrigenous grains	Abundant (quarts grains)	Rare-abundant
Non-skeletal grains	Aggregates, ooids(?)	Absent
Major skeletal grains	Mollusks (chiefly bivalves), barnacles, foraminifers, bryozoans, serpulids, echinoderms, corals (ahermatypic)	Bryozoans, mollusks, foraminifers, barnacles, calcareous red algae, serpulids, corals (ahermatypic), echinoderms, brachiopods
Carbonate grain associations	Barnamol > Bimol >Foramol> Bryomol	Bryomol > Foramol
Trophic class	Mesotropic to eutrophic	Oligotrophic
Nutrient sources	Upwelling, iron-rich desert dust	Riverine input, upwelling, ocean fronts

This internal structure is described in Kidwell and Gyllenhaal (1998) as response of the colony growth under environmental constraints. Specimens associated with the less dynamic channel margin and oyster banks are characterized by a simple internal growth structure, while others from the channel thalweg experienced higher water energies and tend to develop a more complex and often interrupted growth record. The internal anatomy of most high-energy bryoliths indicates multi-colony growth and repeated abandonment of the colony by hermit occupants, features that are completely absent in

Mauritanian bryoliths. As a consequence, the growth history tends to be irregular and bryozoan skeletons are partially overlapping each other. Alternations in the growth record indicate encrustation and bioerosion events, as well as abrasion of the colony by hermit dragging (Kidwell and Gyllenhaal, 1998). Additionally, the presence of pebble and shell-nucleated bryoliths clearly indicates that the Californian symbiotic association was not essential under these environmental settings.

The analogues from the New Zealand Shelf and the fossil examples from the Imperial Fm. of southeastern California provide a range of environmental information that highlight the importance of (1) nutrient supply due to upwelling, (2) the availability of suitable substrate and gastropod nuclei and (3) the hydrodynamic regime that controls the colony growth. Any features that indicate phases of intense bioerosion, enhanced encrustation or a periodic colony die-off as reported from fossil bryoliths of the Imperial Fm. are completely absent in bryoliths from the Mauritanian Shelf. This argues for hydrodynamic stable condition below the storm wave base in a trophic-controlled environment. The regular internal anatomy argues for a single genetic colony that extends the cavity, used by a hermit crab, by a helicospiral growth. To our interpretation this mutualistic relationship is of highest importance for both symbiotic partners and provides a long-term substratum for the bryoliths and a reusable shelter for the hermit crab.

This non-obligatory symbiosis demonstrates the adaptive capabilities and benefits from close partnerships, especially in highly dynamic environments where sessile benthic animals such as bryozoans are prone to disturbance and burial, and shells suitable for occupancy by hermit crabs may be in short supply. The availability of nutrients, either due to ocean upwelling or from terrigenous sources, an unsuitable or even non-existent hardground substrate on which to settle, coupled with an intense hydrodynamic regime, are recognized to be key steering factors favoring this association. Detailed assessment and descriptions of these faunal-ecosystem interactions represents an important challenge for further research.

X.6 Conclusions

Ever since the Middle Jurassic, symbiotic associations between hermit crabs and multilamellar encrusting bryozoans have formed bionodules (bryoliths) in which the hermit crabs reside. The gastropod shell initially inhabited by a pagurid crab forms the nucleus around which the bryozoan colony grows, precipitating skeletal carbonate. End products are subspherical to spherical bionodules occupied by pagurids. Some of the bryozoan symbionts involved have calcitic skeletons, giving the bryoliths a relatively high fossilization potential, documenting this symbiosis over geological timescales. This close association offers advantages to both symbionts and allows them to cope with local environmental constraints and parameters that govern a very complex ecosystem. The

Banc d'Arguin offshore of NW Mauritania provides an important natural laboratory to study the direct response of environmental conditions on faunal communities, and thus the sedimentological record, as it hosts one of the few modern systems in which a heterozoan faunal association develops in the tropics. The entire system shows pronounced upwelling that elevates primary productivity and thus causes low-light to aphotic conditions and reduced oxygen levels in which photoautotrophic organisms are completely absent. Balanids and mollusks are dominant, while gastropod shells are rare, placing greater value on these shelters for the pagurid symbiont.

The bryoliths document a distinctive symbiotic relationship between two different marine organisms that allows the bryozoan partner to live where few or no hardground substrates exist and burial and disturbance present problems, while the hermit crab host gains a long-lasting domicile providing protection against predators and bioerosion. It thus represents a valuable environmental indicator, although reported occurrences, both recent and fossil, are relatively few and knowledge of the interacting symbiotic partners is limited.

X.7 Acknowledgements

Participants and crew of the Maria S. Merian Cruise MSM 16 leg 3 are gratefully acknowledged for providing support and sample background data. Claire Reymond and Julien Michel (both ZMT-Bremen, Germany) are acknowledged for stimulating discussions and comments on an earlier version of this manuscript. Susan M. Kidwell and an anonymous reviewer provided thought-provoking reviews for which we are grateful. The project was funded through the DFG-Research Center/Cluster of Excellence "The Ocean in the Earth System", project SD-2 and is part of the PhD thesis of André Klicpera.

X.8 References

Adey, WH, MacIntyre, IG (1973) Crustose coralline algae: a re-evaluation in the geological sciences. Geological Society of America Bulletin 84:883-903

Aleman N, Certain R, Courp T, Barusseau JP, Vernet R, Dia A (2010) Le Golfe d'Arguin – Carte Morpho – Bathymetricque. IMAGES - Institut de Modélisation et d'Analyse en Géo-Environnement et Santé. Université de Perpignan (France)

Ardovini R, Cossignani T (2004) West African seashells (including Azores, Madeira and Canary Is.) Conchiglie dell'Africa Occidentale (incluse Azzorre, Madeira e Canarie). English-Italian edition. L'Informatore Piceno: Ancona, Italy. 319 pp

Campredon P (2000) Entre le Sahara et L'Atlantique – Le parc National du Banc d'Arguin – Mauritanie. FIBA, la Tour du Valat, Arles, France. pp. 124

Balson PS, Taylor PD (1982) Palaeobiology and systematics of large cyclostome bryozoans from the Pliocene Coralline Crag of Suffolk. Palaeontology 25(3):529-554

Boucher DH (1988) The Biology of Mutualism: Ecology and Evolution. Oxford University Press

Cadée GC (2007) Balanuliths: Free-living clusters of the barnacle *Balanus crenatus*. Palaios 22: 680-681.

Cook PL (1964) Polyzoa from West Africa. Notes on the genera *Hippoporina* Neviani, *Hippoporella* Canu, *Cleidochasma* Harmer and *Hippoporidra* Canu & Bassler (Cheilostomata, Ascophora). Bulletin of the British Museum (Natural History) (Zoology Series) 12:1-35

Cook PL (1968a) Bryozoa (Polyzoa) from the coasts of tropical West Africa. Atlantide Report 10:115-262

Cook PL (1968b) Polyzoa from West Africa. The Malacostega - Part 1. Bulletin of The British Museum (Natural History). Zoology 16:115-160

Cuffey RJ and Johnson ME (1997) Bryozoan nodules built around andesite clasts from upper Pliocene of Baja California: palaeoecological implications and closure of the Panama Isthmus. In Johnson ME and Ledesma-Vázques J (eds.): Pliocene Carbonates and related Facies Flanking the Gulf of California, Baja California, Mexico. Geological Society of America. Special Paper 318:111-117

Douglas AE (1994) Symbiotic Interactions. New York: Oxford University Press on Demand

Ehrenberg K (1931) Über Lebensspuren von Einsiedlerkrebsen. Palaebiologica, 4, 137-174

Eisele M, Frank N, Wienberg C, Titschack J, Mienis F, Beuck L, Tisnerat-Laborde N, Hebbeln, D (2013) From sediment baffling to mass wasting – Sedimentation patterns on a cold-water coral mound in the Banda Mound Province, Mauritania, submitted to Deep Sea Research II

Flor FD (1970) Biometrische Untersuchungen zur Autökologie ober-kretazischer Bryozoen. Dissertation, Fachbereich für Geowissenschaften, Universität Hamburg

Ginsburg RN and James NP (1974) Holocene carbonate sediments of continental shelves, in Burke CA and Drake CL, (eds.): The geology of continental margins. Springer-Verlag, Berlin. p. 137-155

Glynn PW (1974) Rolling stones among the Scleractinia: mobile coralliths in the Gulf of Panama.Proceedings of the 2nd International Coral Reef Synopsium 2:183-198

Gordon, DP (1972) Biological relationships of an intertidal bryozoan population. Journal of Natural History, 6, 503-514

Grischenko AV, Taylor PD, Mawatari SF (2002) A New Cheilostome Bryozoan with Gigantic Zooids from the North-West Pacific. Zoological Science 19:1279–1289.

Hanebuth TJJ, Lantzsch H (2008) A Late Quaternary sedimentary shelf system under hyperarid conditions: Unravelling climatic, oceanographic and sea-level controls (Golfe d'Arguin, Mauritania, NW Africa). Marine Geology 256:77-89

Hanebuth TJJ, Henrich R (2009) Recurrent decadal-scale dust events over Holocene western Africa and their control on canyon turbidite activity (Mauritania). Quaternary Science Reviews 28:261-270

Hanebuth TJJ, Mersmeyer H, Kudrass HR, Westphal H (subm. 09/2012) Aeolian to shallow-marine shelf architecture off a major desert since the Late Pleistocene (Northern Mauritania). Geomorphology

Hayton S, Nelson CS, Hood SD (1995) A skeletal assemblage classification system for non-tropical carbonate deposits based on New Zealand Cenozoic limestones. Sedimentary Geology v. 100, 1–4, pp.123-141

Hoffmann L (1988) The Banc d'Arguin: nature in harmony with man. WWF News, June/July: 10-11

Hayward PJ and Ryland JS (1979) Bristish ascophoran bryozoans. Synopses of the British Fauna (New Series), 14, 1-312

IMROP (2013) Atlas maritime des zones vulnérables en Mauritanie - Un appui à la gestion écosystémique et équitable. IMROP, Nouhadibou, Mauritania, 152 pp., in press

James DW, Foster MS and O'Sullivan J (2006) Bryoliths (Bryozoa) in the Gulf of California. Pacific Science 60:117-124

James NP (1997) The cool-water carbonate depositional realm, in James NP and Clarke JAD (eds.). Cool-Water Carbonates. SEPM Special Publication 56 pp. 1–20

Johnson NM, Officer CB, Opdyke ND, Woodard GD, Zeitler PK & Lindsay EH (1983) Rates of late Cenozoic tectonism in the Vallecito-Fish Creek Basin, western Imperial Valley, California. Geology 11, 664-667
Karleskint G, Turner RL, and Small, JW (2009) Introduction to Marine Biology. Brooks/Cole. ISBN: 0495561975
Kellog CW (1976) Gastropods shells: a potential limiting resource for hermit crabs. J. Exp. Mar. Biol. Ecol., 22:101-111
Kirkpatrick R and Metzelaar J (1922) On an instance of commensalism between hermit crabs and a polyzoon. Proceedings of the Zoological Society of London 1922:983-990.
Kidwell SM and Gyllenhaal ED (1998) Symbiosis, competition, and physical disturbance in the growth histories of Pliocene cheilostome bryoliths. Lethaia vol. 31:221-239
Kissling DL (1973) Circumrotatory growth form in Recent and Silurian corals. In Boardman RS, Cheetham AH & Oliver WA (eds.): Animal Colonies 43-58. Dowden, Hutchinson & Ross, Stroudsburg
Klicpera A, Taylor PD, Westphal H (2013) Bryoliths constructed by bryozoans in symbiotic associations with hermit crabs in a tropical heterozoan carbonate system, Golfe d'Arguin, Mauritania. Marine Biodiversity 43:429–444, DOI 10.1007/s12526-013-0173-4
Koopmann B, Lees A, Piessens P, and Sarnthein M (1979) Skeletal carbonate sands and wind-derived silty-marls off the Saharan coast: Baie du Lévrier, Arguin Platform, Mauritania: Meteor Forschungsergebnisse, Reihe C 30:15–57
Lagaaij R (1952) The Pliocene Bryozoa of the Low Countries and their bearing on the Marine Stratigraphy of the North Sea Region. Proefschrift Robert Lagaaij, Ernest van Aelst
Lagaaij, R (1963) New additions to the bryozoan fauna of the Gulf of Mexico. Publications of the Institute of Marine Science, Texas, 9, 162-236
Lees A and Buller AT (1972) Modern temperate water and warm-water shelf carbonate sediments contrasted: Marine Geology 13:67–73
McKinney FK, Jackson JBC (1991) Bryozoan Evolution. University of Chicago Press edition 1991
McLaughlin P (2012) *Pseudopagurus granulimanus* (Miers, 1881). In: Lemaitre R, McLaughlin P, (2012). World Paguroidea & Lomisoidea database. Accessed through: World Register of Marine Species at http://www.marinespecies.org/
Maranon E and Holligan PM (1999) Photosynthetic parameters of phytoplankton from 50 °N to 50 °S in the Atlantic Ocean. Mar Ecol Prog Ser 176:191–203
Michel J, Westphal H, and Hanebuth TJJ (2009) Sediment partitioning and winnowing in a mixed eolian–marine system (Mauritanian shelf). Geo-Marine Letters 29:221–232
Michel J, Mateu-Vicens G, Westphal H (2011a) Modern heterozoan carbonates from a eutrophic tropical shelf (Mauritania). Journal of Sedimentary Research 8:641-655
Michel J, Westphal H, Von Cosel (2011b) The Mollusk Fauna of Soft Sediments from the tropical, upwelling-influenced shelf of Mauritania (Northwestern Africa). Palaios 26(7):447-460
Moen FE, Svensen E (2004) Marine fish & invertebrates of Northern Europe. AquaPress. ISBN: 0-9544060-2-8
Moran NA (2006) Symbiosis. Current Biology Volume 16, Issue 20, 24:866-871
Morris PA, Soule DF, Soule, JD (1989) Bryozoans, Hermit Crabs, and Gastropods: Life strategies can affect the fossil record. Bull. Southern California Acad. Sci. 88(2):45-60.
Nelson CS, Keane SL, Head PS (1988a) Non-tropical carbonate deposits on the modern New Zealand shelf. Sedimentary Geology 60(1988):71-94
Nelson CS, Hyden FM, Keane SL, Leask WL and Gordon DP (1988b) Application of bryozoan zoarial growth-form studies in facies analysis of non-tropical carbonate deposits in New Zealand. Sedimentary Geology 60(1988):301-322
Ould Mahfoudh M, Dobrovine B, Ould Dedah S (1991) Hydrologique des eaux superficilles du Banc d'Arguin, Département Ressources et Environment et Laboratoire d'Hydrologie et Environment, Centre National de Recherches Oceanographiques et des Peches; http://hdl.handle.net/1834/518
Palmer TJ and Hancock CD (1973) Symbiotic relationships between ectoprocts and gastropods, and between ectoprocts and hermit crabs in the French Jurassic. Palaeontology 16:563-566
Piessens P (1979) Influence relative des sources de production et du transport dans la formation de facies calcaires biogéniques: les sédiments quaternaires de la plate-forme d'Arguin (Mauritanie) et comparaison avec des régions cotières européennes (Irlande et Hébrides). Dissertation, Université Catholique de Louvain
Reguant S, Fernandez J, Rodriguez-Fernandez J, and Serra-Kiel J (1991) Bryozoan biofacies, zoarial forms and sedimentary environments in the Tertiary of Spain. In Bigey FP (ed.): Bryozoaires actuels et fossiles 361-370. Bulletin de la Société Sciences Naturelle d'Ouest France, Memoires, H.S. 1
Reymond CE, Mateu-Vicens G, Westphal H (2013) More than latitude: controlling factors shaping foraminiferal assemblages from the Golfe d'Arguin, Mauritania. Submitted to Estuarine, Coastal and Shelf Science

Rider J and Enrico R (1979) Structural and functional adaptations of mobile anascan ectoproct colonies (ectoproctaliths). In Larwood EP and Abbott MB (eds.): Advances in Bryozoology, 297-320. Academic Press, London
Roff G (2007) Corals on the move: morphological and reproductive strategies of reef flat coralliths. Coral Reefs 27:343-344
Ryland JS (1976) Physiology and ecology of marine bryozoans. *In* Advances in Marine Biology, 14:285-443. Academic Press, London
Smith DC (1992) The symbiotic condition. Symbiosis 14:3-15
Smith AM, Key Jr. MM, Gordon DP (2006) Skeletal mineralogy of bryozoans: Taxonomic and temporal patterns. Earth-Science Reviews 78 (3–4):287-306
Stachowitsch M (1980) The epibiotic and endolithic species associated with the gastropod shells inhabited by the hermit crabs Paguristes oculatus and Paguristes cuanensis, PSZNI Mar. Ecol., 1, 73–101, 1980. 4386
Taylor PD (1976) Multilamellar growth in two Jurassic cyclostomatous Bryozoa. Palaeontology 19:293-306
Taylor PD (1991) Observations on symbiotic associations of bryozoans and hermit crabs from the Otago Shelf of New Zealand. In Bigey FP (ed.): Bryozoaires actuels et fossils, 487-495. Bullétin de la Societé des Sciences Naturelle de l`Quest de la France, Momoires, H.S. 1
Taylor PD (1994) Evolutionary palaeoecology of symbioses between bryozoans and hermit crabs. Historical Biology 9:147-205
Taylor PD (2005) Bryozoans and palaeoenvironmental interpretation. Journal of the Palaeontological Society of India 50(2):1-11
Taylor PD and Monks N (1997) A new cheilostome bryozoan genus pseudoplanktonic on molluscs and algae. Invertebrate Biology 116 (1):39-51
Taylor PD and Schindler KS (2004) A new Eocene species of the hermit-crab symbiont *Hippoporidra* (Bryozoa) from the Ocala Limestone of Florida. Journal of Paleontology 78:790-794
Taylor PD, Schembri PJ, Cook PL (1989) Symbiotic associations between hermit crabs and bryozoans from the Otago region, southeastern New Zealand. Journal of Natural History 23:1059-1085
Vermaat JE, Beijer JAJ, Gijlstra R, Hootsmans MJM, Philippart CJM (1993) Leaf dynamics and standing stocks of intertidal *Zostera noltii* Hornem, and *Cymodocea nodosa* (Ucira) Ascherson on the Banc d'Arguin (Mauritania). Hydrobiology 258:59–72
Westphal H, Freiwald A, Hanebuth TJJ, Eisele M, Gürs K, Heindel K, Michel J and Reumont J (2007) Report and preliminary results of Poseidon cruise 346 — MACUMA: integrating carbonates, siliciclastics and deep-water reefs for understanding a complex environment, Las Palmas (Spain)–Las Palmas (Spain), 28.12.2006–15.1.2007. Reports of the Dept. of Geosciences, University of Bremen, Germany, 49 pp.
Westphal H, Beuck L, Braun S, Freiwald A, Hanebuth TJJ, Hetzinger S, Klicpera A, Kudrass H, Lantzsch H, Lundälv T, Mateu-Vicens G, Preto N, Reumont J, Schilling S, Taviani M and Wienberg C (2013) Report of Cruise Maria S. Merian 16/3 — Phaeton – Paleoceanographic and paleo-climatic record on the Mauritanian shelf. Oct. 13 – Nov. 20, 2010, Bremerhaven (Allemagne) – Mindelo (Cap Verde). Maria S. Merian-Berichte, Leibniz-ZMT, Bremen, Germany, 136 pp.
Westphal H, Halfar J and Freiwald A (2010) Heterozoan carbonates in subtropical to tropical settings in the present and in the past: International Journal of Earth Sciences 99:153–159
Williams JD, McDermott JJ (2004) Hermit crab biocoenoses: a worldwide review of the diversity and natural history of hermit crab associates. Journal of Experimental Marine Biology and Ecology 305:1-128
Winker CD and Kidwell SM (1996) Stratigraphy of marine rift basin: Neogene of the western Salton Trough, California. In Abbott PL and Cooper JD (eds.): Field Conference Guide 1996. Pacific Section AAPG Guide Book 73, Pacific SEPM Book 80:295-336
Winston JE (1982) Marine bryozoans (Ectoprocta) of the Indian River area (Florida). Bulletin of the American Museum of Natural History, 173, 99-176
Winston JA and Heimberg BF (1986) Bryozoans from Bali, Lombok, and Komodo. American Museum Novitates 2847, 99:1-49
Wolff WJ, Van Der Land J, Nienhuis PH and De Wilde PAWJ (1993) The functioning of the ecosystem of the Banc d'Arguin, Mauritania: a review. Hydrobiologia 258:211–222

XI. Third publication

Bryozoans on the move: Adaptations to hard substrate–limiting tropical heterozoan carbonates (Banc d'Arguin, Mauritania)

André Klicpera, Paul D. Taylor, Hildegard Westphal

Marine Biodiversity (Oct. 2014, online first)
Doi:10.1007/s12526-014-0279-3

this page is intentionally left blank

Bryozoans on the move: Adaptations to hard substrate–limiting tropical heterozoan carbonates (Banc d'Arguin, Mauritania)

André Klicpera[1], Paul D. Taylor[2], Hildegard Westphal[1,3]

1 Leibniz Center for Tropical Marine Ecology (ZMT), Bremen, Germany
2 Department of Earth Sciences, Natural History Museum London, UK
3 Department of Geosciences, University Bremen, Germany

The Banc d'Arguin off Mauritania hosts an extensive warm-water heterozoan carbonate factory that is unique in the present-day world. Tropical waters characterize this epicontinental gulf that lacks photosymbiotic fauna because of increased nutrient levels, low water transparencies and dust from the Sahara. Dominated by eutrophic conditions, this atypical carbonate system does not fit into commonly used classifications. However, in representing a depositional paradox, the Banc d'Arguin serves as a modern analogue for the geological record and future perspectives of marine environments affected by eutrophication and desertification. The heterozoan community is low in biodiversity because tropical elements are suppressed by dysphotic conditions and partly anoxic settings, a result of high primary productivity induced by upwelling. Paucity of hard substrates and the hydrodynamic regime make this ecosystem particularly challenging for marine organisms. Profiteers are specialized suspension feeders, such as molluscs, balanids and bryozoans (Fig. XI.1A).

By forming free-living, semi-mobile colonies, cupuladriid bryozoans (e.g. *Reussirella* sp., Fig. XI.1B) are well adapted to distinct niche habitats characterized by sandy substrates. Locomotion is made possible by using semi-rigid setae that act as legs. This adaptation enables colonies to resurface if buried, as well as to move on or within the sediment (O'Dea et al. 2009). High population densities (>500 colonies m^{-2}) in Mauritanian sediments and similar occurrences reported from other mixed carbonate-siliciclastic shelves off Florida, Brazil (Winston & Migotto 2005) and Ghana (Cook 1965) indicate that these interstitial bryozoans may be more common and of greater relevance than marine ecologists have realized so far.

Another extraordinary adaptation to environmental constraints is the symbiotic partnership between bryozoans (*Acanthodesia commensale*) and a hermit crab (*Pseudopagurus granulimanus*). This non-obligatory cooperation provides benefits to both symbiotic partners. As the bryozoan colony grows, it furnishes an ever-enlarging shelter for the growing hermit crab occupant (Fig. XI.1C). In exchange, the crab offers a hard substrate on which to settle, moves the colony to new feeding grounds or protects it against hazards and endobiotic bioerosion (Klicpera et al. 2013).

These new records from the Mauritanian Shelf highlight that our perspective on subtidal sand communities deserves more attention and how such potential bioarchives can increase our understanding of environmental control factors.

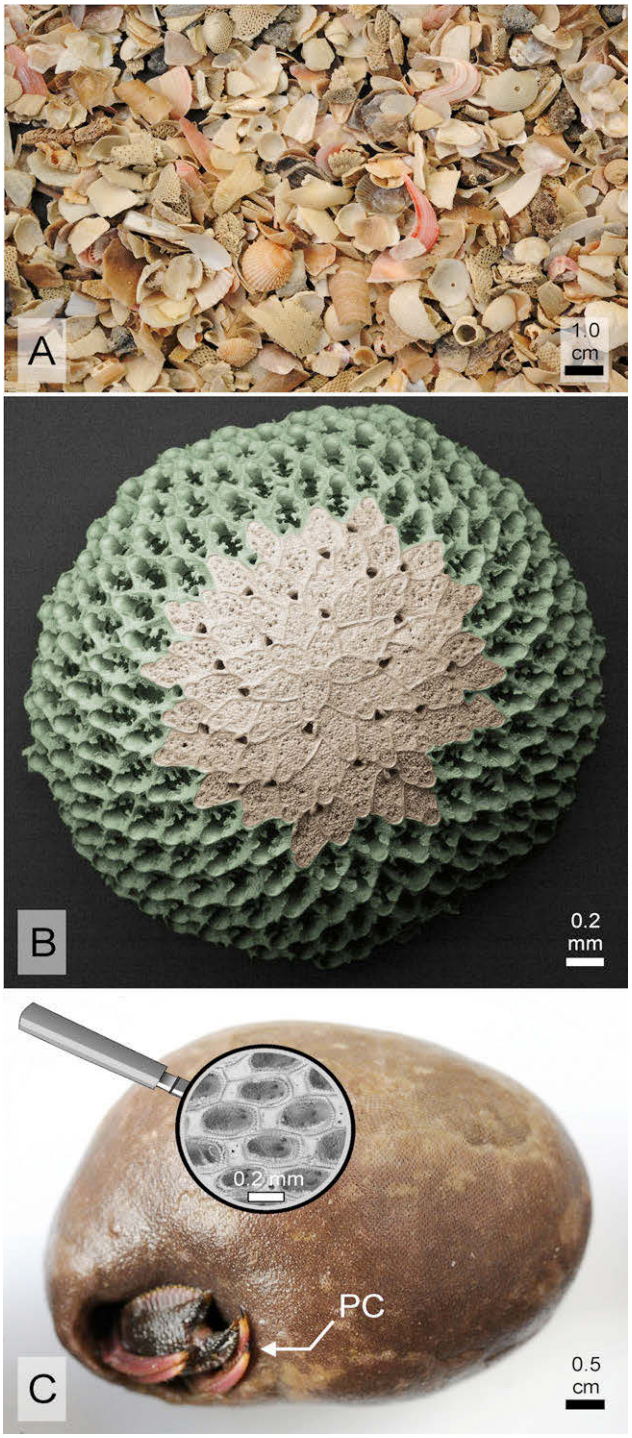

Fig. XI.1: (A) Heterozoan carbonates form the Banc d'Arguin; (B) SEM image of *Reussirella* sp.; (C) Mauritanian bryolith encrusted by *Acanthodesia commensale* and occupied by pagurid crab (PC).

References:

Cook PL (1965) Polyzoa from West Africa: The Cupuladriidae (Cheilostomata, Anasca). British Museum (Natural History).

Klicpera A, et al. (2013) Bryoliths constructed by bryozoans in symbiotic associations with hermit crabs in a tropical heterozoan carbonate system, Golfe d'Arguin, Mauritania. Mar. Biodiv. 43:429–444.

O'Dea A, et al. (2009) Relation of form to life habit in free-living cupuladriid bryozoans. Aquat. Biol. 7:1–18.

Winston JE & Migotto AE (2005) A new encrusting interstitial marine fauna from Brazil. Invertebr. Biol. 124:79–87.

XII. Bivalve shells as environmental archives

Invertebrates are the most common constituents of the metazoan fossil record, and since they are abundant in Phanerozoic marine sedimentary deposits worldwide, they are of great utility in reconstructing ancient climates and environments (Gaines and Droser, 2009). Among the marine invertebrates, the mollusks or more specifically, bivalves provide a number of important biorecorders, because they are able to store environmental proxies such as seawater properties within their shells and skeletons. Morphological features, shell size and sculpture are furthermore valuable indicators of certain environmental constraints governing their habitats and lifestyle (Stanley, 1975). Today it is known that the marine biodiversity of modern marine environments is greatest at equatorial latitudes and declines towards higher latitudes. In general, this pattern is in accord with data from the fossil record (Hallam, 1994; Parrish, 1998). This characteristic is making especially long-living large and robust carbonate secretors such as bivalves and corals to ideal environmental archives covering recent to geological time-scales (Wefer, 1985).

Although the primary factors, which govern this pattern are a subject of debate, many environmental factors other than temperature are clearly important (Gaines and Droser, 2009). These include (1) the availability of nutrients (e.g., Halfar et al., 2004; Westphal et al., 2010; Reijmer et al., 2012); (2) decreased environmental stability at high latitudes (Sanders, 1968); (3) dominance of trophic generalists in resource-limited high latitude regions as opposed to high niche partitioning in resource-rich low latitude regions (as a result of e.g., seasonality) (Valentine, 1973); and (4) variation in light incidents across latitudinal gradients (Ziegler et al., 1984). As a consequence, various concepts evolved during the last decades that focus on the distributions of faunal assemblages in relation to their latitudinal setting and environmental steering parameters, see e.g., Addicott (1969); Roy et al. (1996); Nakashima (2002) and Westphal et al. (2010).

Whereas species distribution, assemblage content, presence/absence pattern and diversity may be used to address a wide range of palaeo-climatological questions, some specific geobiochemical signals within the shells or skeletons of carbonate precipitating invertebrates (such as e.g., corals, mollusks, brachiopods and foraminifers) can provide highly sensitive proxies for palaeo-temperature and related environmental conditions (Wefer, 1985; Gaines and Droser, 2009; Schöne and Gillikin, 2012). However, since biogenic carbonate minerals are extremely sensitive to alteration or recrystallization during post-burial processes (e.g., bioerosion, diagenesis) the original carbonatic microstructure and mineralogy of a sub-recent or fossil sample is of highest importance for accurate geochemical analyses. Otherwise, the geochemical footprint of a sample can

also represent characteristics and processes, which took place within the diagenetic environment (see e.g., Nothdurft and Webb, 2009 and references therein).

The ratio of stable oxygen isotopes ($\delta^{18}O = {}^{18}O/{}^{16}O$) and, to a lesser extend, stable carbon isotopes ($\delta^{13}C = {}^{13}C/{}^{12}C$) from shells and skeletons of carbonate precipitating organisms have proven particularly valuable for palaeoclimate reconstructions. The relationship between the ratios of oxygen isotopes ($\delta^{18}O$) is closely coupled to warm and cold periods in earth history. In general, cool waters are enriched in ^{18}O, while warms waters are relatively depleted. For any given time in the past, however, the ratio of $^{18}O/^{16}O$ is also influenced by the $^{18}O/^{16}O$ ratio of the ocean water, which in turn is controlled by the extent of planetary ice volume (known as "Ice volume effect"). The carbon cycle, on the other hand, is driven by biologic productivity; organisms selectively take up the light isotope, leaving productive surface waters isotopically heavy, and bottom waters isotopically light with respect to $\delta^{13}C$ (Wefer, 1985; Gaines and Droser, 2009).

These specific seawater signatures are incorporated into the shells and hard parts of marine organisms and thus represent valuable biogeochemical proxies where metabolically induced fractionation processes or precipitation out of seawater equilibrium can be excluded. Isotopic studies using marine carbonate secreting organisms consequently had to focus on two primary goals: (1) Large-scale and thus low-resolution analyses of global trends of $\delta^{18}O$ and $\delta^{13}C$ through time (see e.g., Hudson and Anderson, 1989) and (2) more localized, small-scale but high-resolution studies uncovering regional trends. Since the very first pioneering studies by Urey (1951) and Epstein (1951) and the further development of various palaeo-thermometer (palaeotemperature equations *sensu* Anderson and Arthur (1983) and Grossman and Ku (1986)) in the following years, the geochemical approach exposed as a valuable tool in geosciences. However, as the topic 'sclerochronology' is booming and analytical procedures increase in accuracy and, the need for more detailed calibrating studies arises that help to interpret and understand such biogeochemical signatures (Schöne and Gillikin, 2012).

The following study highlights the potential of bivalve shells from the Late Pleistocene as biogenic archive of environmental proxies ($\delta^{18}O$ and $\delta^{13}C$). Serially micro-drilled samples from the growth record within the shell exhibit isotopic signatures indicating local shifts in water temperature that are associated with movements of different temperate water masses offshore Uruguay. The geochemical analyses are supported by faunistic studies that show that cold-water related Magellanic bivalve species were common constituents off Uruguay during the Deglacial. These observations are contrary to the modern assemblage that indicated that the confluences offshore northern Argentina acts today as natural boundary (see e.g., Aguirre, 1993; Aguirre et al., 2005).

XIII. Fourth manuscript

The stable oxygen isotope record of a Late Pleistocene bivalve (*Eurhomalea exalbida*) from the Uruguayan Shelf: implications for palaeoenvironmental reconstructions

André Klicpera, Till J.J. Hanebuth, Alvar Carranza, Hildegard Westphal

In preparation for submission

this page is intentionally left blank

The stable oxygen isotope record of a Late Pleistocene bivalve (*Eurhomalea exalbida*) from the Uruguayan Shelf: implications for palaeoenvironmental reconstructions

André Klicpera[1, 3], Till J. J. Hanebuth[2,3], Alvar Carranza[4], Hildegard Westphal[1,5]

1 Leibniz Center for Tropical Marine Ecology (ZMT), Bremen, Germany;
2 School of Coastal and Marine Systems Sciences, Coastal Carolina University, Conway/SC, USA;
3 Formerly at: MARUM – Center for Marine Environmental Sciences, University Bremen, Germany;
4 CURE – Centro Universitario de la Región Este, Universidad de la República, Maldonado, Uruguay
5 Department of Geosciences, University Bremen, Germany

Abstract

Modern seasonality in the southeastern South American continental shelf system is influenced primarily by the interaction of subtropical waters of the Brazil Current, cold waters of the Malvinas Current and the continental runoff supplied through the Río de la Plata estuary. Little is known, however, about the seasonality history in this region during the past millennia. Understanding the past oceanographic condition is of highest significance, because of its a key role in both, the regional climatic system and the general South Atlantic Ocean circulation.

For the analysis of stable isotopes, a fossil bivalve shell of the temperate-to-cold water species *Eurhomalea exalbida* was collected from a vibro core taken in 141 m modern water depth. AMS-^{14}C dating of shell material delivered an age of 16.9 cal kyrs BP corresponding to deglacial times (Heinrich Event 1). δ^{18}O mean values of 3.27 ± 0.4 ‰ with amplitude variations of up to 1.69 ‰ indicate cooler water temperatures and a more pronounced seasonality than observed for modern conditions. Moreover, the δ^{13}O signature exhibits abrupt negative peaks during the warm season that indicates short-term freshwater intrusions as a result of enhanced continental runoff. Such palaeoenvironmental conditions are supported by biogeographic distribution patterns of *E. exalbida* that shifted continuously southwards since the LGM.

The presented data imply a stronger influence of the South American summer monsoon during 16.9 cal kyrs BP. Moreover, the northward flowing cold Malvinas Current was stronger during this time, also pushing the Subtropical Shelf Front offshore Uruguay northwards of its current position.

Corresponding author: André Klicpera, Leibniz Center for Tropical Marine Ecology (ZMT), Fahrenheitstraße 6, D-28359 Bremen, Germany and Center for Marine Environmental Sciences (MARUM), University of Bremen, Germany

XIII.1 Introduction

The southeastern South American continental shelf offshore Argentina and Uruguay is of special interest for oceanographic studies because it hosts: (1) the worldwide highest-energetic confluence zone, formed by the collision of Malvinas Current and Brazil Current (Arz et al., 1999; Curry and Oppo, 2005; Negre et al., 2010); (2) the Rió de la Plata estuary and connected river systems in the hinterland which transport freshwater and suspended sediments from the second largest drainage system of South America into the ocean (Iriondo et al., 2007; Campos et al., 2008); and (3) an atmospheric system that is characterized by the South American monsoon and seasonally varying winds from southwest (Pampero) and southeast (Sudestada) (Clapperton, 1993; Garzoli and Giulivi, 1994). This wind system with its strong seasonal contrasts has strong control on precipitation and runoff.

Such ocean-atmosphere couplings are also known for their capability to displace shelf water bodies and thus play a key role in the distribution of physico-chemical seawater properties on a continental shelf, strongly influencing the associated ecosystems. Moreover, these couplings usually display a highly dynamic behavior with variability at short (seasonal to annual) to long (millennial to glacial/interglacial) time scales (Zhou and Lau, 1998; Piola et al., 2000, 2005, 2008; Gan et al., 2004; Cruzjr et al., 2007). The complexity and climatological importance of the marine system for the South Atlantic circulation and beyond highlights the need for environmental studies in good spatial and temporal resolution. Although a certain number of palaeoclimatological studies for the deglacial and Holocene period were conducted offshore Brazil and in the southern Patagonian shelf already, the knowledge of the palaeodynamics of the subtropical shelf front off Uruguay is still limited and clearly deserves more attention (Chiessi et al., 2007; Cruzjr et al., 2007; Leduc et al., 2010; Wanner et al., 2011; Bender et al., 2013; Lantzsch et al., 2014).

In this context, sclerochronological approaches may serve as valuable tool for the interpretation of ancient environmental conditions in annual to sub-seasonal resolution over years to centuries (e.g., Dettman and Lohmann, 1994; Weidman, 1995; Jones and Quitmyer, 1996; Schöne et al., 2005a, 2005b; Wisshak et al., 2009; Ivany and Runnegar, 2010; Nützel et al., 2010; Schöne and Gillikin, 2012). Bivalve molluscs, for example, represent valuable, but little-used high-resolution bio-archives. In part, this little attention results from the fact that vital effects often bias biological materials with regard to the precipitation of biogenic carbonate on a geochemical level (see e.g., Yan et al., 2012; Gordillo et al., 2013). Consequently, most biogenic materials, useful for sclerochronological approaches studies, demand for a detailed species-specific calibration study, ideally using modern representatives. Besides these limitations, that need to be addressed when using sub-recent and fossil material as environmental archive, bivalve shells are important climate recorders (cf. Schöne and Gillikin, 2012 and references therein) in the marine realm from tropics to high latitudes.

The presented study uses bivalve shells in their function as high-resolution bio-archive. We micro-sampled shell carbonate and analyzed the stable oxygen ($\delta^{18}O$) and carbon ($\delta^{13}C$) isotopes of accretionarily precipitated increments. This approach aims to sheds light on the palaeodynamics of different temperate-climate water bodies that characterized the southeastern South American shelf during the past deglacial period. The purpose of this study is to get a detailed insight into the respective climatic conditions in highest (sub-seasonal to daily) resolution. We hypothesize that (1) a displacement of the Subtropical Shelf Front took place recurrently as result of the reciprocal dominance of Malvinas Current and Brazil Current; and (2) a freshwater signal has incurred occasionally caused by the enhanced influence of the South American summer monsoon, both being deciphered from the multi-annual shell increments of bivalves.

XIII.2 Study area

The Uruguayan continental shelf spans for over 150 km from the modern shoreline to the shelf break in 150 meters below modern sea level (mbsl). This shelf hosts the following contrasting environmental settings in terms of morphology and seabottom sediments (Campos et al., 2008). The current-controlled generally coarse-grained shelf sediments exhibit a range of local relief-confined mud depocenters in shallower waters, while patchy outcrops (e.g., carbonate 'tosca' crusts, rocks) in deeper waters provide a hard-substrate for extensive mollusc banks (Brazeiro et al., 2003; Violante and Parker, 2004; Ayup-Zouain, 2006; Carranza et al., 2010; Krastel et al., 2012; Lantzsch et al., 2014).

The inner shelf is characterized by two morphological features: (1) a depression at the modern seafloor that is refilled by younger sediments (muds and sands) indicating an ancient fluvial pathway of deglacial times (Fig. XIII.1) and, (2) adjacent to this depression, a chain of sandy, partly carbonate-rich ridges (for details see Lantzsch et al., 2014).

The middle and outer shelf shows a number of local autochthonous and parautochthonous shell beds with fine to coarse calcareous detritus and sedimentary bodies enriched in sand-sized materials (mostly quartz and glaucony; Krastel et al., 2012; Lantzsch et al., 2014). Towards the shelf break, most depositional features are overprinted by the intense hydrodynamic regime as a result of strong bottom currents (Matano et al., 2010).

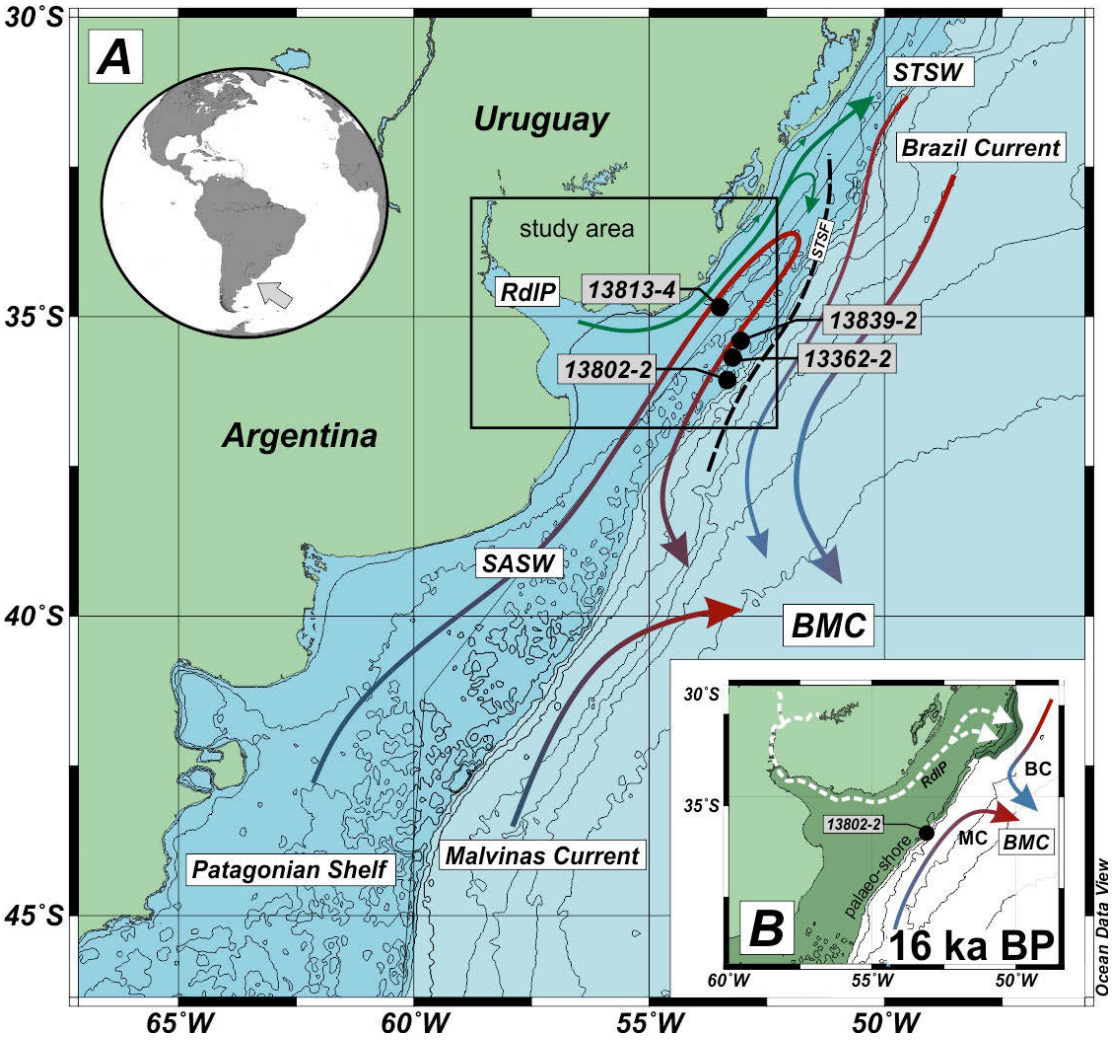

Figure XIII.1: Present-day oceanographic setting of the study area in southeastern South America and locations of the sedimentary cores (grey signs) taken in the inner and outer shelf setting (A). The ancient run of the Río de la Plata (deglacial times; 16 ka BP) is illustrated as dashed white line in (B), also showing the northward displacement of the Brazil-Malvinas Confluence Zone. *SASW*, Sub-Antarctic shelf waters; *RdlP*, Río de la Plata; *STSW*, Sub-tropical shelf waters; *STSF*, Sub-tropical shelf front; *BMC*, Brazil-Malvinas Confluence zone; *BC*, Brazil Current; *MC*, Malvinas Current.

XIII.2.1 Regional Oceanography

The oceanography of southeastern South America is characterized by the collision of two major ocean currents (Fig. XIII.1 and Fig. XIII.2), namely, the warm and saline Brazil Current (BC, >20 °C, >36 ‰) from the North and the cold and less saline Malvinas Current (MC, <15 °C, <34 ‰) from the South (Piola et al., 2000; Piola and Matano, 2001; Matano et al., 2010). Both currents collide between 32 °S and 40 °S and form the high-energetic Brazil-Malvinas Confluence zone (BMC; Fig. XIII.1). On the shelf off Uruguay, the oceanographic setting show a sharp hydrographic boundary (32 to 36°S) that separates

the cool sub-antarctic shelf waters (SASW, <11 °C, <34.5 ‰) from the warm sub-tropical shelf waters (STSW, >16 °C, >34.8 ‰) (Brandani et al., 2000; Piola et al., 2000, 2008). This boundary shows large horizontal temperature and salinity gradients and is known as the Subtropical Shelf Front (STSF).

Shelf surface waters (<20 mbsl) undergo large seasonal temperature changes south of 33 °S with a sea surface temperature (SST) amplitude exceeding 9 °C and reducing to <3 °C north of 23 °S (Piola et al., 2000). The sea surface salinity (SSS) pattern, in contrast, shows little variations (~33.6 to 33.7 ‰) south of 37 °S. Between 37 °S and 35 °S, however, low saline waters (<25 to 30.0 ‰) provided by the Rió de la Plata estuary reach the open shelf (Fig. XIII.1 and Fig. XIII.2) and form a buoyant northeast-directed plume (Emilsson, 1961; Piola et al., 2000).

XIII.2.2 Regional freshwater runoff

Besides a major contribution of suspended sediments ($130*10^6$ $km^2\ yr^{-1}$), the Rió de la Plata provides freshwater (PPW; 670 $km^2\ yr^{-1}$) to the shelf (Depetris and Griffin, 1968). The Paraná and Uruguay Rivers, which drain from different basins, that together form a drainage area covering 20 % ($3.2*10^6\ km^2$) of the South American continent (Campos et al., 2008), provide more than 97 % of the total freshwater runoff. However, since the discharge of these rivers peaks at different times during the year, the seasonal variation of freshwater discharge into the shelf environment is relatively small (5 % of the annual mean) (Burrage et al., 2008). Freshwater mixing with marine waters only occurs in the mouth of the Rió de la Plata estuary that opens up to more than 250 km at its widest dimension.

A second large source of freshwater provides the Patos Lagoon (32 °S). It drains a 200,000 km^2 basin formed by the Guaiba and Camaquã Rivers, which exhibit a high discharge in late winter and early spring and a low to moderate discharge in summer and autumn. The mean annual discharge is 2,000 $m^3\ s^{-1}$ (Vaz et al., 2006), the seasonal mean ranges from 700 $m^3\ s^{-1}$ in summer to 3,000 $m^3\ s^{-1}$ in spring (Moller et al., 2001).

XIII.2.3 Malacofaunal provinces

Biogeographically, the Uruguayan shelf hosts a malacofaunal transition zone (e.g., Olivier and Scarabino, 1972; Kaiser, 1977; Floeter and Soares-Gomes, 1999; Scarabino, 2003). Benthic mollusc assemblages within the outer Rió de la Plata estuary and continental shelf show two main subunits:

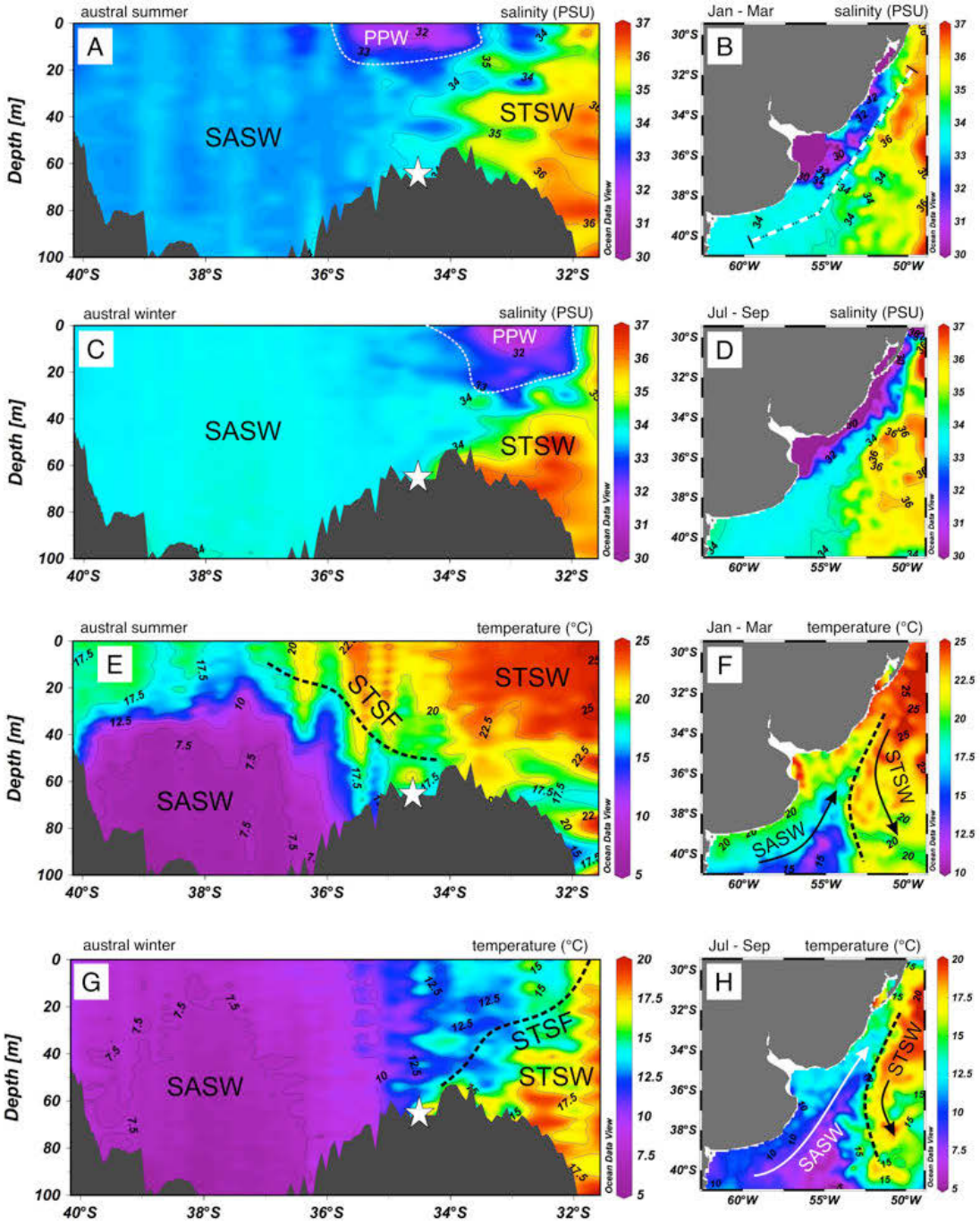

Figure XIII.2: Modern oceanographic settings of the Argentinean and Uruguayan shelf for austral summer (A, B and E, F) and austral winter (C, D and G, H). Seawater salinity pattern for both seasons is shown in (A to D), the seawater temperature pattern is presented in (E to H). The shelf profiles (left column) follow a southeast-northwest transect marked as dashed line in (B). Abbreviations used: *SASW* sub-antarctic shelf waters, *PPW* Río de la Plata plume waters, *STSW* sub-tropical shelf waters, *STSF* sub-tropical shelf front. Data extracted from World Ocean Atlas 2009 (Antonov et al., 2010; Locarnini et al., 2010) and computed in Ocean Data View (Schlitzer, 2012; http://odv.awi.de/).

(1) a zone under the influence of the freshwater discharge of the Rió de la Plata in the shallow waters along the inner shelf and (2) a marine zone in the deeper outer shelf, which hosts both, magellanic and subtropical benthic faunas (Carranza et al., 2008). In the region, beta diversity is strongly influenced by the saline gradient operating at the inner shelf, while a species turnover associated with latitude occurs in the outer shelf. The temperature gradient characterizing the BMC offshore northern Argentina and Uruguay acts therefore as a biogeographic barrier preventing Antarctic cold-water species to pass into warm-temperate and subtropical waters north of the BMC and vice versa.

XIII.3 Material

During research cruise M78 leg 3-a conducted with the German research vessel Meteor in 2009 (Krastel et al., 2012) a number of sedimentary cores (Tab. XIII.1) were taken on the Uruguayan shelf and slope (Fig. XIII.1 and Suppl. XIX.1):

Tab. XIII.1: Sampling locations of bivalve shell material recovered from cores taken during R/V Meteor cruise M78-3a offshore Uruguay. Abbreviations used: *Env* Environment, *IS* inner shelf, *OS* outer shelf, *US* upper slope; gears used: *VC* vibro core, *GC* gravity core, *BC* box core; analyses applied: *OM* optical microscopy, *SEM* scanning electron microscopy, *14C* radiocarbon dating, *18O* oxygen isotopes, *13C* carbon isotopes, *XRD* X-ray scattering technique

Core ID [GeoB-]	Date [m/d/y]	Station Coordinates		Depth [mbsl]	Env.	Core rec. [cm]	Gear	Sample Material; Core-Position; Applied analyses
		LAT [°S]	LON [°W]					
13802-2	05/20/09	36°05.30'	53°20.72'	141.1	US	341	VC	***Eurhomalea exalbida***, fossil; in-core (core base) sample; OM, SEM, 14C, 18O, 13C, XRD
13813-4	05/27/09	34°44.22'	53°33.27'	57.6	IS	1028	GC	***Pitar rostratus***, modern; surface sample; OM, SEM, 14C, 18O, 13C, XRD
13836-2	06/10/09	35°44.72'	53°03.66'	134.0	OS	507	VC	***Zygochlamys patagonica***, subrecent; surface sample; OM, 14C, 18O, 13C
13839-2	06/10/09	35°30.87'	53°16.43'	67.0	OS	18	BC	***Venus antiqua***, subrecent; surface sample; OM, 14C, 18O, 13C

XIII.3.1 Sediment core material

Vibro core (core GeoB13802-2) was taken from the upper slope (141 mbsl) providing a total recovery of 341 cm. The base of the core (interval 335 to 341 cm) contained one large articulated venerid shell, preserved in an excellent condition. Preliminary investigations of thin sections and mineralogical analyses (using XRD) confirmed, that this specimen was an exceptionally suitable candidate for high-resolution isotopic sampling and radiocarbon dating.

Besides vibro core GeoB13082-2, further sedimentary cores (GeoB13813-4, GeoB13839-2 and GeoB13836-2; Fig. XIII.1) were taken on the inner and outer shelf and examined for bioarchives. Bivalve shells listed in Tab. XIII.1 were sampled for additional radiocarbon ages and stable isotopic data (Fig. XIII.1).

All shells were compared with reference material housed at the Museo Nacional de Historia Natural (MNHN), Montevideo, Uruguay, and identified down to species level (pers. comm. F. Scarabino). For high-resolution geochemical analysis, large articulated (both valves preserved) specimens were examined exclusively. Species nomenclature used in this study is based on the World's Register of Marine Species (WoRMS, 2014) and on the taxonomic catalogue of Scarabino (2003).

XIII.3.2 Ecology of bivalve shells sampled as bioarchive

The articulated bivalve shell collected at the base of core GeoB13802-2 was identified as the cold-water species *Eurhomalea exalbida* (Dillwyn, 1817). The exact taxonomic position of this species is under discussion; consequently various scientific names are in use. The most common synonyms are *Eurhomalea exalbida* (accepted name according to WoRMS and thus used in the present study) and the newer, but not yet accepted, name *Retrotapes exalbidus* (WoRMS, accessed 10-2014; Gordillo et al., 2013). The bivalve genus is a neoaustral taxon that has first appeared in Patagonia and Antarctica during the early Tertiary with numerous Miocene and Holocene records in southern South America (Del Rio, 1997; Gordillo, 2006). Today, *E. exalbida* is largely extant in South American waters; however, smaller retreat areas are present in the Magellanic Region and Beagle Channel (Aguirre and Farinati, 1999; Del Rio, 1997; Gordillo, 1999; Gordillo et al., 2013, 2014; Lomovasky et al., 2002a, 2002b; Yan et al., 2012). The Beagle Channel population, in particular, hosts the southernmost occurrence of this species, withstanding temperatures as low as 4 to 11 °C (Gordillo et al., 2013, 2014). A maximum life span of up to 70 years and large, massy shells make this bivalve to an appropriate climate recorder (Lomovasky et al., 2002a). Species-specific calibration studies (e.g. vital effects causing disequilibrium fractionation effects) were recently investigated from *E. exalbida* shells collected in the Malvinas (Falkland Islands) (Yan et al., 2012). The biogeographic

distribution of the genus *Eurhomalea* shows a maximum northern extent up to 38 °S (Penchaszadeh et al., 2008), which coincides with the northernmost position of cool waters provided by the Malvinas Current and associated shelf currents (see Fig. XIII.1 and Fig. XIII.2). The fossil specimen sampled for this study at 36 °S, however, is located more than 100 km north of the reported species distribution limit and within the subtropical convergence zone which makes it to a particularly interesting biogeochemical archive.

Other frequent bivalve sources on the inner Uruguayan shelf are subrecent shell deposits that show an association to cold waters of the Magellan Province. Abundant taxa are the Patagonian scallop *Zygochlamys patagonica* (core GeoB13836-2; 134 mbsl) with a species tolerant limit at 9 °C (Gutiérrez et al. 2008), and *Venus antiqua* clams (core GeoB13839-2; 67 mbsl) indicating normal to reduced saline waters and temperatures between 4 °C and 20 °C. These autochthonous and parautochthonous deposits (for radiocarbon ages see Tab. XIII.2) occur as extensive shell banks along the northern Argentinean and Uruguayan shelf (Martins et al., 2003; Campos et al., 2008). Recent *in-situ* records of the sub-tropical species *Pitar rostratus* (Koch, 1844) were recovered from the surface of core GeoB13813-4 taken in 57 mbsl. This species is characterized by a wide intra-specific variability (Huber, 2010) and prospers under euryhaline (13.3–33.6‰) conditions (Olivier and Scarabino, 1972; Scarabino, 1977; Giberto et al., 2004).

XIII.4 Methods

XIII.4.1 Radiocarbon dating

Powder samples (~30–50 mg each) were drilled parallel to the growth bands from both, juvenile (dorsal hinge) and adult (ventral shell margin) shell positions (Fig. XIII.3A; C14 sample). Sampling in organic-rich layers (e.g., periostracum organic layer) or diagenetically altered shell layers (indicated by dark staining cf. Fig. XIII.3D) was avoided. The AMS-^{14}C dating was carried out at the Poznan Radiocarbon Laboratory, Poland. Radiocarbon concentrations of modern shell material is reported in percent modern carbon (pMC; 1950 AD = BP = 100 % pMC cf. Stuiver and Polach, 1977), whereas radiocarbon ages of subrecent (herein referred to Holocene material) and fossil material (older than Holocene) are reported as uncalibrated ages (^{14}C yrs BP), as -σ range given in calibrated thousands of years before present (cal yrs BP) and as intercepts in cal yrs BP (Tab. XIII.2). Radiocarbon raw ages were calibrated according to the MARINE09 dataset using the conservative, though maybe imprecise, reservoir age of about 400 years (Reimer et al., 2009).

XIII.4.2 Thin-section analysis

Suitability of specimens with respect to diagenetic alteration (e.g., bioerosion, recrystallization, and physical abrasion) was assessed by reflected and transmitted light microscopy of thin sections, each 50 µm in thickness and orientated along the maximum growth axis of the shell valve. Growth increment widths were measured over the total outer shell record (Fig. XIII.3A) and along the chondrophore record (see Fig. XIII.5B) using the image analysis software ImageJ 1.45s (Schneider et al., 2012). Detailed analyses of stable oxygen and carbon isotopes were applied on thick sections (2 mm in thickness each). For this, a sampling transect in the outer shell layer was micro sampled that represents shell growth over 6 consecutive years. Digital images of sections slides cf. Fig. XIII.3B were taken with a Leica DFC-280 digital camera attached to a Leica binocular microscope.

XIII.4.3 SEM analysis

Shell-intern microstructures were investigated with a Tescan Vega 3 XMU scanning electron microscope (20.0 kV; secondary electron mode) at the Leibniz Center for Tropical Marine Ecology, Bremen, Germany. SEM sample chunks were cut from umbonal and central shell positions (Fig. XIII.3A; SEM sample), which provide a well-preserved growth line pattern and clear microstructures of the skeletal mineralogy. Prior to SEM analysis, all samples were slightly etched with hydrochloric acid (HCl 0.25 %) for 10 to 20 seconds to excavate the acid-resistant growth lines and after drying sputtered with gold.

XIII.4.4 XRD of shell carbonate

The Central Laboratory for Crystallography and Applied Material Sciences (ZEKAM, University of Bremen) analyzed the X-ray diffraction pattern of the carbonate powder (Fig. XIII.3A; XRD sample). A Philips X'Pert Pro multipurpose diffractometer equipped with a Cu-tube (k" 1.541, 45 kV, 40 mA), a secondary Ni-Filter, and the X'Celerator detector system were used for continuous scans from 3–85° 2θ with a calculated step size of 0.016° 2θ. Mineral identification was achieved by means of the Philips software X'Pert HighScore as well as detailed identification of calcite and aragonite by using the X-ray diffraction interpretation software MacDiff version 4.25. Additionally, the entire shell was treated with Feigl's solution to confirm its aragonitic mineralogy throughout the entire shell (Leitmeier and Feigl, 1934).

XIII.4.1 Micromill sampling

The high-resolution sampling of accretionary-grown increments was achieved by using a Micromill (New Wave Research) following Dettman and Lohmann (1994). In order to avoid cross-contamination of individual microsamples, diagenetically altered dark stained shell increments were omitted. Horizontal drilling speed of the drill bit was set 100 µm/sec, with a maximum drilling depth of ~280 µm, milled in eight, consecutive passes of 35 µm depth each.

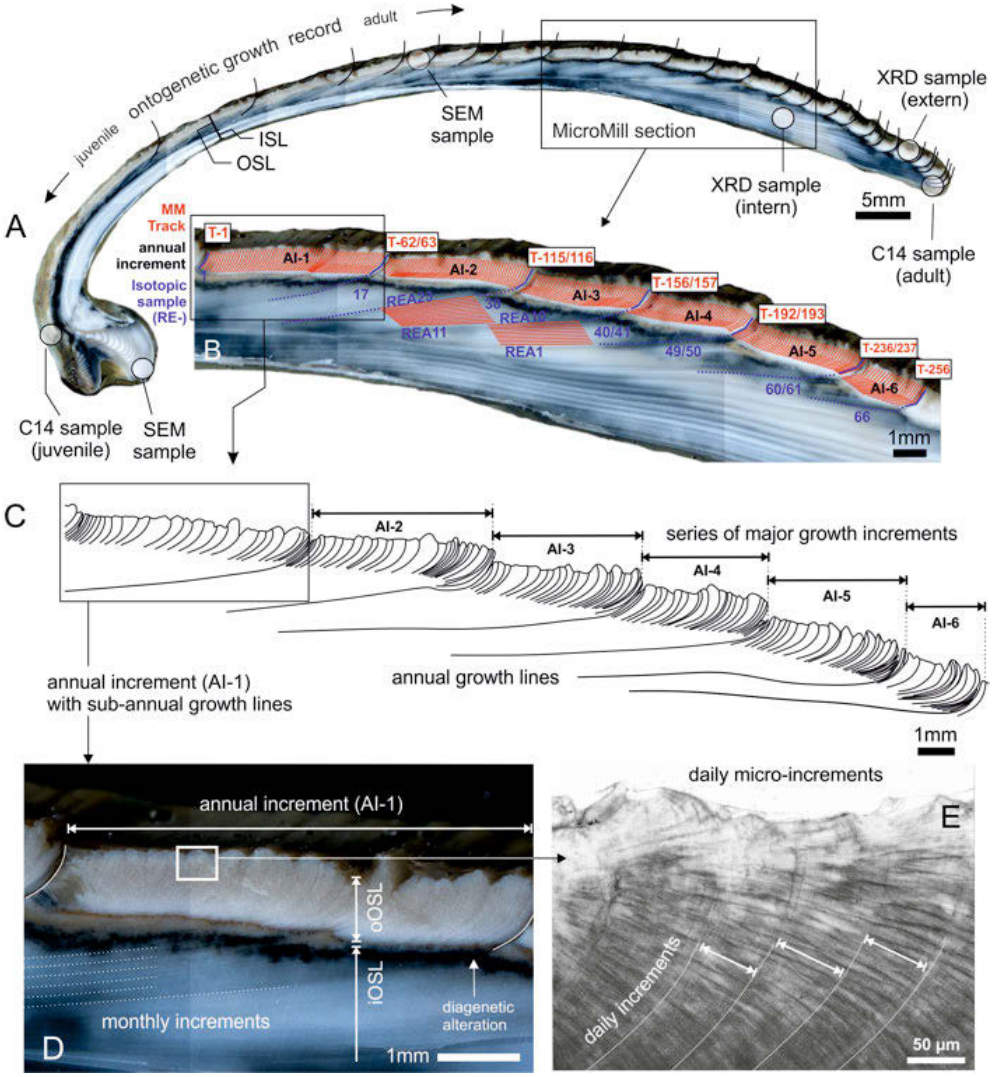

Figure XIII.3: (A) The fossil specimen *Eurhomalea exalbida* and the Micromill transect as photograph (B) and illustration (C) within increments of the outer shell. Accretionary increments were sampled from shell material at age 9 years onward in order to avoid metabolically driven fractionation effects during early ontogeny (B, C; AI-1 to AI-6). (D) At a higher resolution, each annual growth increment provides a record of several, herein monthly sub-increments, which at highest resolution (E) show daily micro-growth increments of 30-80 µm in width each. Abbreviations used: *ISL inner shell layer*, *OSL* outer shell layer, *iOSL* innermost outer shell layer, *oOSL* outermost outer shell layer.

The fossil bivalve *E. exalbida* was sampled over 22.5 mm in the outermost outer shell layer (oOSL) by 256 single tracks (MM tracks; T1 to T256 Fig. XIII.3B) with a distance of 50 µm between each track. This sampling transect covers 6 consecutive annual increments (AI-1 to AI6; Fig. XIII.3B), however, in order to obtain sufficient material for an accurate geochemical analysis of stable isotopes, 2-3 drilling tracks were combined to one isotopic sample (RE1 to RE66; Fig. XIII.3B) of approx. 40-50 µg each.

A second transect (Fig. XIII.3B; REA1-23) was drilled in two annual increments of the innermost outer shell layer (iOSL) in order to estimate potential fractionation processes between the two different shell layers.

XIII.4.2 Shell $\delta^{18}O$ and $\delta^{13}C$ analyses

Micro-drilled powder samples were analyzed for stable oxygen isotopes ($\delta^{18}O_{shell}$) and stable carbon isotopes ($\delta^{13}C_{shell}$) using a Kiel III carbonate preparation line connected online to a ThermoFinnigan MAT 252 mass-spectrometer (Kim et al., 2007; Rosenbaum and Sheppard, 1986). All isotope values are reported in the conventional δ-notation in parts per mil (‰) relative to Vienna Pee Dee Belemnite (V-PDB) by assigning a $\delta^{13}C_{shell}$ value of +1.95 ‰ and a $\delta^{18}O_{shell}$ value of -2.20 ‰ to NBS19. Reproducibility was checked by replicate analyses of laboratory standards and is better than ± 0.05 ‰ 1σ (standard deviation, SD) for $\delta^{18}O_{shell}$ and better than ± 0.03 ‰ 1σ (SD) for $\delta^{13}C_{shell}$.

XIII.4.3 Environmental monitoring

Monthly records of recent SST and SSS remote sensing data (Modis *aqua*) were obtained in 4 km resolution from NASA Giovanni (http://disc.sci.gsfc.nasa.gov/giovanni) and from oceanographic stations near La Barra, Uruguay, situated in the vicinity of the core collection at the inner shelf (Acker and Leptoukh, 2007). Temperature and salinity changes through water depth were calculated by linear regression from *in situ* CTD measurements that were compiled from World Ocean Atlas (WOA09) data (Antonov et al., 2010; Locarnini et al., 2010). Additional measurements of water temperature and salinity were extracted from the literature (e.g., Provost et al., 1992; Wells and Daborn, 1997; and Braga et al., 2008) and processed in Ocean Data View ver. 4.5.6 (Schlitzer, 2012).

XIII.4.4 Environmental reconstruction

Seawater temperatures were calculated from $\delta^{18}O_{shell}$ values by using the palaeothermometry equation (1) of Grossman and Ku (1986) considering modifications

for a SMOW correction (-0.27 ‰) as given in Dettman et al. (1999). Therefore, a 1 ‰ change in $\delta^{18}O_{shell}$ accounts for a temperature change of 4.34 °C if $\delta^{18}O_{water}$ remains unchanged:

$$T_{\delta 18O}(°C) = 20.6 - 4.34 * (\delta^{18}O_{shell} - (\delta^{18}O_{water} - 0.27)) \quad (1)$$

Due to the close correlation of $\delta^{18}O_{water}$ and salinity, the $\delta^{18}O_{shell}$ values may also reflect changes in ambient seawater salinity (Sal). Major freshwater influence caused by a continuous runoff of terrestrial freshwaters are not expected for the time period 15–20 cal kyrs BP due to a drastically northward displacement of the river drainage pathway (Fig. XIII.1B) as shown by Lantzsch et al., 2014. Influences of periodical freshwater pulses (e.g., lagoonal discharges, monsoon-related peaks), however, cannot be completely excluded due to a near-coastal habitat of the analyzed bivalve. The $\delta^{18}O_{water}$ value for the study area was thus reconstructed from the modern freshwater mixing line (Fig. XIII.4A, B) as shown in equation (2):

$$\delta^{18}O_{water}(‰) = 0.54 * Sal - 18.593 \quad (2)$$

By means of a linear regression analysis, the modern $\delta^{18}O_{water}$/Sal slope of 0.54 ‰ PSU^{-1} was calculated which is in general accordance with the global gridded data set of LeGrande and Schmidt (2006) and Bigg and Rohling (2000) who reported a $\delta^{18}O_{water}$/Sal slope of 0.51 ‰ PSU^{-1} for the South Atlantic.

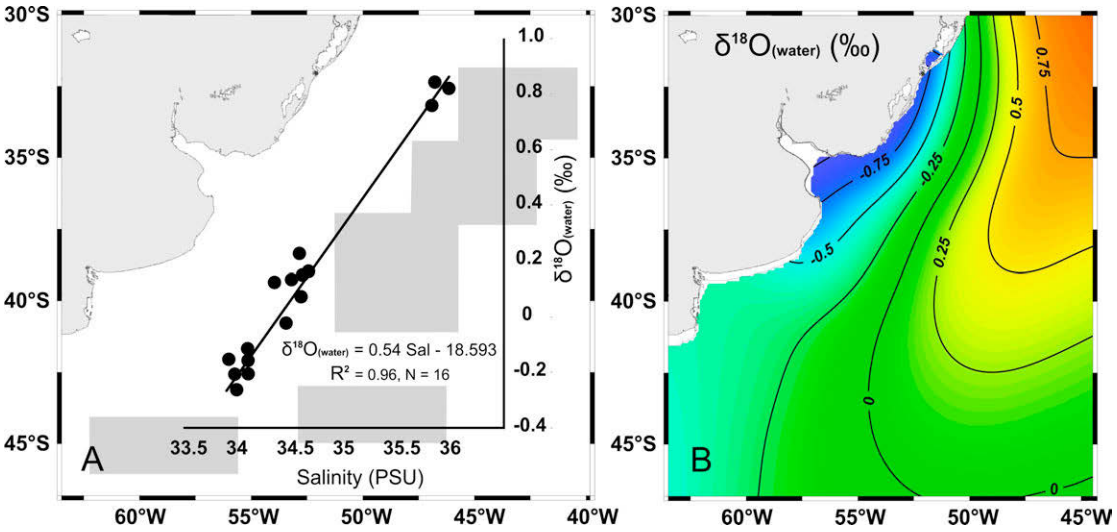

Figure XIII.4: Regional map of southeastern South America showing areas (grey polygons) providing $\delta^{18}O_{water}$ and salinity (Sal) data of surface waters <200 mbsl. The resulting freshwater mixing line is displayed as salinity versus $\delta^{18}O_{water}$ diagram within (A). The shelf current-related distribution of the modern $\delta^{18}O_{water}$ pattern is presented in (B). Note, for the deglacial $\delta^{18}O_{water}$ value an ice-volume correction of +0.9 ‰ ($\delta^{18}O_{IVC}$) was taken into account in order to calibrate ocean waters enriched in heavier $\delta^{18}O$, while lighter $\delta^{16}O$ was stored in land ice masses.

XIII.5 Results and Discussion

XIII.5.1 Radiocarbon dating

Accelerated mass spectroscopy (AMS-^{14}C) revealed radiocarbon ages of biogenic surface materials (bivalve shells, Tab. XIII.2) indicating both, the presence modern material (core GeoB13813-4; inner shelf) and deposits of subrecent ages dating at 1.69 (core GeoB13839-2; outer shelf) and 2.82 cal kyrs BP (core GeoB13836-2, outer shelf) that both correspond to late Holocene times. These shell accumulations formed in the form of *in situ* shell banks (articulated valves) that prospered under a slightly elevated sea level (<2.5 m) relative to the modern settings (e.g., Martínez and Rojas, 2013; Gyllencreutz et al., 2010; Bracco et al., 2005).

Oldest shell material (articulated *E. exalbida* valves) was recovered from the base of core GeoB13802-2 (upper slope) and reveals a deglacial age of 16.9 cal kyrs BP (Tab. XIII.2) which corresponds to the Heinrich 1 stadial and thus to a sea level between 102 and 118 m below the modern level (Guilderson et al., 2000; Hanebuth et al., 2009; Lambeck and Chappell, 2001). Similarly, the oldest bivalve shell sampled from the core material shows an excellent shell-intern growth record that, at least to our knowledge, makes the fossil *E. exalbida* presented in this study to one of the oldest and best-preserved bio-recorders of this species reported from the southeastern South American shelf.

Tab. XIII.2: Radiocarbon ages of shell-carbonate samples taken from juvenile and adult shell positions. For calibration the marine dataset MARINE09 (Reimer et al., 2009) was applied. D, dorsal sample (juvenile); V, ventral sample (adult); POZ, Poznan Radiocarbon Laboratory, Poland; pMC, percent modern carbon.

Species (core label)	Core depth [cm]	Sample position	Lab ID [POZ-]	^{14}C ages [^{14}C yrs BP (*); pMC (**)]	1σ cal age range [cal yrs BP]	Intercept [cal yrs BP]
E. exalbida (13802-2)	341 (base)	D V	36091 36092	14200 ± 70* 14060 ± 60*	16800 – 16980 16720 – 16890	16890 ± 90 16805 ± 10
P. patagonica (13836-2)	0-1 (surface)	D V	36094 36059	3010 ± 35* 3060 ± 30*	2735 – 2820 2770 – 2865	2778 ± 40 2818 ± 50
V. antiqua (13839-2)	0-1 (surface)	D V	36060 36095	2085 ± 30* 2075 ± 30*	1605 – 1770 1595 – 1700	1688 ± 80 1648 ± 50
P. rostratus (13813-4)	0-1 (surface)	D V	36057 36058	109.35 ± 0.30** 104.18 ± 0.32**	n/a n/a	modern modern

The isotopic analyses and palaeoenvironmental interpretation presented in this study thus focus on the late Pleistocene specimen exclusively, while additional analyses of the other late Modern and Holocene shell materials (Tab. XIII.1 and Tab. XIII.2; Fig. XIII.1) are presented for the sake of completeness.

XIII.5.2 Shell mineralogy and preservation

The original aragonitic mineralogy of the deglacial shell was confirmed by a series of 3 individual tests: (1) Feigl's solution stained the entire shell record black, which indicates the presence of aragonite, (2) SEM scans of individual shell layers, which showed characteristic aragonitic skeletal microstructures (see details in Taylor et al., 1969; Chateigner et al., 2000; Kobayashi and Samata, 2006; Gobac et al., 2009) and, (3) XRD measurements of shell carbonate sampled from the iOSL (100 % aragonite) and oOSL (92 % aragonite, 8 % calcite).

Although not very common as other aragonitic venerids, *E. exalbida* provides abundant shell material in the fossil record of southeastern South America that is often well preserved in original mineralogy (Gordillo, 2006; Aguirre et al., 2008; Gordillo et al., 2013 and references therein). The same applies for the herein presented specimen (dated at 16.9 cal kyrs BP) thus fulfilling an important prerequisite for using bivalve shells material as geochemical bioarchive (see e.g., Kaltenegger et al., 1971; Wefer, 1985).

Thin sections show accretionary-grown bands in both, the outer shell layer (OSL; Fig. XIII.3A) and chondrophore section (Fig. XIII.5B) with both records largely free from bioerosion. Minor diagenetic-altered shell carbonate, however, was identified between the iOSL and oOSL (see Fig. XIII.3D for dark stained shell carbonate), which consequently was omitted from sampling. These altered areas, in particular, are interpreted as the result of sulphate reducing nannobacteria that concentrate along protein and organic-enriched shell layers (see e.g., Gosling, 2003). This interpretation is confirmed by the presence micromorphological iron sulphide framboids (Suppl. XIX.2) in between the annual growth increments in the oOSL.

XIII.5.3 Shell growth periodicities

Light microscopy reveals up to 25 successive paired major growth increments (annual) of first order subdivided by growth increments of second order (sub-annual), which characterize the entire oOSL record (Fig. XIII.3A and Fig. XIII.4A). This continuous pattern is also preserved as a compressed record in the chondrophore section (Fig. XIII.5B) and iOSL (Fig. XIII.3B, D). The width of annual growth increments is not constant throughout the shell record, but shows an ontogenetic-controlled increase within the juvenile stage

and a remarkable decrease during adult stages of the shell (Fig. XIII.5A). As a typical feature in bivalve shells, this pattern is related to the onset of sexual maturity during which the organism prefers to invest available energy in reproduction processes instead of growth (Lomovasky et al., 2002; Gosling, 2003).

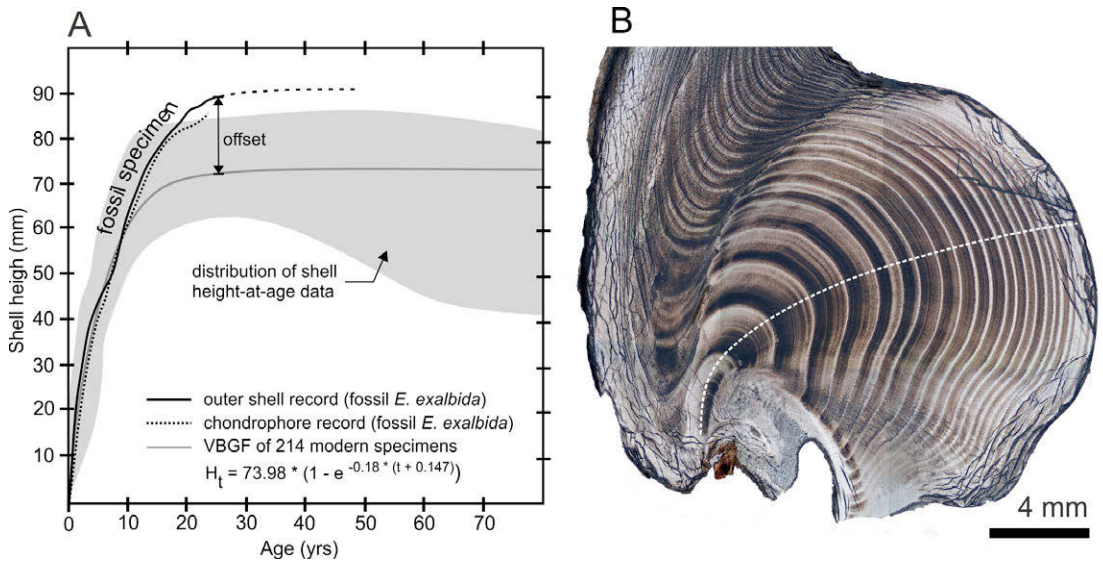

Figure XIII.5: Shell height-at-age curves of fossil and modern specimens of bivalve species *E. exalbida*. A remarkable offset between the fossil (this study) and modern bivalve shells calculated from 214 modern specimens (cf. Lomovasky et al., 2002a) indicate a later onset of maturity in the fossil specimen (A). The full growth record of the chondrophore (hinge section) is presented as a mosaic of ten thin sections in (B).

Accretionary-precipitated major growth structures (first order increments) in *E. exalbida* range from 0.23 mm (latest adult increment) to 23.11 mm (earliest juvenile increment) with an average increment width of 4.03 mm (N=25, total shell record; Fig. XIII.5A). The onset of maturity is indicated by growth increments showing a remarkable decrease in width, which happened during an individual age of 25-30 years (Fig. XIII.5A). Such increments of first order were interpreted in previous studies as the carbonate precipitation over one annual growth cycle (=annual increment; e.g., Lomovasky et al., 2002; Ivany et al., 2008 and references therein).

On an intra-annual scale, these annual increments can host valuable environmental information in a high resolution and thus help to identify environmental conditions that might affect the precipitation of biogenic calcium carbonate during the lifetime of the organism (Marchitto et al., 2000).

Higher magnified photographs of thin sections (40 x – 100 x) reveal subordinate increments (herein called micro-increments) in a sub-annual resolution (second order

increments; Fig. XIII.3C, D, E). In the analyzed shell record of *E. exalbida*, (Fig. XIII.3C, AI1 to AI6) such micro-increments typically range between 9 and 164 µm in width (mean=46 µm), being narrowest towards the annual growth lines and widest in the centre of the increment (Fig. XIII.6C). Contrary to the metabolic-controlled growth of first order increments, intra-annual growth structures show a coupling with environmental parameters that, besides water temperatures, also include the availability of food (primary production) and environmental stress (spawning seasons), see also Gordillo et al. (2013).

Moreover, such micro-scale increments can reach a temporal resolution covering fortnightly, diurnal or even tidal-related cycles and thus represent valuable reference features (Goodwin et al., 2001; Schöne et al., 2005, Azzoug et al., 2012; Yan et al., 2012). By correlating micro-growth bands with stable oxygen isotope-derived temperature data, the shell record of *E. exalbida* serves as a high-resolution bioarchive that allows to track growing seasons, or to assign precise calendar dates to certain shell features, if at least one shell reference date is known (e.g., bivalve death, growth line formation).

The sub-recent and fossil material presented in this study, however, allows not for such precise correlations, not least, because a detailed reference date is not available for ancient shells and the radiocarbon dating method is too imprecise to yield temporal information in high resolution.

XIII.5.4 Shell growth rate

The analysis of the first 20 years of growth (*E. exalbida*) shows that the late Pleistocene sample exhibits a higher growth rate (mean 3.96 mm yr^{-1} = 10.85 µm day^{-1}) and a later onset of maturity (25-30 years) relative to the corresponding time-intervals of modern representatives (Fig. XIII.5A). Modern specimens sampled in Ushuaia Bay (Tierra del Fuego, South America) show an average growth rate not exceeding 2.50 mm yr^{-1} (N=214; Fig. XIII.5A) and an early onset of the adult stage already at 15-20 years (Lomovasky et al., 2002a). This offset is well known for Pleistocene shells of the species *E. exalbida* and probably indicates water conditions closer to the species optimum range (e.g., cooler water temperature, normal salinity, sufficient food supply) or exposure to higher alkalinity and calcium concentrations associated with fully marine environments during the deglacial period (Gordillo, 2006).

XIII.5.5 Growth line formation

Growth lines in the fossil *E. exalbida* specimen correlate with lowest $\delta^{18}O_{shell}$ values (equiv. to highest temperatures) and lowest $\delta^{13}C_{shell}$ values, while the positive $\delta^{18}O_{shell}$

excursions (equiv. to lowest temperatures) are reached shortly after the formation of a growth line (see Fig. XIII.6C). Highest $\delta^{13}C_{shell}$ values, in contrast, show no distinct pattern, while the correlation to shell-intern features might be overprinted as a result of fractionation processes.

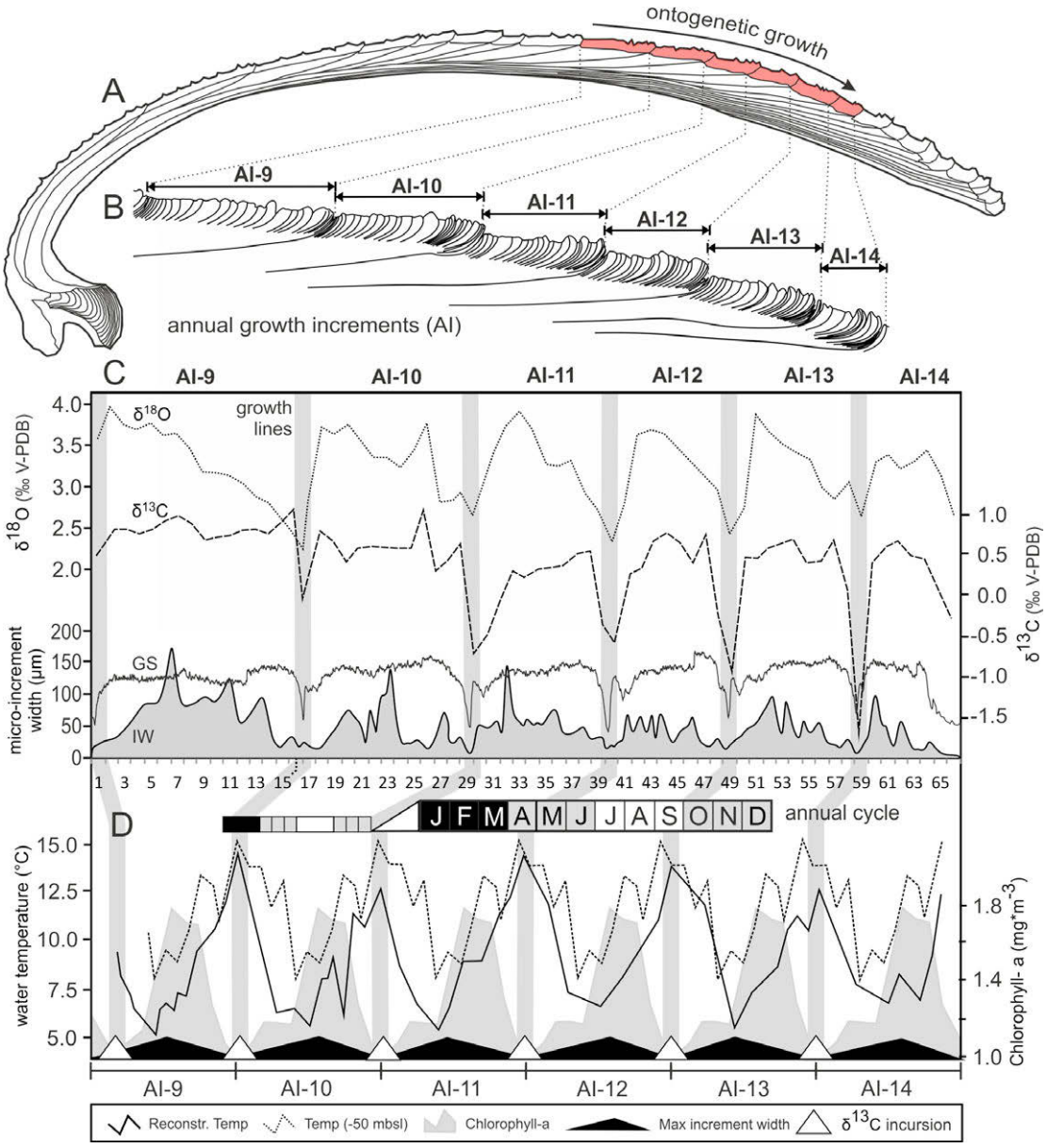

Figure XIII.6: The shell-intern growth record of the fossil specimen *E. exalbida* (A) shows annual (AI) to sub-seasonal precipitated growth increments within the analyzed transect (B). The stable isotopic $\delta^{18}O_{shell}$ (dotted curve) signature and $\delta^{13}C_{shell}$ (dashed curve) signature of shell carbonate with corresponding micro-incremental widths (IW) and increment grey scale intensity (GS) indicating growth-line incisions are shown in the upper panel (C). Temporal aligned data with calculated palaeowater temperatures (black solid curve) and present-day sea surface temperatures (SST, dotted curve) and chlorophyll-a levels (Chl-a, grey shaded curve) are shown in the lower panel (D). Black and white triangles at the panel bottom indicate maximal increment growth and $\delta^{18}O/\delta^{13}C$ incisions, respectively.

The exact timing of growth line formation is still matter of debate (see e.g., Jones and Quitmeyr, 1996; Yan et al., 2012 and references therein). While some authors relate growth line formation simply to winter lines, analogous to growth rings of trees (e.g., Dextraze and Zinsmeister, 1987), it became obvious that species-specific shell growth is by far more complex, especially for sensible stenothermal taxa such as *E. exalbida*.

The annual growth pattern of *E. exalbida* shells, in particular, was discussed before in a number of studies (see e.g., Dextraze and Zinsmeister, 1987; Lomovasky et al., 2002a; 2002b; Ivany et al., 2008). The exact timing of shell growth in *E. exalbida* was presented, for the first time, in a detailed calibration study by Yan et al. (2012). The authors concluded that growth lines in modern shells do not simply reflect cold water-related winter lines, as previously assumed, but also suggest that key-drivers other than temperature (e.g., food availability coupled to primary production) might affect carbonate precipitation and thus shell growth (Ansell, 1968; Yan et al., 2012). Similar findings were reported for other control factors causing environmental and biological stress (e.g., changing seasonality, limited food availability, marine pollution, reproduction cycle; see Morriconi et al., 2002; Elliot et al., 2003; Schöne et al., 2003), and for other long-lived cold-water species such as *Artica islandica* from the northern North Atlantic (Jones, 1980; Schöne, 2005b) and the Patagonian scallop *Zygochlamys patagonica* (Lomovasky et al., 2008). It is thus obvious that this control may also account for fossil specimens of the taxon *Eurhomalea* in southern South America.

XIII.5.6 Shell oxygen and carbon isotopes

The high-resolution profile (N=66, Fig. XIII.6A) analyzed in the oOSL of *E. exalbida* reveals mean $\delta^{18}O_{shell(oOSL)}$ values of 3.27 ± 0.42 ‰. The $\delta^{18}O_{shell(oOSL)}$ amplitude range is 1.69 ‰ with a maximum of 3.98 ‰ and a minimum of 2.29 ‰ (Tab. XIII.3). The temporal unaligned $\delta^{18}O_{shell(oOSL)}$ signature (Fig. XIII.6C) exhibits successive cycles of rapidly increasing values shortly after growth line formation and continuously regressing values within the accretionary intervals in-between the growth-lines. As a result, the $\delta^{18}O_{shell(oOSL)}$ signature forms a characteristic asymmetric sawtooth pattern. The temporal-aligned signature (Fig. XIII.6C) shows most negative $\delta^{18}O_{shell(oOSL)}$ values (=highest water temperatures) associated with growth lines, while the most positive $\delta^{18}O_{shell(oOSL)}$ values (=lowest water temperatures) appear shortly after the first third of growth increment formation (Fig. XIII.6A).

Tab. XIII.3: Shell carbon ($\delta^{13}C_{shell}$) and oxygen ($\delta^{18}O_{shell}$) isotopes from bivalve sample material with corresponding shell ages. Radiocarbon ages cf. Tab. 2.

Species	Shell layer	Age (epoch)*	$\delta^{13}C$ Range [‰]	$\delta^{13}C$ Ampl. [‰]	$\delta^{13}C$ Mean/Stdev [‰]	$\delta^{18}O$ Range [‰]	$\delta^{18}O$ Mean/ Stdev [‰]	$\delta^{18}O$ Ampl. [‰]
E. exalbida	oOSL	LP	-1.74–1.02	2.76	0.41 ± 0.49	2.29–3.98	3.27 ± 0.42	1.69
E. exalbida	iOSL	LP	0.25–1.62	1.37	1.17 ± 0.37	2.93–3.97	3.44 ± 0.30	1.04
P. patagonica	oOSL	LH	1.55–2.77	1.22	2.17 ± 0.39	1.78–2.37	1.98 ± 0.21	0.59
V. antiqua	oOSL	LH	1.42–2.20	0.78	1.99 ± 0.34	0.62–1.63	1.59 ± 0.43	1.01
P. rostratus	iOSL	recent	-1.48–1.80	3.28	0.07 ± 0.75	-0.39–0.68	0.14 ± 0.28	1.07

The $\delta^{13}C_{shell(oOSL)}$ signal reveals mean values of 0.41 ± 0.49 ‰. The $\delta^{13}C_{shell(oOSL)}$ amplitude range is 2.76 ‰ with a maximum of 1.02 ‰ and a minimum of -1.74 ‰. The unaligned $\delta^{13}C_{shell(oOSL)}$ signature exhibits a slight trend towards lighter values characterized by sharp cyclic minima, progressively pronouncing with ontogeny. These negative incursions are closely associated with the five growth lines (Fig. XIII.6C) and thus show a distinct positive correlation with $\delta^{18}O_{shell(oOSL)}$ minimum values.

Besides the high-resolution sampling profile in the oOSL, an additional set of samples was analyzed from the iOSL (Fig. XIII.3B) in order to compare the isotopic signature increments precipitated within different sub-shell layers (Fig. XIII.7A, B; Tab. XIII.3). The isotopic signatures from two major growth increments within the iOSL (sample step 100 µm, N=23) show mean $\delta^{18}O_{shell(iOSL)}$ values of 3.44 ± 0.30 ‰ and mean $\delta^{13}C_{shell(iOSL)}$ values of 1.17 ± 0.37 ‰ (see Fig. XIII.3B, REA1 to REA23). These data indicate that while $\delta^{18}O_{shell(iOSL)}$ and $\delta^{18}O_{shell(oOSL)}$ values show a high correlation ($r^2 = 0.85$), the $\delta^{13}C_{shell(iOSL)}$ values exhibit a remarkable positive offset ($r^2 = 0.36$) by about 1.1 ‰ (Fig. XIII.7C) relative to $\delta^{13}C_{shell\,(oOSL)}$ values. This offset is interpreted as the result of species-specific metabolic fractionation processes and indicates that incorporation of $\delta^{13}C$ in bivalve shells and different shell layers should be regarded critically (see also Krantz et al., 1987; Wefer, 1985 and references therein).

Additional surface-collected bivalve shells (different taxa cf. Tab. XIII.1) were analyzed for stable oxygen and carbon isotopes and radiocarbon ages in order to provide a calibration dataset for geochemical data (see Tabs. 2, 3 for details). This material, however, suffered from intense bioerosion and was consequently not micro-sampled in high-resolution.

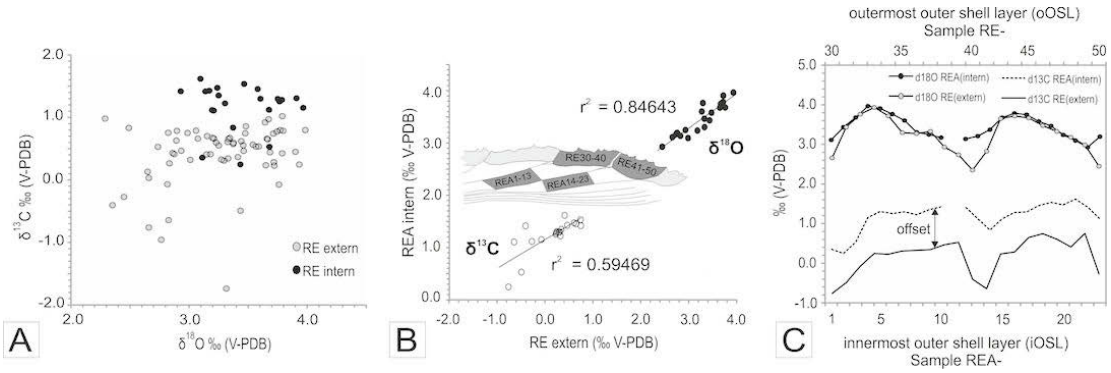

Figure XIII.7: Stable oxygen and carbon isotope profiles analyzed in the oOSL and iOSL of *E. exalbida*. Total $\delta^{13}C_{shell}$ versus $\delta^{18}O_{shell}$ signatures are presented in (A), while the correlation of stable oxygen and carbon isotopes of the iOSL (REA intern) and oOSL (RE extern) is shown in (B). This analysis indicates that while the $\delta^{18}O_{shell}$ (intern vs. extern) signatures show a high correlation, the $\delta^{13}C_{shell}$ (intern vs. extern) signatures show a remarkable offset of about 1 ‰ that is attributed to shell intern metabolically fractionation processes (C).

XIII.5.7 Palaeoenvironmental interpretation

Species-specific ecological information is a prerequisite in order to establish a robust palaeoenvironmental reconstruction based on fossil shell material (Vogel, 1984). In addition to sedimentological core data (Krastel et al., 2012; Lantzsch et al., 2014) and sea level reconstructions (Lambeck and Chappell, 2001; Guilderson et al., 2000; Lantzsch et al., 2014), we applied the analysis of the stable oxygen ($\delta^{18}O_{shell}$) and carbon ($\delta^{13}C_{shell}$) isotopic fingerprint. This approach aims to shed light for the first time on a fossil *E. exalbida* bivalve shell dated at 16.9 cal kyrs BP. Variations in $\delta^{18}O_{shell}$ and $\delta^{13}C_{shell}$ signatures are dependent on three major drivers, which affect the isotopic composition of marine shells: (1) water temperature under which the organism precipitates shell material; (2) isotopic composition of the surrounding seawater ($\delta^{18}O_{water}$) and; (3) $\delta^{13}C$ of the dissolved HCO_3^- from which the carbonate formed (see details in Aguirre et al., 1998; Wefer, 1985).

XIII.5.7.1 Habitat reconstruction

The habitat water depth of the bivalve *E. exalbida* was extracted from palaeo sea level considering a modern water depth of 141 mbsl plus 3.4 m sediment cover. Currently well-established sea level curves for the deglacial period argue for a near-coastal shallow subtidal environment at a water depth between 26 and 40 mbsl. This part of the Uruguayan shelf is primarily influenced by cool (SASW) and warm (STSW) shelf currents (Fig. XIII.1), but is also situated within the reach of continental freshwater influence (cf. Braga et al., 2008; Burrage et al., 2008; Möller, 2008).

While seasonal short-term freshwater intrusions cannot be excluded for the investigated time interval, a permanent and year-round freshwater runoff by the Rio de la Plata is unlikely due to the following reasons: (1) Morphological and sediment-acoustic data show a coastal-parallel northward-directed palaeo-river depression along the Uruguayan shore indicating a runoff scenario of the Rio de la Plata displaced more than 200 km northward of its present-day setting (see Fig. XIII.1B; Lantzsch et al., 2014); (2) The maximum range of the $\delta^{18}O_{shell}$ signature (1.69 ‰ equivalent to 8.0 ± 0.7 °C) is in agreement the variation in water temperature for a water depth in 26 to 40 mbsl (see Fig. XIII.6D; Braga et al., 2008). Therefore, the analyzed shell micro-transect indicates no disequilibrium effects caused by large-scale freshwater runoff as shown in Aguirre et al. (1998) for modern shells collected from the Río de la Plata mouth ($\delta^{18}O_{shell}$ amplitudes of ~ 4.5 ‰). Slightly colder water temperatures during cold seasons (austral winter; Fig. XIII.6D) may be seen as the response to a stronger influence of the Malvinas Current and SASW during deglacial times. This situation would, furthermore, result in a northward displacement of the STSF and slightly cooler mean annual water temperatures (Fig. XIII.6C); (3) Most significant, the stable isotopic signatures ($\delta^{18}O_{shell}$, $\delta^{13}C_{shell}$) exhibit coincident and abrupt negative peaks during austral summer, which is a clear diagnostic for short-term freshwater intrusions into the marine system (Fig. XIII.6C).

XIII.5.7.2 Freshwater influence

The amplitude of variation in the $\delta^{13}C_{shell}$ signatures in the fossil specimen *E. exalbida* (Fig. XIII.6C; Fig. XIII.7A) is a significant characteristic related to water mass and carbon sources. Principally, a more or less constant intra-annual $\delta^{13}C_{shell}$ value with minor excursions indicates that water column mixing in austral spring, summer, and autumn (April – November) may result in a relatively homogeneous spatial distribution of carbon isotopes in particulate organic matter (POM) and seawater dissolved inorganic carbon (DIC). During summer, however, the analyzed $\delta^{13}C_{shell}$ record shows significant negative peaks in inter-annual growth increments, which correlate with the formation of growth lines and most negative $\delta^{18}O_{shell}$ values (Fig. XIII.6C). Assuming that bivalve specimens form their carbonate shells using carbon from the DIC pool, such seasonal deviations may indicate seasonal $\delta^{13}C_{shell}$ variations of seawater DIC controlled by phytoplankton productivity (Mook and Vogel, 1968). However, there is no evidence for a high nutrient setting (e.g., upwelling induced primary production) that may initiate phytoplankton blooms during summer, as this period of the year is dominated by the warm STSW and a strong Brazil Current with comparatively low Chl-a levels (Fig. XIII.6D; Piola et al., 2008). Therefore, seasonal production and remineralization of phytoplankton organic matter are not likely to exert a significant influence on seawater DIC and the $\delta^{13}C_{shell}$ record in the fossil specimen *E. exalbida.*

The following, not mutually exclusive, processes may have influence on the $\delta^{13}C_{shell}$ variations observed in the analyzed *E. exalbida* shell record: (1) outflow of low-salinity coastal waters (e.g., lagoonal runoff) from the hinterland onto the shelf and within the reach of the habitat of *E. exalbida*. Co-varying negative peaks of both, the $\delta^{18}O_{shell}$ and $\delta^{13}C_{shell}$ signature during summer (Fig. XIII.6C) strongly argue for $\delta^{18}O_{seawater}$ value and $\delta^{13}C$ of DIC lowered as a result of freshwater intrusions; (2) the outflow from the hinterland also carries POM of terrestrial origin with relatively lower $\delta^{13}C$ than that of marine phytoplankton. Filter feeding molluscs, such as *E. exalbida* living in a near-coastal setting and within the realm of freshwater influence, could ingest a large percentage of POM with a terrestrial source than molluscs living in fully marine conditions; (3) after depositions of terrestrial POM on the inner shelf, oxidation and remineralization would release ^{12}C-enriched CO_2 into the bottom water, decreasing the $\delta^{13}C$ of the DIC.

Runoff during summer transports large masses of terrestrial organic matter to the deglacial coastal hinterland that is characterized by extensive grasslands (humid pampas) with wetlands and lagoons in near-coastal settings (see Clapperton, 1993; Violante and Parker, 2004 for details). We interpret the negative excursions in the $\delta^{13}C$ values of the fossil specimen *E. exalbida* as recording the cyclic outflow of salinity reduced lagoonal waters onto the shelf for a short period each summer (weeks to month), with an associated transport of terrestrial organic carbon. This increasing freshwater influence as shown in Fig. XIII.6C might indicate a stronger influence of the South American summer monsoon (SASM), which is in perfect agreement with findings from speleothems showing a southward displacement of the SASM during deglacial times (see, Cruz et al., 2005).

XIII.5.7.3 Water temperatures

$\delta^{18}O$-derived seawater temperatures range from 5.6 to 14.3 °C (mean = 9.4 °C) for the deglacial time interval, which is slightly above the species tolerance limit of *E. exalbida* (4 to 11 °C cf. Gordillo et al., 2013, 2014), but still colder than modern seawater temperatures (8 to >15 °C) at a water depth of 50 mbsl (see WOA09 dataset and Braga et al.,2008, for details). On the one hand, Yan et al. (2012) have shown that shells of the species *E. exalbida* from the Falkland Islands are able to withstand water temperatures as low as 11.5 ± 1.2 °C and probably have a wider temperature tolerance than previously thought.

On the other hand, the identified temperature offset between tolerance range and reconstructed water temperatures might also be the result of the following processes: (1) a disfractionation effect of stable oxygen isotopes causing an overestimate of reconstructed water temperatures during the ontogeny as identified by Yan et al. (2012). This effect was, however, extrapolated from juvenile shells of the species *E. exalbida* exclusively (4 to 10 years old) and results, thus, in an unrealistically large offset at the maximum reported age for this species (would be +564 °C at an age of 70 years, cf.

Lomovasky et al., 2002a, 2002b). For comparison, such a large disfractionation effect transferred to the specimen presented in this study would cause an temperature offset of about 7.9 to 12.9 °C (=1.8 to 3.0 ‰ $\delta^{18}O_{shell}$) for the analyzed shell interval (age 9 to 16) and more than 24 °C for the maximum age of 25 years. To our interpretation, it is possible that the offset described in Yan et al. (2012) does indeed exist, but does for sure not describe an exponential function throughout the entire growth record; (2) the isotopic composition ($\delta^{18}O_{seawater}$) of coastal marine waters adjacent to the Río de la Plata estuary, which is known to be extremely variable Aguirre et al. (1998). Estimating the $\delta^{18}O_{seawater}$ value is significant for a robust palaeotemperature equation, nonetheless it remains an estimation, which is usually not representing seasonal variations in their full potential. The colder $\delta^{18}O_{shell}$-derived water temperatures reporting the cold seasons are interpreted to be the result of a stronger influence of Malvinas Current and its shallow marine shelfal water body the SASW. As a consequence, the STSF moved northward relative to its current position and enabled cold and temperate water species to pass into lower latitudes, such as *E. exalbida* did (see e.g., Bender et al., 2013 for Holocene shifts of STSF).

Considering the modern biogeographic distribution of *E. exalbida*, it is obvious that the southernmost-located Patagonian shelf serves as the retreat area for this cold-water species. These findings are in agreement with the palaeo-biogeographic distribution of faunal elements suggesting colder water temperature during deglacial times off Uruguay. For instance, Aguirre and Farinati (1999) reported that post-LGM faunal associations show typically cold-water elements north of their present-day northernmost life limit, locally coinciding with the BMC (~38°S) off northern Argentina. These post-LGM faunal associations relate to the cold-water mollusc fauna referred to as the Magellanic Faunal Province (MFP) as reported in a number of taxonomic and palaeo-geographical studies (Gordillo, 2006; Lomovasky et al., 2002a; Scarabino, 1977).

XIII.6 Conclusions

(1) A shell of the species *Eurhomalea exalbida* was collected from sedimentary core material offshore Uruguay and shows an exceptional well-preserved shell record, which provides valuable climatic information in a temporal highest resolution. This bivalve species is largely extant in southeastern South America; however, it provides abundant sub-recent and fossil shell material in the geological record, often preserved in original mineralogy and free of bioerosion. Radiocarbon dating delivered an age of 16.9 cal kyrs BP corresponding to the Deglacial period, which makes the bivalve shell presented in this study to one of the oldest and best-preserved environmental biorecorder of the taxon *E. exalbida* for southeastern South America.

(2) Thin sections of the shell-intern growth record exhibit clear annual increments characterized by subordinate micro-increments that provide a daily record of

environmental parameters. Although the formation of the shell is strongly influenced by bivalve-specific growth effects that are elated to juvenile and adult growth phases of the organisms, it clearly shows a continuous record palaeoenvironmental conditions that characterized the habitat during over a time span of 25 years. With a maximum reported age of 70 years and its high preservation potential, *E. exalbida* shells are perfect bivalve biorecorders that allow deriving a number of palaeoenvironmental implications for the deglacial period of the southeastern South American Shelf.

(3) $\delta^{13}C$ signatures exhibit abrupt negative peaks associated with shell growth lines formed during summer season. This signature clearly indicates short-term intrusions of terrestrial waters (e.g., lagoon discharges) in the near-coastal hinterland. Because of the large drainage area that characterize the Río de la Plata source rivers and a northward-displaced palaeo-river mouth during deglacial time, a permanent year-round runoff in the study area could be excluded, while a seasonal short-term freshwater discharge (negative $\delta^{13}C$ peaks) related to an increased South American summer monsoon is reasonable.

(4) $\delta^{18}O$ signatures show continuously decreasing values with most negative values associated with shell growth lines (summer season) and negative $\delta^{13}C$ peaks. Mean $\delta^{18}O$ values indicate water temperatures up to 3.5 °C cooler than today for a water depth in 26 to 40 meters below sea level. This situation is interpreted as a stronger influence of the Malvinas Current during cold season that has also a significant influence on shelf water circulation. Furthermore, the stronger influence of cool Antarctic waters resulted in a northward displacement of the sub-tropical shelf front, thus allowing cool water taxa such as *E. exalbida* to pass into water regimes that are characterized today by subtropical and tropical biota.

(5) Although this study suffered from limited shell material present in sedimentary cores (see e.g., Carre et al., 2012) for statistical robustness of mollusc-based studies), which meet the high requirements of sclerochronological studies (e.g., specimen size, *in-situ* preservation, limited diagenetic alteration), it has been shown that *E. exalbida* can serve as valuable high-resolution archive of palaeoclimatic conditions. As already suggested by Yan et al. (2012) more geochemical research based on *E. exalbida* shell material is important in order to establish a robust master chronology of one of the best bivalve biorecorders in southeastern South America.

XIII.7 Acknowledgements

Chief Scientist Sebastian Krastel-Gudegast and the participants and crew of the Meteor Cruise M78/3a are gratefully acknowledged for collecting the sample material and for providing sample background data. Matthias López Correa (GeoZentrum Nordbayern, Germany) is thanked for support during the Micromill sampling and for constructive comments on the manuscript. Michael Joachimski, Daniele Lutz (both GeoZentrum Nordbayern, Germany) performed the mass spectrometric measurements of the oxygen and carbon isotopes. We also would like to acknowledge Felipe García-Rodríguez (Facultad de Ciencias, Centro Universitario Regional del Este (CURE/Rocha), Universidade de la Republica, Uruguay) and Fabrizio Scarabino (Museo Nacional de Historia Natural in Montevideo, Uruguay) for their local support and discussions. The project was funded through the DFG-Research Center/Cluster of Excellence "The Ocean in the Earth System", MARUM project SD2 and is part of the PhD thesis of AK.

XIII.8 References

Acker JG, Leptoukh G (2007) Online analysis enhances use of NASA Earth science data. Eos, Transactions American Geophysical Union 88, 14–17.

Aguirre ML, Farinati EA (1999) Paleogeografia de las faunas de moluscos marinos del Neogeno y Cuaternario del Atlantico sudoccidental. Rev. Soc. Geol. Espana 12, 93–112.

Aguirre ML, Leng MJ, Spiro B (1998) Variation in isotopic composition (C, O and Sr) of Holocene Mactra isabelleana (Bivalvia) from the coast of Buenos Aires Province, Argentina. The Holocene 8, 613–621.

Ansell AD (1968) The rate of growth of the hard clam Mercenaria mercenaria (L) throughout the geographic range. Journal du Conseil Permanent Internatinal pour l'Exploration de la Mer 31, 364–409.

Antonov JI, Seidov D, Boyer TP, Locarnini RA, Mishonov AV, Garcia HE, Baranova OK, Zwerg MM, Johnson DR (2010) World Ocean Atlas 2009, Volume 2: Salinity.

Arz HW, Pätzold J, Wefer G (1999) The deglacial history of the Western Tropical Atlantic as inferred from high resolution stable isotope reords off Northeastern Brazil. Earth and Planetary Science Letters 167, 105–117.

Ayup-Zouain RN (2006) Evolucíon paleogeográafica y dispersióon de los sedimentos del Río de la Plata. Bases para la conservación y el manejo de la costa uruguaya. VIDA SILVESTRE URUGUAY, Montevideo.

Azzoug M, Carré M, Schauer AJ (2012) Reconstructing the duration of the West African Monsoon season from growth patterns and isotopic signals of shells of Anadara senilis (Saloum Delta, Senegal). Palaeogeography, Palaeoclimatology, Palaeoecology 346–347, 145–152.

Bender VB, Hanebuth TJJ, Chiessi CM (2013) Holocene shifts of the Subtropical Shelf Front off southeastern South America controlled by high and low latitude atmospheric forcings. Paleoceanography 28, 1–10.

Bigg GR, Rohling EJ (2000) An oxygen isotope data set for marine waters. Journal of Geophysical Research 105, 8527–8535.

Braga ES, Chiozzini VC, Berbel GBB, Maluf JCC, Aguiar VMC, Charo M, Molina D, Romero SI, Eichler BB (2008) Nutrient distributions over the Southwestern South Atlantic continental shelf from Mar del Plata (Argentina) to Itajaí (Brazil): Winter–summer aspects. Continental Shelf Research 28, 1649–1661.

Brandini FP, Boltovskoy D, Piola A, Kocmur S, Röttgers R, Cesar Abreu P, Mendes Lopes R (2000) Multiannual trends in fronts and distribution of nutrients and chlorophyll in the southwestern Atlantic (30–62°S), Deep-Sea Res. Pt. I - Oceanogr. Res. Pap., 47(6), 1015–1033, doi:10.1016/s0967-0637(99)00075-8.

Bracco R, Inda H, del Puerto L, Castiñeira C, Sprechmann P, García-Rodríguez F (2005) Relationships between Holocene sea-level variations, trophic development, and climatic change in Negra Lagoon, Southern Uruguay. Journal of Paleolimnology 33 (3), 253–263.

Brazeiro A, Acha EM, Mianzan H, Gómez-Erache M, Fernández V (2003) Aquatic priority areas for the conservation and management of the ecological integrety of the Rio de la Plata and its maritime front. Technical Report PNUD Project / GEF RLA/99/G31

Burrage D, Wesson J, Martinez C, Pérez T, Möller O, Piola A (2008) Patos Lagoon outflow within the Río de la Plata plume using an airborne salinity mapper: Observing an embedded plume. Continental Shelf Research 28, 1625–1638.

Butler PG, Wanamaker AD, Scourse J, Richardson CA, Reynolds DJ (2013): Variability of marine climate on the North Icelandic Shelf in a 1357-year proxy archive based on growth increments in the bivalve Arctica islandica. Palaeogeography, Palaeoclimatology, Palaeoecology, 373, 141-151

Campodonico S, Macchi G, Lomovasky B, Lasta M (2008) Reproductive cycle of the Patagonian scallop Zygochlamys patagonica in the south-western Atlantic. *Journal of the Marine Biological Association of the UK*, *88*(03), 603-611.

Campos E, Piola A, Matano R, Miller J (2008) PLATA: A synoptic characterization of the southwest Atlantic shelf under influence of the Plata River and Patos Lagoon outflows. Continental Shelf Research 28, 1551–1555.

Carlson AE, Oppo DW, Came RE, LeGrande AN, Keigwin LD, Curry WB (2008) Subtropical Atlantic salinity variability and Atlantic meridional circulation during the last deglaciation. Geology 36, 991.

Carranza A, Arim M, Scarabino F, Defeo O (2010) Coexistence patterns of benthic gastropods on the Uruguayan shelf. Oikos 119, 1312–1318.

Carranza A, Scarabino F, Brazeiro A, Ortega L, Martínez S (2008) Assemblages of megabenthic gastropods from Uruguayan and northern Argentinean shelf: Spatial structure and environmental controls. Continental Shelf Research 28, 788–796.

Carré M, Sachs JP, Wallace JM, Favier C (2012) Exploring errors in paleoclimate proxy reconstructions using Monte Carlo simulations: paleotemperature from mollusk and coral geochemistry. Clim. Past 8:433–450. doi:10.5194/cp-8-433-2012

Chateigner D (2000) Mollusc shell microstructures and crystallographic textures. Journal of Structural Geology 22, 1723–1735.
Chiessi CM, Ulrich S, Mulitza S, Pätzold J, Wefer G (2007) Signature of the Brazil-Malvinas Confluence (Argentine Basin) in the isotopic composition of planktonic foraminifera from surface sediments. Marine Micropaleontology 64, 52–66.
Chiessi CM, Mulitza S, Paul A, Pätzold J, Groeneveld J, Wefer G (2008) South Atlantic interocean exchange as the trigger for the Bølling warm event. Geology 36, 919.
Clapperton C (1993) Nature of environmental changes in South America at the Last Glacial Maximum. Palaeogeography, Palaeoclimatology, Palaeoecology 101, 189–208.
Cruz F, Burns S, Karmann I, Sharp W (2005) Insolation-driven changes in atmospheric circulation over the past 116,000 years in subtropical Brazil. Nature 434:63-66.
Cruzjr F, Burns S, Jercinovic M, Karmann I, Sharp W, Vuille M (2007) Evidence of rainfall variations in Southern Brazil from trace element ratios (Mg/Ca and Sr/Ca) in a Late Pleistocene stalagmite. Geochimica et Cosmochimica Acta 71, 2250–2263.
Curry WB, Oppo DW (2005) Glacial water mass geometry and the distribution of delta C-13 of Sigma CO2 in the western Atlantic Ocean. Paleoceanography 20, PA1017.
Del Rio CJ (1997) Cenozoic Biogeographic History of the Eurythermal Genus Retrotapes, New Genus (Subfamily Tapetinae) from Southern South America and Antarctica. The Nautilus 110, 77–93.
Depetris PJ, Griffin JJ (1968) Suspended Load in the Rio De La Plata Drainage Basin. Sedimentology 11, 53–60.
Dettman DL, Goodwin D, Flessa K, Schöne B (2001) Cross-Calibration of Daily Growth Increments , Stable Isotope Variation, and Temperature in the Gulf of California Bivalve Mollusk Chione cortezi : Implications for Paleoenvironmental Analysis. Palaios 16, 387–398.
Dettman DL (1999) Controls on the stable isotope composition of seasonal growth bands in aragonitic fresh-water bivalves (unionidae). Geochimica et Cosmochimica Acta 63, 1049–1057.
Dettman DL, Lohmann KC (1994) Microsampling Carbonates for stable Isotope and minor Element Analysis. Research Methods Papers 566–569.
Dextraze BL, Zinsmeister WJ (1987) A study of the internal annual growth lines of the late Eocene mollusk Eurhomalea Antarctica. Antarctic Journal of the United States 22, 14–15.
Elliot M, DeMenocal PB, Linsley BK and Howe SS (2003) Environmental controls on the stable isotopic composition of Mercenaria mercenaria: Potential application to paleoenvironmental studies, Geochem. Geophys. Geosyst., 4(7), 1056, doi:10.1029/2002GC000425, 2003.
Emilsson I (1961) The shelf and coastal waters off southern Brazil. Boletim do Instituto Oceanográfico da Universidade de São Paulo 11, 102–112.
Fairbanks RG, Matthews RK (1978) The Marine Oxygen Isotope Record in Pleistocene Coral, Barbados, West Indies. Quaternary Research 10, 181–196.
Floeter SR, Soares-Gomes A (1999) Biogeographic and Species Richness Patterns of Gastropoda on the Southwestern Atlantic. Revista Brasileira De Biologia 59, 567–575.
Gallardo MH, Mena C, Lomovasky B, Morriconi E, Clasing E (2003) Allozymic variation in the clam genus Eurhomalea (Bivalvia : Veneriidae) along southern South American coast. Methods 76, 501–507.
Gan MA, Kousky VE, Ropelewski CF (2004) The South America Monsoon Circulation and Its Relationship to Rainfall over West-Central Brazil. Journal of Climate 17, 47–66.
Garzoli SL, Giulivi C (1994) What forces the variability of the southwestern Atlantic boundary currents ? Deep Sea Research Part I: Oceanographic Research Papers 41, 1527–1550.
Giberto DA, Bremec CS, Acha EM, Mianzan H (2004) Large-scale spatial patterns of benthic assemblages in the SW Atlantic: the Rio de la Plata estuary and adjacent shelf waters. Estuarine, Coastal and Shelf Science 61, 1–13.
Gillikin DP (2005) Strong biological controls on Sr/Ca ratios in aragonitic marine bivalve shells. Geochemistry Geophysics Geosystems 6.
Gobac ZZ, Posilovic H, Bermanec V (2009) Identification of biogenic Calcite and Aragonite using SEM. Geologia Croatica 9611, 201–206.
Goodwin DH., Flessa KW, Schöne BR and Dettman DL (2001) Cross-calibration of daily growth increments, stable isotope variation, and temperature in the Gulf of California bivalve mollusk Chione cortezi: implications for environmental analysis. Palaios. 16, 387–398.
Gordillo S, et al. (2014) *Mollusk shells as bio-geo-archives: Evaluating environmental changes during the Quaternary*. SpringerBriefs in Earth System Sciences, ISBN: 978-3-319-03475-1 (Print) 978-3-319-03476-8 (Online).
Gordillo S (1999) Holocene molluscan assemblages in the Magellan region *. Holocene 63, 15–22.
Gordillo S (2006) Pleistocene Retrotapes de Rió, 1997 (Veneridae, Bivalvia) from Tierra del Fuego, Argentinia. Ameghiniana 43.

Gordillo S, Brey T, Beyer K, Lomovasky B (2013) Retrotapes exalbidus from southern SouthAmerica: are fossil shells reliable proxy archives for Holocene climate, in: 3rd International Sclerochronology Conference. Caernarfon, Wales, UK.
Gordillo S, Rabassa J, Coronato A (2008) Paleoecology and paleobiogeographic patterns of mid-Holocene mollusks from the Beagle Channel (southern Tierra del Fuego, Argentina). Revista Geolólogia de Chile 35, 321–333.
Gosling E (2003) Bivalve Molluscs: Biology, Ecology and Culture, Blackwell Publishing Ltd, Oxford, UK. doi: 10.1002/9780470995532
Grossman E, Ku TL (1986) Oxygen and carbon isotope fractionation in biogenic aragonite: Temperature effects. Chemical Geology 59, 59–74.
Guilderson TP, Burckle L (2000) Late Pleistocene sea level variations derived from the Argentine Shelf. Geochemistry, Geophysics, Geosystems. 1:2000GC00098.
Guilderson TP, Pak DK (2005) Reconstructing Past Ocean Salinity ((delta)18Owater). Encyclopedia of Quaternary Science. URL-BOOK-217238
Gutiérrez F, Guerrero J, Lucha P (2008) A genetic classification of sinkholes illustrate fromevaporite paleokarst exposures in Spain. Environmental Geology 53, 993–1006.
Gyllencreutz R, Mahiques MM, Alves DVP, Wainer IKC (2010) Mid- to late-Holocene paleoceanographic changes on the southeastern Brazilian shelf based on grain size records. Holocene 20 (6), 863–875
Haddock S (2010) A plea for meaningful colors in odv. Limnology and Oceanography 19, 2010.
Hanebuth TJJ, Stattegger K, Bojanowski A (2009) Termination of the last glacial maximum sea-level lowstand: the Sunda-Shelf data revisited. Global and Planetary Change 66(1–2):76–84
Huber, M (2010) Compendium of Bivalves, 901 p. ConchBooks, Hackenheim.
Iriondo MH, Paggi JC, Parma MJ (2007) The Middle Parana River: Limnology of a Subtropical Wetland. , XII, 382 p. 128 illus. Springer Verlag.
Ivany LC, Runnegar B (2010) Early Permian seasonality from bivalve 18O and implications for the oxygen isotopic composition of seawater. Geology 38, 1027–1030.
Jones DS (1980) Annual cycle of shell growth increment formation in two continental shelf bivalves and its paleoecologic significance. Paleobiology 6, 331–340.
Jones DS, Quitmyer IR (1996) Marking time with bivalve shells.pdf. Palaios 11, 340–346.
Kaiser P (1977) Beiträge zur Kenntnis der Voluten (Mollusca) in argentinisch-brasilianischen Gewässern (mit der Beschreibung zweier neuer Arten). Mittel Hamburg Zool Mus Inst 74.
Kaltenegger W, Preisinger A, Rögl F (1971) Paläotemperaturbestimmungen an aragonitischen en aus dem aplinen Mesozoikum. Palaeogeogr. Palaeoclimatol. Palaeoecol. 10, 273–285.
Kanazawa T, Sato S (2007) Environmental and physiological controls on shell microgrowth pattern of Ruditapes philippinarum (Bivalvia: Veneridae) from Japan. J. Molluscan Stud. 74, 89–95.
Kim S-T, Mucci A, Taylor BE (2007) Phosphoric acid fractionation factors for calcite and aragonite between 25 and 75 °C: Revisited. Chemical Geology 246, 135–146.
Kobayashi I, Samata T (2006) Bivalve shell structure and organic matrix. Mater. Sci. Eng. C 26, 692–698. doi:10.1016/j.msec.2005.09.101
Krantz DE, Williams DF, Jones DS (1987) Ecological and paleoenvironmental information using stable isotope profiles from living and fossil molluscs. Palaeogeography, Palaeoclimatology, Palaeoecology 58, 249–266.
Krastel S, Wefer G and cruise participants (2012) Report and preliminary results of RV METEOR Cruise M78/3. Sediment transport off Uruguay and Argentina: From the shelf to the deep sea. 19.05.2009 – 06.07.2009, Montevideo (Uruguay) – Montevideo (Uruguay).
Lambeck K, Chappell J (2001) Sea level change through the last glacial cycle. Science (New York, N.Y.) 292, 679–86.
Lantzsch H, Hanebuth TJJ, Chiessi CM, Schwenk T, Violante R (2014) The high-supply, current-dominated continental margin of southeastern South America during the late Quaternary. Quat. Res. doi:10.1016/j.yqres.2014.01.003
Leduc G, Schneider R, Kim J-H, Lohmann G (2010) Holocene and Eemian sea surface temperature trends as revealed by alkenone and Mg/Ca paleothermometry. Quaternary Science Reviews 29, 989–1004.
LeGrande AN, Schmidt GA (2006) Global gridded data set of the oxygen isotopic composition in seawater. Geophys. Res. Lett. 33, 1–5. doi:10.1029/2006GL026011
Leitmeier H, Feigl F (1934) Eine einfache Reaktion zur Unterscheidung von Calcit und Aragonit. Zeitschrift für Krist. Mineral. und Petrogr. 45, 447–456. doi:10.1007/BF02943377
Locarnini RA, Mishonov AV, Antonov JI, Boyer TP, Garcia HE, Baranova OK, Zweng MM, Johnson DR (2010) World Ocean Atlas 2009, Volume 1: Temperature.

Lomovasky BJ, Brey T, Morriconi E, Calvo J (2002a) Growth and production of the venerid bivalve Eurhomalea exalbida in the Beagle Channel, Tierra del Fuego. Journal of Sea Research 48, 209–216.
Lomovasky BJ, Morriconi E, Brey T, Calvo J (2002b) Individual age and connective tissue lipofuscin in the hard clam Eurhomalea exalbida. Journal of Experimental Marine Biology and Ecology 276, 83–94.
Maier E, Titschack J (2010) Spondylus gaederopus: A new Mediterranean climate archive — Based on high-resolution oxygen and carbon isotope analyses. Palaeogeography, Palaeoclimatology, Palaeoecology 291, 228–238.
Marchitto TA, Jones GA, Goodfriend GA, Weidmann CR (2000) Precise temporal correlation of Holocene mollusk shells using sclerochronology. Quat. Res. 53, 236–246.
Martínez, S., Rojas, A., 2013. Relative sea level during the Holocene in Uruguay. Palaeogeography, Palaeoclimatology, Palaeoecology 374, 123–131.
Martins LR, Martins IR, Urien CM (2003) Aspectos sedimentares da plataforma continental na a´rea de Influe ˆncia do Rio de La Plata. Gravel 1, 68–80.
Matano RP, Palma ED, Piola AR (2010) The influence of the Brazil and Malvinas Currents on the Southwestern Atlantic Shelf circulation. Ocean Science 6, 983–995.
Moller OO, Castaing P, Salomon J-C, Lazure P (2001) The Influence of Local and Non-Local Forcing Effects on the Subtidal Circulation of Patos Lagoon. Estuaries 24, 297.
Mook WG, Vogel JC (1968) Isotopic equilibrium between shells and their environment. Science 159:874-875.
Morriconi E, Lomovasky BJ, Calvo J, Brey T (2002) The reproductive cycle of Eurhomalea exalbida (Chemnitz, 1795) (Bivalvia: Veneridae) in Ushuaia Bay (54 degrees 50′ S), Beagle Channel (Argentina). Invertebrate Reproduction and Devel- opment 42, 61–68.
Morris PJ, Rosenberg G (2005) Search interface and documentation for Malacolog, an online database of Western Atlantic marine Mollusks. [WWW database (version 4.1.1)] URL http://www.malacolog.org.
Negre C, Zahn R, Thomas AL, Masqué P, Henderson GM, Martínez-Méndez G, Hall IR, Mas JL (2010) Reversed flow of Atlantic deep water during the Last Glacial Maximum. Nature 468, 84–8.
Nützel A, Joachimski M, López Correa M (2010) Seasonal climatic fluctuations in the Late Triassic tropics—High-resolution oxygen isotope records from aragonitic bivalve shells (Cassian Formation, Northern Italy). Palaeogeography, Palaeoclimatology, Palaeoecology 285, 194–204.
Olivier SR, Scarabino V (1972) Distribución ecológica de algunos moluscos recogidos por la expedición del "Walther Herwig" (R.F.A.) al Atlántico sudoccidental (1966). Rev Bras Biol 32, 235–247.
Pannella G, MacClintock C (1968) Paleontological Society Biological and Environmental Rhythms Reflected in Molluscan Shell Growth. Memoir (The Paleontological Society) 2, 64–80.
Penchaszadeh PE, Pastorino G, Brogger MI (2008) Atlas de sensibilidad ambiental del mar y de la costa, www.atlas.ambiente.gov.ar.
Piola AR, Campos EJD, Möller OO, Charo M, Martinez C (2000) Subtropical Shelf Front off eastern South America. Journal of Geophysical Research 105, 6565–6578.
Piola AR, Matano RP (2001) Brazil and Falklands (Malvinas) Currents. Encyclopedia of Ocean Sciences 1, 340–349.
Piola AR, Matano RP, Palma ED, Ller OOM, Campos EJD (2005) The influence of the Plata River discharge on the western South Atlantic shelf, Geophys. Geophysical Research Letters 32.
Piola AR, Romero SI, Zajaczkovski U (2008) Space-time variability of the Plata plume inferred from ocean color. Continental Shelf Research, doi: 101016/jcsr200702013.
Provost C, Garcia O, Garcon V (1992) Analysis of Satellite Sea Surface Temperature Time Series in the Brazil-Malvinas Current Confluence Region: Dominance of the Annual and Semiannual Periods. Journal of Geophysical Research 97, 17,841–17,858.
Reimer P, Baillie M, Bard E, Bayliss A, Beck J, Blackwell P, Bronk Ramsey C, Buck C, Burr G, Edwards R, Friedrich M, Grootes P, Guilderson T, Hajdas I, Heaton T, Hogg A, Hughen K, Kaiser K, Kromer B, McCormac F, Manning S, Reimer R, Richards D, Southon J, Talamo S, Turney C, van der Plicht J, Weyhenmeyer C (2009) IntCal09 and Marine09 radiocarbon age calibration curves, 0–50, 000 years cal BP. Radiocarbon 51(4), 1111–50.
Rios EC (1994) Seashells of Brazil. Fundação Cidade do Rio Grande, Rio Grande.
Rosell-Melé A, Bard E, Emeis K (2004) Sea surface temperature anomalies in the oceans at the LGM estimated from the alkenone-U37K′ index: comparison with GCMs. Geophysical ResearchLetters 31, 1–4.
Rosenbaum J, Sheppard SMF (1986) An isotopic study of siderites, dolomites and ankerites at high temperatures. Geochimica et Cosmochimica Acta 50, 1147–1150.
Scarabino F (2003) Lista Sistematica de los Bivalvos Marinos Y Estuarios de Uruguay. Comunicaciones de la Sociedad Malacológica del Uruguay 8, 227–258.
Scarabino V (1977) Moluscos del Golfo San Matías. Comun. Soc. Malacol. Uruguay 4 31, 177–263.

Schlitzer R (2012) Ocean Data View (ODV). http://www.odv.awi.de
Schmidt GA, Bigg GR, Rohling EJ (1999) Gloabl Seawater Oxygen-18 Database v1.21. http://data.giss.nasa.gov/o18data/
Schneider CA, Rasband WS, Eliceiri KW (2012) NIH Image to ImageJ: 25 years of image analysis. *Nat Methods* 9 (7): 671–675. doi:10.1038/nmeth.2089
Schöne BR, Dunca E, Fiebig J, Pfeiffer M (2005a) Mutvei's solution: An ideal agent for resolving microgrowth structures of biogenic carbonates. Palaeogeography, Palaeoclimatology, Palaeoecology 228, 149–166.
Schöne BR, Fiebig J, Pfeiffer M, Gleβ R, Hickson J, Johnson A, Dreyer W, Oschmann W (2005b) Climate records from a bivalved Methuselah (Arctica islandica, Mollusca; Iceland). Palaeogeography, Palaeoclimatology, Palaeoecology 228, 130–148.
Schöne BR, Houk S, Freyre Castro A, Fiebig J, Oschmann W, Kroncke I, Dreyer W, Gosselck F (2005c) Daily Growth Rates in Shells of Arctica islandica: Assessing Sub-seasonal Environmental Controls on a Long-lived Bivalve Mollusk. Palaios 20, 78–92.
Schöne BR, Gillikin, DP (2012) Unraveling environmental histories from skeletal diaries - advances in sclerochronology. Palaeogeography, Palaeoclimatology, Palaeoecology.
Schöne BR, Radermacher P, Zhang Z, Jacob DE (2011) Crystal fabrics and element impurities (Sr/Ca, Mg/Ca, and Ba/Ca) in shells of Arctica islandica—Implications for paleoclimate reconstructions. Palaeogeography, Palaeoclimatology, Palaeoecology 373, 50–59.
Schrag DP, Adkins JF, McIntyre K, Alexander JL, Hodell DA, Charles CD, and McManus JF (2002) The oxygen isotopic composition of seawater during the Last Glacial Maximum, Quat. Sci. Rev., 21(1-3), 331–342, doi:10.1016/S0277-3791(01)00110-X.
Seibold, E (1982) Geology of the Northwest African continental margin. Berlin, New York, Heidelberg: Springer-Verlag, 1982.
Stuiver M, Polach HA (1977) Discussion: reporting of 14C data. Radiocarbon 19(3):355–63
Taylor JD (1969) The shell structure and mineralogy of the Bivalvia. Introduction. Nuculacea-Trigonacea. *Bull. Br. Mus. Nat. Hist.(Zool.)*, 3, 1-125.
Vaz AC, Möller Jr. OO, Almeida TL (2006) Sobre a descarga dos rios afluentes a Lagoa dos Patos. Atlantica 28, 13–23.
Violante R, Parker G (2004) The post-last glacial maximum transgression in the de la Plata River and adjacent inner continental shelf, Argentina. Quaternary International 114, 167–181.
Vogel K (1984) Lebensweise und Umwelt fossiler Tiere: eine Einführung in die Ökologie der Vorzeit. Quelle & Meyer. Heidelberg
Waelbroeck C, Paul A, Kucera M, Rosell-Melé A, Weinelt M (2009) Constraints on the magnitude and patterns of ocean cooling at the Last Glacial Maximum. Nature Geoscience 2, 127–132.
Wanner H, Solomina O, Grosjean M, Ritz SP, Jetel M (2011) Structure and origin of Holocene cold events. Quaternary Science Reviews 30, 3109–3123.
Weidman CR (1995) Development and Application of the Mollusc Arctica islandica as a Paleoceanographic Tool for the North Atlantic Ocean. Marine Geology. State University of New York at Oneonta.
Wefer G (1985) Die Verteilung stabiler Isotope in Kalkschalen mariner Organismen. Geol. Jahrb. 82-A.
Wells PG, Daborn GR (1997) The Río de la Plata - An Environmental Overview. EcoPlata Project.
Wisshak M, López Correa M, Gofas S, Salas C, Taviani M, Jakobsen J, Freiwald A (2009) Shell architecture, element composition, and stable isotope signature of the giant deep-sea oyster Neopycnodonte zibrowii sp. n. from the NE Atlantic. Deep Sea Research Part I: Oceanographic Research Papers 56, 374–407.
WoRMS Editorial Board (2014). World Register of Marine Species. Available from http://www.marinespecies.org at VLIZ. Accessed 2014-09-26
Yan L, Schöne BR, Arkhipkin A (2012) Eurhomalea exalbida (Bivalvia): A reliable recorder of climate in southern South America? Palaeogeography, Palaeoclimatology, Palaeoecology 350-352, 91–100.
Zhou J, Lau K-M (1998) Does a Monsoon Climate Exist over South America? Journal of Climate 11, 1020–1040.

XIV. Summary and conclusions

This dissertation clearly highlights the importance of modern analogue studies in order to evaluate past and present marine ecosystems. In order to investigate the complex sedimentological nature of shelfal depositional systems, three different interdisciplinary approaches were used, whose outcomes and conclusions are presented in the following paragraphs. The investigated study areas offshore Mauritania and Uruguay are characterized by a number of environmental steering factors (e.g., oceanographic conditions, ocean-atmosphere-couplings, terrestrial influence) that manifest in the modern and ancient sedimentological record, thus providing a 'window into the past' from short (sub-seasonal) to geological time-scales.

The focus of this study is the role of carbonate secreting organisms in clastic shelf systems and their potential as environmental bioarchive. Of course, this study provides no master plan that allows characterizing marine ecosystems on the basis of carbonate secretors only. However, the insights we get from such organisms, often living in close equilibrium with environmental conditions, and that are able to adapt their morphology in order to cope with environmental constraints over short to geological time-scales is a significant contribution to understand specific ecosystems or habitats in the context of climate change. Ecosystem-based studies and monitoring programs are of fundamental value, not only to understand the response of marine systems under future perspectives, but also for the interpretation and palaeo-environmental reconstructions of ancient marine environments preserved the sedimentological and geological record.

XIV.1 Main outcomes of the first publication

1) The Golfe d'Arguin offshore Mauritania hosts a valuable analogue model of a heterozoan carbonate system that developed under tropical eutrophic conditions.

2) Sedimentary constituents clearly highlight the multidimensional control under which the shells and remains of carbonate secreting organisms developed.

3) Detailed taxonomic studies on species level can provide information on ecosystem level that clearly highlights the influence of upwelling and low-light conditions as main-drivers of carbonate productions.

4) Carbonate grain associations and gulf-wide facies pattern provide insights into shelf morphology and water circulation on the shallow Banc d'Arguin.

XIV.2 Main outcomes of the second and third publication

1) Bryozoan taxa identified in the Golfe d'Arguin show different adaptation strategies to environmental steering factors, such as mobile to semi-mobile colonies that are able to cope with the hydrodynamic regime and high sedimentation rate.

2) Bryoliths, for example, form subspherical to spherical bionodules that result from the symbiotic proto-cooperation of encrusting bryozoans and hermit crabs.

3) Both symbiotic partners form a non-obligatory partnership, this relationship represents an adaptation to environmental constraints such as limited hardbottom availability and an intense hydrodynamic regime with high sedimentation loads.

4) Bryoliths are rare constituents in modern systems, but show a high variety with a documented fossil records dating back to the Middle Jurassic. These modern occurrences provide valuable insights that are of interest for the interpretation of fossil records with a poor fossilization potential.

XIV.3 Main outcomes of the fourth manuscript

1) This study clearly highlights the high potential of accretionary biogenic carbonate from growth increments of venerid bivalve shells as environmental archive.

2) The temporal resolution covering sub-seasonal to daily cycles provides a high-resolution climate archive of ambient water conditions over the lifetime of the organism that spans from years to centuries.

3) However, calibration studies of modern representatives are of significant importance in order to exclude metabolically-influenced disfractionation effects of the stable isotopic composition.

4) The outcome of the presented study is a more pronounced deglacial seasonality offshore Uruguay and a stronger seasonal influence of the cold-water Malvinas Current (also Sub-Antarctic Shelf Current) thus displacing the sub-tropical shelf front offshore Uruguay in a more northward position. Also, a very prominent freshwater signal in the stable carbon isotopic signature argues for a stronger influence of the South American summer monsoon.

XV. Perspectives and implications for future research

The investigated research areas offshore northwest Africa (Golf d'Arguin) and offshore Uruguay (Río de la Plata Shelf) are valuable locations to study the effect of environmental steering factors on carbonate secreting organisms. Both mixed carbonate-siliciclastic systems lie adjacent to a complex oceanographic system with distinct seasonal shifting thermal fronts, confluence zones of different-temperated water masses and upwelling phenomena. Understanding the effect of those environmental conditions on carbonate secreting organisms is a crucial prerequisite in order to reconstruct modern and ancient marine ecosystems and palaeo-climatic conditions during that time.

The results presented in this dissertation help do define accurate models which allow for a better interpretation of the environment, and hence, for a better evaluation and monitoring of threatened marine ecosystems that are affected by the consequences of climate change.

However, such localized studies are just initial steps that help to demonstrate how future research can contribute to a better knowledge of complex marine ecosystems. As shown in the publications attached to this research project, the presence is a valuable key to the past throughout, nonetheless, when comparing modern analogues with ancient counterparts, a third variable has to be considered, which was not a topic of this study, but always an important aspect: Diagenetic alteration can modify the sedimentological record and, in particular, the geochemical fingerprint of environmental archives. Bioerosion and hydrodynamically induced abrasion processes are always important factors in shallow marine settings that often determine the preservation and lithification potential of such carbonate deposits. When applying the provided techniques to the fossil record, a critical reflection on diagenetic processes is an important prerequisite.

The facies study presented in the First publication provides for the first time a conclusive, large-scale carbonate depositional model for the Golfe d'Arguin. Additional environmental data and sedimentological core and surface material are now available and allow the reconstruction of modern 'atypical' conditions (e.g., heterozoan carbonates in tropical latitudes) through time. Future research should include core material dating back to Late Pleistocene times in order to look for changes in upwelling intensities and biotic community structures offshore Mauritania. As already noted by Michel et al. 2009, the comparison of such modern heterozoan carbonates from the Golfe d'Arguin with those from other upwelling-influences shelves would improve our knowledge of the palaeo-environmental and palaeo-oceanographic interpretation of ancient heterozoan carbonates.

A fist step in this direction was done in the Second publication and Third publication in which the modern bryomol sediments of the shallow Banc d'Arguin and the larger bryolith constituents were compared with environmental settings of the New Zealand Shelf. However, *in situ* bryoliths are extremely rare in modern marine settings and a comparison of bryoliths from different locations and different time intervals is thus of highest importance in order to better understand the benefits and circumstances that favor such a proto-cooperation (symbiosis) of two different marine species.

Future research is also crucial when using large venerid clams as palaeo-environmental bioarchive. As shown in the Fourth manuscript, modern analogue studies are essentials in order to calibrate past oceanographic conditions using fossil material. The presented study, however, is based on a single large clam only, thus more replicates are needed in order to establish the investigated bivalve species *E. exalbida* as environmental bioarchive in southeastern South America. Besides an extended dataset of sub-recent and fossil shell material, more detailed calibration studies under natural and artificial conditions are needed, as it has shown that modern representatives of the species *E. exalbida* precipitate calcium carbonate out of equilibrium with seawater conditions. Although this trend could not be confirmed with fossil material, more calibration studies would improve the applicability of the geochemical fingerprint and the use of marine bioarchives as palaeo-environmental proxy.

XVI. Appendix

XVI.1 Institutional cooperation

Center for Marine Environmental Sciences (MARUM)
University Bremen,
Leobener Str., D-28359 Bremen, Germany
http://www.marum.de

Leibniz Center for Tropical Marine Ecology (ZMT)
Fahrenheitstraße 6,
D-28359 Bremen, Germany
http://www.zmt-bremen.de

Natural History Museum (NHM)
Department for Earth Sciences,
Cromwell Road, London, SW7 5BD, UK
http://www.nhm.ac.uk

Museo Nacional de History Natural (MNHN)
Malacología y Zoología Invertebrados
25 de mayo 582 – CC. 399, CP. 11000
Montevideo, Uruguay
http://www.mnhn.gub.uy

Universidad de la República (UdelaR)
Seccion Oceanologia / Facultad de Ciencias
Avenida 18 de Julio 1824
Montevideo 11100, Uruguay
http://www.udelar.edu.uy

XVI.2 List of co-authors

Prof. Dr. Hildegard Westphal
Leibniz Center for Tropical Marine Ecology (ZMT), Bremen, Germany, and
University of Bremen, Bremen, Germany
✉ Hildegard.westphal [at] zmt-bremen.de

Prof. Dr. Till J.J. Hanebuth
School of Coastal and Marine Systems Sciences, Coastal Carolina University, Conway/SC, USA
✉ thanebuth [at] coastal.edu

Dr. Paul D. Taylor
Natural History Museum, Department of Earth Sciences, London, United Kingdom
✉ p.taylor [at] nhm.ac.uk

Dr. Alvar Carranza
Centro Universitario Regional Este (CURE), Universidad de la República, Maldonado, Uruguay and
Museo Nacional de Historia Natural (MNHN), Montevideo, Uruguay
✉ alvardoc [at] fcien.edu.uy

Dr. Julien Michel

Department of Earth Sciences, cluster DERC , VU University Amsterdam, The Netherlands
Formerly at: Center for Marine Environmental Sciences (MARUM), University Bremen, Germany
✉ jmichel [at] marum.de

André Klicpera (MSc Geol., PhD cand.)
Leibniz Center for Tropical Marine Ecology (ZMT), Bremen, Germany, and
Center for Marine Environmental Sciences (MARUM), University Bremen, Germany
✉ klicpera [at] uni-bremen.de

XVI.3 Compiled literature

The following literature, research articles and scientific reports build the basis of relevant research conducted in the field of the presented dissertation. For detailed information on a certain topic please refer the references given in the chapters of publications and manuscripts.

Abrantes FF (1991) Variability of upwelling Oof NW Africa during the latest Quaternary: Diatom evidence. Paleoceanography, 6. No. 4: 431-460.

Acker JG, Leptoukh G (2007) Online analysis enhances use of NASA Earth science data. Eos, Transactions American Geophysical Union 88, 14–17.

Addicott WO (1969) Tertiary climatic change in the marginal northeastern Pacific Ocean. Science, 165, 583–586.

Adey WH, MacIntyre IG (1973) Crustose coralline algae: a re-evaluation in the geological sciences. Geological Society of America Bulletin 84:883-903

André L, Planchon F, Dehairs F, Bauwens M, Beelaerts V, Mas R, Blust R, Hansen H, Dubois Ph., Borremans C, Willenz Ph., Gosselin P, Hermans J (2009) Critical evaluation of marine calcareous skeletons as recorders of global climate change "CALMARS II" Final Report Ph 1. Brussels : Belgian Science Policy 2009 – 132 p. (Research Programme Science for a Sustainable Development)

Aguirre ML (1993) Palaeobiogeography of the Holocene molluscan fauna from northeastern Buenos Aires Province, Argentina: its relation to coastal evolution and sea level changes. Palaeogeogr. Palaeoclimatol. Palaeoecol. 102, 1–26.

Aguirre ML, Farinati EA (1999) Paleogeografia de las faunas de moluscos marinos del Neogeno y Cuaternario del Atlantico sudoccidental.pdf. Rev. Soc. Geol. Espana 12, 93–112.

Aguirre ML, Leng MJ, Spiro B (1998) Variation in isotopic composition (C, O and Sr) of Holocene Mactra isabelleana (Bivalvia) from the coast of Buenos Aires Province, Argentina. The Holocene 8, 613–621.

Aguirre ML, Sirch YN, Richiano S (2005) Late Quaternary molluscan assemblages from the coastal area of Bahía Bustamante (Patagonia, Argentina): Paleoecology and paleoenvironments. J. South Am. Earth Sci. 20, 13–32.

Aleman N, Certain R, Courp T, Barusseau JP, Vernet R, Dia A (2010) Le Golfe d'Arguin – Carte Morpho – Bathymetricque. IMAGES - Institut de Modélisation et d'Analyse en Géo-Environnement et Santé. Université de Perpignan (France)

Anderson TF, Arthur MA (1983) Stable isotopes of oxygen and carbon and their applications to sedimentological and paleoenvironmental problems. In M. A. Arthur, T. F. Anderson, I. R. Kaplan, J. Veizer, & L. S. Land (Eds.), *Stable Isotopes in Sedimentary Geology* (Soc. Econ., pp. 1-151).

Ansell AD (1968) The rate of growth of the hard clam Mercenaria mercenaria (L) throughout the geographic range. Journal du Conseil Permanent Internatinal pour l'Exploration de la Mer 31, 364–409.

Ansell, AD (1983) The biology of the genus Donax, in McLachlan, A., and Erasmus, T., eds., Sandy Beaches as Ecosystems: The Hague, Dr .W. Junk Publishers, p. 607–636

Antonov JI, Seidov D, Boyer TP, Locarnini RA, Mishonov AV, Garcia HE, Baranova OK, Zwerg MM, Johnson DR (2010) World Ocean Atlas 2009, Volume 2: Salinity.

Ardovini R, Cossignani T (2004) West African seashells (including Azores, Madeira and Canary Is.) Conchiglie dell'Africa Occidentale (incluse Azzorre, Madeira e Canarie). English-Italian edition. L'Informatore Piceno: Ancona, Italy. 319 pp

Arz HW, Pätzold J, Wefer G (1999) The deglacial history of the Western Tropical Atlantic as inferred from high resolution stable isotope reords off Northeastern Brazil. Earth and Planetary Science Letters 167, 105–117.

Ayup-Zouain RN (2006) Evolucíon paleogeográafica y dispersióon de los sedimentos del Río de la Plata. Bases para la conservación y el manejo de la costa uruguaya. VIDA SILVESTRE URUGUAY, Montevideo.

Azzoug M, Carré M, Schauer AJ (2012) Reconstructing the duration of the West African Monsoon season from growth patterns and isotopic signals of shells of Anadara senilis (Saloum Delta, Senegal). Palaeogeogr. Palaeoclimatol. Palaeoecol. 346-347, 145–152. doi:10.1016/j.palaeo.2012.06.001

Balson PS, Taylor PD (1982) Palaeobiology and systematics of large cyclostome bryozoans from the Pliocene Coralline Crag of Suffolk. Palaeontology 25(3):529-554

Barange M, Field J, Harris R, Hofmann E (2010) Marine ecosystems and global change. OUP Oxford

Barton ED (1998) Eastern boundary of the North Atlantic: Northwest Africa and Iberia. In: Robinson AR, Brink KH (eds) The Sea. JohnWiley & Sons Inc., New York, pp pp. 633–657

Batten ML, Martinez JR, Bryan DW, Buch EJ (2000) A modeling study of the coastal eastern boundary current system off Iberia and Morocco. Journal of Geophysical Research, 105, 14173-14195.

Bender VB, Hanebuth TJJ, Chiessi CM (2013) Holocene shifts of the Subtropical Shelf Front off southeastern South America controlled by high and low latitude atmospheric forcings. Paleoceanography 28, 1–10.

Berghuis EM, Duineveld GCA, Hegeman J (1993) Primary production and distribution of phytopigments in the water column and sediments on the upwelling shelf off the Mauritanian coast (Northwest Africa). Hydrobiologia 258:81–93.

Binet D, Samb B, Ould Taleb MM (1998) Sardine and other pelagic fisheries changes associated with multi-year trade wind increases in the southern Canary Current. In: Durand M-H, Cury P, Mendelssohn R, et al. (eds) Global versus Local Changes in Upwelling Systems. ORSTOM Colloques et Seminaires, Paris, pp 211–233.

Bigg GR, Rohling EJ (2000) An oxygen isotope data set for marine waters. Journal of Geophysical Research 105, 8527–8535.

Bisbal GA (1995) The Southeast South American shelf large marine ecosystem: Evolution and components, Marine Policy, 19-1:21-38, ISSN 0308-597X, doi:10.1016/0308-597X(95)92570-W.

Blott SJ, Croft DJ, Pye K, et al. (2004) Particle size analysis by laser diffraction. Geological Society, London, Special Publications 232:63–73. doi: 10.1144/GSL.SP.2004.232.01.08

Blott, S. J., & Pye, K. (2001). GRADISTAT: a grain size distribution and statistics package for the analysis of unconsolidated sediments. *Earth surface processes and Landforms*, *26*(11), 1237-1248.

Boucher DH (1988) The Biology of Mutualism: Ecology and Evolution. Oxford University Press

Bourrouilh-Le Jan F, Hottinger L (1988) Occurrence of rhodolites in the tropical Pacific — a consequence of Mid-Miocene paleo-oceanographic change. Sediment Geol 60:355–367.

Bosch T, Colijn F, Ebinghaus R, Körtzinger A, Latif M, Matthiessen B, Melzner F, Oschlies A, Petersen S, Proelß A, Quaas M, Requate T, Reusch TBH, Rosenstiel P, Schrottke K, Sichelschmidt H, Siebert U, Soltwedel R, Sommer U, Stattegger K, Sterr H, Sturm R, Treude T, Vafeidis A, van Bernem C, van Beusekom J, Visbeck M, Wahl M, Wallmann KJG, Weinberger F, Bollmann M, Froese R, Khalilian S, Reichenbach J, Schmidt J, Voss R and M, Future Ocean - Cluster of Excellence (2010) *World Ocean Review 2010 : Mit den Meeren leben* , ed. by Gelpke, N and Visbeck M. Mare, Hamburg, 234 pp. ISBN 978-3-86648-000-1

Boschma H (1955) The described species of the family Sacculinidae. Zoologische Verhandelingen 27 (1): 1–76.

Bradford MD, Schwab E (2012) Symbiosis: 'Living together' in chaos, Studies in the History of Biology 4 (4): 7–25.

Bracco R, Inda H, del Puerto L, Castiñeira C, Sprechmann P, García-Rodríguez F (2005) Relationships between Holocene sea-level variations, trophic development, and climatic change in Negra Lagoon, Southern Uruguay. Journal of Paleolimnology 33 (3), 253–263.

Braga ES, Chiozzini VC, Berbel GBB, Maluf JCC, Aguiar VMC, Charo M, Molina D, Romero SI, Eichler BB (2008) Nutrient distributions over the Southwestern South Atlantic continental shelf from Mar del Plata (Argentina) to Itajaí (Brazil): Winter–summer aspects. Continental Shelf Research 28, 1649–1661.

Brandano M, Corda L (2002) Nutrients, sea level and tectonics: constrains for the facies architecture of a Miocene carbonate ramp in central Italy. Terra Nova 14:257–262.

Brandini FP, Boltovskoy D, Piola A, Kocmur S, Röttgers R, Cesar Abreu P, Mendes Lopes R (2000) Multiannual trends in fronts and distribution of nutrients and chlorophyll in the southwestern Atlantic (30–62°S), Deep-Sea Res. Pt. I - Oceanogr. Res. Pap., 47(6), 1015–1033, doi:10.1016/s0967-0637(99)00075-8.

Brazeiro A, Acha EM, Mianzan H, Gómez-Erache M, Fernández V (2003) Aquatic priority areas for the conservation and management of the ecological integrety of the Rio de la Plata and its maritime front. Technical Report PNUD Project / GEF RLA/99/G31

Burke L, Bryant D, McManus J, Spalding M (2011) Reefs at Risk. World Ressorce Insitute, http://www.wri.org/our-work/project/reefs-risk

Burrage D, Wesson J, Martinez C, Pérez T, Möller O, Piola A (2008) Patos Lagoon outflow within the Río de la Plata plume using an airborne salinity mapper: Observing an embedded plume. Continental Shelf Research 28, 1625–1638.

Butler PG, Wanamaker AD, Scourse J, Richardson CA, Reynolds DJ (2013): Variability of marine climate on the North Icelandic Shelf in a 1357-year proxy archive based on growth increments in the bivalve Arctica islandica. Palaeogeography, Palaeoclimatology, Palaeoecology, 373, 141-151

Cadée GC (2007) Balanuliths: Free-living clusters of the barnacle *Balanus crenatus*. Palaios 22: 680-681.

Van Camp L, Nykjaer L, Mittelstaedt E, Schlittenhardt P (1991) Upwelling and boundary circulation off Northwest Africa as depicted by infrared and visible satellite observations. Progress in Oceanography 26:357–402.

Campodonico S, Macchi G, Lomovasky B, Lasta M (2008) Reproductive cycle of the Patagonian scallop Zygochlamys patagonica in the south-western Atlantic. *Journal of the Marine Biological Association of the UK*, *88*(03), 603-611.

Campos E, Piola A, Matano R, Miller J (2008) PLATA: A synoptic characterization of the southwest Atlantic shelf under influence of the Plata River and Patos Lagoon outflows. Continental Shelf Research 28, 1551–1555.

Campredon P (2000) Entre le Sahara et L'Atlantique – Le parc National du Banc d'Arguin – Mauritanie. FIBA, la Tour du Valat, Arles, France. pp. 124

Carlson AE, Oppo DW, Came RE, LeGrande AN, Keigwin LD, Curry WB (2008) Subtropical Atlantic salinity variability and Atlantic meridional circulation during the last deglaciation. Geology 36, 991.

Carannante G, Esteban M, Milliman JD, Simone L (1988) Carbonate lithofacies as paleolatitude indicators: problems and limitations. Sediment Geol 60:333–346.

Carranza A, Arim M, Scarabino F, Defeo O (2010) Coexistence patterns of benthic gastropods on the Uruguayan shelf. Oikos 119, 1312–1318.

Carranza A, Scarabino F, Brazeiro A, Ortega L, Martínez S (2008) Assemblages of megabenthic gastropods from Uruguayan and northern Argentinean shelf: Spatial structure and environmental controls. Continental Shelf Research 28, 788–796.

Cesero P, Ponte FC (1997) Análise comparativa da paleogeologia dos litorais atlânticos brasileiro e africano. Boletim de Geociências, PETROBRAS, 11(1/2): 1–18.

Chateigner D (2000) Mollusc shell microstructures and crystallographic textures. Journal of Structural Geology 22, 1723–1735.

Chave K (1967) Recent carbonate sediments: an unconventional view. Geol Educ 5:200–204.

Chiessi CM, Ulrich S, Mulitza S, Pätzold J, Wefer G (2007) Signature of the Brazil-Malvinas Confluence (Argentine Basin) in the isotopic composition of planktonic foraminifera from surface sediments. Marine Micropaleontology 64, 52–66.

Chiessi CM, Mulitza S, Paul A, Pätzold J, Groeneveld J, Wefer G (2008) South Atlantic interocean exchange as the trigger for the Bølling warm event. Geology 36, 919.

Clapperton C (1993) Nature of environmental changes in South America at the Last Glacial Maximum. Palaeogeography, Palaeoclimatology, Palaeoecology 101, 189–208.

Cook J, Nuccitelli D, Green SA (2013) Quantifying the consensus on anthropogenic global warming in the scientific literature. Environmental Research Letters 8:7 pp. doi: 10.1088/1748-9326/8/2/024024

Cook PL (1964) Polyzoa from West Africa. Notes on the genera *Hippoporina* Neviani, *Hippoporella* Canu, *Cleidochasma* Harmer and *Hippoporidra* Canu & Bassler (Cheilostomata, Ascophora). Bulletin of the British Museum (Natural History) (Zoology Series) 12:1-35

Cook PL (1968a) Bryozoa (Polyzoa) from the coasts of tropical West Africa. Atlantide Report 10:115-262

Cook PL (1968b) Polyzoa from West Africa. The Malacostega - Part 1. Bulletin of The British Museum (Natural History). Zoology 16:115-160

Cruzjr F, Burns S, Jercinovic M, Karmann I, Sharp W, Vuille M (2007) Evidence of rainfall variations in Southern Brazil from trace element ratios (Mg/Ca and Sr/Ca) in a Late Pleistocene stalagmite. Geochimica et Cosmochimica Acta 71, 2250–2263.

Cuffey RJ and Johnson ME (1997) Bryozoan nodules built around andesite clasts from upper Pliocene of Baja California: palaeoecological implications and closure of the Panama Isthmus. In Johnson ME and Ledesma-Vázques J (eds.): Pliocene Carbonates and related Facies Flanking the Gulf of California, Baja California, Mexico. Geological Society of America. Special Paper 318:111-117

Curry WB, Oppo DW (2005) Glacial water mass geometry and the distribution of delta C-13 of Sigma CO2 in the western Atlantic Ocean. PALEOCEANOGRAPHY 20, PA1017.

Davison I (2005) Central Atlantic Margin Basins of North West Africa: Geology and hydrocarbon potential (Morocco to Guinea). Journal of African Earth Sciences 43, 254-274.

Dedah SO (1993) Wind, surface water temperature, surface salinity and pollution in the area of the Banc d'Arguin, Mauritania. Hydrobiologia 258:9–19.

De Mello e Sousa SH, Passos RF, Fukumoto M, Almeida da Silveira IC, Lopes Figueira RC, Koutsoukos EAM, De Mahiques MM, Rezende CE (2006) Mid-lower bathyal benthic foraminifera of the Campos Basin, Southeastern Brazilian margin: Biotopes and controlling ecological factors, Marine Micropaleontology, 61/1–3:40-57, doi:10.1016/j.marmicro.2006.05.003.

Del Rio CJ (1997) Cenozoic Biogeographic History of the Eurythermal Genus Retrotapes, New Genus (Subfamily Tapetinae) from Southern South America and Antarctica. The Nautilus 110, 77–93.

Depetris PJ and Pasquini AI (2007) The Middle Paraná River: Limnology of a Subtropical Wetland ed M H Iriondo et al. (Berlin, Springer-Verlag) p 143

Depetris PJ, Griffin JJ (1968) Suspended Load in the Rio De La Plata Drainage Basin. Sedimentology 11, 53–60.

Depetris PJ (1973) Hydrochemistry of the Para& River. Limnol. Oceanogr. 21, 736–739.
Dettman D, Goodwin D, Flessa K, Schöne B (2001) Cross-Calibration of Daily Growth Increments , Stable Isotope Variation , and Temperature in the Gulf of California Bivalve Mollusk Chione cortezi : Implications for Paleoenvironmental Analysis. Palaios 16, 387–398.
Dettman DL (1999) Controls on the stable isotope composition of seasonal growth bands in aragonitic fresh-water bivalves (unionidae). Geochimica et Cosmochimica Acta 63, 1049–1057.
Dettman DL, Lohmann KC (1994) Microsampling Carbonates for stable Isotope and minor Element Analysis.pdf. Research Methods Papers 566–569.
Dextraze BL, Zinsmeister WJ (1987) A study of the internal annual growth lines of the late Eocene mollusk Eurhomalea Antarctica. Antarctic Journal of the United States 22, 14–15.
Diop MS (1988) Biologie et Dynamique des populations de praires (Venus rosalina) a l'ouest du Banc d'Arguin Mauritanie.
Douglas AE (1994) Symbiotic Interactions. New York: Oxford University Press on Demand
Douglas AE (2010) The symbiotic habit, New Jersey: Princeton University Press, pp. 5–12, ISBN 978-0-691-11341-8
Domain F (1985) Carte Sédimentologigue du plateu continental Mauretanien 1:200.000. Nouadhibou
Doney SC, Ruckelshaus MJ, Duffy E, et al. (2012) Climate Change Impacts on Marine Ecosystems. Annual Review of Marine Science 4:11–37. doi: doi:10.1146/annurev-marine-041911-111611
Duineveld GCA, Lavaleye MSS, Noort GJ Van (1993) The trawlfauna of the Mauritanian shelf (Northwest Africa): density, species composition, and biomass. Hydrobiologia 258:165–173.
Edinger EN Copper P, Risk MJ, Atmojo W (2002) Oceanography and reefs of recent and Paleozoic tropical epeiric seas. Facies 47: 127–149.
Ehrenberg K (1931) Über Lebensspuren von Einsiedlerkrebsen. Palaebiologica, 4, 137-174
Eisele M, Frank N, Wienberg C, Titschack J, Mienis F, Beuck L, Tisnerat-Laborde N, Hebbeln, D (2013) From sediment baffling to mass wasting – Sedimentation patterns on a cold-water coral mound in the Banda Mound Province, Mauritania, submitted to Deep Sea Research II
Elliot M, DeMenocal PB, Linsley BK and Howe SS (2003) Environmental controls on the stable isotopic composition of Mercenaria mercenaria: Potential application to paleoenvironmental studies, Geochem. Geophys. Geosyst., 4(7), 1056, doi:10.1029/2002GC000425, 2003.
Emilsson I (1961) The shelf and coastal waters off southern Brazil. Boletim do Instituto Oceanográfico da Universidade de São Paulo 11, 102–112.
Epstein (1951) Carbonate-Water Isotopic Temperature Scale. *Geological Society of America*, 62, 417-426.
Fairbanks RG, Matthews RK (1978) The Marine Oxygen Isotope Record in Pleistocene Coral, Barbados, West Indies. Quaternary Research 10, 181–196.
Falabella V, Campagna C, Croxall J (2009) Atlas del Mar Patagónico. Especies y Espacios. Wildlife Conservation Society y BirdLife International. http://www.atlas-marpatagonico.org
Fedoseev A (1970) Geostrophic circulation of surface waters on the shelf of north-west Africa. Rapp. P.-V. Reun. Cons. Int. Explor. Mer., 159, 32-37.
Floeter SR, Soares-Gomes A (1999) Biogeographic and Species Richness Patterns of Gastropoda on the Southwestern Atlantic. Revista Brasileira De Biologia 59, 567–575.
Flor FD (1970) Biometrische Untersuchungen zur Autökologie ober-kretazischer Bryozoen. Dissertation, Fachbereich für Geowissenschaften, Universität Hamburg
Flügel E (2004) Microfacies of carbonate rocks: analysis, interpretation and application. Springer Berlin Heidelberg
Fourqurean JW, Duarte CM, Kennedy H (2012) Seagrass ecosystems as a globally significant carbon stock. Nature Geoscience 5:505–509. doi: 10.1038/ngeo1477
Freiwald A, Fosså JH, Grehan A, Koslow T, Roberts JM (2004) Cold-water Coral Reefs. UNEP-WCMC, Cambridge, UK.
Fütterer DK (1980) Sedimentation am NW-afrikanischen Kontinentalrand: Quantitative Zusammensetzung und Verteilung der Siltfraktion in den Oberflächensedimenten. 'Meteor' Forsch.ergeb. C (33), 15–60.
Fütterer DK (1983) The modern upwelling record off Northwest Africa. In Thiede, J. & Suess, E. (Eds.), Coastal upwelling: its sediment record, Part B. Sedimentary records of ancient coastal upwelling, 105-121. Plenum Press, London.
Gallardo MH, Mena C, Lomovasky B, Morriconi E, Clasing E (2003) Allozymic variation in the clam genus Eurhomalea (Bivalvia : Veneriidae) along southern South American coast. Methods 76, 501–507.
Gan MA, Kousky VE, Ropelewski CF (2004) The South America Monsoon Circulation and Its Relationship to Rainfall over West-Central Brazil. Journal of Climate 17, 47–66.

Gaines RR, and Droser ML (2009) "Animal proxies - Invertebrates". In Gornitz V Encyclopedia of paleoclimatology and ancient environments. M.L. Springer. p. 11. ISBN 1-4020-4551-4. Retrieved 15 November 2009.
Garzoli SL, Giulivi C (1994) What forces the variability of the southwestern Atlantic boundary currents ? Deep Sea Research Part I: Oceanographic Research Papers 41, 1527–1550.
Gattuso JP, Hansson L (2011) Ocean Acidification. Oxford University Press
Giberto DA, Bremec CS, Acha EM, Mianzan H (2004) Large-scale spatial patterns of benthic assemblages in the SW Atlantic: the Rio de la Plata estuary and adjacent shelf waters. Estuarine, Coastal and Shelf Science 61, 1–13.
Gillikin, DP (2005) Geochemistry of Marine Bivalve Shells: the potential for paleoenvironmental reconstruction, PhD Thesis. Faculty of Science. Vrije Universiteit Brussel
Gillikin, DP (2005) Strong biological controls on Sr/Ca ratios in aragonitic marine bivalve shells. Geochemistry Geophysics Geosystems 6.
Gilman EL, Ellison J, Duke NC, Field C (2008) Threats to mangroves from climate change and adaptation options: A review. Aquatic Botany 89:237–250. doi: 10.1016/j.aquabot.2007.12.009
Ginsburg RN and James NP (1974) Holocene carbonate sediments of continental shelves, in Burke CA and Drake CL, (eds.): The geology of continental margins. Springer-Verlag, Berlin. p. 137-155
Glynn PW (1974) Rolling stones among the Scleractinia: mobile coralliths in the Gulf of Panama.Proceedings of the 2nd International Coral Reef Synopsium 2:183-198
Gobac ZZ, Posilovic H, Bermanec V (2009) Identification of biogenic Calcite and Aragonite using SEM. Geologia Croatica 9611, 201–206.
Goodwin DH., Flessa KW, Schöne BR and Dettman DL (2001) Cross-calibration of daily growth increments, stable isotope variation, and temperature in the Gulf of California bivalve mollusk Chione cortezi: implications for environmental analysis. Palaios. 16, 387–398.
Gordillo S, et al. (2014) *Mollusk shells as bio-geo-archives: Evaluating environmental changes during the Quaternary*. SpringerBriefs in Earth System Sciences, ISBN: 978-3-319-03475-1 (Print) 978-3-319-03476-8 (Online).
Gordillo S (1999) Holocene molluscan assemblages in the Magellan region *. Holocene 63, 15–22.
Gordillo S (2006) Pleistocene Retrotapes de Rió, 1997 (Veneridae, Bivalvia) from Tierra del Fuego, Argentinia. Ameghiniana 43.
Gordillo S, Brey T, Beyer K, Lomovasky B (2013) Retrotapes exalbidus from southern SouthAmerica: are fossil shells reliable proxy archives for Holocene climate, in: 3rd International Sclerochronology Conference. Caernarfon, Wales, UK.
Gordillo S, Rabassa J, Coronato A (2008) Paleoecology and paleobiogeographic patterns of mid-Holocene mollusks from the Beagle Channel (southern Tierra del Fuego, Argentina). Revista Geolólogia de Chile 35, 321–333.
Gordon, DP (1972) Biological relationships of an intertidal bryozoan population. Journal of Natural History, 6, 503-514
Gosling E (2003) Bivalve Molluscs: Biology, Ecology and Culture, Blackwell Publishing Ltd, Oxford, UK. doi: 10.1002/9780470995532
Goudswaard PC, Smaal AC, Wagué A (2007) The ecological implications of exploitation of the bivalve Venus rosalina in Mauritanian waters. 132.
Greene RW (1974) in Symbiosis in the Sea, ed. Vernberg, W. B. (Univ. of South Carolina Press, Columbia), pp. 21-27.
Grischenko AV, Taylor PD, Mawatari SF (2002) A New Cheilostome Bryozoan with Gigantic Zooids from the North-West Pacific. Zoological Science 19:1279–1289.
Grossman E, Ku T-L (1986) Oxygen and carbon isotope fractionation in biogenic aragonite: Temperature effects. Chemical Geology 59, 59–74.
Guilderson TP, Burckle L (2000) Late Pleistocene sea level variations derived from the Argentine Shelf. Geochemistry, Geophysics, Geosystems. 1:2000GC00098.
Guilderson TP, Pak DK (2005) Reconstructing Past Ocean Salinity ((delta)18Owater). Encyclopedia of Quaternary Science. URL-BOOK-217238
Gutiérrez F, Guerrero J, Lucha P (2008) A genetic classification of sinkholes illustrate fromevaporite paleokarst exposures in Spain. Environmental Geology 53, 993–1006.
Gyllencreutz R, Mahiques MM, Alves DVP, Wainer IKC (2010) Mid- to late-Holocene paleoceanographic changes on the southeastern Brazilian shelf based on grain size records. Holocene 20 (6), 863–875
Gyory J, Mariano AJ, Ryan EH (2013) "The Canary Current." Ocean Surface Currents. (http://oceancurrents.rsmas.miami.edu/atlantic/canary.html)
Haddock S (2010) A plea for meaningful colors in odv. Limnology and Oceanography 19, 2010.

Hagen E (2001) Northwest African upwelling scenario. Oceanologica Acta 24:113–128.
Halfar J, Godinez-Orta L, Mutti M, et al. (2004) Nutrient and temperature controls on modern carbonate production: An example from the Gulf of California, Mexico. Geology 32:213. doi: 10.1130/G20298.1
Hallock P (2005) Global change and modern coral reefs: New opportunities to understand shallow-water carbonate depositional processes. Sedimentary Geology 175:19–33. doi: 10.1016/j.sedgeo.2004.12.027
Hallock P (1988) The role of nutrient availability in bioerosion: consequences to carbonate buildups. Palaeogeogr Palaeoclimatol Palaeoecol 63:
Hallock P (1981) Production of carbonate sediments by selected large benthic foraminifera on two Pacific coral reefs. J Sediment Petrol 51:467–474
Hallock P, Schlager W (1986) Nutrient excess and the demise of coral reefs and carbonate platforms. Palaios 1:389–398.
Hallam A (1994) An outline of Phanerozoic biogeography, Oxford Biogeography Series, 10.
Hanebuth TJJ, Henrich R (2009) Recurrent decadal-scale dust events over Holocene western Africa and their control on canyon turbidite activity (Mauritania). Quaternary Science Reviews 28:261-270
Hanebuth TJJ, Lantzsch H (2008) A Late Quaternary sedimentary shelf system under hyperarid conditions: Unravelling climatic, oceanographic and sea-level controls (Golfe d'Arguin, Mauritania, NW Africa). Marine Geology 256:77-89
Hanebuth TJJ, Mersmeyer H, Kudrass HR, Westphal H (2013) Aeolian to shallow-marine shelf architecture off a major desert since the Late Pleistocene (Northern Mauritania). Geomorphology 213, 132–147.
Hayton S, Nelson C, Hood S (1995) A skeletal assemblage classification system for non-tropical carbonate deposits based on New Zealand Cenozoic limestones. Sedimentary Geology
Hayward PJ and Ryland JS (1979) Bristish ascophoran bryozoans. Synopses of the British Fauna (New Series), 14, 1-312
Hoegh-Guldberg O, Mumby PJ, Hooten a J, et al. (2007) Coral reefs under rapid climate change and ocean acidification. Science (New York, NY) 318:1737–42. doi: 10.1126/science.1152509
Hoffmann L (1988) The Banc d'Arguin: nature in harmony with man. WWF News, June/July: 10-11
Holz C, Stuut JW, Henrich R (2004) Terrigenous sedimentation processes along the continental margin off NW Africa: implications from grain-size analysis of seabed sediments. Sedimentology 51, 1145–1154.
Honkoop PJC, Berghuis EM, Holthuijsen S, et al. (2008) Molluscan assemblages of seagrass-covered and bare intertidal flats on the Banc d'Arguin, Mauritania, in relation to characteristics of sediment and organic matter. Journal of Sea Research 60:255–263. doi: 10.1016/j.seares.2008.07.005
Huber M (2010) Compendium of Bivalves, 901 p. ConchBooks, Hackenheim.
Hudson JD, Anderson TF (1989) Ocean temperatures and isotopic compositions through time. Trans R Soc Edinb, 80, 183–192.
IMROP (2013) Atlas maritime des zones vulnérables en Mauritanie - Un appui à la gestion écosystémique et équitable. IMROP, Nouhadibou, Mauritania, 152 pp.
IPCC board members (2013) IPCC 2013: Climate change 2013: The physical science basis. Intergovernmental Panel on Climate Change, Working Group I Contribution to the IPCC Fifth Assessment Report (AR5)(Cambridge Univ Press, New York) (2013).
IPCC board members (2007) IPCC, 2007: Climate change 2007: the physical science basis. Contribution of Working Group I to the fourth assessment report of the Intergovernmental Panel on Climate Change (2007).
Iriondo MH, Paggi JC, Parma MJ (2007) The Middle Parana River: Limnology of a Subtropical Wetland. , XII, 382 p. 128 illus. Springer Verlag.
Ivany LC., Runnegar B (2010) Early Permian seasonality from bivalve 18O and implications for the oxygen isotopic composition of seawater. Geology 38, 1027–1030.
James DW, Foster MS and O'Sullivan J (2006) Bryoliths (Bryozoa) in the Gulf of California. Pacific Science 60:117-124
James NP (1997) The cool-water carbonate depositional realm, in James NP and Clarke JAD (eds.). Cool-Water Carbonates. SEPM Special Publication 56 pp. 1–20
Johnson NM, Officer CB, Opdyke ND, Woodard GD, Zeitler PK & Lindsay EH (1983) Rates of late Cenozoic tectonism in the Vallecito-Fish Creek Basin, western Imperial Valley, California. Geology 11, 664-667
Jones DS (1980) Annual cycle of shell growth increment formation in two continental shelf bivalves and its paleoecologic significance. Paleobiology 6, 331–340.
Jones DS, Quitmyer IR (1996) Marking time with bivalve shells.pdf. Palaios 11, 340–346.
Kaiser P (1977) Beiträge zur Kenntnis der Voluten (Mollusca) in argentinisch-brasilianischen Gewässern (mit der Beschreibung zweier neuer Arten). Mittel Hamburg Zool Mus Inst 74.
Kaltenegger W, Preisinger A, Rögl F (1971) Paläotemperaturbestimmungen an aragonitischen Mollusken aus dem aplinen Mesozoikum. Palaeogeogr. Palaeoclimatol. Palaeoecol. 10, 273–285.Kanazawa T, Sato S

(2007) Environmental and physiological controls on shell microgrowth pattern of Ruditapes philippinarum (Bivalvia: Veneridae) from Japan. J. Molluscan Stud. 74, 89–95.
Kendall CGSC, Schlager W (1981) Carbonates and relative changes in sea level. Mar. Geol. 44, 181–212. doi:10.1016/0025-3227(81)90118-3
Karleskint G, Turner RL, and Small, JW (2009) Introduction to Marine Biology. Brooks/Cole. ISBN: 0495561975
Kellog CW (1976) Gastropods shells: a potential limiting resource for hermit crabs. J. Exp. Mar. Biol. Ecol., 22:101-111
Kirkpatrick R and Metzelaar J (1922) On an instance of commensalism between hermit crabs and a polyzoon. Proceedings of the Zoological Society of London 1922:983-990.
Kidwell SM and Gyllenhaal ED (1998) Symbiosis, competition, and physical disturbance in the growth histories of Pliocene cheilostome bryoliths. Lethaia vol. 31:221-239
Kim S-T, Mucci A, Taylor BE (2007) Phosphoric acid fractionation factors for calcite and aragonite between 25 and 75 [degree sign]C: Revisited. Chemical Geology 246, 135–146.
Kindler P, Wilson M (2010) Carbonate grain associations: their use and environmental significance, a brief review. Carbonate Syst. Dur. 42, 35–48.
Kissling DL (1973) Circumrotatory growth form in Recent and Silurian corals. In Boardman RS, Cheetham AH & Oliver WA (eds.): Animal Colonies 43-58. Dowden, Hutchinson & Ross, Stroudsburg
Kleypas JA, Feely RA, Fabry VJ, Langdon C, Sabine CL, Robbins LL (2006) Impacts of Ocean Acidification on Coral Reefs and Other Marine Calcifiers: A Guide for Future Research, report of a workshop held 18–20 April 2005, St. Petersburg, FL, sponsored by NSF, NOAA, and the U.S. Geological Survey, 88 pp.
Klicpera A, Michel J, Westphal H. (2015) Facies patterns of a tropical heterozoan carbonate platform under eutrophic conditions: the Banc d'Arguin, Mauritania. Facies 61:421 Doi:10.1007/s10347-014-0421-5
Klicpera A, Taylor PD, Westphal H (2014) Bryozoans on the move: Adaptations to hard substrate–limiting tropical heterozoan carbonates (Banc d'Arguin, Mauritania) Marine Biodiversity (Oct. 2014, online first) Doi:10.1007/s12526-014-0279-3
Klicpera A, Taylor PD, Westphal H (2013) Bryoliths constructed by bryozoans in symbiotic associations with hermit crabs in a tropical heterozoan carbonate system, Golfe d'Arguin, Mauritania. Marine Biodiversity 43:429–444, DOI 10.1007/s12526-013-0173-4
Kloff S, Trebaol L, Lacroix E (2007) Pêche aux bivalves & environnement Panorama mondial - études de cas - application à l'exploitation des praires en Mauritanie. Fondation Internationale du Banc d'Arguin, FIBA, La tour du Valat, Arles, France, 191 pp.
Kobayashi I, Samata T (2006) Bivalve shell structure and organic matrix. Mater. Sci. Eng. C 26, 692–698. doi:10.1016/j.msec.2005.09.101Krantz DE, Williams DF, Jones DS (1987) Ecological and paleoenvironmental information using stable isotope profiles from living and fossil molluscs. Palaeogeography, Palaeoclimatology, Palaeoecology 58, 249–266.
Koopmann B, Lees A, Piessens P, and Sarnthein M (1979) Skeletal carbonate sands and wind-derived silty-marls off the Saharan coast: Baie du Lévrier, Arguin Platform, Mauritania: Meteor Forschungsergebnisse, Reihe C 30:15–57
Kuipers BR, Witte HJ, Gonzalez SR (1993) Zooplankton distribution in the coastal upwelling system along the Banc d'Arguin, Mauritania. Hydrobiologia 258:133–149.
Krantz DE, Williams DF, Jones DS (1987) Ecological and paleoenvironmental information using stable isotope profiles from living and fossil molluscs. Palaeogeography, Palaeoclimatology, Palaeoecology 58, 249–266.
Krastel S, Wefer G and cruise participants (2012) Report and preliminary results of RV METEOR Cruise M78/3. Sediment transport off Uruguay and Argentina: From the shelf to the deep sea. 19.05.2009 – 06.07.2009, Montevideo (Uruguay) – Montevideo (Uruguay).
Lagaaij R (1952) The Pliocene Bryozoa of the Low Countries and their bearing on the Marine Stratigraphy of the North Sea Region. Proefschrift Robert Lagaaij, Ernest van Aelst
Lagaaij R (1963) New additions to the bryozoan fauna of the Gulf of Mexico. Publications of the Institute of Marine Science, Texas, 9, 162-236
Lambeck K, Chappell J (2001) Sea level change through the last glacial cycle. Science (New York, N.Y.) 292, 679–86.
Lantzsch H, Hanebuth TJJ, Chiessi CM, Schwenk T, Violante R (2014) The high-supply, current-dominated continental margin of southeastern South America during the late Quaternary. Quat. Res. doi:10.1016/j.yqres.2014.01.003
Lees A and Buller AT (1972) Modern temperate water and warm-water shelf carbonate sediments contrasted: Marine Geology 13:67–73
Leduc G, Schneider R, Kim JH, Lohmann G (2010) Holocene and Eemian sea surface temperature trends as revealed by alkenone and Mg/Ca paleothermometry. Quaternary Science Reviews 29, 989–1004.

LeGrande AN, Schmidt GA (2006) Global gridded data set of the oxygen isotopic composition in seawater. Geophys. Res. Lett. 33, 1–5. doi:10.1029/2006GL026011
Leinfelder RR, Nose, M (1999) Increasing complexity - decreasing flexibility. A different perspective of reef evolution through time. Profil 17:135-147
Leitmeier H, Feigl F (1934) Eine einfache Reaktion zur Unterscheidung von Calcit und Aragonit. Zeitschrift für Krist. Mineral. und Petrogr. 45, 447–456. doi:10.1007/BF02943377
Locarnini RA, Mishonov AV, Antonov JI, Boyer TP, Garcia HE, Baranova OK, Zweng MM, Johnson DR (2010) World Ocean Atlas 2009, Volume 1: Temperature.
Lomovasky BJ (2002) Growth and production of the venerid bivalve Eurhomalea exalbida in the Beagle Channel, Tierra del Fuego. Journal of Sea Research 48, 209–216.
Lomovasky BJ, Morriconi E, Brey T, Calvo J (2002) Individual age and connective tissue lipofuscin in the hard clam Eurhomalea exalbida. Journal of Experimental Marine Biology and Ecology 276, 83–94.
López Correa M, Montagna P, Vendrell-Simón B, McCulloch M, Taviani M (2010) Stable isotopes (δ18O and δ13C), trace and minor element compositions of Recent scleractinians and Last Glacial bivalves at the Santa Maria di Leuca deep-water coral province, Ionian Sea. Deep Sea Res. Part II Top. Stud. Oceanogr. 57, 471–486.
Marañón E, Holligan PM (1999) Photosynthetic parameters of phytoplankton from 50 " N to 50 " S in the Atlantic Ocean. Marine Ecology Progress Series 176
Martínez, S., Rojas, A., 2013. Relative sea level during the Holocene in Uruguay. Palaeogeography, Palaeoclimatology, Palaeoecology 374, 123–131.
Martins LR, Martins IR, Urien CM (2003) Aspectos sedimentares da plataforma continental na a´rea de Influe ˆncia do Rio de La Plata. Gravel 1, 68–80.
Martinez P, Bertrand P, Shimmield GB, et al. (1999) Upwelling intensity and ocean productivity changes off Cape Blanc (northwest Africa) during the last 70,000 years: geochemical and micropalaeontological evidence. Marine Geology 158:57–74.
Matsuzaki kmR., Eynaud F, Malaizé B, Grousset FE, Tisserand A, Rossignol L, Charlier K, Jullien E (2011) Paleoceanography of the Mauritanian margin during the last two climatic cycles: From planktonic foraminifera to African climate dynamics. Mar. Micropaleontol. 79, 67–79.
McKinney FK, Jackson JBC (1991) Bryozoan Evolution. University of Chicago Press edition 1991
McLaughlin P (2012) *Pseudopagurus granulimanus* (Miers, 1881). In: Lemaitre R, McLaughlin P, (2012). World Paguroidea & Lomisoidea database. Accessed through: World Register of Marine Species at http://www.marinespecies.org/
Maier E, Titschack J (2010) Spondylus gaederopus: A new Mediterranean climate archive — Based on high-resolution oxygen and carbon isotope analyses. Palaeogeography, Palaeoclimatology, Palaeoecology 291, 228–238.
Maranon E and Holligan PM (1999) Photosynthetic parameters of phytoplankton from 50 °N to 50 °S in the Atlantic Ocean. Mar Ecol Prog Ser 176:191–203
Matano RP, Palma ED, Piola AR (2010) The influence of the Brazil and Malvinas Currents on the Southwestern Atlantic Shelf circulation. Ocean Science 6, 983–995.
Marchitto TA, Jones GA, Goodfriend GA, Weidmann CR (2000) Precise temporal correlation of Holocene mollusk shells using sclerochronology. Quat. Res. 53, 236–246.
Martínez, S., Rojas, A., 2013. Relative sea level during the Holocene in Uruguay. Palaeogeography, Palaeoclimatology, Palaeoecology 374, 123–131.
Menon N (1972) Heat tolerance, growth and regeneration in three North Sea bryozoans exposed to different constant temperatures. Mar. Biol. 15, 1–11.
Michel J, Westphal H, and Hanebuth TJJ (2009) Sediment partitioning and winnowing in a mixed eolian–marine system (Mauritanian shelf). Geo-Marine Letters 29:221–232
Michel J, Mateu-Vicens G, Westphal H (2011a) Modern heterozoan carbonates from a eutrophic tropical shelf (Mauritania). Journal of Sedimentary Research 8:641-655
Michel J, Westphal H, Von Cosel (2011b) The Mollusk Fauna of Soft Sediments from the tropical, upwelling-influenced shelf of Mauritania (Northwestern Africa). Palaios 26(7):447-460
Milliman, JD (1974). Marine carbonates. Berlin; Heidelberg; New York: Springer, 375 p.
Mittelstaedt E (1991) The ocean boundary along the northwest African coast: Circulation and oceanographic properties at the sea surface. Prog Oceanogr 26:307–355. doi: doi:10.1016/0079-6611(91)90011-A.
Moen FE, Svensen E (2004) Marine fish & invertebrates of Northern Europe. AquaPress. ISBN: 0-9544060-2-8
Moran NA (2006) Symbiosis. Current Biology Volume 16, Issue 20, 24:866-871
Moller OO, Castaing P, Salomon J-C, Lazure P (2001) The Influence of Local and Non-Local Forcing Effects on the Subtidal Circulation of Patos Lagoon. Estuaries 24, 297.

Morriconi E, Lomovasky BJ, Calvo J, Brey T (2002) The reproductive cycle of Eurhomalea exalbida (Chemnitz, 1795) (Bivalvia: Veneridae) in Ushuaia Bay, Beagle Channel (Argentina). Invertebrate Reproduction and Devel- opment 42, 61–68.
Morris PA, Soule DF, Soule, JD (1989) Bryozoans, Hermit Crabs, and Gastropods: Life strategies can affect the fossil record. Bull. Southern California Acad. Sci. 88(2):45-60.
Morris PJ, Rosenberg G (2005) Search interface and documentation for Malacolog, an online database of Western Atlantic marine Mollusks. http://www.malacolog.org
Mulitza S, Heslop D, Pittauerova D, et al. (2010) Increase in African dust flux at the onset of commercial agriculture in the Sahel region. Nature 466:226–8. doi: 10.1038/nature09213
Müller G, Gastner M (1971) The "Karbonate-Bombe", a simple device for the determination of the carbonate content in sediments, soils and other materials. N Jb Miner Mh 10:446–469.
Mutti M, Hallock P (2003) Carbonate systems along nutrient and temperature gradients: some sedimentological and geochemical constraints. International Journal of Earth Sciences 92:465–475. doi: 10.1007/s00531-003-0350-y
Myers N, Mittermeier R a, Mittermeier CG, et al. (2000) Biodiversity hotspots for conservation priorities. Nature 403:853–8. doi: 10.1038/35002501
Nakashima R (2002) Geographic distribution of the late Cenozoic bivalve Fortipecten in the northwestern Pacific. Palaeogeogr, Palaeoclimatol, Palaeoecol, 186, 261–274.
Negre C, Zahn R, Thomas AL, Masqué P, Henderson GM, Martínez-Méndez G, Hall IR, Mas JL (2010) Reversed flow of Atlantic deep water during the Last Glacial Maximum. Nature 468, 84–8.
Nelson CS, Keane SL, Head PS (1988a) Non-tropical carbonate deposits on the modern New Zealand shelf. Sedimentary Geology 60:71-94
Nelson CS, Hyden FM, Keane SL, Leask WL and Gordon DP (1988b) Application of bryozoan zoarial growth-form studies in facies analysis of non-tropical carbonate deposits in New Zealand. Sedimentary Geology 60(1988):301-322
Nothdurft LD, Webb GE (2008) Earliest diagenesis in scleractinian coral skeletons: implications for palaeoclimate-sensitive geochemical archives. Facies 55, 161–201.
Nutter AH, Summerhayes CP, Tooms JS (1971) Geological structure and development of the continental margin of northwest Africa. Mar. Geol. 11, 1–25.
Nützel A, Joachimski M, López Correa M (2010) Seasonal climatic fluctuations in the Late Triassic tropics—High-resolution oxygen isotope records from aragonitic bivalve shells (Cassian Formation, Northern Italy). Palaeogeography, Palaeoclimatology, Palaeoecology 285, 194–204.
O'Dea A, Jackson J (2008) Modes of reproduction in recent and fossil cupuladriid bryozoans. Palaeontology 51, 847–864.
O'Dea A (2009) Relation of form to life habit in free-living cupuladriid bryozoans. Aquat. Biol. 7, 1–18.
O'Dea A, Jackson J (2009) Environmental change drove macroevolution in cupuladriid bryozoans. Proc. Biol. Sci. 276, 3629–34.
Olivier SR, Scarabino V (1972) Distribución ecológica de algunos moluscos recogidos por la expedición del "Walther Herwig" (R.F.A.) al Atlántico sudoccidental (1966). Rev Bras Biol 32, 235–247.
Ortega L, Martínez A (2007) Multiannual and Seasonal Variability of Water Masses and Fronts Over the Uruguayan Shelf. J. Coast. Res. 233, 618–629.
Ould Mahfoudh M, Dobrovine B, Ould Dedah S (1991) Hydrologique des eaux superficilles du Banc d'Arguin, Département Ressources et Environment et Laboratoire d'Hydrologie et Environment, Centre National de Recherches Oceanographiques et des Peches; http://hdl.handle.net/1834/518
Palma ED, Matano RP, Piola AR (2008) A numerical study of the Southwestern Atlantic Shelf circulation: Stratified ocean response to local and offshore forcing. J. Geophys. Res. 113, 1–22.
Palmer TJ and Hancock CD (1973) Symbiotic relationships between ectoprocts and gastropods, and between ectoprocts and hermit crabs in the French Jurassic. Palaeontology 16:563-566
Pannella G, MacClintock C (1968) Paleontological Society Biological and Environmental Rhythms Reflected in Molluscan Shell Growth. Memoir (The Paleontological Society) 2, 64–80.
Pastor M, Pelegri J, Hernandezguerra A, et al. (2008) Water and nutrient fluxes off Northwest Africa. Continental Shelf Research 28:915–936. doi: 10.1016/j.csr.2008.01.011
Penchaszadeh PE, Pastorino G, Brogger MI (2008) Atlas de sensibilidad ambiental del mar y de la costa, www.atlas.ambiente.gov.ar.
Parrish JT (1998) Interpreting Pre-Quaternary Climate from the Geologic Record. New York: Columbia University Press.
Perry C, Taylor K (2009) Environmental sedimentology. Wiley
Peters H (1976) The spreading of the water masses of the Banc d'Arguin in the upwelling area off the northern Mauritanian coast. Meteor Forsch Ergeb 18:78–100.

Peterson RG, Stramma L, Kortum G (1996) Early concepts and charts of ocean circulation. Progress in Oceanography, 37, 1-115.
Petschick R (1996) "Mac Diff version 3." Online: http://www. servermac. geologie. uni-frankfurt. de.
Piessens P (1979) Influence relative des sources de production et du transport dans la formation de facies calcaires biogéniques: les sédiments quaternaires de la plate-forme d'Arguin (Mauritanie) et comparaison avec des régions cotières européennes (Irlande et Hébrides). Dissertation, Université Catholique de Louvain
Piessens P, Chabot AG (1977) Bathymetry and Sediments of the Arguin Platform, Mauritania, West Africa. Mém. Inst. géol. Univ. Louvain, t. 29, pp. 369-379.
Piola AR, Campos EJD, Möller OO, Charo M, Martinez C (2000) Subtropical Shelf Front off eastern South America. Journal of Geophysical Research 105, 6565–6578.
Piola AR, Matano RP (2001) Brazil and Falklands (Malvinas) Currents. Encyclopedia of Ocean Sciences 1, 340–349.
Piola AR, Matano RP, Palma ED, Ller OOM, Campos EJD (2005) The influence of the Plata River discharge on the western South Atlantic shelf, Geophys. Geophysical Research Letters 32.
Piola AR, Romero SI, Zajaczkovski U (2008) Space-time variability of the Plata plume inferred from ocean color. Continental Shelf Research thisissued, 101016/jcsr200702013.
Pomar L (2001) Types of carbonate platforms: a genetic approach. Basin Research 13:313–334. doi: 10.1046/j.0950-091x.2001.00152.x
Pomar L, Brandano M, Westphal H (2004) Environmental factors influencing skeletal grain sediment associations: a critical review of Miocene examples from the western Mediterranean. Sedimentology 51:627–651. doi: 10.1111/j.1365-3091.2004.00640.x
Pomar L, Ward W (1995) Sea-level changes, carbonate production and platform architecture: the Llucmajor platform, Mallorca, Spain. Sequence stratigraphy and depositional response to eustatic, tectonic and climatic forcing. Academic Press, Dordrecht, p 87
Pomar L, Ward W (1999) Reservoir-scale heterogeneity in depositional packages and diagenetic patterns on a reef-rimmed platform, upper Spain Miocene, Mallorca. Bull AAPG 83:1759– 1773.
Preisendorfer RW (1986) Secchi disk science: Visual optics of natural waters. Limnol Oceanogr 31:909–26.
Provost C, Garcia O, Garcon V (1992) Analysis of Satellite Sea Surface Temperature Time Series in the Brazil-Malvinas Current Confluence Region: Dominance of the Annual and Semiannual Periods. Journal of Geophysical Research 97, 17,841–17,858.
Quack B, Peeken I, Petrick G, Nachtigall K (2007) Oceanic distribution and sources of bromoform and dibromomethane in the Mauritanian upwelling. Journal of Geophysical …
Reijmer JJG, Bauch T, Schäfer P (2012) Carbonate facies patterns in surface sediments of upwelling and non-upwelling shelf environments (Panama, East Pacific). Sedimentology 59:32–56. doi: 10.1111/j.1365-3091.2010.01214.x
Reguant S, Fernandez J, Rodriguez-Fernandez J, and Serra-Kiel J (1991) Bryozoan biofacies, zoarial forms and sedimentary environments in the Tertiary of Spain. In Bigey FP (ed.): Bryozoaires actuels et fossiles 361-370. Bulletin de la Société Sciences Naturelle d'Ouest France, Memoires, H.S. 1
Reymond CE, Mateu-Vicens G, Westphal H (2014) Foraminiferal assemblages from a transitional tropical upwelling zone in the Golfe d'Arguin, Mauritania. *Estuarine, Coastal and Shelf Science* 148 (2014): 70-84.
Reimer P, Baillie M, Bard E, Bayliss A, Beck J, Blackwell P, Bronk Ramsey C, Buck C, Burr G, Edwards R, Friedrich M, Grootes P, Guilderson T, Hajdas I, Heaton T, Hogg A, Hughen K, Kaiser K, Kromer B, McCormac F, Manning S, Reimer R, Richards D, Southon J, Talamo S, Turney C, van der Plicht J, Weyhenmeyer C (2009) IntCal09 and Marine09 radiocarbon age calibration curves, 0–50, 000 years cal BP. Radiocarbon 51(4), 1111–50.
Ribeiro A (2006) Tectonic history and the biogeography of the freshwater fishes from the coastal drainages of eastern Brazil: an example of faunal evolution associated with a divergent continental margin. Soc. Bras. Ictiol. 4, 225–246.
Rider J and Enrico R (1979) Structural and functional adaptations of mobile anascan ectoproct colonies (ectoproctaliths). In Larwood EP and Abbott MB (eds.): Advances in Bryozoology, 297-320. Academic Press, London
Riegl BM, Lirman, GD (2013) Benthic Gabitat: Coral and hardbottom. In Integrated Conceptual Ecosystem Model Development for the Southeast Florida Coastal Marine Ecosystem, W.K. Nuttle and P.J. Fletcher (eds.). NOAA Technical Memorandum, OAR-AOML-103 and NOS-NCCOS-163. Miami, Florida. 53-62.
Rios EC (1994) Seashells of Brazil. Fundação Cidade do Rio Grande, Rio Grande.

Roff G (2007) Corals on the move: morphological and reproductive strategies of reef flat coralliths. Coral Reefs 27:343-344
Rosell-Melé A, Bard E, Emeis K (2004) Sea surface temperature anomalies in the oceans at the LGM estimated from the alkenone-U37K′ index: comparison with GCMs. Geophysical ResearchLetters 31, 1–4.
Rosenbaum J, Sheppard SMF (1986) An isotopic study of siderites, dolomites and ankerites at high temperatures. Geochimica et Cosmochimica Acta 50, 1147–1150.
Rosenberg G (2009) Malacolog 4.1. 1: a database of Western Atlantic marine Mollusca. *WWW database (version 4.1. 1)] http://www. malacolog. org*.
Roy K, Valentine JW, Jablonski D, and Kidwell SM (1996). Scales of climatic variability and time averaging in Pleistocene biotas: implications for ecology and evolution. Trends Ecol Evol, 11, 458–463.
Ryland JS (1976) Physiology and ecology of marine bryozoans. *In* Advances in Marine Biology, 14:285-443. Academic Press, London
Samankassou E (2002) Cool-water carbonates in a paleoequatorial shallow-water environment: The paradox of the Auernig cyclic sediments (Upper Pennsylvanian, Carnic Alps, Austria-Italy) and its implications. Geology 655–658.
Sanders HL (1968) Marine benthic diversity: a comparative study. Am Nat, 102, 243–282.
Scarabino F (2003) Lista Sistematica de los Bivalvos Marinos Y Estuarios de Uruguay. Comunicaciones de la Sociedad Malacológica del Uruguay 8, 227–258.
Scarabino V (1977) Moluscos del Golfo San Matías. Comun. Soc. Malacol. Uruguay 4 31, 177–263.
Schemainda R, Nehring D, Schulz S (1975) Ozeanologische Unter- suchungen zum Produktionspotential der nordwestafrikanischen Wasserauftriebsregion 1970–1973. Geophys Veröff 88.
Schlitzer R (2012) Ocean Data View (ODV). http://odv.awi.de
Schmidt GA, Bigg GR, Rohling EJ (1999) Gloabl Seawater Oxygen-18 Database v1.21. http://data.giss.nasa.gov/o18data/
Schneider CA, Rasband WS, Eliceiri KW (2012) NIH Image to ImageJ: 25 years of image analysis. *Nat Methods* 9 (7): 671–675. doi:10.1038/nmeth.2089
Schöne BR, Dunca E, Fiebig J, Pfeiffer M (2005a) Mutvei's solution: An ideal agent for resolving microgrowth structures of biogenic carbonates. Palaeogeography, Palaeoclimatology, Palaeoecology 228, 149–166.
Schöne BR, Fiebig J, Pfeiffer M, Gleβ R, Hickson J, Johnson A, Dreyer W, Oschmann W (2005b) Climate records from a bivalved Methuselah (Arctica islandica, Mollusca; Iceland). Palaeogeography, Palaeoclimatology, Palaeoecology 228, 130–148.
Schöne BR, Houk S, Freyre CA, Fiebig J, Oschmann W, Kroncke I, Dreyer W, Gosselck F (2005) Daily Growth Rates in Shells of Arctica islandica: Assessing Sub-seasonal Environmental Controls on a Long-lived Bivalve Mollusk. Palaios 20, 78–92.
Schöne BR, Gillikin DP (2012) Unraveling environmental histories from skeletal diaries - advances in sclerochronology. Palaeogeography, Palaeoclimatology, Palaeoecology, 373:1-5.
Schöne BR, Radermacher P, Zhang Z, Jacob DE (2011) Crystal fabrics and element impurities (Sr/Ca, Mg/Ca, and Ba/Ca) in shells of Arctica islandica — Implications for paleoclimate reconstructions. Palaeogeography, Palaeoclimatology, Palaeoecology 373, 50–59.
Scholle PA, Bebout DG, Moore CH (1983) Carbonate depositional environments / edited by Peter A. Scholle, Don G. Bebout, Clyde H. Moore. xi, 708 p. :
Schrag DP, Adkins JF, McIntyre K, Alexander JL, Hodell DA, Charles CD, and McManus JF (2002) The oxygen isotopic composi- tion of seawater during the Last Glacial Maximum, Quat. Sci. Rev., 21(1-3), 331–342, doi:10.1016/S0277-3791(01)00110-X.
Seibold, E (1982) Geology of the Northwest African continental margin. Berlin, New York, Heidelberg: Springer-Verlag, 1982.
Sevrin-Reyssac J (1993) Hydrology and underwater climate of the Banc d'Arguin, Mauritania: a review. Hydrobiologia 258, 1–8.
Sharkey C (2013) Migration and Climate Change by Étienne Piguet , Antoine Pécoud and Paul De Guchteneire (eds). Cambridge: Cambridge University Press, 2011. 425pp.
Smith AM (1995) Palaeoenvironmental interpretation using bryozoans: a review. Geol. Soc. London, Spec. Publ. 83, 231–243.
Smith DC (1992) The symbiotic condition. Symbiosis 14:3-15
Smith AM, Key Jr. MM, Gordon DP (2006) Skeletal mineralogy of bryozoans: Taxonomic and temporal patterns. Earth-Science Reviews 78 (3–4):287-306
Stachowitsch M (1980) The epibiotic and endolithic species associated with the gastropod shells inhabited by the hermit crabs Paguristes oculatus and Paguristes cuanensis, PSZNI Mar. Ecol., 1, 73–101, 1980. 4386

Stanley SM (1975) Adaptive themes in the evolution of the Bivalvia (Mollusca). Annu. Rev. Earth Planet. Sci. 361–385.
Stramma L, Siedler G (1988) Seasonal changes in the North Atlantic sub-tropical gyre. Journal of Geophysical Research, 93, 8111-8118
Stuiver M, Polach HA (1977) Discussion: reporting of 14C data. Radiocarbon 19(3):355–63
Summerhayes CP, Milliman JD, Briggs SR, Bee AG, Hogan C (1976) Northwest African shelf sediments: influence of climate and sedimentary processes. J. Geol. 84, 277–300.
Sverdrup KA, Duxbury A, and Duxbury AC (2006) Fundamentals of oceanography. McGraw-Hill Higher Education, 2006.
Taylor JD (1969) The shell structure and mineralogy of the Bivalvia. Introduction. Nuculacea-Trigonacea. *Bull. Br. Mus. Nat. Hist.(Zool.)*, 3, 1-125.
Taylor GT, Muller-Karger FE, Thunell RC, et al. (2012) Ecosystem responses in the southern Caribbean Sea to global climate change. Proceedings of the National Academy of Sciences of the United States of America 109:19315–20. doi: 10.1073/pnas.1207514109
Taylor PD (1976) Multilamellar growth in two Jurassic cyclostomatous Bryozoa. Palaeontology 19:293-306
Taylor PD (1991) Observations on symbiotic associations of bryozoans and hermit crabs from the Otago Shelf of New Zealand. In Bigey FP (ed.): Bryozoaires actuels et fossils, 487-495. Bullétin de la Societé des Sciences Naturelle de l`Quest de la France, Momoires, H.S. 1
Taylor PD (1994) Evolutionary palaeoecology of symbioses between bryozoans and hermit crabs. Historical Biology 9:147-205
Taylor PD (2005) Bryozoans and palaeoenvironmental interpretation. Journal of the Palaeontological Society of India 50(2):1-11
Taylor PD and Monks N (1997) A new cheilostome bryozoan genus pseudoplanktonic on molluscs and algae. Invertebrate Biology 116 (1):39-51
Taylor PD and Schindler KS (2004) A new Eocene species of the hermit-crab symbiont *Hippoporidra* (Bryozoa) from the Ocala Limestone of Florida. Journal of Paleontology 78:790-794
Taylor PD, Schembri PJ, Cook PL (1989) Symbiotic associations between hermit crabs and bryozoans from the Otago region, southeastern New Zealand. Journal of Natural History 23:1059-1085
Tossili L (1959) Sistema hidrográfico y Cuenca del Río de la Plata. Contribución al estudio de su régimen hidrológico. An. Soc. Cient. Arg. 167 (3-4): 41-64.
Tucker ME (1996) Methoden der Sedimentologie. Enke, Stuttgart
Tucker ME and Wright PV (2009) Carbonate sedimentology. John Wiley & Sons, 2009. ISBN 1444314165
UNESCO (1981) The Practical Salinity Scale 1978 and the International Equation of State of Seawater 1980. Tech. Pap. Mar. Sci. 36:
Urey (1951) Measurement of paleotemperatures and temperatures of the Upper Cretaceous of England, Denmark, and the southeastern United States. *Geol. Soc. Am. Bul.*, 62, 399-416.
Van Camp L, Nykjaer L, Mittelstaedt E, Schlittenhardt P (1991) Upwelling and boundary circulation off Northwest Africa as depicted by infrared and visible satellite observations. Prog. Oceanogr. 26, 357–402.
Van der Geest M (2013) Multi-trophic interactions within the seagrass beds of Banc d'Arguin, Mauritania: a chemosynthesis-based intertidal ecosystem. PhD Thesis, University of Groningen, Groningen, The Netherlands
Vaz AC, Möller Jr OO, Almeida TL (2006) Sobre a descarga dos rios afluentes a Lagoa dos Patos. Atlantica 28, 13–23.
Valentine JW (1973) Evolutionary Paleoecology of the Marine Biosphere. New Jersey: Prentice Hall.
Vermaat JE, Beijer JAJ, Gijlstra R, Hootsmans MJM, Philippart CJM (1993) Leaf dynamics and standing stocks of intertidal *Zostera noltii* Hornem, and *Cymodocea nodosa* (Ucira) Ascherson on the Banc d'Arguin (Mauritania). Hydrobiology 258:59–72
Vernet R (2007) Le Golfe d'Arguin de la préhistoire à l'histoire: littoral et plaines intérieures. 202 pp.
Violante R, Parker G (2004) The post-last glacial maximum transgression in the de la Plata River and adjacent inner continental shelf, Argentina. Quaternary International 114, 167–181.
Vogel K (1984) Lebensweise und Umwelt fossiler Tiere eine Einführung in die Ökologie der Vorzeit; Biologische Arbeitsbücher; 39. Quelle und Meyer, Heidelberg
Wainwright PC, Reilly SM (1994) Functional Morphology as a Tool in Ecological Research in Ecological Morphology: Integrative Organismal Biology. University of Chicago Press, 15.08.1994 - 367 p.
Ward JHJ (1963) Hierarchical Grouping to Optimize an Objective Function. Journal of the American Statistical Association 58:236–244.

Wass, RE (1991) Intracolonial variation in the cheilostome genera, Adeona and Adeonellopsis. In: Bigey, FP. (Wd.) Bryozoaires Actuels et Fossiles: Bryozoa Living and Fossil. Bulletin de la Societe des Sciences Naturelles de l'Ouest de la France, Memoire HS 1, 523-529.
Waelbroeck C, Paul A, Kucera M, Rosell-Melé A, Weinelt M, et al. (2009) Constraints on the magnitude and patterns of ocean cooling at the Last Glacial Maximum. Nature Geoscience 2, 127–132.
Wanner H, Solomina O, Grosjean M, Ritz SP, Jetel M (2011) Structure and origin of Holocene cold events. Quaternary Science Reviews 30:3109–3123.
Wefer G (1985) Die Verteilung stabiler Isotope in Kalkschalen mariner Organismen. Geol. Jahrb. 82-A.
Weidman CR (1995) Development and Application of the Mollusc Arctica islandica as a Paleoceanographic Tool for the North Atlantic Ocean. Marine Geology. State University of New York at Oneonta.
Wells PG, Daborn GR (1997) The Rio de La Plata: an Environmental Overview. An EcoPlata Project Background Report. Dalhousie University, Halifax, NS. 248p.
Wentworth CK (1922) A scale of grade and class terms for clastic sediments. Geology 30:7–392.
Westphal H, Beuck L, Braun S, Freiwald A, Hanebuth TJJ, Hetzinger S, Klicpera A, Kudrass H, Lantzsch H, Lundälv T, Mateu-Vicens G, Preto N, Reumont J, Schilling S, Taviani M and Wienberg C (2014) Report of Cruise Maria S. Merian 16/3 — Phaeton – Paleoceanographic and paleo-climatic record on the Mauritanian shelf. Oct. 13 – Nov. 20, 2010, Bremerhaven (Allemagne) – Mindelo (Cap Verde). Maria S. Merian-Berichte, Leibniz-ZMT, Bremen, Germany, 136 pp. Doi:10.2312/cr_msm16_3
Westphal H, Halfar J and Freiwald A (2010) Heterozoan carbonates in subtropical to tropical settings in the present and in the past: International Journal of Earth Sciences 99:153–159
Westphal H, Freiwald A, Hanebuth TJJ, Eisele M, Gürs K, Heindel K, Michel J and Reumont J (2007) Report and preliminary results of Poseidon cruise 346 — MACUMA: integrating carbonates, siliciclastics and deep-water reefs for understanding a complex environment, Las Palmas (Spain)–Las Palmas (Spain), 28.12.2006–15.1.2007. Reports of the Dept. of Geosciences, University of Bremen, Germany, 49 pp.
Williams JD, McDermott JJ (2004) Hermit crab biocoenoses: a worldwide review of the diversity and natural history of hermit crab associates. Journal of Experimental Marine Biology and Ecology 305:1-128
Winker CD and Kidwell SM (1996) Stratigraphy of marine rift basin: Neogene of the western Salton Trough, California. In Abbott PL and Cooper JD (eds.): Field Conference Guide 1996. Pacific Section AAPG Guide Book 73, Pacific SEPM Book 80:295-336
Winston JE (1982) Marine bryozoans (Ectoprocta) of the Indian River area (Florida). Bulletin of the American Museum of Natural History, 173, 99-176
Winston JA and Heimberg BF (1986) Bryozoans from Bali, Lombok, and Komodo. American Museum Novitates 2847, 99:1-49
Wisshak M, López Correa M, Gofas S, Salas C, Taviani M, Jakobsen J, Freiwald A (2009) Shell architecture, element composition, and stable isotope signature of the giant deep-sea oyster Neopycnodonte zibrowii sp. n. from the NE Atlantic. Deep Sea Research Part I: Oceanographic Research Papers 56, 374–407.
Wissmann G (1982) Stratigraphy and Structural Features of the Con- tinental Margin Basin of Senegal and Mauritania. In von Rad, U., Hinz, K., Sarnthein, M. & Seibold, E. (Eds.), Geology of the North- west African continental margin, 160-181. Springer-Verlag, Berlin.
Wolff WJ, Duiven AG, Duiven P, et al. (1993a) Biomass of macrobenthic tidal flat fauna of the Banc d'Arguin, Mauritania. Hydrobiologia 258:151–163.
Wolff WJ, Land J Van Der, Nienhuis PH, Wilde PAWJ De (1993b) The functioning of the ecosystem of the Banc d'Arguin, Mauritania: a review. Hydrobiologia 258:211–222.
Wolff WJ, Van der Land J, Nienhuis PH, De Wilde PAWJ (1993c) Ecological Studies in the Coastal Waters of Mauritania. Hydrobiologia 258:
Wooster WS, Bakum A, McLain DR (1976) The seasonal upwelling cycle along the eastern boundary of the North Atlantic. Journal of Marine Research, 34, 131-140.
World Population Prospects (WPP 2012): The 2012 Revision, Methodology of the United Nations Population Estimates and Projections, Working Paper No. ESA/P/WP.235. United Nations, Department of Economic and Social Affairs.
WoRMS Editorial Board (2014). World Register of Marine Species. Available from http://www.marinespecies.org at VLIZ. Accessed 2014-09-26
Wright V, Burgess P (2005) The carbonate factory continuum, facies mosaics and microfacies: an appraisal of some of the key concepts underpinning carbonate sedimentology. Facies 51:19–25.
Yan L, Schöne BR, Arkhipkin A (2012) Eurhomalea exalbida (Bivalvia): A reliable recorder of climate in southern South America? Palaeogeography, Palaeoclimatology, Palaeoecology 350-352, 91–100.

Ziegler AM, Hulver ML, Lottes AL, and Schmachtenberg WF (1984) Uniformitarianism and paleoclimates: inferences from the distribution of carbonate rocks. In Brenchley, P.J. (ed.), Fossils and Climate. Chichester: Wiley, pp. 3–25.

Zhou J, Lau K-M (1998) Does a Monsoon Climate Exist over South America? Journal of Climate 11, 1020–1040.

Zonneveld K and cruise participants (2010) Report and preliminary results of R/V Poseidon Cruises P 366-1 and P 366-2, Las Palmas - Las Palmas - Vigo, 03 -19 May 2008 and 22 -30 May 2008. PERGAMOM Proxy Education and Research cruise off Galicai, Morocco and Mauretania. 47 pages.

XVI.4 Peer-reviewed conference contributions and cruise reports

Westphal H, Beuck L, Braun S, Freiwald A, Hanebuth TJJ, Hetzinger S, **Klicpera A**, Kudrass H, Lantzsch H, Lundälv T, Mateu-Vicens G, Preto N, Reumont J, Schilling S, Taviani M and Wienberg C (2014) Report of Cruise Maria S. Merian 16/3 – Phaeton – Paleoceanographic and paleo-climatic record on the Mauritanian shelf. October 13 – November 20, 2010 – Bremerhaven (Germany) – Mindelo (Cap Verde). Maria S. Merian-Berichte, 57 pp, DFG-Senatskommission für Ozeanographie. Doi: 10.2312/cr_msm16_3

Müller P, **Klicpera A**, Lopez-Correa M, Vernet R, Tous P, Westphal H (2013) δ18O records of catfish otoliths (Arius heudelotii) and their potential for paleoclimatological reconstructions. International Sclerochronological Conference 2013, Bangor, UK

Hanebuth TJJ, Bender VB, Lantzsch H, Perez L, **Klicpera A**, Chiessi C, García-Rodríguez F, Violante R, Westphal H (2012) Reconstructing rapid changes in fluvial runoff, shelf currents and human activity over the past 100, 1,000 and 10,000 years (the shelf system off Uruguay). CERF 2012, Mar del Plata, Argentina

Michel J, Reymond C, **Klicpera A**, Hanebuth TJJ, Westphal H (2012) Last transgression heterozoan carbonate and siliciclastic sedimentation on a tropical, upwelling-influenced shelf (Mauritania), (Talk). 29th International Association of Sedimentologists Meeting (IAS 2012), Schladming, Austria

Klicpera A, Michel J, Reymond C, Westphal H (2012) The Banc d'Arguin off Mauritania: An extreme example of shallow-water heterozoan carbonate production under eutrophic tropical conditions, (Talk). 29th International Association of Sedimentologists Meeting (IAS 2012), Schladming, Austria

Müller P, **Klicpera A**, Westphal H (2012) Analysis of paleoenvironmental proxies in fish-otoliths: A high resolution archive for Holocene upwelling variations offshore Mauritania, NW-Africa, (Talk); Sediment & GV Meeting 2012, University Hamburg, Hamburg, Germany

Klicpera A, Hanebuth TJJ, Michel J, Mersmeyer H, Kudrass H, Westphal H (2012) A mixed carbonate-siliciclastic system under hyperarid and eutrophic conditions (the Arguin Shelf off Mauritania since late Pleistocene), (Poster). MARUM Klausurtagung Farge (2012), Bremen, Germany

Klicpera A, Westphal H, Michel J, Taviani M, Mateu G (2011) The Banc d'Arguin off Mauritania: Shallow-water carbonate production under eutrophic tropical conditions, (Talk).14th Bathurst Meeting of Carbonate Sedimentologists 2011, University of Bristol, Bristol, UK

Klicpera A, Hanebuth TJJ, Westphal H (2011) Reconstructing Holocene palaeoenvironmental conditions offshore Uruguay by using growth-line periodicity and high-resolution shell geochemistry on large clam Retrotapes exalbidus, (Talk). 28th International Association of Sedimentologists Meeting (IAS 2011), Zaragoza, Spain

Klicpera A, Westphal H (2010) Geobiochemical investigations on large-shelled clams Retrotapes and Pitar (Bivalvia, Veneridae) sampled offshore Uruguay: Analyses of growth line periodicity and shell-geochemistry as useable tools for ecological reconstructions of paleoceanic parameters, (Talk). 18th International Sedimentological Congress (ISC 2010), Mendoza, Argentina

XVII. Supplements to the first publication (Mauritania)

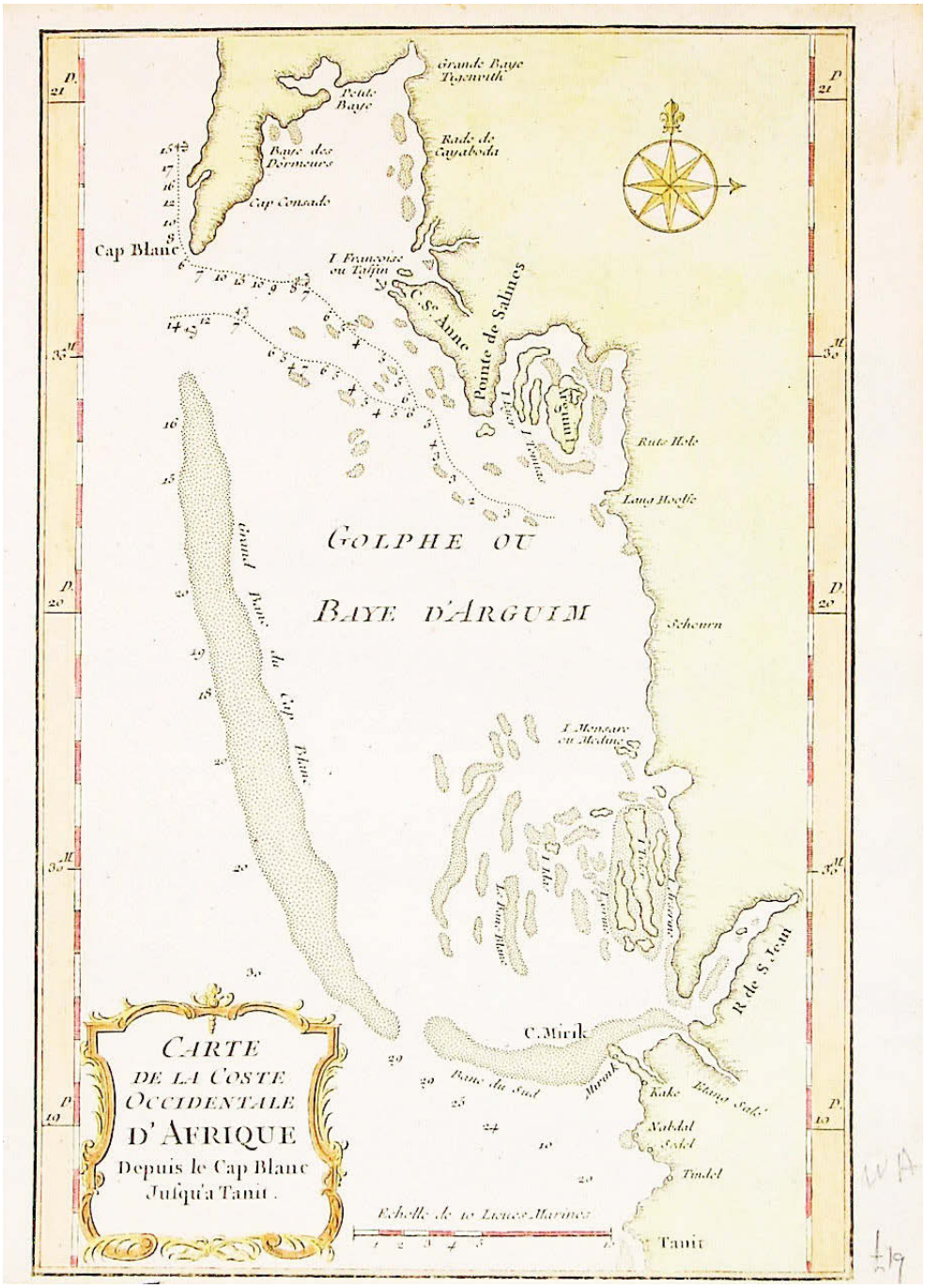

Suppl. XVII.1: Map of the Golfe d'Arguin. Published in Antoine-François Prevost's 20 volume edition of L`Histoire Generale des Voyages published by Pierre de Hondt, The Hague between 1747 & 1780.

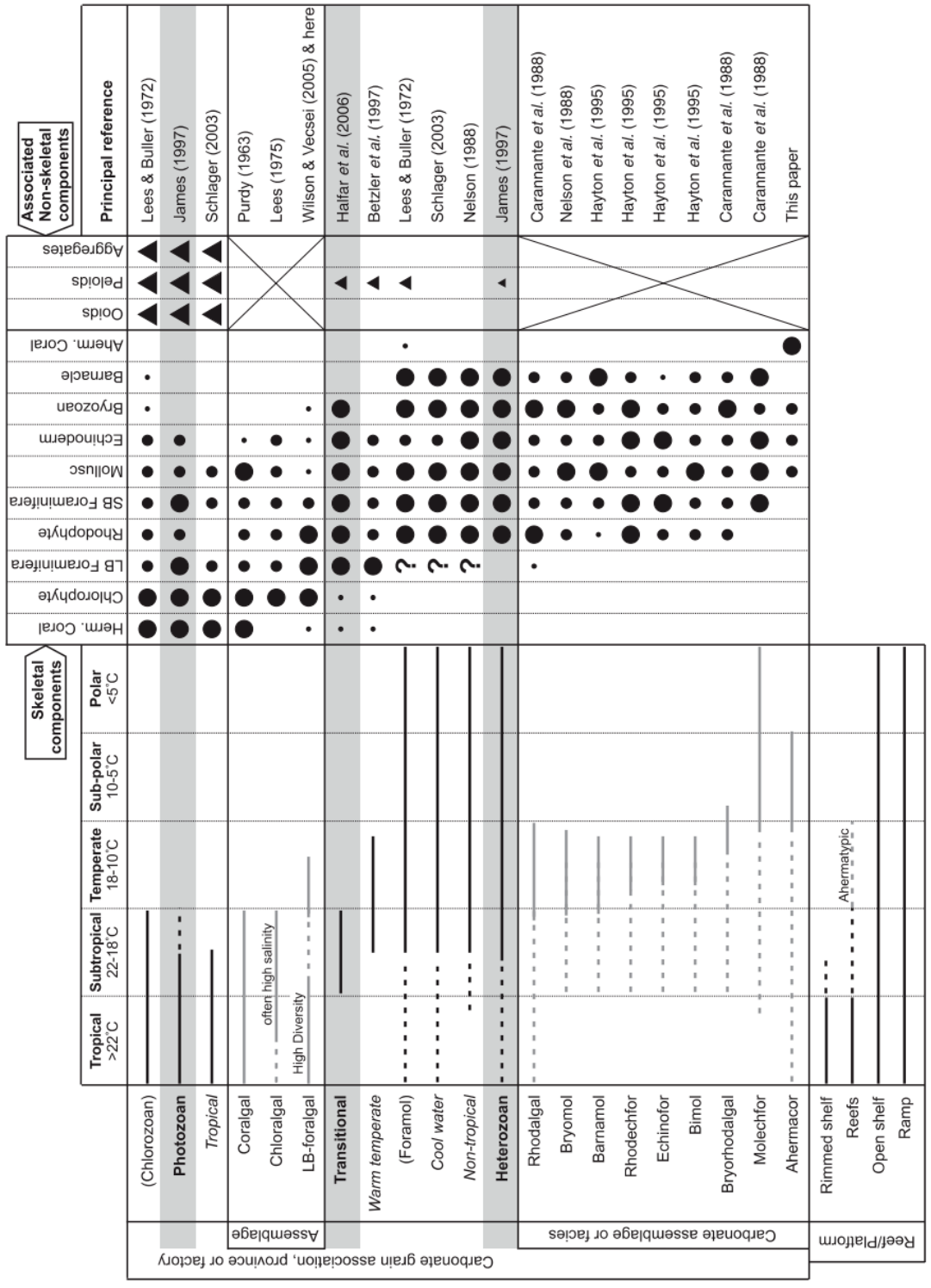

Suppl. XVII.2: Summary of Cenozoic carbonate deposit types based on benthic (skeletal and non-skeletal) components (after Wilson & Vecsei, 2005; taken from Kindler and Wilson, 2010).

Suppl. XVII.3: Component analysis and determination of bivalve grains from the outer Banc d'Arguin (14833, 14812, 14748, 14725), the Baie du Lévrier (14786, 25783), and the Baie de Saint Jean. Values in percentages (%), total bivalve point counts and total undetermined bivalve point counts for each sampling site is shown at the bottom of each table.

Bivalvia		14833-7	14833-21	14812-10	14748-11	14748-10	14725-2	14783-7	14786-9	Baie de Saint Jean
Nuculanidae	*Nuculana bicuspidata*							1,62	12,63	
Nuculidae	*Nucula nitidosa*							2,65	4,25	
	Nucula crassicostata							0,29		
	Nuculidae							2,06		
Arcidae	*Arcopsis afra*			2,57			0,35			
	Anadara polii			0,32						
	Bathyarca sp.			0,51						
	Arcidae			0,32						
Glycymeridae	*Glycymeris concentrica*	0,22	0,13	0,26						
Limopsidae	*Limopsis sp.*						0,35			
Mytilidae	*Modiolus sp.*	1,70	0,55	0,26						
	Musculus subpictus			0,51				0,59		
	Gregariella pentagnae			4,99		0,98	17,86			
	Solamen dollfusi			0,51						
	Mytilidae			0,96				0,29	0,87	
Pinnidae	*Atrina sp.*				0,09					
Pectinidae	*Aequipecten flabellum*	0,58	0,46							
	Aequipecten sp.								0,87	
	Pectinidae			1,73		0,49		0,22		
Ostreidae	*Ostreidae*			3,15	0,84	1,30	0,69	0,15	1,98	
Gryphaeidae	*Gryphaeidae*			0,51						
Anomiidae	*Anomia ephippium*	0,15	0,07					0,59	0,12	
Limidae	*Limatula gwyni*				0,38					
Lucinidae	*Lucinidae sp.1*								0,12	
	Lucinidae sp.2									0,90
Montacutidae	*Montacutidae*			0,51				0,07		
Lasaeidae	*Scacchia sp.*					0,49	0,69		0,99	
Pharidae	*Ensis goreensis*	0,07		0,51						
Crassatellidae	*Crassatina marchadi*	0,58	0,33					0,44		
	Crassatina sp.	0,07						1,62		
Astartidae	*Digitaria digitata*	0,22								
Carditidae	*Carditamera contigua*			5,06			6,92	0,29		
	Cardiocardita ajar							0,59	1,16	
Condylocardiidae	*Cuna gambiensis*			0,64	0,75	1,47		8,60	9,20	
Chamidae	*Chama crenulata*	1,00	0,27	11,30	0,38	2,02	6,53	0,15		
Cardiidae	*Laevicardium crassum*	0,15								
	Papillicardium papillosum	0,92		0,26	0,38			45,70	14,55	
	Fraginae juveniles	0,85		0,32						
	Fraginae sp.1									10,04
	Cerastoderma cf. edule									16,97
	Acanthocardia-like								1,34	
	Cardiidae					0,49				

Bivalvia

		14833-7	14833-21	14812-10	14748-11	14748-10	14725-2	14783-7	14786-9	Baie de Saint Jean
Mactridae	*Mactridae*			0,77						
Tellinidae	*Macoma cumana*								2,85	
	Tellina boucheti			0,77	0,09	0,60				
	Tellina cf. boucheti									0,45
	Tellina densestriata								5,41	
	Tellina hanleyi				1,17					
	Tellina rubicincta								5,65	
	Tellina sp.				1,13	0,49	0,35	0,59	4,37	
	Tellinidae			0,26			0,35			
Donacidae	*Donax burnupi*	78,13	74,53	5,64	48,61	30,17	2,85	1,40	2,97	
Semelidae	*Abra sp.1*								0,99	
	Abra sp.2									4,81
	Ervilia castanea	4,05	0,20							
Psammobiidae	*Gari fervensis*								3,73	
Veneridae	*Dosinia sp.*	0,36	0,07	0,51	1,13	1,97		3,82	7,86	16,78
	Pitar sp.							0,29	1,75	
	Tivela sp.			0,26						
	Callista floridella			0,26		0,05		5,36	1,11	0,45
	Timoclea ovata	4,13	16,49	33,14	43,85	57,00	17,38	1,18	1,98	
	Timoclea sp.		0,07							
	Venus crebrisulca	0,73	1,26				19,02			
	Venus sp.1			0,51			3,76			
	Venus spp.	1,70	3,28	0,58	0,46			0,29		
	Circomphalus							0,29		
	Clausinella punctigera		0,07							
	Veneridae	0,85		0,51		0,49	1,25			
Corbulidae	*Corbula gibba*		0,13					10,29	10,42	
	Corbula laticostata		0,07	3,67				0,51		
Total Bivalves (point counts)		**652**	**716**	**294**	**413**	**318**	**195**	**360**	**217**	**122**
Bivalves undetermined (point counts)		**563**	**507**	**77**	**290**	**240**	**56**	**45**	**207**	**120**

Suppl. XVII.4: Component analysis and determination of gastropod grains from the Banc d'Arguin (14833, 14812, 14748, 14725), the Baie du Lévrier (14786, 25783), and the Baie de Saint Jean. Values in percent (%).

Gastropoda		14833-7	14833-21	14812-10	14748-11	14748-10	14725-2	14783-7	14786-9	Baie de Saint Jean
Fissurellidae	*Fissurella sp.*			0,26			0,69			
Trochidae	*Gibbula joubini* *Trochidae*	1,70	0,55	2,57 1,15		0,49 0,49	2,42 2,98	0,29 2,20		
Tricoliidae	*Tricolia pullus*			4,10			7,61			
Cerithiidae	*Bittium sp.*									6,64
Rissoidae	*Alvania sp.* *Pusillina sp.*			1,60			0,69			12,27
Barleeidae	*Barleeia sp.*			2,24			3,46			
Rissooidea	*Rissooidea*									24,77
Calyptraeidae	*Calyptrea africana* *Crepidula porcellana* *Crepidula sp.*	0,07		1,80			1,04	0,07 2,87		0,25 2,05
Turritellidae	*Mesalia freytagi* *Turritellidae*	0,92	0,07				0,69	0,51	0,12	
Triphoridae	*Marshallora sp.* *Triphoridae*		0,55	2,18				0,59		
Naticidae	*Natica sp.* *Naticidae*		0,61	0,51			1,04	0,15		
Buccinidae	*Buccinidae*									0,45
Olividae	*Aragonia acuminata*			0,26						
Cystiscidae	*Gibberula sp.* *Persicula blanda* *Cystiscidae*		0,07					1,47	1,75	0,45
Marginellidae	*Granulina sp.* *Marginella sp.* *Volvarina ambigua* *Marginellidae*		0,07 0,07 0,07					0,59	0,87	1,35
Marginellidae	*Marginellidae/Cystiscidae*						0,35	0,15		
Turridae	*Turridae*			0,26				0,29		
Mangeliidae	*Mangelia sp.*	0,85								
Architectonicidae	*Architectonicidae*				0,38	0,49				
Pyramidellidae	*Odostomia sp* *Turbonilla sp.* *Pyramidellidae*			0,96			0,35 0,35	0,29		
Bullidae	*Bulla sp.*									1,35
Cylichnidae	*Acteocina knockeri* *Cylichna cylindracea*					0,49			0,12	
Acteonicidae	*Acteon senegalensis*				0,38					
Scaphopoda	*Scaphopoda*							0,59		
Fissurellidae	*Fissurella sp.*			0,26			0,69			
Trochidae	*Gibbula joubini* *Trochidae*	1,70	0,55	2,57 1,15		0,49 0,49	2,42 2,98	0,29 2,20		
Tricoliidae	*Tricolia pullus*			4,10			7,61			
Cerithiidae	*Bittium sp.*									6,64
Total Gastropods (point counts)		**6**	**9**	**61**	**2**	**4**	**60**	**42**	**5**	**179**
Gastropods undetermined (point counts)		**43**	**48**	**45**	**14**	**16**	**6**	**2**	**10**	**102**

XVIII. Supplements to the second and third publication (Mauritania)

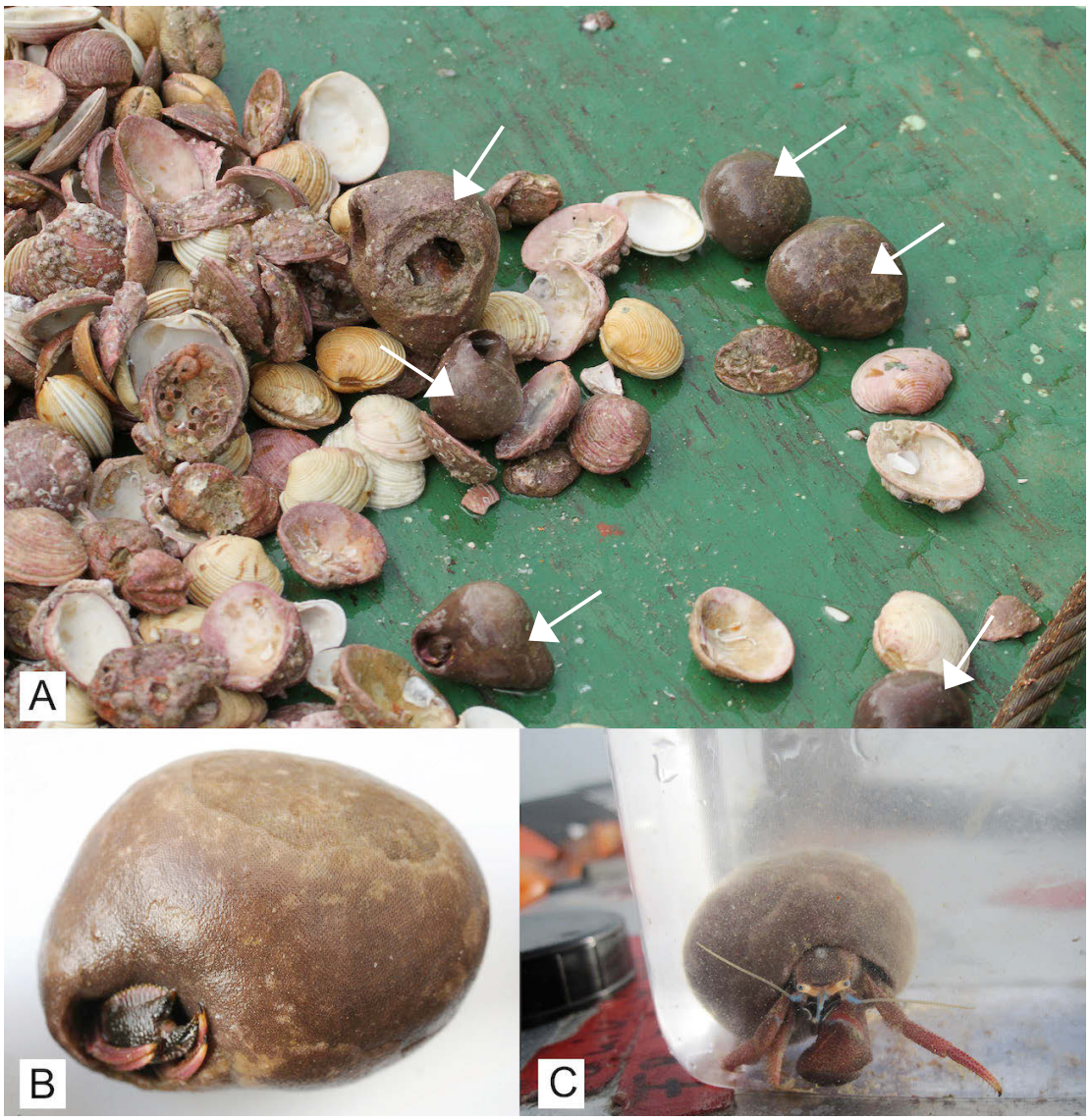

Supplement XVIII.1: Living bryoliths photographed offshore Mauritania. (A) Dredge recovery south of Cap Blanc (Banc d'Arguin); (B) Bryolith specimen with living crab inside and; (C) Hermit crab symbiont carrying bryolith shelter, temporarily stored in Kautex bottle. Photographed and documented during MSM16-3 (2010).

Suppl. XVIII.2: Bryozoan skeletons identified from Mauritanian sediments

Sample ID: pdt12874
Name: *Acanthodesia sp. A*
Age: Recent
Cruise/Expedition: MSM16-3
Station ID: GeoB14789-1
Location: Central Banc d'Arguin
Country: Mauritania
Water depth: 32 mbsl
GPS: N20°10.062' / W17°22.788'
Date: November 2010

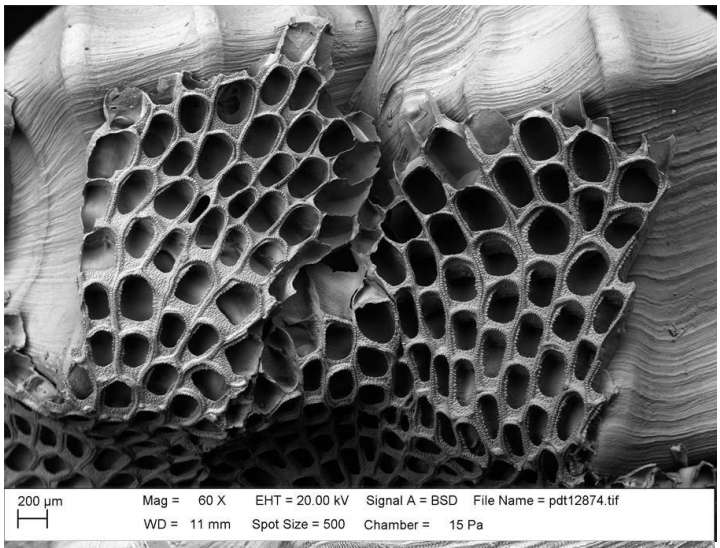

Sample ID: pdt12876
Name: *Acanthodesia sp. A*
Age: Recent
Cruise/Expedition: MSM16-3
Station ID: GeoB14789-1
Location: Central Banc d'Arguin
Country: Mauritania
Water depth: 32 mbsl
GPS: N20°10.062' / W17°22.788'
Date: November 2010

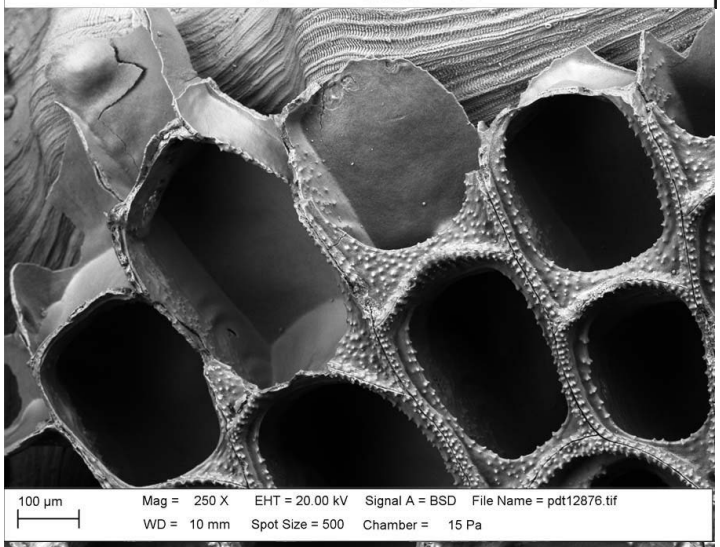

Sample ID: pdt12877
Name: *Acanthodesia sp. A*
Age: Recent
Cruise/Expedition: MSM16-3
Station ID: GeoB14789-1
Location: Central Banc d'Arguin
Country: Mauritania
Water depth: 32 mbsl
GPS: N20°10.062' / W17°22.788'
Date: November 2010

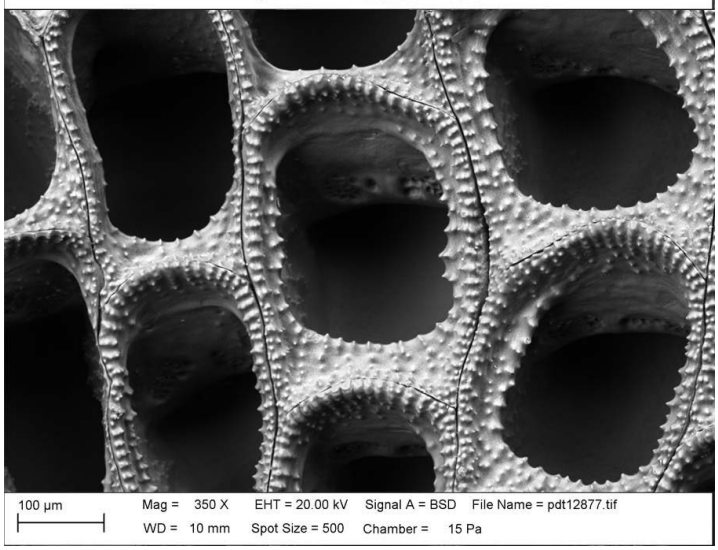

Sample ID: pdt12878
Name: *Hippoporidra picardi (Gautier, 1962)*
Age: Recent
Cruise/Expedition: MSM16-3
Station ID: GeoB14714-1
Location: Outer Banc d'Arguin
Country: Mauritania
Water depth: 52 mbsl
GPS: N20°02.627' / W17°27.420'
Date: October 2010

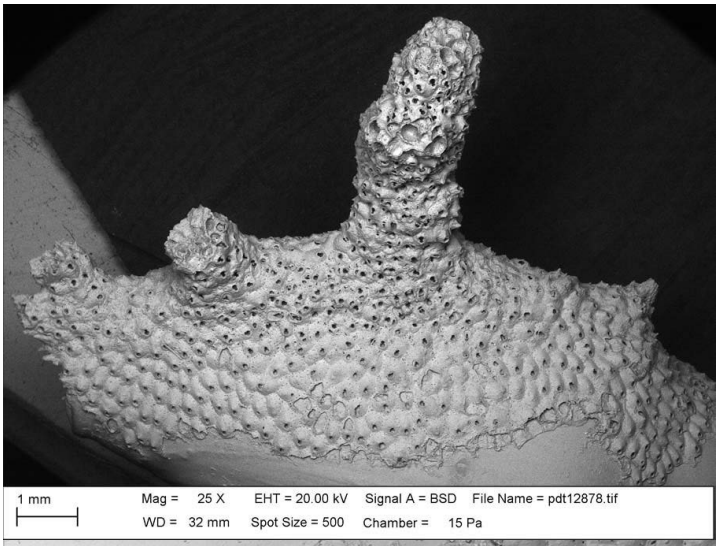

Sample ID: pdt12879
Name: *Hippoporidra picardi (Gautier, 1962)*
Age: Recent
Cruise/Expedition: MSM16-3
Station ID: GeoB14714-1
Location: Outer Banc d'Arguin
Country: Mauritania
Water depth: 52 mbsl
GPS: N20°02.627' / W17°27.420'
Date: October 2010

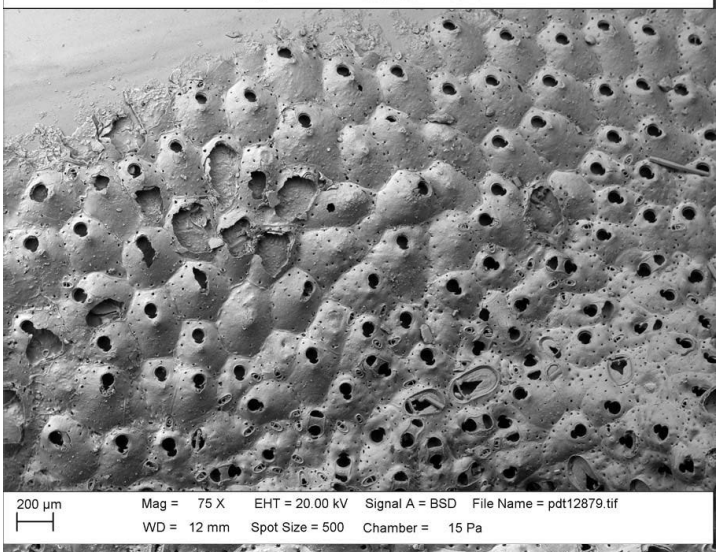

Sample ID: pdt12880
Name: *Hippoporidra picardi (Gautier, 1962)*
Age: Recent
Cruise/Expedition: MSM16-3
Station ID: GeoB14714-1
Location: Outer Banc d'Arguin
Country: Mauritania
Water depth: 52 mbsl
GPS: N20°02.627' / W17°27.420'
Date: October 2010

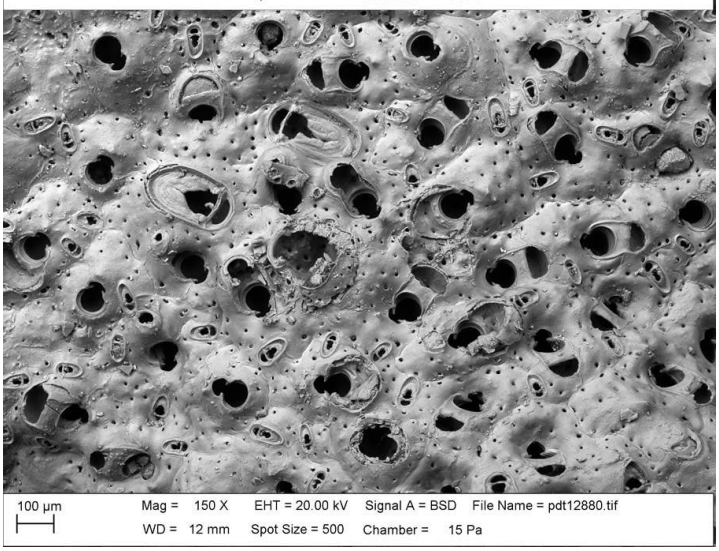

Sample ID: pdt128881
Name: *Reteporella*
Age: Recent
Cruise/Expedition: MSM16-3
Station ID: n/A
Location: Outer Shelf
Country: Mauritania
Water depth: n.A., but associated with Lophelia, Madrepora corals, thus assumed to be 500-800 mbsl
Date: November2010

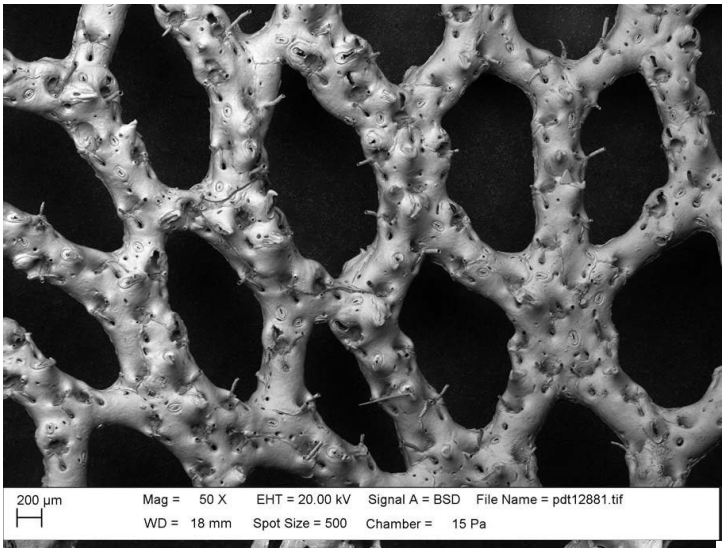

Sample ID: pdt128882
Name: *Reteporella*
Age: Recent
Cruise/Expedition: MSM16-3
Station ID: n/A
Location: Outer Shelf
Country: Mauritania
Water depth: n.A., but associated with Lophelia, Madrepora corals, thus assumed to be 500-800 mbsl
Date: November2010

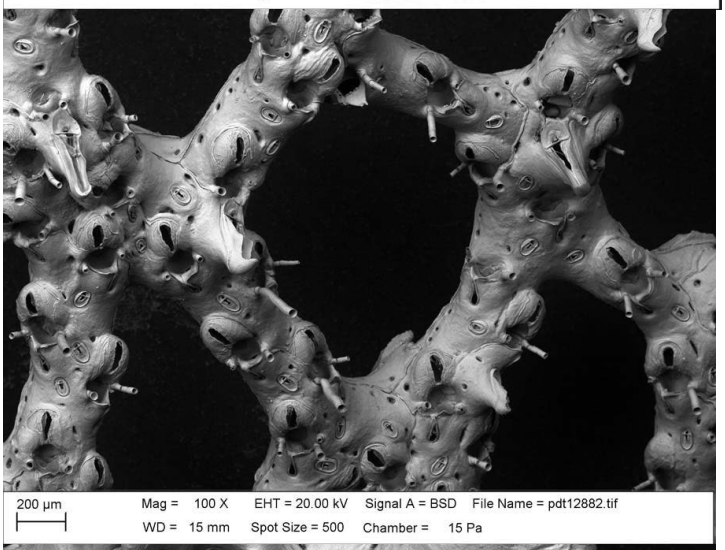

Sample ID: pdt128883
Name: *Reteporella*
Age: Recent
Cruise/Expedition: MSM16-3
Station ID: n/A
Location: Outer Shelf
Country: Mauritania
Water depth: n.A., but associated with Lophelia, Madrepora corals, thus assumed to be 500-800 mbsl
Date: November2010

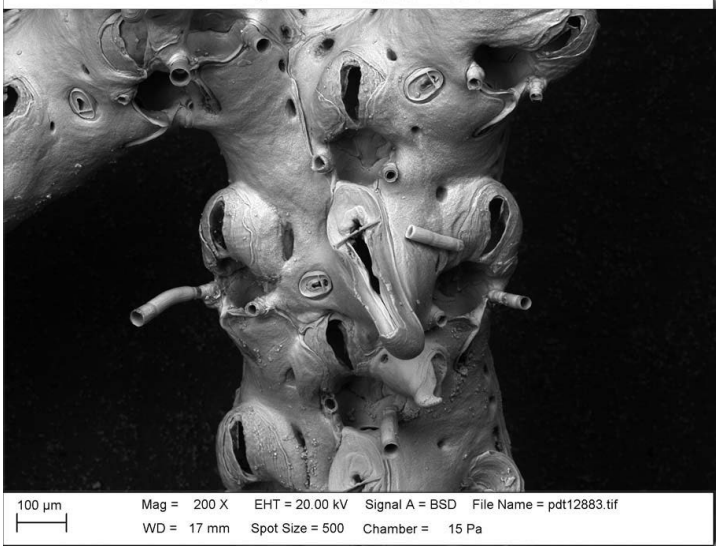

Sample ID: pdt12879
Name: *Hippoporidra senegambiensis (Carter, 1882)*
Age: Recent
Cruise/Expedition: MSM16-3
Station ID: GeoB14714-1
Location: Outer Banc d'Arguin
Country: Mauritania
Water depth: 52 mbsl
GPS: N20°02.627' / W17°27.420'
Date: October 2010

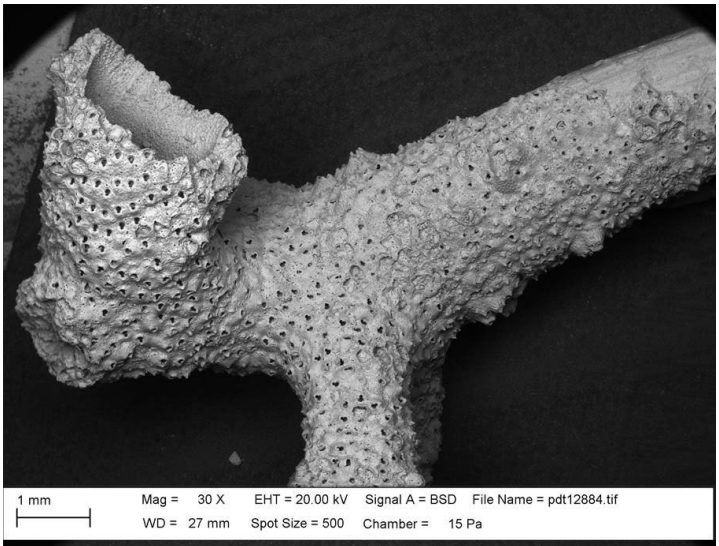

Sample ID: pdt12879
Name: *Hippoporidra senegambiensis (Carter, 1882)*
Age: Recent
Cruise/Expedition: MSM16-3
Station ID: GeoB14714-1
Location: Outer Banc d'Arguin
Country: Mauritania
Water depth: 52 mbsl
GPS: N20°02.627' / W17°27.420'
Date: October 2010

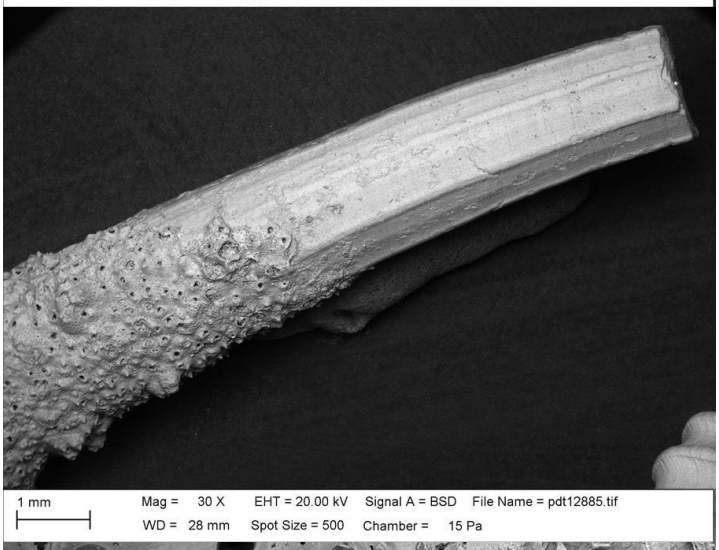

Sample ID: pdt12879
Name: *Hippoporidra senegambiensis (Carter, 1882)*
Age: Recent
Cruise/Expedition: MSM16-3
Station ID: GeoB14714-1
Location: Outer Banc d'Arguin
Country: Mauritania
Water depth: 52 mbsl
GPS: N20°02.627' / W17°27.420'
Date: October 2010

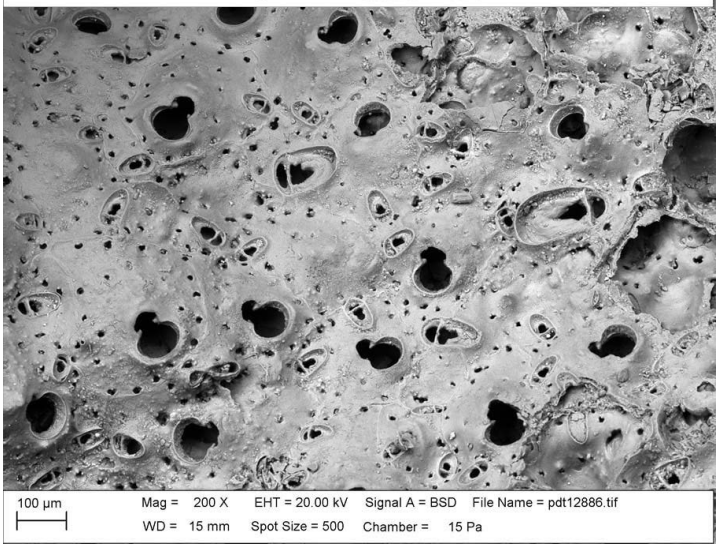

Sample ID: pdt12887
Name: *Discoporella sp.A*
Age: Recent
Cruise/Expedition: MSM16-3
Station ID: GeoB14766-2
Location: Cap Timiris Shelf
Country: Mauritania
Water depth: 60 mbsl
GPS: N19°07.230' / W16°34.530'
Date: October 2010

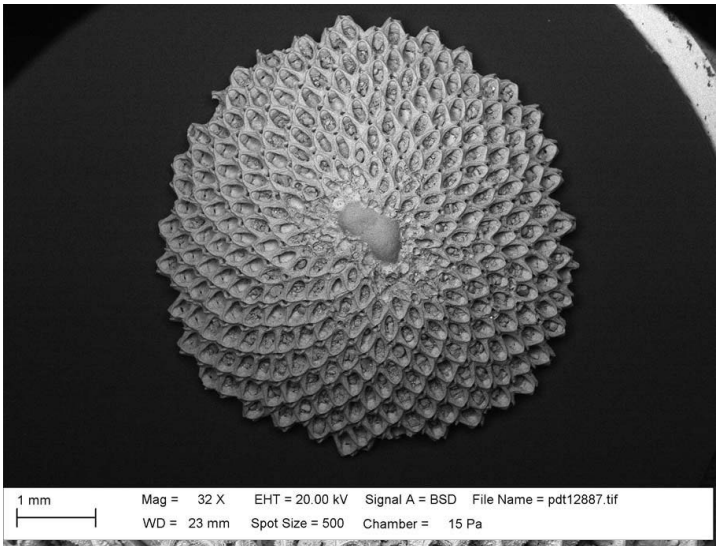

Sample ID: pdt12888
Name: *Discoporella sp.A*
Age: Recent
Cruise/Expedition: MSM16-3
Station ID: GeoB14766-2
Location: Cap Timiris Shelf
Country: Mauritania
Water depth: 60 mbsl
GPS: N19°07.230' / W16°34.530'
Date: October 2010

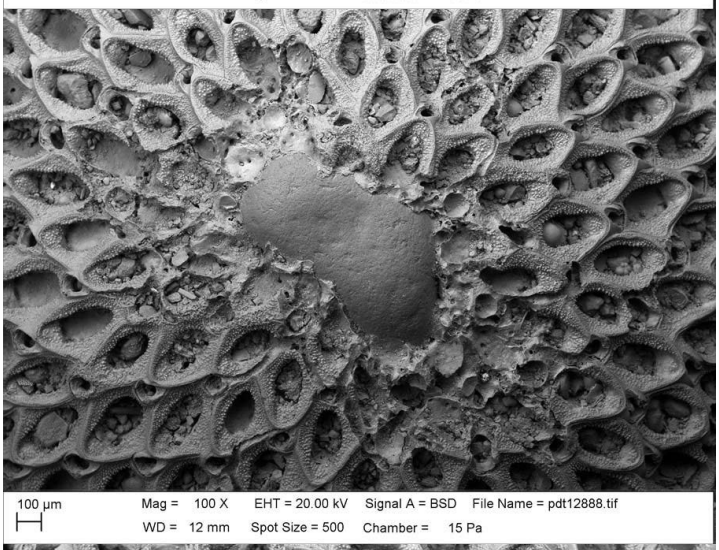

Sample ID: pdt12889
Name: *Discoporella sp.A*
Age: Recent
Cruise/Expedition: MSM16-3
Station ID: GeoB14766-2
Location: Cap Timiris Shelf
Country: Mauritania
Water depth: 60 mbsl
GPS: N19°07.230' / W16°34.530'
Date: October 2010

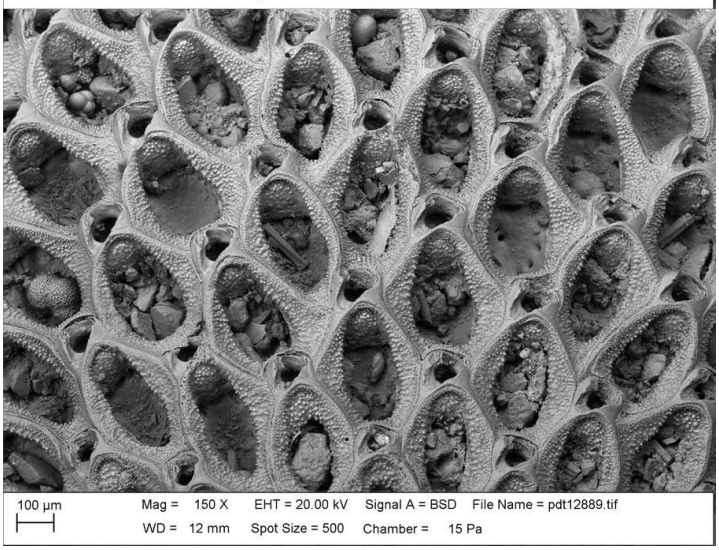

Sample ID: pdt12891
Name: *Discoporella sp.B*
Age: Recent
Cruise/Expedition: MSM16-3
Station ID: GeoB14765-1
Location: Cap Timiris Shelf
Country: Mauritania
Water depth: 60 mbsl
GPS: N19°07.230' / W16°34.530'
Date: October 2010

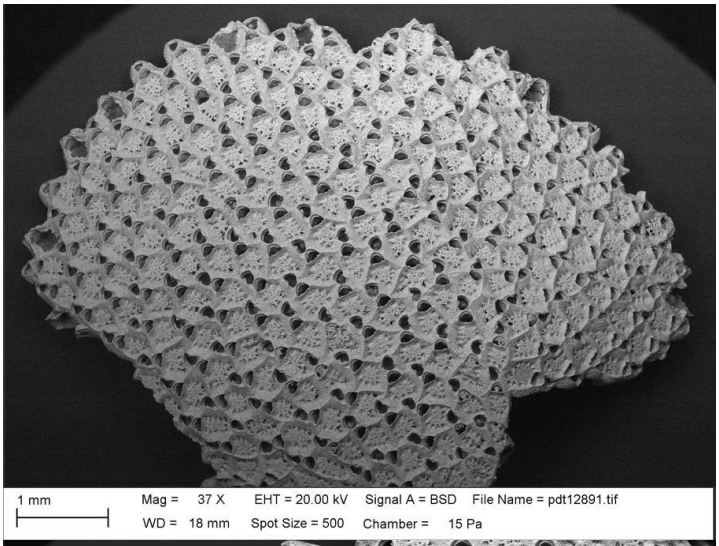

Sample ID: pdt12892
Name: *Discoporella sp.B*
Age: Recent
Cruise/Expedition: MSM16-3
Station ID: GeoB14765-1
Location: Cap Timiris Shelf
Country: Mauritania
Water depth: 60 mbsl
GPS: N19°07.230' / W16°34.530'
Date: October 2010

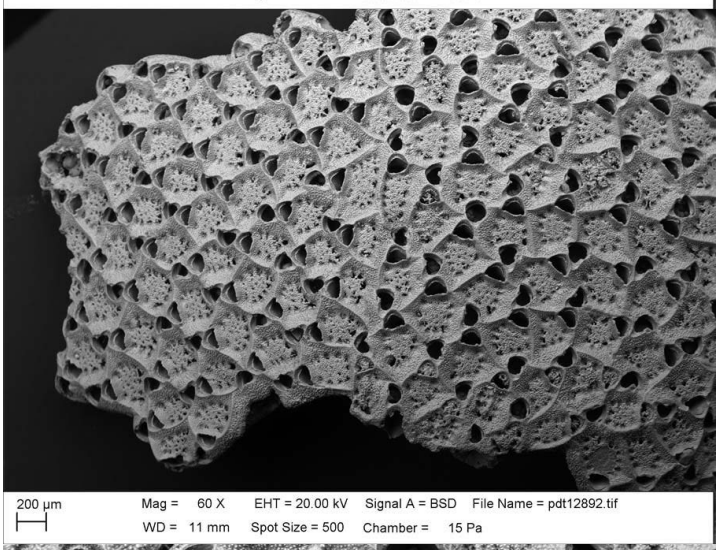

Sample ID: pdt12893
Name: *Discoporella sp.B*
Age: Recent
Cruise/Expedition: MSM16-3
Station ID: GeoB14765-1
Location: Cap Timiris Shelf
Country: Mauritania
Water depth: 60 mbsl
GPS: N19°07.230' / W16°34.530'
Date: October 2010

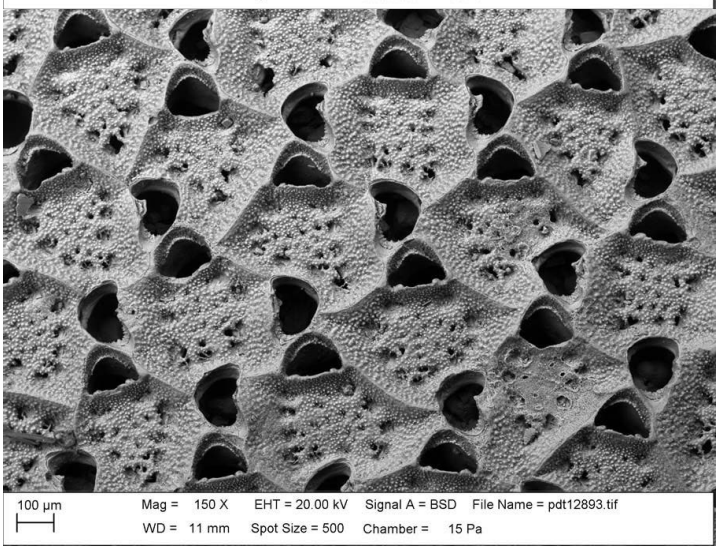

Sample ID: pdt12894
Name: *Microporella*
Age: Recent
Cruise/Expedition: POS366
Station ID: POS13015
Location: Outer Banc d'Arguin
Country: Mauritania
Water depth: 125 mbsl
GPS: N20°33.99' / W17°31.98'
Date: 2009

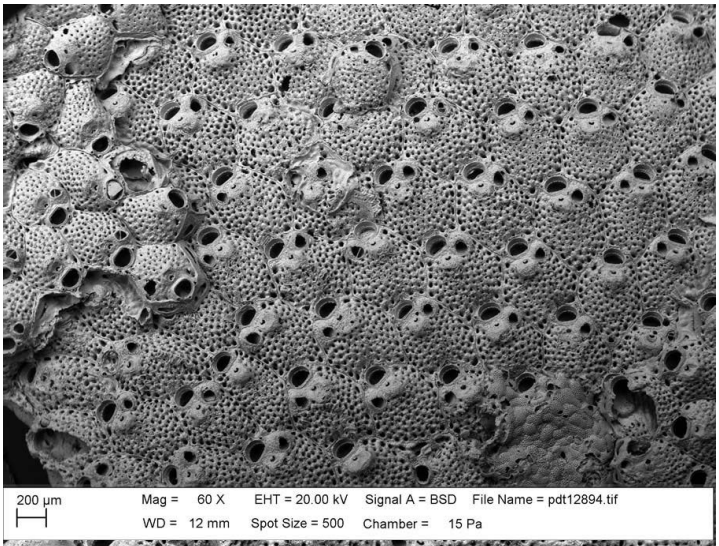

Sample ID: pdt12895
Name: *Microporella*
Age: Recent
Cruise/Expedition: POS366
Station ID: POS13015
Location: Outer Banc d'Arguin
Country: Mauritania
Water depth: 125 mbsl
GPS: N20°33.99' / W17°31.98'
Date: 2009

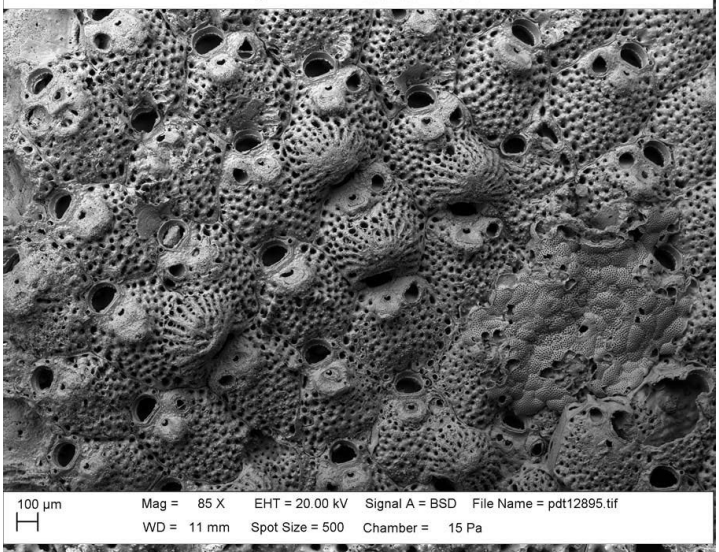

Sample ID: pdt12896
Name: *Microporella*
Age: Recent
Cruise/Expedition: POS366
Station ID: POS13015
Location: Outer Banc d'Arguin
Country: Mauritania
Water depth: 125 mbsl
GPS: N20°33.99' / W17°31.98'
Date: 2009

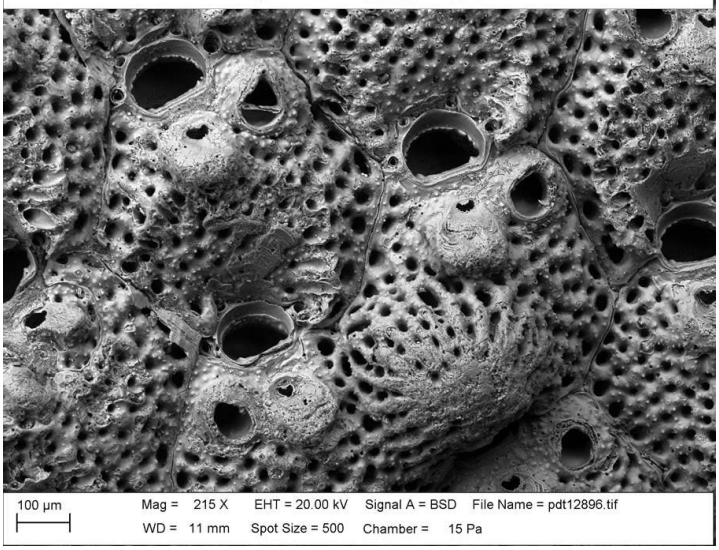

Sample ID: pdt12897
Name: *Porella cf. cervicornis (Pallas, 1766)*
Age: Recent
Cruise/Expedition: POS366
Station ID: POS13015
Location: Outer Banc d'Arguin
Country: Mauritania
Water depth: 125 mbsl
GPS: N20°33.99' / W17°31.98'
Date: 2009

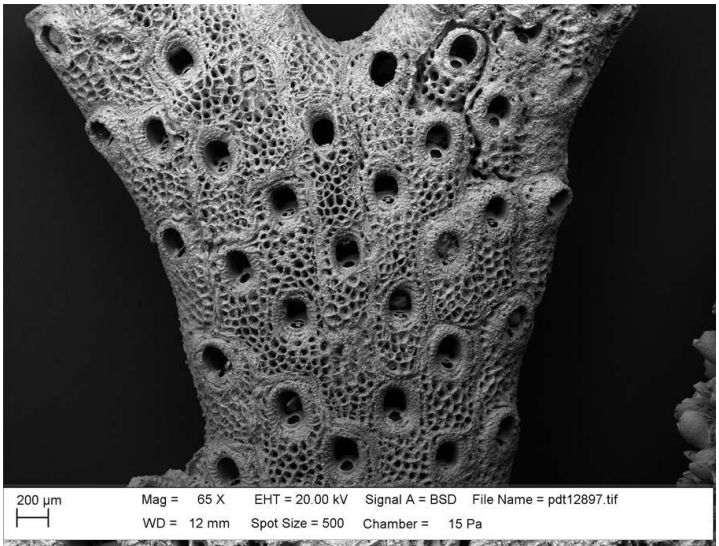

Sample ID: pdt12898
Name: *Porella cf. cervicornis (Pallas, 1766)*
Age: Recent
Cruise/Expedition: POS366
Station ID: POS13015
Location: Outer Banc d'Arguin
Country: Mauritania
Water depth: 125 mbsl
GPS: N20°33.99' / W17°31.98'
Date: 2009

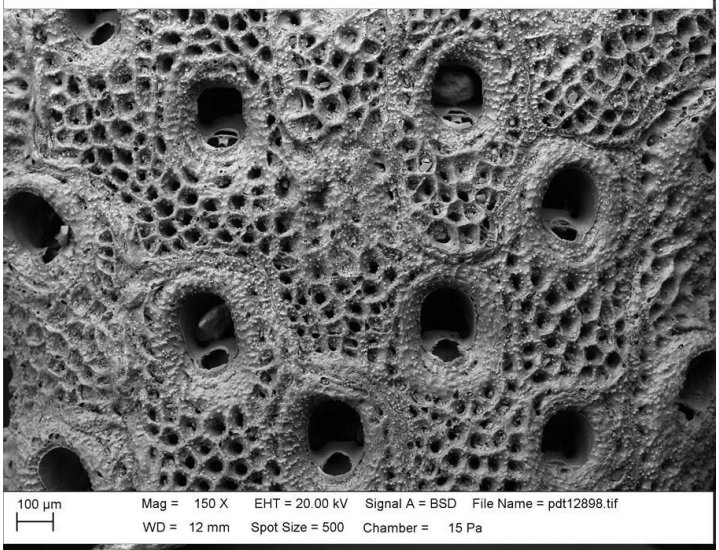

Sample ID: pdt12899
Name: *celleporina parvula (Canu & BAssler, 1928)*
Age: Recent
Cruise/Expedition: POS366
Station ID: POS13015
Location: Outer Banc d'Arguin
Country: Mauritania
Water depth: 125 mbsl
GPS: N20°33.99' / W17°31.98'
Date: 2009

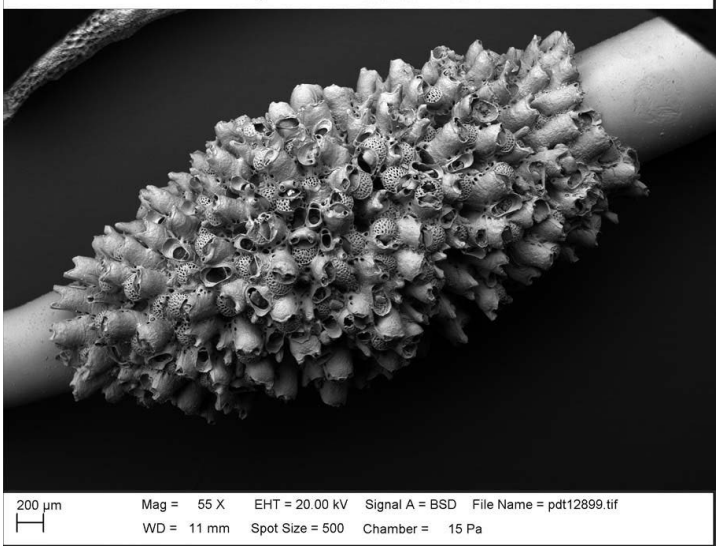

Sample ID: pdt12900
Name: *Porella cf. cervicornis (Pallas, 1766)*
Age: Recent
Cruise/Expedition: POS366
Station ID: POS13015
Location: Outer Banc d'Arguin
Country: Mauritania
Water depth: 125 mbsl
GPS: N20°33.99' / W17°31.98'
Date: 2009

Sample ID: pdt12901
Name: *Turbicellepora coronopus (Wood, 1844)*
Age: Recent
Cruise/Expedition: MSM16-3
Station ID: GeoB14717-1
Location: Outer Shelf of Golfe d'Arguin
Country: Mauritania
Water depth: 69 mbsl
GPS: N20°01.573'/ W17°29.265'
Date: October 2010

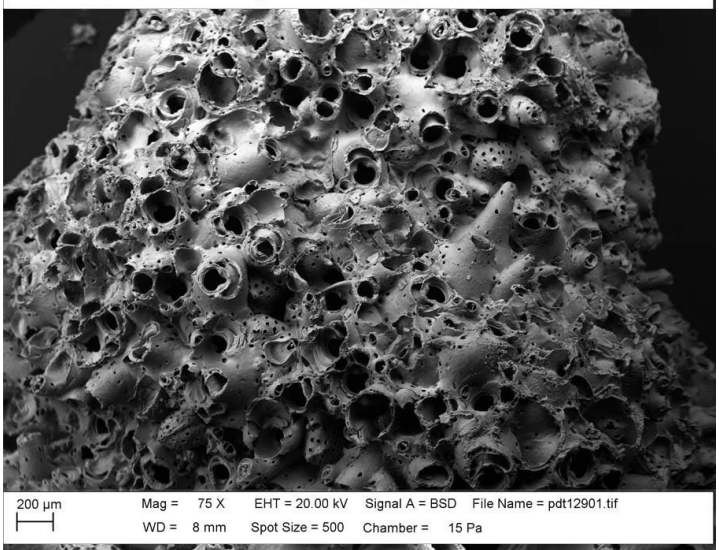

Sample ID: pdt12902
Name: *Turbicellepora coronopus (Wood, 1844)*
Age: Recent
Cruise/Expedition: MSM16-3
Station ID: GeoB14717-1
Location: Outer Shelf of Golfe d'Arguin
Country: Mauritania
Water depth: 69 mbsl
GPS: N20°01.573'/ W17°29.265'
Date: October 2010

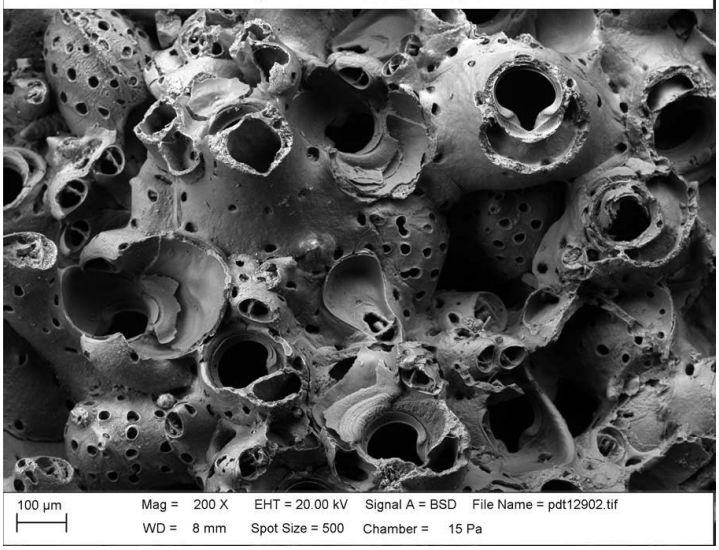

Sample ID: pdt12903
Name: *Poricella oranensis (Waters, 1918)*
Age: Recent
Cruise/Expedition: MSM16-3
Station ID: GeoB14764-1
Location: Cap Timiris Shelf
Country: Mauritania
Water depth: 56 mbsl
GPS: N19°07.381' / W16°34.976'
Date: October 2010

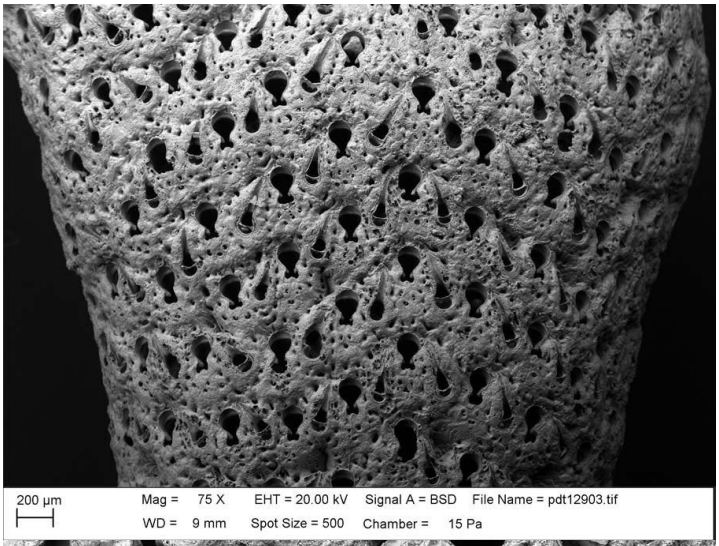

Sample ID: pdt12904
Name: *Poricella oranensis (Waters, 1918)*
Age: Recent
Cruise/Expedition: MSM16-3
Station ID: GeoB14764-1
Location: Cap Timiris Shelf
Country: Mauritania
Water depth: 56 mbsl
GPS: N19°07.381' / W16°34.976'
Date: October 2010

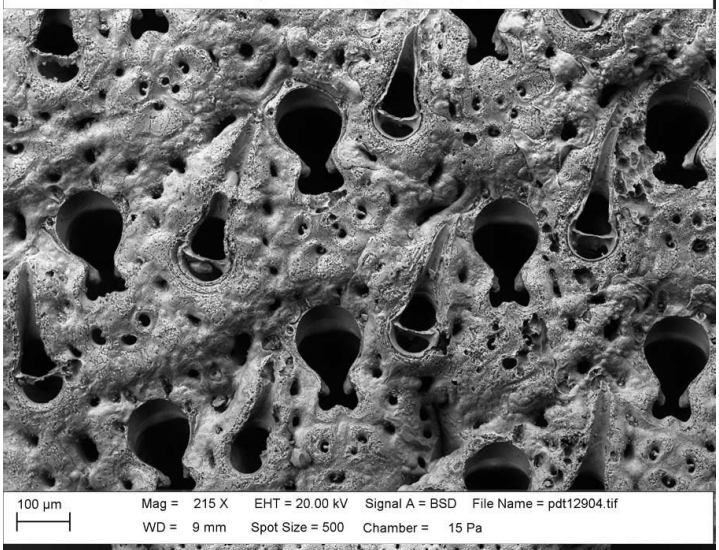

Sample ID: pdt12905
Name: *Diporula verrucosa (Peachs, 1968)*
Age: Recent
Cruise/Expedition: MSM16-3
Station ID: GeoB14764-1
Location: Cap Timiris Shelf
Country: Mauritania
Water depth: 56 mbsl
GPS: N19°07.381' / W16°34.976'
Date: October 2010

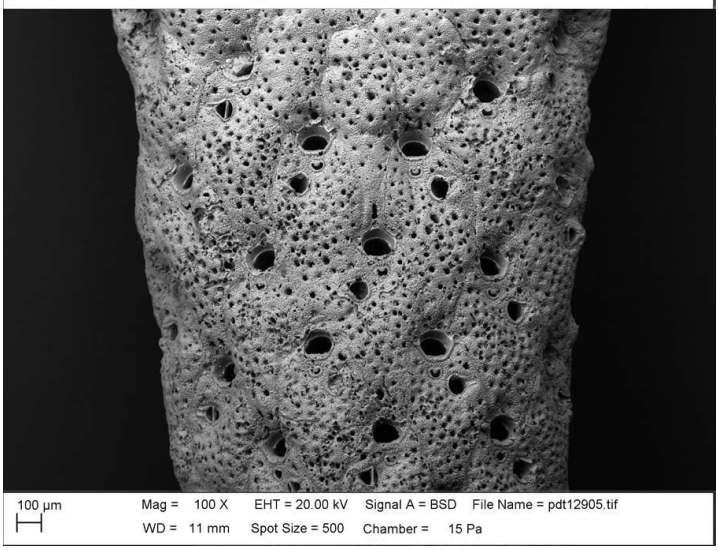

Sample ID: pdt12906
Name: *Diporula verrucosa (Peachs, 1968)*
Age: Recent
Cruise/Expedition: MSM16-3
Station ID: GeoB14764-1
Location: Cap Timiris Shelf
Country: Mauritania
Water depth: 56 mbsl
GPS: N19°07.381' / W16°34.976'
Date: October 2010

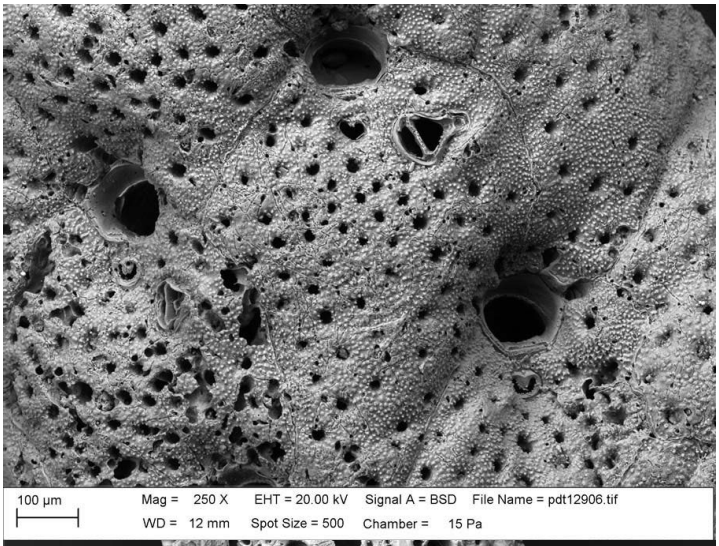

Sample ID: pdt12907
Name: *Arachnipusia*
Age: Recent
Cruise/Expedition: MSM16-3
Station ID: GeoB14764-1
Location: Cap Timiris Shelf
Country: Mauritania
Water depth: 56 mbsl
GPS: N19°07.381' / W16°34.976'
Date: October 2010

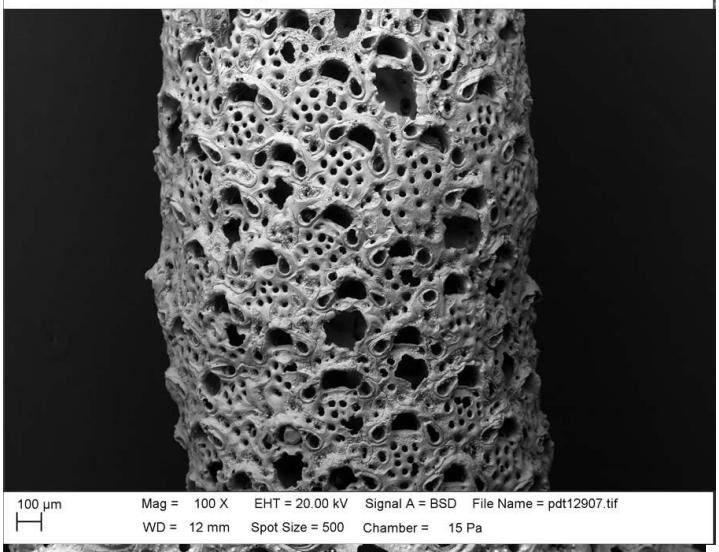

Sample ID: pdt12908
Name: *Arachnipusia*
Age: Recent
Cruise/Expedition: MSM16-3
Station ID: GeoB14764-1
Location: Cap Timiris Shelf
Country: Mauritania
Water depth: 56 mbsl
GPS: N19°07.381' / W16°34.976'
Date: October 2010

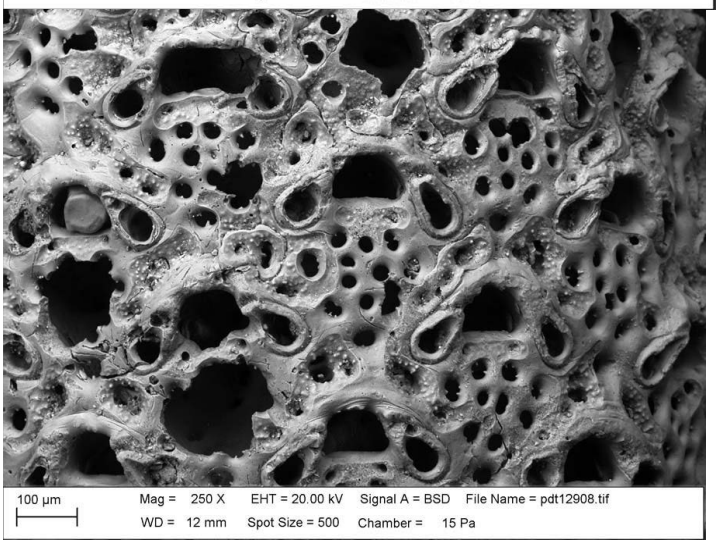

Sample ID: pdt12909
Name: *Exidmonea ingens (Canu & Bassler, 1928)*
Age: Recent
Cruise/Expedition: MSM16-3
Station ID: GeoB14764-1
Location: Cap Timiris Shelf
Country: Mauritania
Water depth: 56 mbsl
GPS: N19°07.381' / W16°34.976'
Date: October 2010

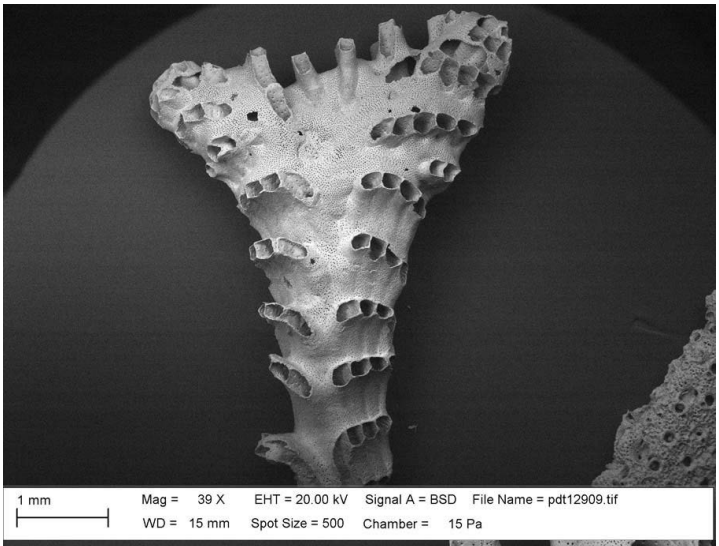

Sample ID: pdt12910
Name: *Exidmonea ingens (Canu & Bassler, 1928)*
Age: Recent
Cruise/Expedition: MSM16-3
Station ID: GeoB14764-1
Location: Cap Timiris Shelf
Country: Mauritania
Water depth: 56 mbsl
GPS: N19°07.381' / W16°34.976'
Date: October 2010

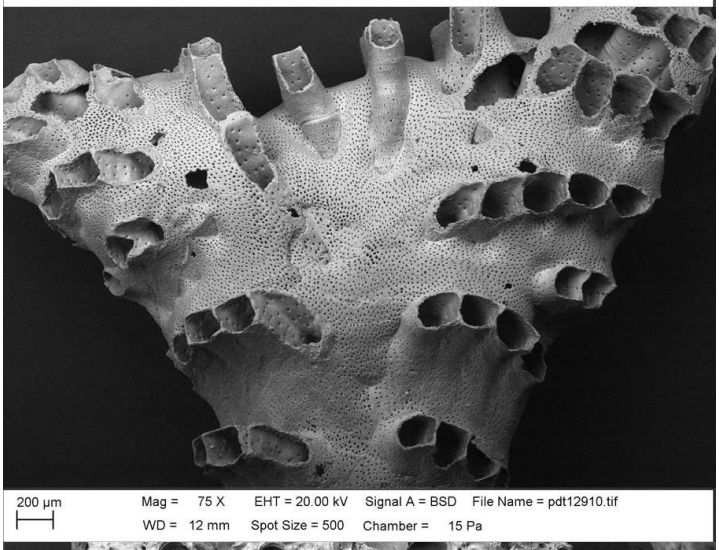

Sample ID: pdt12911
Name: *cf. Cosciniopsis*
Age: Recent
Cruise/Expedition: MSM16-3
Station ID: GeoB14764-1
Location: Cap Timiris Shelf
Country: Mauritania
Water depth: 56 mbsl
GPS: N19°07.381' / W16°34.976'
Date: October 2010

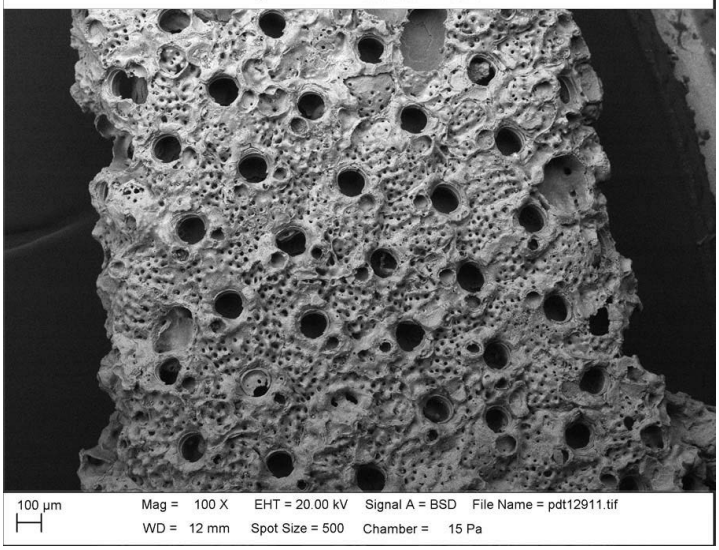

Sample ID: pdt12912
Name: *cf. Cosciniopsis*
Age: Recent
Cruise/Expedition: MSM16-3
Station ID: GeoB14764-1
Location: Cap Timiris Shelf
Country: Mauritania
Water depth: 56 mbsl
GPS: N19°07.381' / W16°34.976'
Date: October 2010

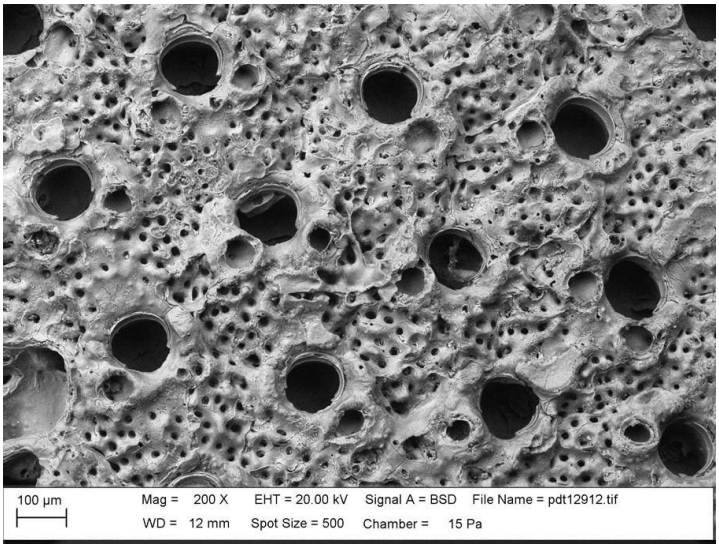

Sample ID: pdt12913
Name: *Reussirella sp.A*
Age: Recent
Cruise/Expedition: MSM16-3
Station ID: GeoB14764-1
Location: Cap Timiris Shelf
Country: Mauritania
Water depth: 56 mbsl
GPS: N19°07.381' / W16°34.976'
Date: October 2010

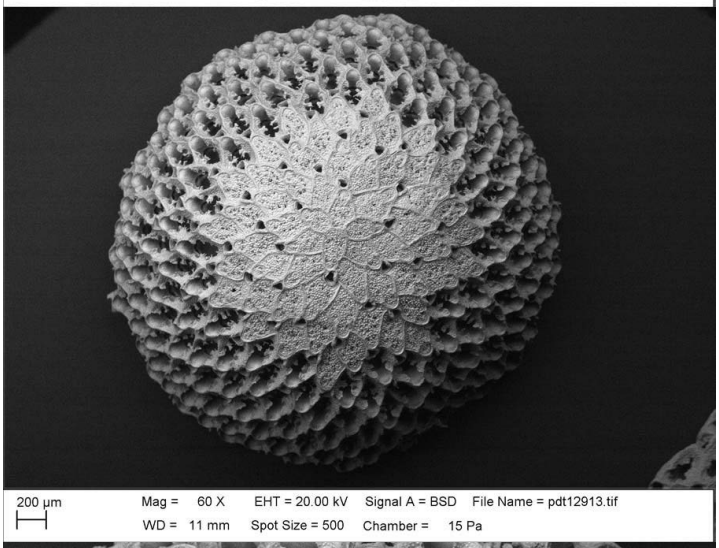

Sample ID: pdt12914
Name: *Reussirella sp.A*
Age: Recent
Cruise/Expedition: MSM16-3
Station ID: GeoB14764-1
Location: Cap Timiris Shelf
Country: Mauritania
Water depth: 56 mbsl
GPS: N19°07.381' / W16°34.976'
Date: October 2010

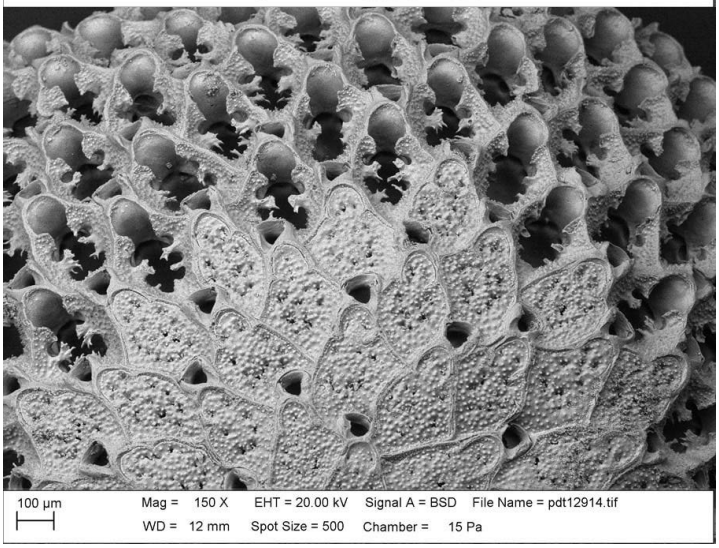

Sample ID: pdt12915
Name: *Reussirella sp.B*
Age: Recent
Cruise/Expedition: MSM16-3
Station ID: GeoB14764-1
Location: Cap Timiris Shelf
Country: Mauritania
Water depth: 56 mbsl
GPS: N19°07.381' / W16°34.976'
Date: October 2010

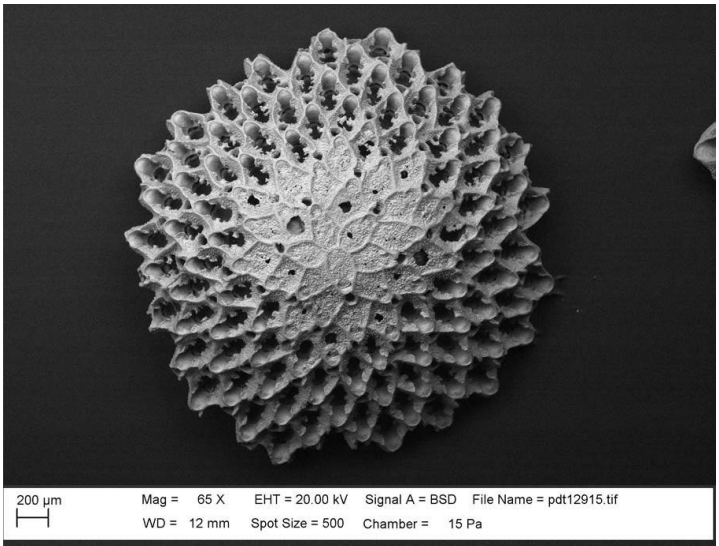

Sample ID: pdt12916
Name: *Reussirella sp.B*
Age: Recent
Cruise/Expedition: MSM16-3
Station ID: GeoB14764-1
Location: Cap Timiris Shelf
Country: Mauritania
Water depth: 56 mbsl
GPS: N19°07.381' / W16°34.976'
Date: October 2010

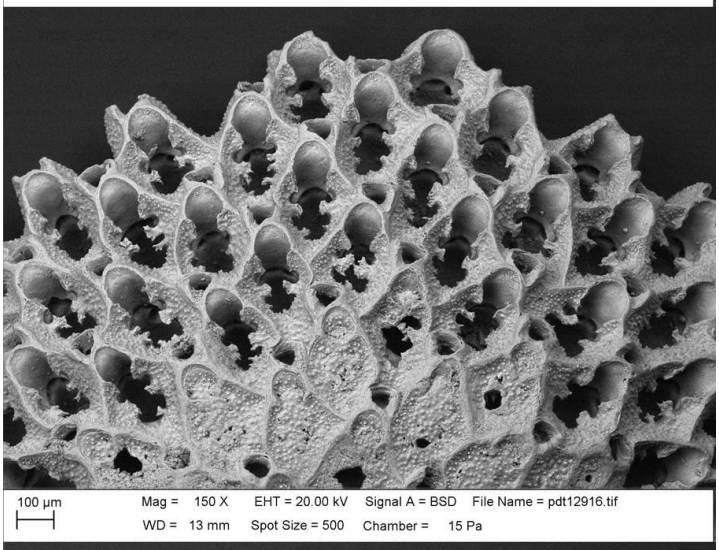

Sample ID: pdt12917
Name: *Reussirella sp.C*
Age: Recent
Cruise/Expedition: MSM16-3
Station ID: GeoB14764-1
Location: Cap Timiris Shelf
Country: Mauritania
Water depth: 56 mbsl
GPS: N19°07.381' / W16°34.976'
Date: October 2010

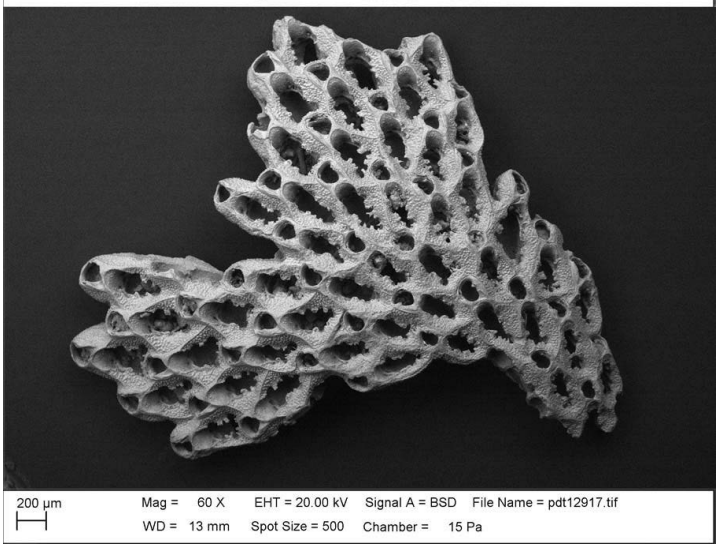

Sample ID: pdt12918
Name: *Reussirella sp.C*
Age: Recent
Cruise/Expedition: MSM16-3
Station ID: GeoB14764-1
Location: Cap Timiris Shelf
Country: Mauritania
Water depth: 56 mbsl
GPS: N19°07.381' / W16°34.976'
Date: October 2010

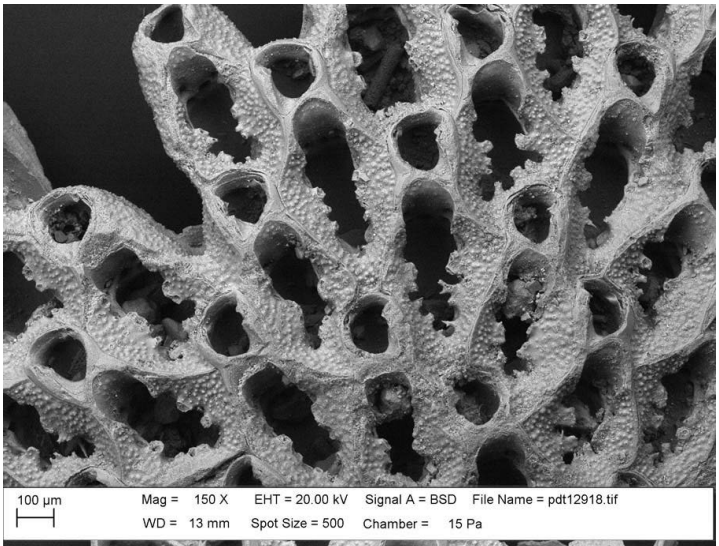

Sample ID: pdt12920
Name: *Reussirella sp.C*
Age: Recent
Cruise/Expedition: MSM16-3
Station ID: GeoB14764-1
Location: Cap Timiris Shelf
Country: Mauritania
Water depth: 56 mbsl
GPS: N19°07.381' / W16°34.976'
Date: October 2010

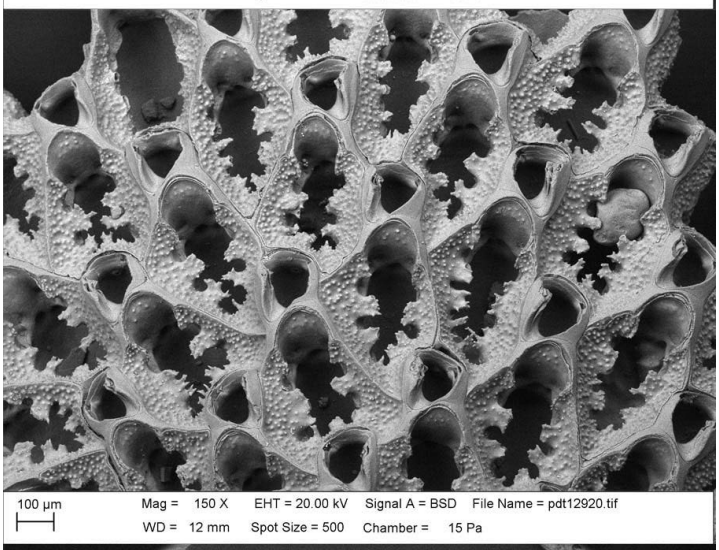

Sample ID: pdt12921
Name: *Discoporella*
Age: Recent
Cruise/Expedition: MSM16-3
Station ID: GeoB14764-1
Location: Cap Timiris Shelf
Country: Mauritania
Water depth: 56 mbsl
GPS: N19°07.381' / W16°34.976'
Date: October 2010

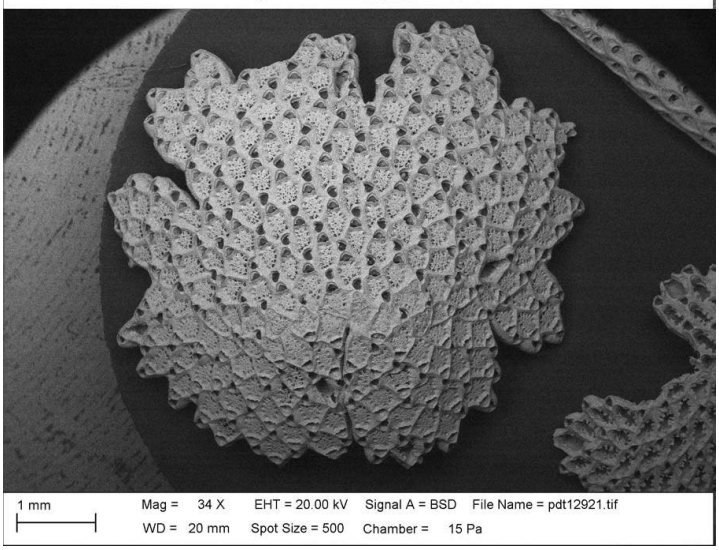

Sample ID: pdt12922
Name: *Discoporella*
Age: Recent
Cruise/Expedition: MSM16-3
Station ID: GeoB14764-1
Location: Cap Timiris Shelf
Country: Mauritania
Water depth: 56 mbsl
GPS: N19°07.381' / W16°34.976'
Date: October 2010

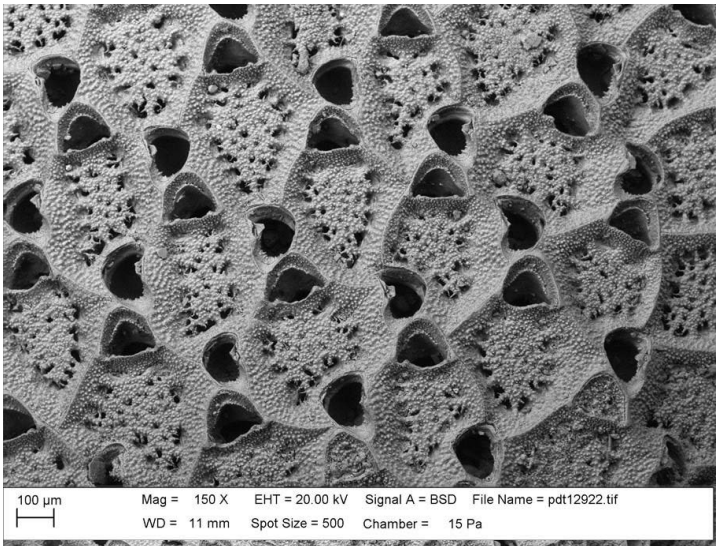

Sample ID: pdt12923
Name: *Discoporella*
Age: Recent
Cruise/Expedition: MSM16-3
Station ID: GeoB14764-1
Location: Cap Timiris Shelf
Country: Mauritania
Water depth: 56 mbsl
GPS: N19°07.381' / W16°34.976'
Date: October 2010

Auto-fragmentation sutur

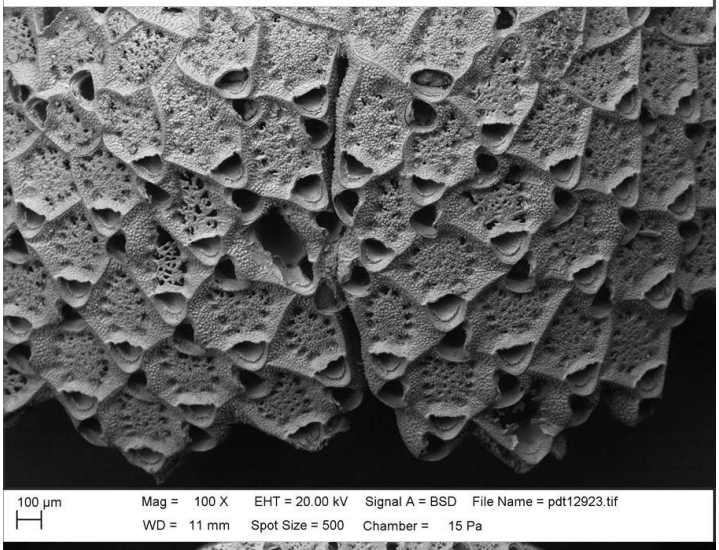

Sample ID: pdt12926
Name: *Discoporella*
Age: Recent
Cruise/Expedition:MSM16-3
Station ID: GeoB14764-1
Location: Cap Timiris Shelf
Country: Mauritania
Water depth: 56 mbsl
GPS: N19°07.381' / W16°34.976'
Date: October 2010

Asexual fragment

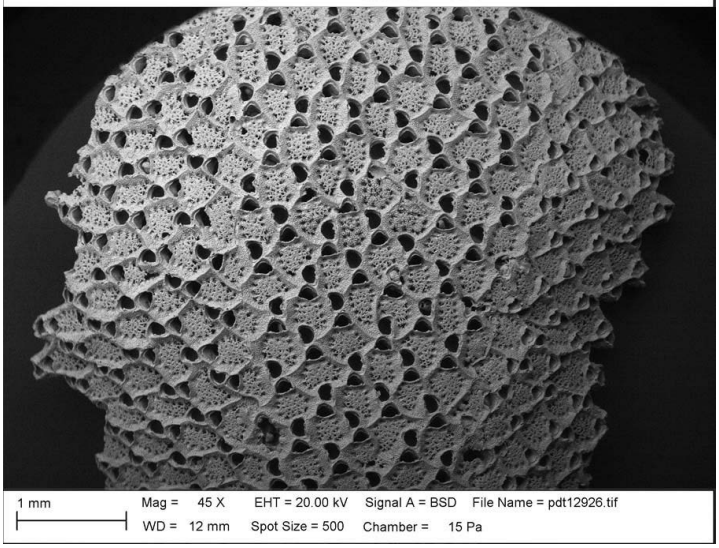

Sample ID: pdt12926
Name: *Discoporella*
Age: Recent
Cruise/Expedition: MSM16-3
Station ID: GeoB14764-1
Location: Cap Timiris Shelf
Country: Mauritania
Water depth: 56 mbsl
GPS: N19°07.381' / W16°34.976'
Date: October 2010

Asexual fragment

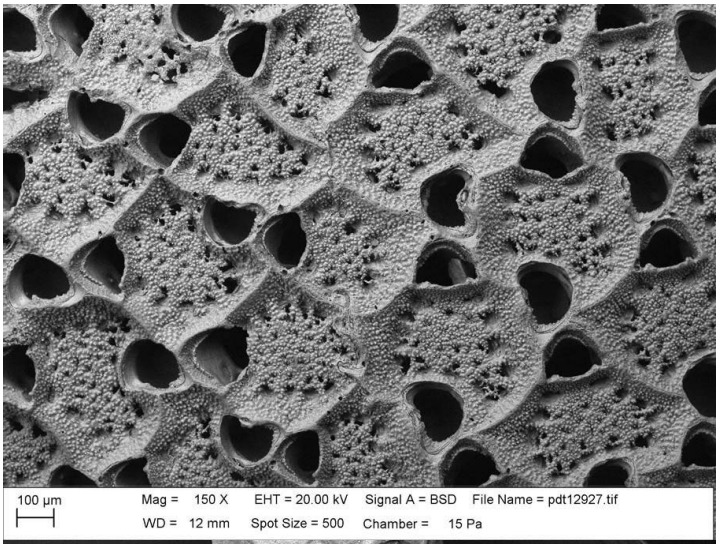

Sample ID: pdt12924
Name: *Cellaria elongata (Canu & Bassler, 1928)*
Age: Recent
Cruise/Expedition: MSM16-3
Station ID: GeoB14764-1
Location: Cap Timiris Shelf
Country: Mauritania
Water depth: 56 mbsl
GPS: N19°07.381' / W16°34.976'
Date: October 2010

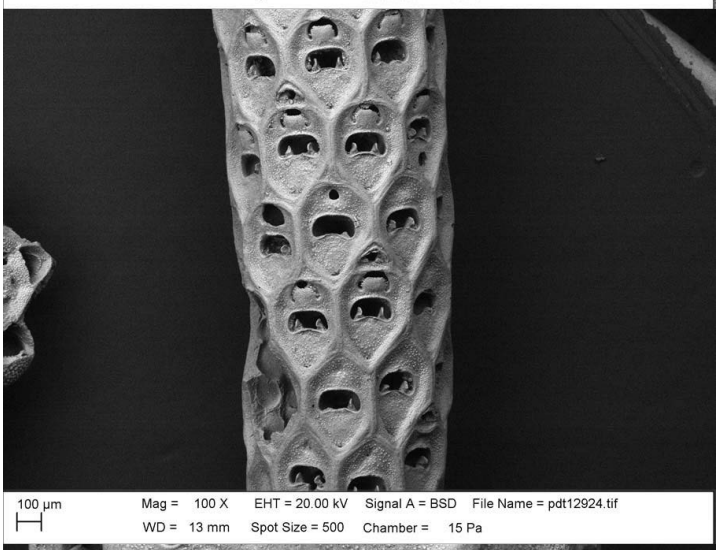

Sample ID: pdt12925
Name: *Cellaria elongata (Canu & Bassler, 1928)*
Age: Recent
Cruise/Expedition: MSM16-3
Station ID: GeoB14764-1
Location: Cap Timiris Shelf
Country: Mauritania
Water depth: 56 mbsl
GPS: N19°07.381' / W16°34.976'
Date: October 2010

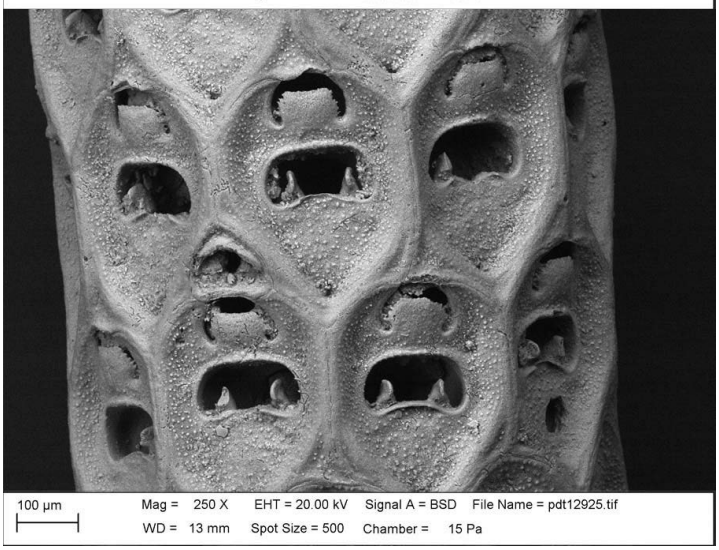

Sample ID: pdt12929
Name: *Acanthodesia sp.B*
Age: Recent
Cruise/Expedition: MSM16-3
Station ID: GeoB14764-1
Location: Cap Timiris Shelf
Country: Mauritania
Water depth: 56 mbsl
GPS: N19°07.381' / W16°34.976'
Date: October 2010

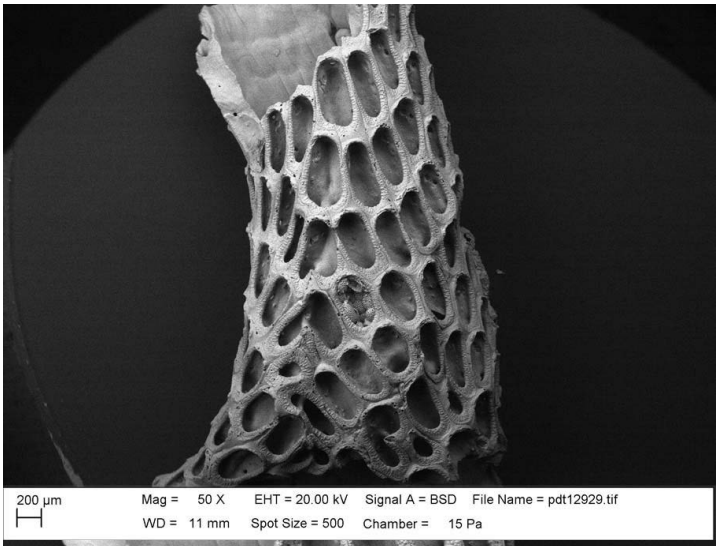

Sample ID: pdt12929
Name: *Acanthodesia sp.B*
Age: Recent
Cruise/Expedition: MSM16-3
Station ID: GeoB14764-1
Location: Cap Timiris Shelf
Country: Mauritania
Water depth: 56 mbsl
GPS: N19°07.381' / W16°34.976'
Date: October 2010

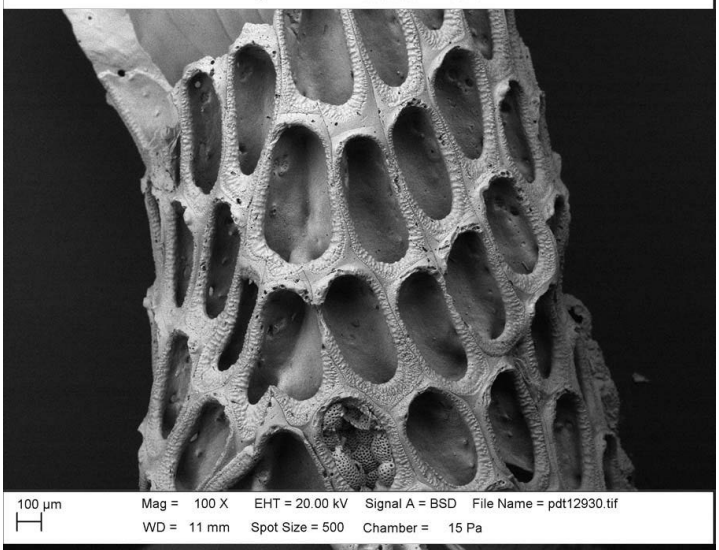

Sample ID: pdt12931
Name: *Buskea*
Age: Recent
Cruise/Expedition: MSM16-3
Station ID: GeoB14764-1
Location: Cap Timiris Shelf
Country: Mauritania
Water depth: 56 mbsl
GPS: N19°07.381' / W16°34.976'
Date: October 2010

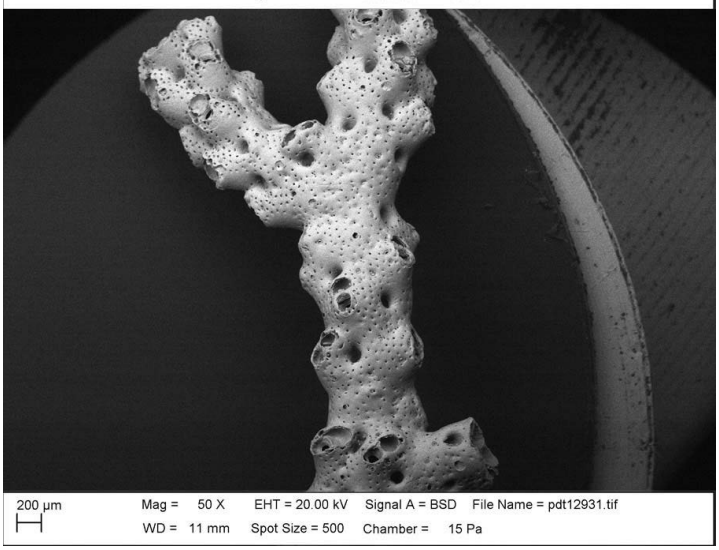

Sample ID: pdt12931
Name: *Buskea*
Age: Recent
Cruise/Expedition: MSM16-3
Station ID: GeoB14764-1
Location: Cap Timiris Shelf
Country: Mauritania
Water depth: 56 mbsl
GPS: N19°07.381' / W16°34.976'
Date: October 2010

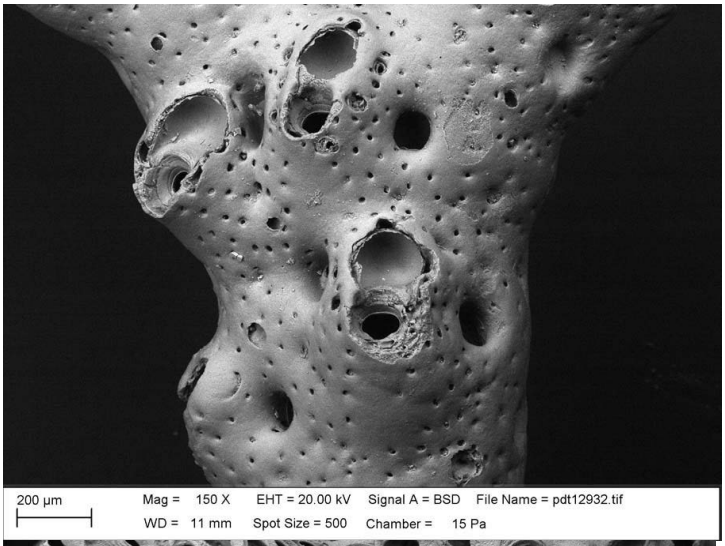

Sample ID: pdt12933
Name: *Onychocella cf. marioni (Jullien, 1881)*
Age: Recent
Cruise/Expedition: MSM16-3
Station ID: GeoB14764-1
Location: Cap Timiris Shelf
Country: Mauritania
Water depth: 56 mbsl
GPS: N19°07.381' / W16°34.976'
Date: October 2010

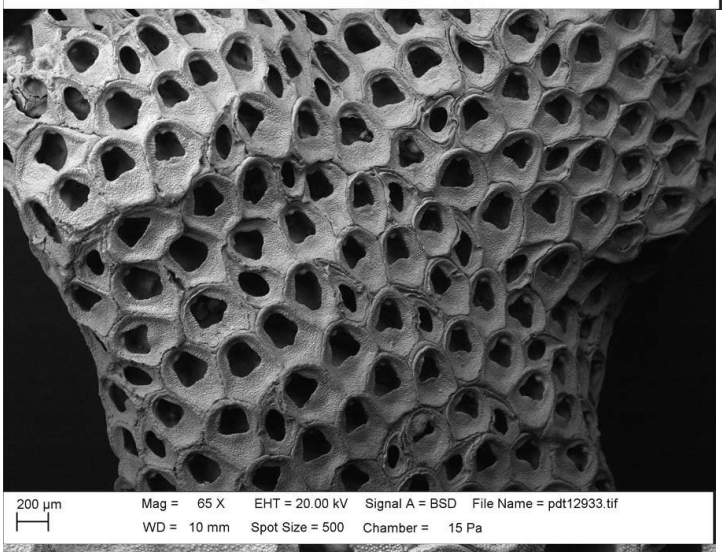

S Sample ID: pdt12934
Name: *Onychocella cf. marioni (Jullien, 1881)*
Age: Recent
Cruise/Expedition: MSM16-3
Station ID: GeoB14764-1
Location: Cap Timiris Shelf
Country: Mauritania
Water depth: 56 mbsl
GPS: N19°07.381' / W16°34.976'
Date: October 2010

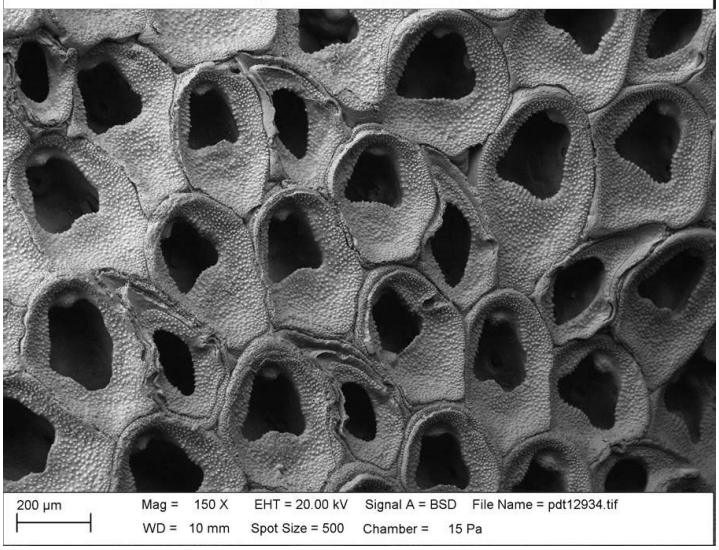

Sample ID: pdt12935
Name: *Acanthodesia commensale (Kirkpatrick & Metzelaar, 1922)*
Age: Recent
Cruise/Expedition: MSM16-3
Station ID: GeoB14833-8
Location: Central Banc d'Arguin
Country: Mauritania
Water depth: 24 mbsl
GPS: N20°09.460'/W17°19.267'
Date: November 2010

Pagurid symbiont

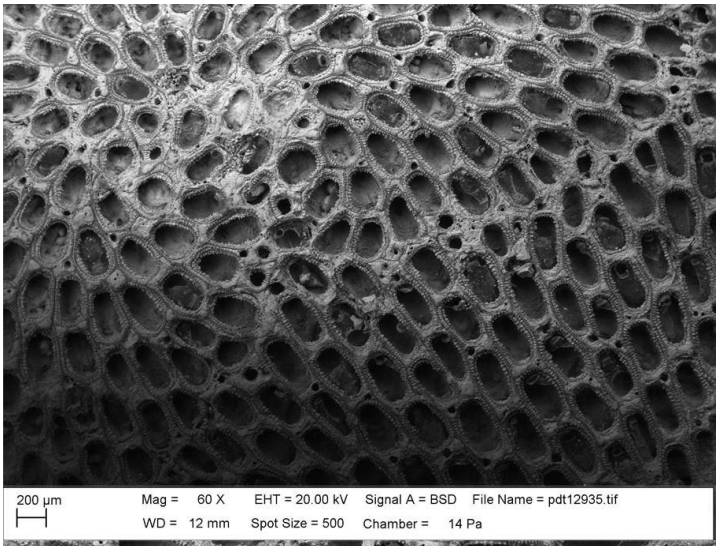

Sample ID: pdt12936
Name: *Acanthodesia commensale (Kirkpatrick & Metzelaar, 1922)*
Age: Recent
Cruise/Expedition: MSM16-3
Station ID: GeoB14833-8
Location: Central Banc d'Arguin
Country: Mauritania
Water depth: 24 mbsl
GPS: N20°09.460'/W17°19.267'
Date: November 2010

Pagurid symbiont

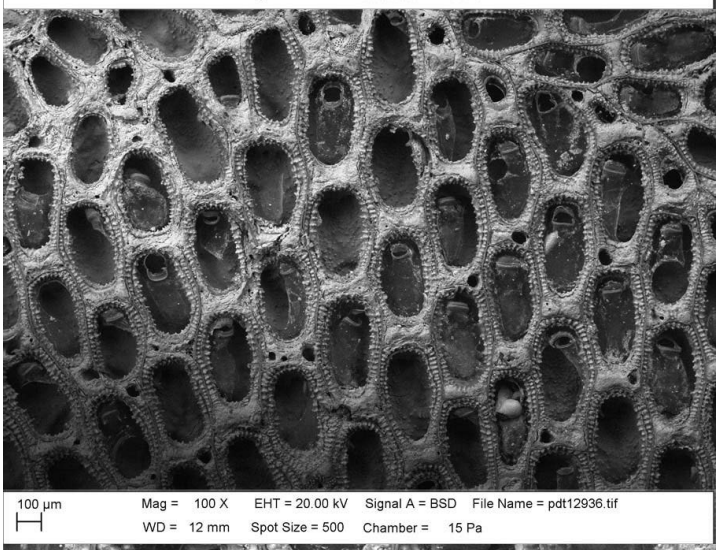

Sample ID: pdt12937
Name: *Acanthodesia commensale (Kirkpatrick & Metzelaar, 1922)*
Age: Recent
Cruise/Expedition: MSM16-3
Station ID: GeoB14833-8
Location: Central Banc d'Arguin
Country: Mauritania
Water depth: 24 mbsl
GPS: N20°09.460'/W17°19.267'
Date: November 2010

Pagurid symbiont

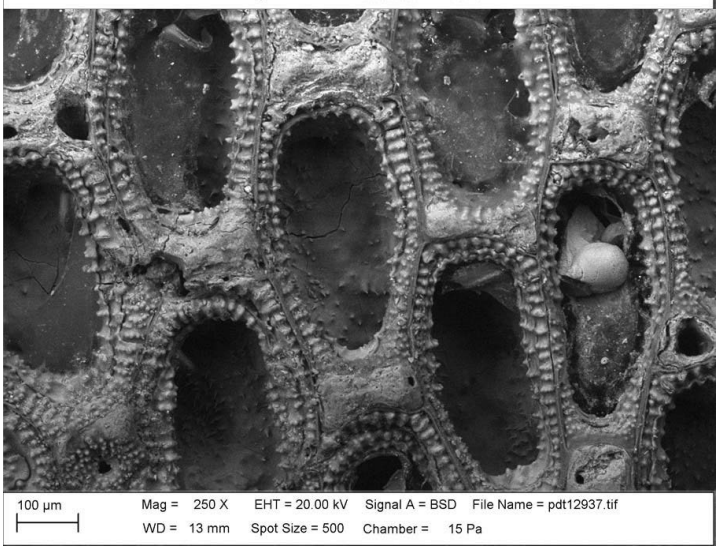

XIX. Supplements to the fourth manuscript (Uruguay)

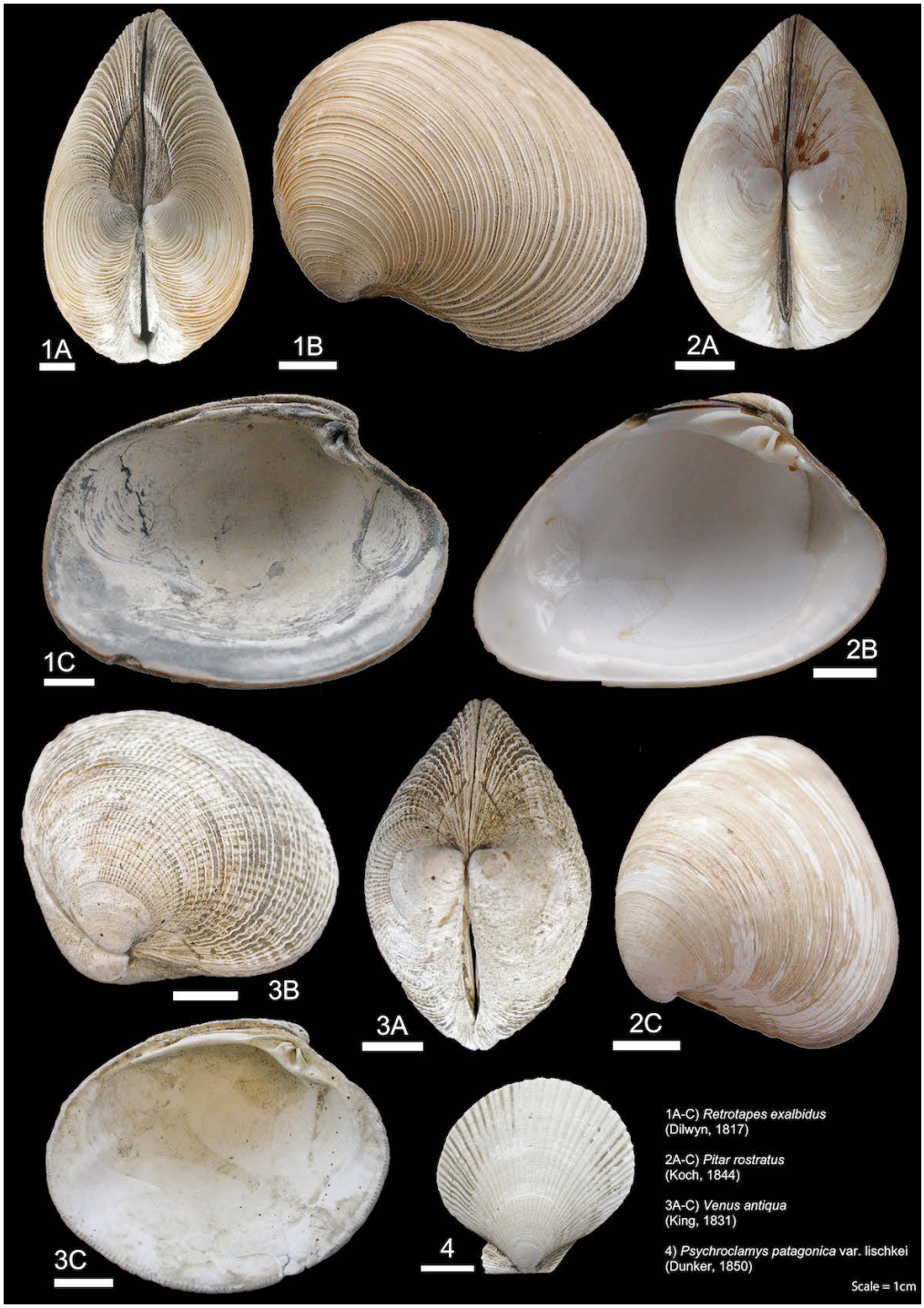

Supplement XIX.1: Fossil and recent bivalve shells sampled offshore Uruguay. *Retrotapes exalbidus (=Eurhomalea exalbida)* (1A to 1C) presented in dorsal view (1A), dorso-lateral view (1B) and internal view (1C); modern *Pitar rostratus* (2A to 2C) presented in dorsal view (2A), dorso-lateral view (2B) and internal view (2C); fossil *Venus antiqua* (3A to 3) presented in dorsal view (3A), dorso-lateral view (3B) and internal view (3C) and fossil *Zygoclamys patagonica* (4) presented in lateral view.

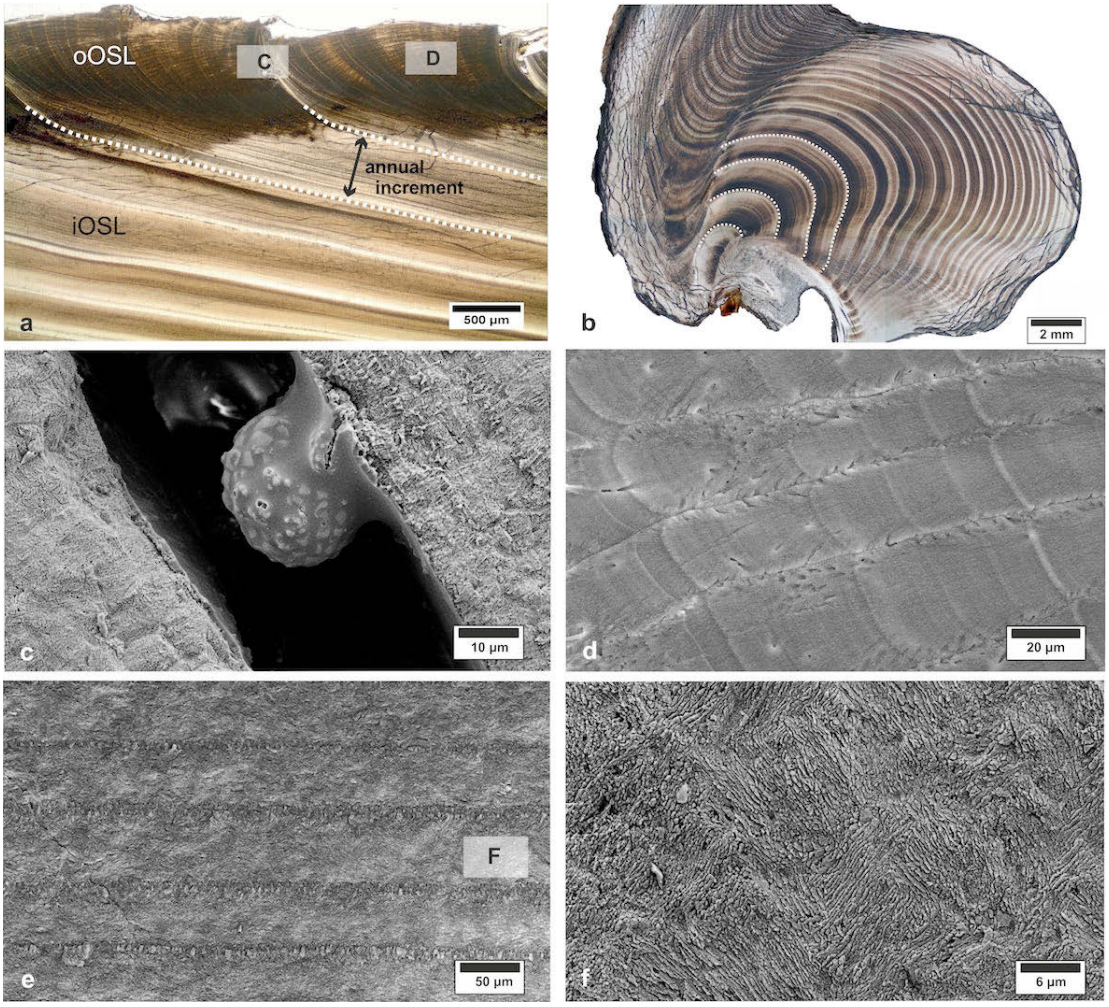

Supplement XIX.2: Thin sections (a - b) and SEM views c - f) of the bivalve samples showing shell microstructures and bioerosion features; a) *R. exalbidus* growth increments perpendicular to shell surface (under transmitted light) showing outermost outer shell layer (oOSL) and inner outer shell layer (iOSL); b) chondrophore growth record under reflected light. Dashed lines separate annual growth increments; c) iron sulphide fromboids in growth line spacing of *R. exalbidus*; d) calcitic prismatic structure in the outer shell structure of R. exalbidus providing an excellent preservation of microstructures; e) detailed view of the inner shell structure of P. rostratus showing successions of growth increments and a detailed view of the cross-lamellar structure in (f).

Supplement XIX.3: *XRD analyses of bivalve shell carbonate,* P. rostratus (extern shell, core 13813-4).

Measurement Conditions:

Probenname Klicpera-PRex
Datum / Zeit der Messung 19-apr-2012 14:37
Herkunft der Rohdaten PHILIPS-ASCII (.UDF)
Scan-Achse Gonio
Startposition [°2Th.] 10,0150
Endposition [°2Th.] 65,0050
Schrittweite [°2Th.] 0,0300
Schrittzeit [s] 2,0000
Scan Modus CONTINUOUS
Offset [°2Th.] 0,0000
Art der Divergenzblende Automatisch
Bestrahlte Länge [mm] 2,00
Probenlänge [mm] 10,00
Grösse Empfangsblende [mm] 0,1000
Temperatur der Messung [°C] 25,00
Anodenmaterial Cu
Generatoreinstellung 40 kV, 30 mA
Diffraktometer Typ ?
Diffraktometer Nummer 1
Goniometer Radius [mm] 240,00
Abstand Focus-Div.blende [mm] 91,00
Primärstrahl-Monochromator Nein
Probendrehung Nein

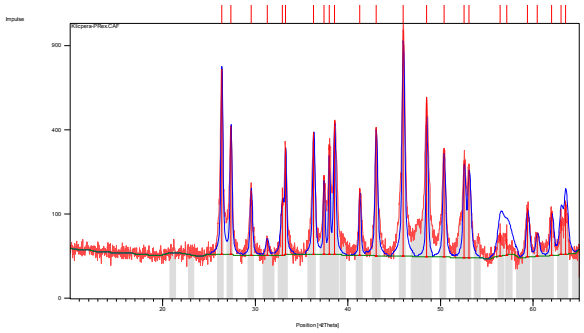

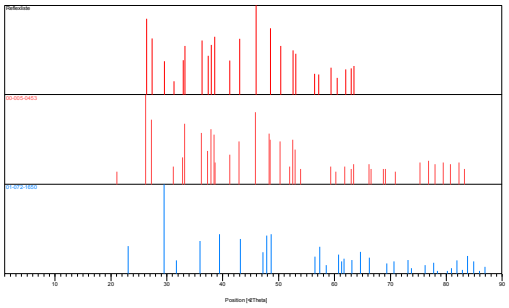

Recognized Minerals:

Score	RIR	Halbquant.[%]	Verbindungsname	ChemischeFormel	Skalierungsfaktor	PDF-Nr.
66	1,140	88	Aragonite, syn	Ca C O3	0,510	00-005-0453
39	3,220	12	Calcite	Ca C O3	0,195	01-072-1650

Peak List:

Pos. [°2Th.]	d-Wert [Å]	Höhe [cts]	FWHM [°2Th.]	Höhe [cps]	Fläche [cps*°2Th.]	Fläche [cts*°2Th.]	Zuordnung	Erklärt durch
26,3770	3,37900	715,89	0,1771	357,94	62,54	125,08	KA1 + KA2	00-005-0453
27,3650	3,25920	391,50	0,1771	195,75	34,20	68,40	KA1 + KA2	00-005-0453
29,5505	3,02295	138,72	0,2362	69,36	16,16	32,32	KA1 + KA2	01-072-1650
31,2765	2,85996	22,93	0,3542	11,46	4,01	8,01	KA1 + KA2	00-005-0453
32,9354	2,71960	146,66	0,3844	73,33	18,79	37,58	KA1 + KA2	00-005-0453
33,2621	2,69362	295,05	0,1476	147,53	21,48	42,96	KA1 + KA2	00-005-0453
36,3002	2,47486	361,47	0,2362	180,73	42,10	84,21	KA1 + KA2	00-005-0453
37,4034	2,40436	185,73	0,1476	92,87	13,52	27,04	KA1 + KA2	00-005-0453
37,9784	2,36927	306,90	0,1181	153,45	17,87	35,75	KA1 + KA2	00-005-0453
38,5530	2,33527	417,27	0,2066	208,63	42,53	85,06	KA1 + KA2	00-005-0453
41,2760	2,18729	144,27	0,1771	72,13	12,60	25,21	KA1 + KA2	00-005-0453
43,0469	2,10132	387,38	0,2362	193,69	45,12	90,24	KA1 + KA2	00-005-0453; 01-072-1650
45,9689	1,97433	993,27	0,2066	496,63	101,23	202,47	KA1 + KA2	00-005-0453
48,5091	1,87671	547,48	0,1476	273,74	39,86	79,71	KA1 + KA2	00-005-0453; 01-072-1650
50,3783	1,81138	293,46	0,2362	146,73	34,18	68,37	KA1 + KA2	00-005-0453
52,5621	1,74115	244,93	0,2362	122,47	28,53	57,06	KA1 + KA2	00-005-0453
53,0938	1,72496	208,21	0,2952	104,10	30,32	60,63	KA1 + KA2	00-005-0453
56,4600	1,62985	53,83	0,6146	26,92	16,54	33,08	KA1 + KA2	01-072-1650
57,1500	1,61180	50,70	1,1566	25,35	29,32	58,64	KA1 + KA2	01-072-1650
59,3923	1,55619	90,75	0,2952	45,38	13,21	26,43	KA1 + KA2	00-005-0453
60,4486	1,53150	34,42	0,3542	17,21	6,01	12,03	KA1 + KA2	00-005-0453; 01-072-1650
62,0114	1,49661	80,30	0,2952	40,15	11,69	23,38	KA1 + KA2	00-005-0453; 01-072-1650
63,0116	1,47524	86,10	0,3666	43,05	15,78	31,57	KA1 + KA2	00-005-0453; 01-072-1650
63,5036	1,46378	102,93	0,3600	51,46	24,70	49,41	Nur KA1	00-005-0453

Supplement XIX.4: *XRD analyses of bivalve shell carbonate*, P. rostratus (intern shell, core 13813-4).

Measurement Conditions:

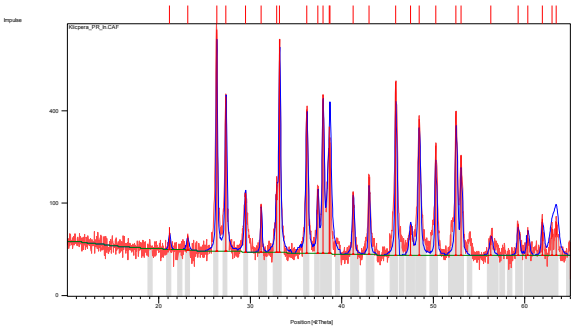

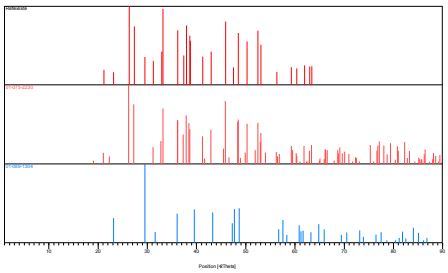

Probenname Klicpera-PRin
Datum / Zeit der Messung 19.04.2012 10:57:59
Bediener mess
Herkunft der Rohdaten XRD measurement (*.XRDML)
Scan-Achse Gonio
Startposition [°2Th.] 10,0150
Endposition [°2Th.] 65,0050
Schrittweite [°2Th.] 0,0300
Schrittzeit [s] 2,0000
Scan Modus Continuous
Offset [°2Th.] 0,0000
Art der Divergenzblende Automatisch
Bestrahlte Länge [mm] 2,00
Probenlänge [mm] 10,00
Grösse Empfangsblende [mm] 0,1000
Temperatur der Messung [°C] 25,00
Anodenmaterial Cu
Generatoreinstellung 40 kV, 30 mA
Goniometer Radius [mm] 200,00
Abstand Focus-Div.blende [mm] 91,00
Primärstrahl-Monochromator Nein
Probendrehung Ja

Recognized Minerals:

Score	RIR	Halbquant.[%]	Verbindungsname	ChemischeFormel	Skalierungsfaktor	PDF-Nr.
76	1,140	94	Aragonite	Ca (C O3)	0,846	01-075-2230
37	3,120	6	Calcite, magn.syn	(Mg0.03Ca0.97)(C O3)	0,144	01-089-1304

Peak List:

Pos. [°2Th.]	d-Wert [Å]	Höhe [cts]	FWHM [°2Th.]	Höhe [cps]	Fläche [cps*°2Th.]	Fläche [cts*°2Th.]	Zuordnung	Erklärt durch
21,1720	4,19647	29,60	0,2122	14,80	2,09	4,19	KA1 + KA2	01-075-2230
23,1483	3,84247	20,86	0,2948	10,43	2,05	4,10	KA1 + KA2	01-089-1304
26,3242	3,38566	803,61	0,1181	401,80	46,80	93,60	KA1 + KA2	01-075-2230
27,3363	3,26257	440,66	0,1771	220,33	38,50	76,99	KA1 + KA2	01-075-2230
29,4779	3,03023	101,20	0,2952	50,60	14,73	29,47	KA1 + KA2	01-089-1304
31,1926	2,86746	74,59	0,1476	37,29	5,43	10,86	KA1 + KA2	01-075-2230
32,9006	2,72240	144,70	0,2651	72,35	12,79	25,57	KA1 + KA2	01-075-2230
33,2040	2,69821	747,11	0,1476	373,55	54,39	108,78	KA1 + KA2	01-075-2230
36,1801	2,48280	384,58	0,2066	192,29	39,20	78,39	KA1 + KA2	01-075-2230; 01-089-1304
37,3799	2,40582	111,30	0,1771	55,65	9,72	19,45	KA1 + KA2	01-075-2230
37,9534	2,37077	453,58	0,1771	226,79	39,62	79,25	KA1 + KA2	01-075-2230
38,6236	2,33117	313,44	0,4313	156,72	45,06	90,12	KA1 + KA2	01-075-2230
38,7204	2,32556	252,90	0,1181	126,45	14,73	29,46	KA1 + KA2	01-075-2230
41,2361	2,18931	104,30	0,2066	52,15	10,63	21,26	KA1 + KA2	01-075-2230
42,9802	2,10443	143,84	0,1476	71,92	10,47	20,94	KA1 + KA2	01-075-2230
45,8986	1,97718	514,18	0,1476	257,09	37,43	74,86	KA1 + KA2	01-075-2230
47,5146	1,91364	39,50	0,3235	19,75	6,39	12,78	KA1 + KA2	01-089-1304
48,4569	1,87861	345,96	0,2066	172,98	35,26	70,52	KA1 + KA2	01-075-2230; 01-089-1304
50,2659	1,81517	244,12	0,1476	122,06	17,77	35,54	KA1 + KA2	01-075-2230
52,4863	1,74349	378,87	0,1771	189,44	33,10	66,20	KA1 + KA2	01-075-2230
53,0403	1,72657	210,10	0,1476	105,05	15,30	30,59	KA1 + KA2	01-075-2230
56,3108	1,63381	22,30	0,3542	11,15	3,90	7,79	KA1 + KA2	01-075-2230
59,2814	1,55884	41,47	0,2362	20,73	4,83	9,66	KA1 + KA2	01-075-2230
60,3325	1,53417	35,60	0,2088	17,80	3,72	7,43	KA1 + KA2	01-075-2230

Supplement XIX.5: *XRD analyses of bivalve shell carbonate*, E. exalbida (extern shell, core 13802-2)

Measurement Conditions:

Probenname Klicpera_re_In
Datum / Zeit der Messung 19.04.2012 13:02:43
Bediener mess
Herkunft der Rohdaten XRD measurement (*.XRDML)
Scan-Achse Gonio
Startposition [°2Th.] 10,0150
Endposition [°2Th.] 65,0050
Schrittweite [°2Th.] 0,0300
Schrittzeit [s] 2,0000
Scan Modus Continuous
Offset [°2Th.] 0,0000
Art der Divergenzblende Automatisch
Bestrahlte Länge [mm] 2,00
Probenlänge [mm] 10,00
Grösse Empfangsblende [mm] 0,1000
Temperatur der Messung [°C] 25,00
Anodenmaterial Cu
Generatoreinstellung 40 kV, 30 mA
Goniometer Radius [mm] 200,00
Abstand Focus-Div.blende [mm] 91,00
Primärstrahl-Monochromator Nein
Probendrehung Ja

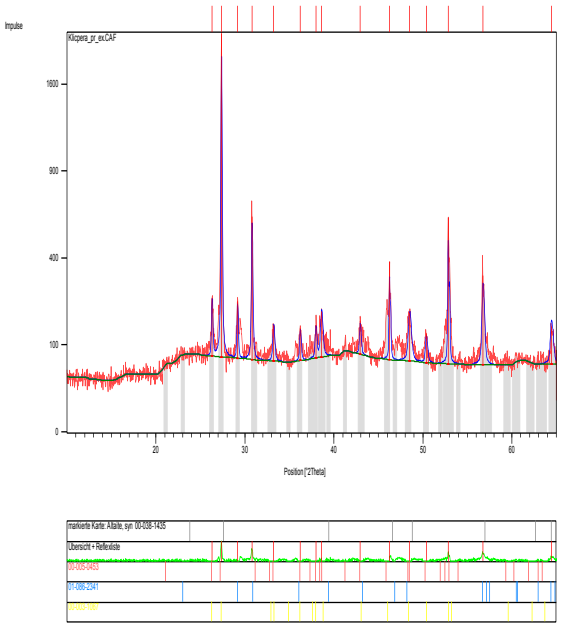

Recognized Minerals:

Score	RIR	Halbquant.[%]	Verbindungsname	ChemischeFormel	Skalierungsfaktor	PDF-Nr.
51	1,140	27	Aragonite, syn	Ca C O3	0,105	00-005-0453
39	2,820	8	Calcite	Ca (C O3)	0,080	01-086-2341
37	1,140	64	Aragonite	Ca C O3	0,243	00-003-1067

Peak List:

Pos. [°2Th.]	d-Wert [Å]	Höhe [cts]	FWHM [°2Th.]	Höhe [cps]	Fläche [cps*°2Th.]	Fläche [cts*°2Th.]	Zuordnung	Erklärt durch
26,3038	3,38823	160,77	0,1476	80,39	11,70	23,41	KA1 + KA2	00-005-0453; 00-003-1067
27,3579	3,26004	2021,69	0,1181	1010,85	117,74	235,49	KA1 + KA2	00-005-0453; 00-003-1067
29,1611	3,06242	153,43	0,1476	76,72	11,17	22,34	KA1 + KA2	01-086-2341
30,7908	2,90395	542,28	0,1476	271,14	39,48	78,96	KA1 + KA2	01-086-2341
33,2264	2,69644	84,04	0,2362	42,02	9,79	19,58	KA1 + KA2	00-005-0453; 00-003-1067
36,2169	2,48036	74,90	0,1771	37,45	6,54	13,09	KA1 + KA2	00-005-0453; 01-086-2341; 00-003-1067
37,9725	2,36963	78,89	0,1771	39,44	6,89	13,78	KA1 + KA2	00-005-0453; 00-003-1067
38,6098	2,33197	118,20	0,2952	59,10	17,21	34,42	KA1 + KA2	00-005-0453; 00-003-1067
42,9469	2,10598	83,53	0,1771	41,77	7,30	14,59	KA1 + KA2	00-005-0453; 00-003-1067
46,2478	1,96307	312,64	0,1181	156,32	18,21	36,42	KA1 + KA2	00-003-1067
48,5079	1,87676	122,36	0,3542	61,18	21,38	42,76	KA1 + KA2	00-005-0453; 00-003-1067
50,3751	1,81148	62,86	0,2362	31,43	7,32	14,64	KA1 + KA2	00-005-0453; 00-003-1067
52,8513	1,73230	545,90	0,1181	272,95	31,79	63,59	KA1 + KA2	00-005-0453; 00-003-1067
56,7435	1,62237	263,09	0,2362	131,54	30,64	61,29	KA1 + KA2	01-086-2341
64,4450	1,44465	85,05	0,2880	42,53	16,33	32,66	Nur KA1	01-086-2341
26,3038	3,38823	160,77	0,1476	80,39	11,70	23,41	KA1 + KA2	00-005-0453; 00-003-1067
27,3579	3,26004	2021,69	0,1181	1010,85	117,74	235,49	KA1 + KA2	00-005-0453; 00-003-1067
29,1611	3,06242	153,43	0,1476	76,72	11,17	22,34	KA1 + KA2	01-086-2341
30,7908	2,90395	542,28	0,1476	271,14	39,48	78,96	KA1 + KA2	01-086-2341
33,2264	2,69644	84,04	0,2362	42,02	9,79	19,58	KA1 + KA2	00-005-0453; 00-003-1067
36,2169	2,48036	74,90	0,1771	37,45	6,54	13,09	KA1 + KA2	00-005-0453; 01-086-2341; 00-003-1067
37,9725	2,36963	78,89	0,1771	39,44	6,89	13,78	KA1 + KA2	00-005-0453; 00-003-1067
38,6098	2,33197	118,20	0,2952	59,10	17,21	34,42	KA1 + KA2	00-005-0453; 00-003-1067
42,9469	2,10598	83,53	0,1771	41,77	7,30	14,59	KA1 + KA2	00-005-0453; 00-003-1067

Supplement XIX.6: *XRD analyses of bivalve shell carbonate*, E. exalbida (intern shell, core 13802-2)

Measurement Conditions:

Probenname Klicpera-REin
Datum / Zeit der Messung 19.04.2012 10:57:59
Bediener mess
Herkunft der Rohdaten XRD measurement (*.XRDML)
Scan-Achse Gonio
Startposition [°2Th.] 10,0150
Endposition [°2Th.] 65,0050
Schrittweite [°2Th.] 0,0300
Schrittzeit [s] 2,0000
Scan Modus Continuous
Offset [°2Th.] 0,0000
Art der Divergenzblende Automatisch
Bestrahlte Länge [mm] 2,00
Probenlänge [mm] 10,00
Grösse Empfangsblende [mm] 0,1000
Temperatur der Messung [°C] 25,00
Anodenmaterial Cu
Generatoreinstellung 40 kV, 30 mA
Goniometer Radius [mm] 200,00
Abstand Focus-Div.blende [mm] 91,00
Primärstrahl-Monochromator Nein
Probendrehung Ja

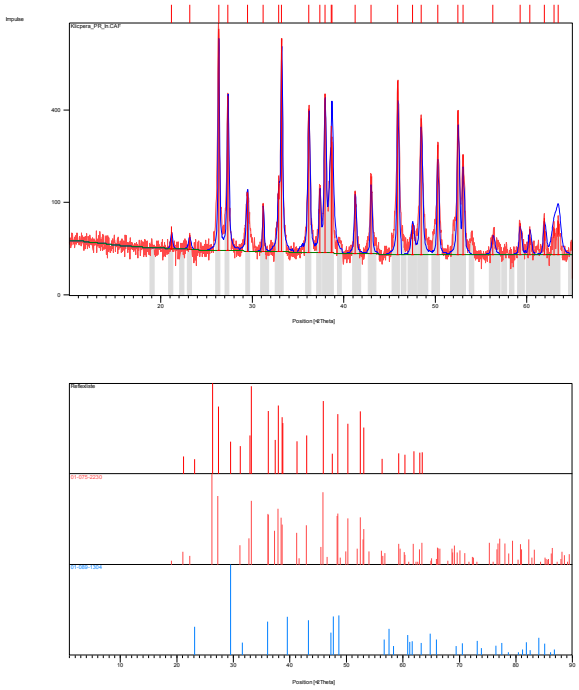

Recognized Minerals:

Score	RIR	Halbquant.[%]	Verbindungsname	ChemischeFormel	Skalierungsfaktor	PDF-Nr.
76	1,140	94	Aragonite	Ca (C O3)	0,846	01-075-2230
37	3,120	6	Calcite, magn.syn	(Mg0.03Ca0.97)(C O3)	0,144	01-089-1304

Peak List:

Pos. [°2Th.]	d-Wert [Å]	Höhe [cts]	FWHM [°2Th.]	Höhe [cps]	Fläche [cps*°2Th.]	Fläche [cts*°2Th.]	Zuordnung	Erklärt durch
21,1720	4,19647	29,60	0,2122	14,80	2,09	4,19	KA1 + KA2	01-075-2230
23,1483	3,84247	20,86	0,2948	10,43	2,05	4,10	KA1 + KA2	01-089-1304
26,3242	3,38566	803,61	0,1181	401,80	46,80	93,60	KA1 + KA2	01-075-2230
27,3363	3,26257	440,66	0,1771	220,33	38,50	76,99	KA1 + KA2	01-075-2230
29,4779	3,03023	101,20	0,2952	50,60	14,73	29,47	KA1 + KA2	01-089-1304
31,1926	2,86746	74,59	0,1476	37,29	5,43	10,86	KA1 + KA2	01-075-2230
32,9006	2,72240	144,70	0,2651	72,35	12,79	25,57	KA1 + KA2	01-075-2230
33,2040	2,69821	747,11	0,1476	373,55	54,39	108,78	KA1 + KA2	01-075-2230
36,1801	2,48280	384,58	0,2066	192,29	39,20	78,39	KA1 + KA2	01-075-2230; 01-089-1304
37,3799	2,40582	111,30	0,1771	55,65	9,72	19,45	KA1 + KA2	01-075-2230
37,9534	2,37077	453,58	0,1771	226,79	39,62	79,25	KA1 + KA2	01-075-2230
38,6236	2,33117	313,44	0,4313	156,72	45,06	90,12	KA1 + KA2	01-075-2230
38,7204	2,32556	252,90	0,1181	126,45	14,73	29,46	KA1 + KA2	01-075-2230
41,2361	2,18931	104,30	0,2066	52,15	10,63	21,26	KA1 + KA2	01-075-2230
42,9802	2,10443	143,84	0,1476	71,92	10,47	20,94	KA1 + KA2	01-075-2230
45,8986	1,97718	514,18	0,1476	257,09	37,43	74,86	KA1 + KA2	01-075-2230
47,5146	1,91364	39,50	0,3235	19,75	6,39	12,78	KA1 + KA2	01-089-1304
48,4569	1,87861	345,96	0,2066	172,98	35,26	70,52	KA1 + KA2	01-075-2230; 01-089-1304
50,2659	1,81517	244,12	0,1476	122,06	17,77	35,54	KA1 + KA2	01-075-2230
52,4863	1,74349	378,87	0,1771	189,44	33,10	66,20	KA1 + KA2	01-075-2230
53,0403	1,72657	210,10	0,1476	105,05	15,30	30,59	KA1 + KA2	01-075-2230
56,3108	1,63381	22,30	0,3542	11,15	3,90	7,79	KA1 + KA2	01-075-2230
59,2814	1,55884	41,47	0,2362	20,73	4,83	9,66	KA1 + KA2	01-075-2230
60,3325	1,53417	35,60	0,2088	17,80	3,72	7,43	KA1 + KA2	01-075-2230

Supplement XIX.7: Pitar rostratus (modern sample) δ13C- and δ18O-values of the high resolution transect from external shell sample (PR1) to shell internal shell sample (PR40) and near the ventral shell margin (PREX, PRIN1, PRIN2). Sampling procedure and sample numbering equates growth from youngest precipitated increments to latest ones, aragonite (ar) and calcite (cc) mineralogy (Min) in %. Carbon and oxygen stable isotope ratios are reported relative to the VPDB (Vienna PDB) standard.

ID	Min [ar/cc]	$\delta^{13}C$* [‰]	$\delta^{13}C$ StdDev	$\delta^{18}O$* [‰]	$\delta^{18}O$ StdDev	ID	Min [ar/cc]	$\delta^{13}C$* [‰]	$\delta^{13}C$ StdDev	$\delta^{18}O$* [‰]	$\delta^{18}O$ StdDev
PR1	94/6	1.80	0.01	0.54	0.02	PR23	94/6	-0.11	0.01	0.28	0.01
PR2	94/6	0.34	0.01	0.08	0.01	PR24	94/6	-0.46	0.01	0.02	0.01
PR3	94/6	0.32	0.01	-0.16	0.01	PR25	94/6	-0.46	0.01	0.07	0.01
PR4	94/6	0.73	0.02	0.60	0.01	PR26	94/6	-0.39	0.01	0.06	0.01
PR5	94/6	0.72	0.01	0.48	0.01	PR27	94/6	-0.09	0.01	0.02	0.01
PR6	94/6	0.97	0.01	0.54	0.01	PR28	94/6	-0.29	0.01	-0.39	0.01
PR7	94/6	1.02	0.01	0.34	0.01	PR29	94/6	-0.37	0.01	-0.09	0.02
PR8	94/6	0.93	0.01	0.18	0.01	PR30	94/6	-0.98	0.01	-0.12	0.02
PR9	94/6	0.65	0.01	-0.10	0.02	PR31	94/6	-1.30	0.01	-0.27	0.01
PR10	94/6	0.50	0.01	0.16	0.01	PR32	94/6	-1.48	0.01	-0.08	0.02
PR11	94/6	0.92	0.01	0.66	0.01	PR33	94/6	-1.35	0.01	-0.10	0.01
PR12	94/6	0.88	0.01	0.55	0.01	PR34	94/6	-1.19	0.01	-0.12	0.02
PR13	94/6	0.39	0.01	0.40	0.01	PR35	94/6	0.10	0.03	0.12	0.02
PR14	94/6	0.54	0.02	-0.09	0.01	PR36	94/6	-0.04	0.01	0.32	0.05
PR15	94/6		sample	lost		PR37	94/6	-0.08	0.01	0.01	0.01
PR16	94/6	0.93	0.01	0.68	0.02	PR38	94/6	-0.33	0.01	0.10	0.01
PR17	94/6	0.50	0.01	0.23	0.02	PR39	94/6	-0.34	0.01	0.28	0.01
PR18	94/6	0.04	0.01	0.05	0.01	PR40	94/6	-0.62	0.01	0.25	0.02
PR19	94/6	0.62	0.01	0.40	0.02						
PR20	94/6	0.06	0.02	-0.29	0.02	PRIN1	94/6	1.99	0.01	0.17	0.01
PR21	94/6	-0.23	0.01	-0.13	0.01	PRIN2	94/6	2.42	0.01	0.80	0.01
PR22	94/6	-0.31	0.01	0.02	0.01	PREX	88/12	0.69	0.01	0.53	0.01

Supplement XIX.8: *Retrotapes exalbidus* δ13C and δ18O values of the high resolution transect from the outer calcitic shell layer (RE1 – RE66) and inner aragonitic shell layer (REA1 – REA23). Sampling procedure and sample numbering equates growth from youngest to oldest increments, aragonite (ar) and calcite (cc) mineralogy (Min) in %. Carbon and oxygen stable isotope ratios are reported relative to the VPDB (Vienna PDB) standard

ID	Min [ar/cc]	$\delta^{13}C$* [‰]	$\delta^{13}C$ StdDev	$\delta^{18}O$* [‰]	$\delta^{18}O$ StdDev	ID	Min [ar/cc]	$\delta^{13}C$* [‰]	$\delta^{13}C$ StdDev	$\delta^{18}O$* [‰]	$\delta^{18}O$ StdDev
RE1	92/8	0.54	0.01	3.59	0.02	RE46	92/8	0.61	0.01	3.33	0.00
RE2	92/8	0.80	0.01	3.98	0.00	RE47	92/8	0.41	0.01	3.18	0.01
RE3	92/8	0.80	0.01	3.77	0.02	RE48	92/8	0.75	0.01	2.99	0.01
RE4	92/8	0.74	0.02	3.71	0.01	RE49	92/8	-0.27	0.01	2.45	0.01
RE5	92/8	0.79	0.01	3.80	0.01	RE50	92/8	-0.96	0.01	2.76	0.01
RE6	92/8	0.92	0.02	3.64	0.02	RE51	92/8	0.45	0.01	3.90	0.02
RE7	92/8	0.97	0.02	3.67	0.01	RE52	92/8	0.44	0.01	3.69	0.01
RE8	92/8	0.86	0.01	3.48	0.02	RE53	92/8	0.56	0.01	3.54	0.01
RE9	92/8	0.66	0.01	3.21	0.01	RE54	92/8	0.62	0.01	3.44	0.01
RE10	92/8	0.67	0.01	3.20	0.02	RE55	92/8	0.67	0.01	3.35	0.02
RE11	92/8	0.70	0.01	3.15	0.02	RE56	92/8	0.32	0.01	3.01	0.02
RE12	92/8	0.79	0.01	3.06	0.01	RE57	92/8	0.41	0.02	2.88	0.01
RE13	92/8	0.79	0.01	2.90	0.01	RE58	92/8	0.66	0.01	3.08	0.01
RE14	92/8	0.75	0.01	2.82	0.02	RE59	92/8	0.03	0.01	2.66	0.01
RE15	92/8	0.83	0.01	2.49	0.01	RE60	92/8	-1.74	0.01	3.32	0.03
RE16	92/8	0.98	0.01	2.29	0.02	RE61	92/8	0.37	0.01	3.41	0.01
RE17	92/8	-0.07	0.01	2.82	0.01	RE62	92/8	0.60	0.02	3.23	0.01
RE18	92/8	0.77	0.01	3.74	0.01	RE63	92/8	0.66	0.01	3.33	0.01
RE19	92/8	0.66	0.01	3.66	0.01	RE64	92/8	0.46	0.01	3.46	0.01
RE20	92/8	0.43	0.01	3.79	0.02	RE65	92/8	0.41	0.01	3.15	0.01
RE21	92/8	0.53	0.01	3.57	0.01	RE66	92/8	0.13	0.01	2.65	0.02
RE22	92/8	0.59	0.01	3.38	0.02						
RE23	92/8	0.57	0.01	3.37	0.01	REA1	100/0	0.36	0.01	3.11	0.01
RE24	92/8	0.55	0.01	3.25	0.01	REA2	100/0	0.25	0.01	3.43	0.03
RE25	92/8	0.55	0.01	3.46	0.01	REA3	100/0	0.53	0.01	3.68	0.01
RE26	92/8	1.02	0.02	3.79	0.03	REA4	100/0	1.15	0.01	3.97	0.01
RE27	92/8	0.27	0.01	2.83	0.01	REA5	100/0	1.31	0.02	3.91	0.02
RE28	92/8	0.43	0.01	2.86	0.01	REA6	100/0	1.25	0.01	3.77	0.01
RE29	92/8	0.63	0.01	2.89	0.02	REA7	100/0	1.30	0.02	3.60	0.03
RE30	92/8	-0.76	0.02	2.66	0.01	REA8	100/0	1.22	0.01	3.30	0.02
RE31	92/8	-0.49	0.01	3.44	0.02	REA9	100/0	1.35	0.01	3.25	0.02
RE32	92/8	-0.08	0.01	3.76	0.01	REA10	100/0	1.43	0.01	3.17	0.02
RE33	92/8	0.25	0.01	3.93	0.03	REA11	100/0		sample	lost	
RE34	92/8	0.23	0.01	3.72	0.01	REA12	100/0	1.42	0.01	3.14	0.01
RE35	92/8	0.31	0.01	3.30	0.02	REA13	100/0	1.11	0.00	3.21	0.01
RE36	92/8	0.33	0.02	3.27	0.01	REA14	100/0	0.84	0.02	3.37	0.03
RE37	92/8	0.34	0.01	3.33	0.02	REA15	100/0	1.12	0.01	3.68	0.01
RE38	92/8	0.47	0.01	2.93	0.01	REA16	100/0	1.28	0.02	3.79	0.02
RE39	92/8	0.53	0.01	2.74	0.01	REA17	100/0	1.30	0.01	3.75	0.01
RE40	92/8	-0.40	0.01	2.35	0.01	REA18	100/0	1.45	0.01	3.58	0.02
RE41	92/8	-0.64	0.01	2.83	0.01	REA19	100/0	1.54	0.01	3.47	0.01
RE42	92/8	0.23	0.01	3.65	0.02	REA20	100/0	1.47	0.01	3.24	0.02
RE43	92/8	0.28	0.01	3.72	0.01	REA21	100/0	1.62	0.01	3.10	0.02
RE44	92/8	0.65	0.01	3.67	0.02	REA22	100/0	1.42	0.01	2.93	0.02
RE45	92/8	0.75	0.01	3.48	0.01	REA23	100/0	1.12	0.01	3.20	0.01

XX. Epilogue

„We are tied to the ocean. And when we go back to the sea, whether it is to sail or to watch - we are going back from whence we came.“

John F. Kennedy